University of Nevada

Reno

Recent Deformation in the Saline Valley Region, Inyo County, California

A dissertation, submitted in partial fulfillment of the requirements for the degree of Doctor of Philosophy,

by

John Theodore Zellmer

May 1980

The dissertation of John Theodore Zellmer is approved:

Dissertation Advisor

Department Chairman

Dean, Graduate School

University of Nevada

Reno

May 1980

ABSTRACT

Saline Valley is a deep rhomb-shaped depression bordered by normal- and oblique-slip fault zones. The faults that offset unconsolidated alluvial sediments and are characteristic of the present tectonic regime can be divided into five fault zones, based on their location and tectonic style. These are: 1) the Grapevine Canyon, 2) the Western Frontal, 3) the Central Valley, 4) the East Side, and 5) the Lee Flat fault zones.

The Grapevine Canyon fault zone trends northwest-southeast from Hunter Mountain to Daisy Canyon. Displacement is primarily right-lateral, strike-slip at Hunter Mountain and becomes increasingly dip-slip toward Daisy Canyon. Total vertical offset at Daisy Canyon is at least 6000 m. Total right-slip displacement appears to be at least 1000 m. Offsets in unconsolidated alluvial and lacustrine sediments are up to 30 m vertically and 22 m right-slip. Evidence for multiple offsets is common.

The Western Frontal fault zone extends from Daisy Canyon to the northern border of the study area. The zone consists of normal-slip faults in unconsolidated alluvium and colluvium. Total offset is at least 6000 m. Three episodes of faulting are evident in the unconsolidated material. One alluvial fan has been offset at least 30 m.

The Central Valley fault zone is located in the playa of Saline Valley. Numerous northwest-southeast to east-west trending faults

offset the recent lacustrine and eolian deposits. There is evidence for continuing deformation of the playa.

The East Side fault zone is located in the northcentral portion of the study area. This is a zone of north-south trending normal faults and grabens in the unconsolidated sediments. The faults are related to step faulting along the west flank of the Panamint Range and east-west extension of Saline Valley. Multiple fault offsets with total displacements of at least 30 m were observed.

The Lee Flat fault zone is located between the Nelson Range and the Inyo Mountains. The zone is cut by northwest-southeast trending normal faults in unconsolidated alluvium and Tertiary-Quarternary basalt.

Ages of faults in unconsolidated alluvial deposits indicate that Saline Valley has been tectonically active during the Pleistocene and Holocene. Fault recurrence rates during the last 2×10^4 yr average about 1.7×10^{-4} yr^{-1}.

An analysis of joint patterns at Hunter Mountain suggest that the high-angle joints resulted from movement along the Grapevine Canyon fault zone. The orientations of the Grapevine Canyon and other fault zones suggest that they resulted from a regional stress system in which the maximum principal stress acted in a NNE-SSW to NE-SW direction.

A rhombochasm origin for Saline Valley is indicated by the style and orientation of the faults and other tectonic and physiographic features in the region. Saline Valley formed as the result of east-west extension due to the western migration of the Sierra Nevada

and right-lateral shearing along the western border of the Basin and Range province. The extension and shearing are attributed to northeasterly-southwesterly trending regional compressive forces. As a result of the regional stress field and deformation, Saline Valley developed in a zone of tension in a transitional area between the Sierra Nevada and Basin and Range Provinces.

CONTENTS

LIST OF FIGURES

LIST OF PHOTOS

LIST OF TABLES

1.0 INTRODUCTION

1.1 PURPOSE AND SCOPE OF INVESTIGATION

This study investigates deformational features in the Saline Valley region of southeastern California that are characteristic of the present tectonic regime. The analysis and interpretation of these deformational features provide insight into the tectonic style and regional stress field responsible for the present topography and structural elements observed in the region. The study area is located in an area between the borders of two physiographic and geologic provinces, the Sierra Nevada and the Basin and Range. Because the study area displays characteristics of both provinces, it is considered to be transitional between the two tectonic styles. Consequently, an analysis of the tectonic features of this area helps provide a clearer understanding of the transition zone and the geologic evolution of both provinces.

The characteristics of Quaternary tectonism in the Saline Valley region can be determined from the style and pattern of the faults and related features that affect the young unconsolidated alluvial deposits. Therefore, this study focuses principally on the young, well preserved fault zones that border the valley and offset unconsolidated sediments on the playa floor. Aerial photographs and aerial reconnaisance were used extensively to assess the style and pattern of faulting and to determine key locations for detailed field study. The field study included fault scarp profiling to estimate the age and number of fault offsets, the determination of grain size distributions

for the scarp material, determination of the in situ seismic velocities of the scarp material, measurement of joint orientations on Hunter Mountain, and general reconnaisance of the region. An interpretation of this data was used to develop a tectonic model that accounts for the tectonic features observed in Saline Valley and the surrounding region.

1.2 LOCATION AND ACCESSIBILITY

The study area (Figure 1.1) occupies approximately 826 km^2 of central Inyo County, southeastern California, and is located in the southwestern portion of the Basin and Range physiographic province. The area includes the Racetrack Valley region of Death Valley National Monument and extends westward across Saline Valley to near the crest of the Inyo Mountains. The eastern boundary is 117°30' West longitude and the western boundary is a NNW-SSE trending line connecting 117°55' and 117°45' West longitudes. The northern and southern boundaries are respectively 36°45' and 36°30' North latitude. Topographic map coverage is provided by the Ubehebe Peak (1950) and New York Butte (1951) 15' (1:62, 500) U.S.G.S. topographic maps with contour intervals of 40 and 80 ft, respectively (Figure 1.2).

The area may be approached from both the north and south by improved dirt roads. The southern route extends north about 50 km from U.S. Hwy 190 which connects U.S. Hwy 395 near Olancha with Death Valley National Monument. The northern route extends south about 64 km from State Hwy 168 which connects U.S. Hwy 395 at Big Pine with Westgard Pass. The access roads are generally well maintained but may

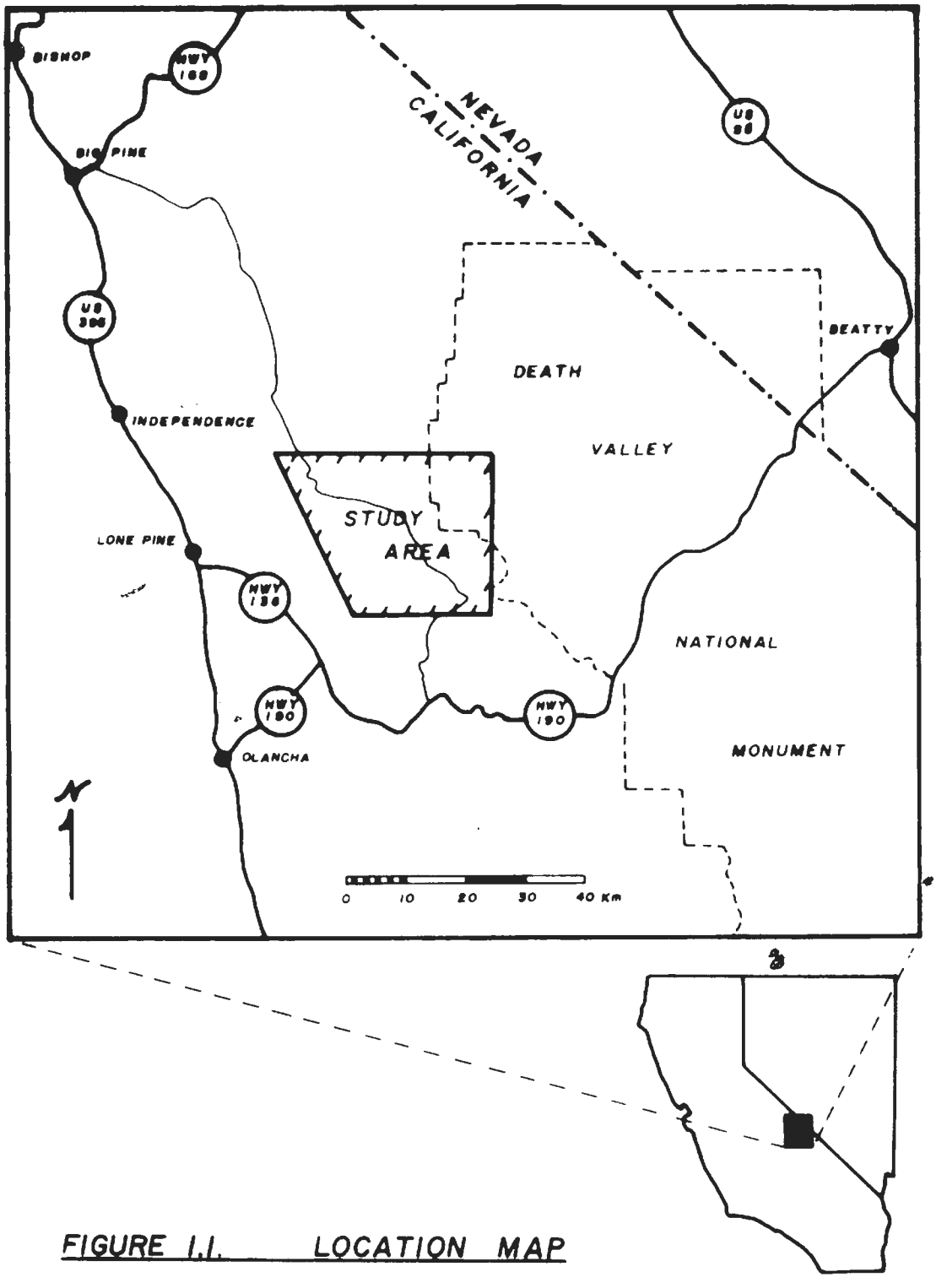

FIGURE I.I. LOCATION MAP

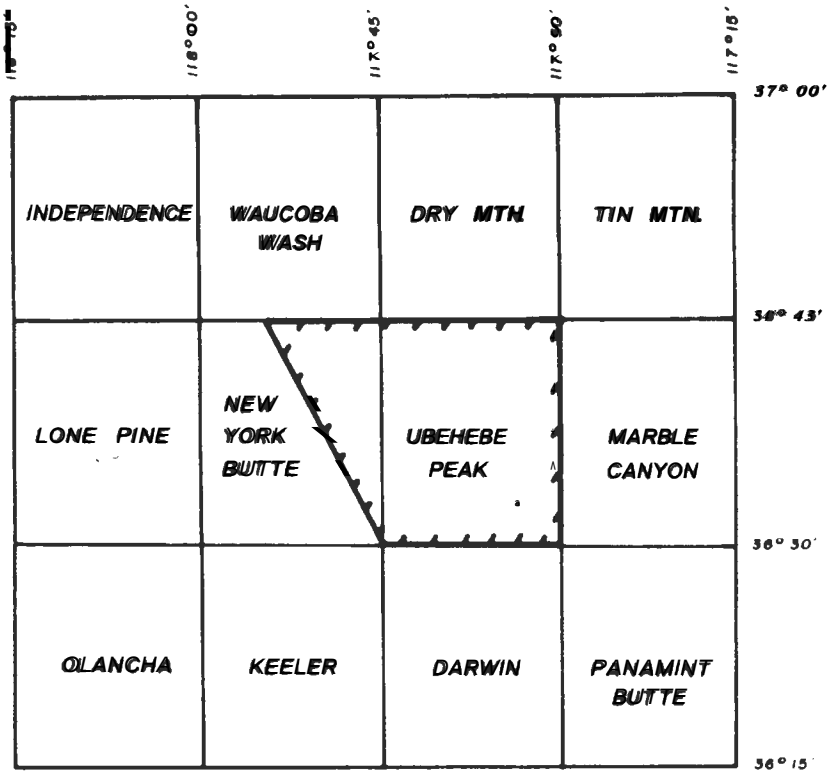

FIGURE 1.2. Topographic map coverage at a scale of 1:62,500.

be impassable seasonally due to snow accumulations at the higher elevations or by being washed-out by heavy rainfall. The area occupies portions of Death Valley National Monument (U.S. Park Service) and the California Desert Conservation Area, Saline Valley Area (U.S. Bureau of Land Management) and so vehicle travel is strictly limited to existing roads. Vehicle access to many localities is quite poor or nonexistent. Roads range in quality from well maintained to locally impassable.

1.3 PHYSIOGRAPHIC SETTING

Physiographically the study area is dominated by tectonic landforms. The Inyo Mountains and Saline Valley are the most prominent physiographic features (Photo 1.1). Approximately 6.5 km west of the study area Keynot Peak, at the crest of the Inyo Mountains, rises to an elevation of 3383.6 m, forming a topographic gradient of 355 m/km. The topographic closure of Saline Valley is approximately 1220 m. The average elevation of the valley rim approximately 2134 m. The playa area of Saline Valley is at an elevation of 325 m.

Other prominent geographic features in the study area are: 1) the Nelson Range which forms the southern border of Saline Valley, rises to a maximum elevation of 2,347 m; 2) Lee Flat, located between the Nelson Range and Inyo Mountains with an average elevation of about 1676 m; 3) the Panamint Range, which forms the eastern border of Saline Valley, and 4) Racetrack Valley, in the northeast corner of the study area, with a playa elevation of 2272 m.

A relief map of the general region is shown in Figure 1.3. A series of east-west topographic profiles through the study area and adjacent region are shown in Plate 1.1.

1.4 CLIMATE

The study area has a desert climate typified by slight rainfall, high summer temperatures, high evaporation, low humidity, wide diurnal and annual temperature fluctuations and frequent strong winds in the spring. The climate is similar to that of Death Valley. Temperatures often may reach 38°C from March to September. Visitors to Saline

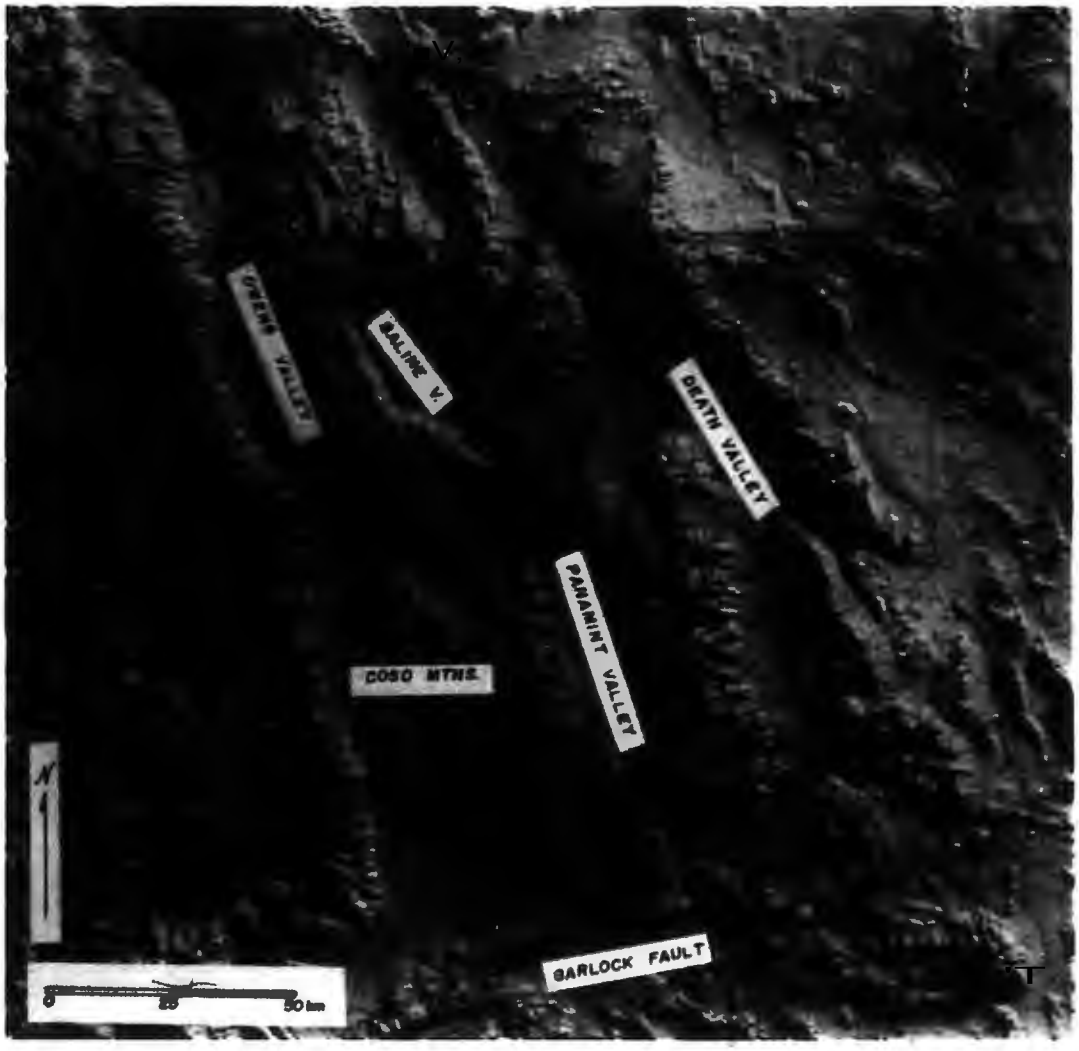

PHOTO 1.1. Topographic relief map of a portion of the Sierra Nevada - Basin and Range transition zone.

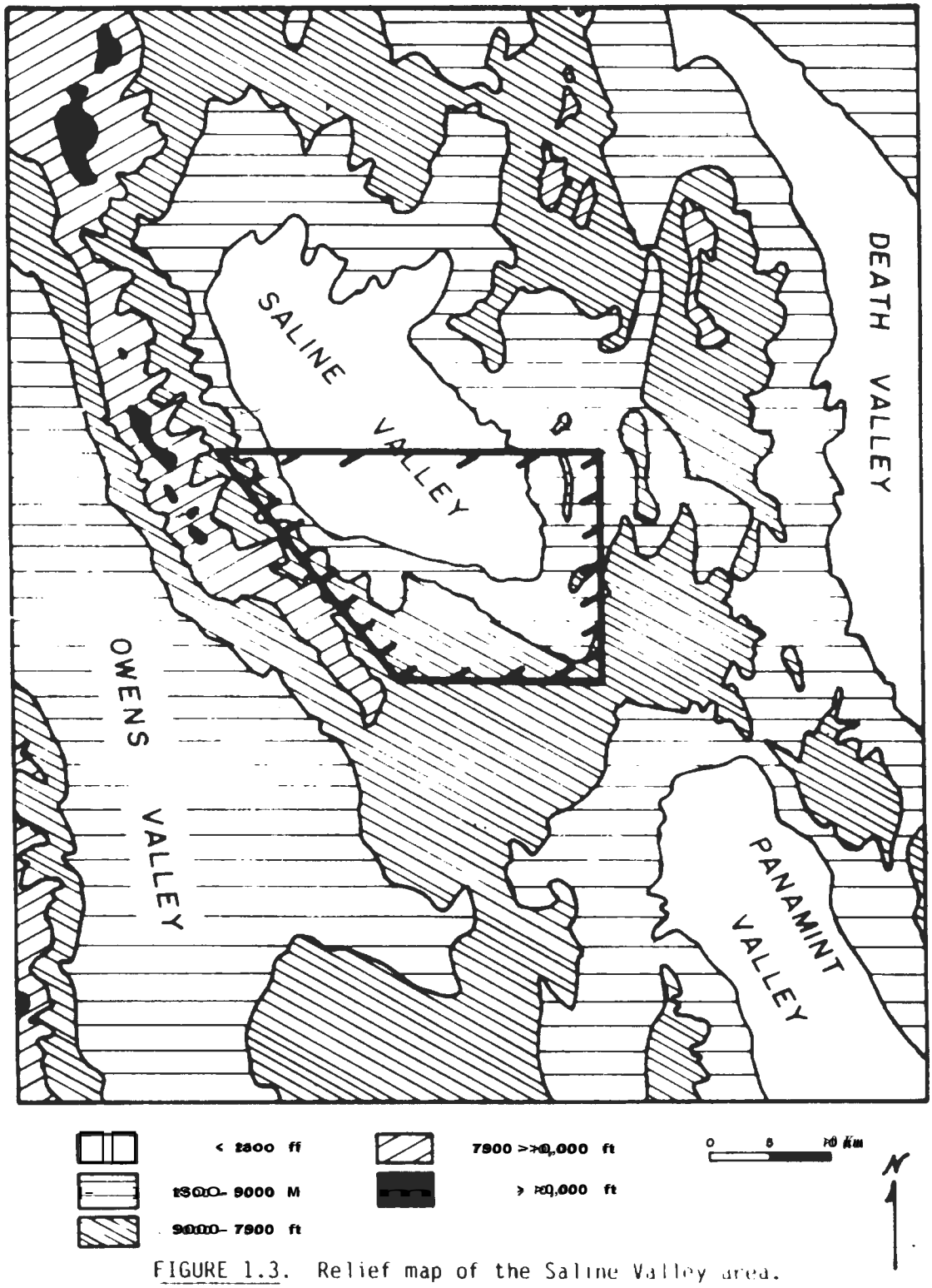

FIGURE 1.3. Relief map of the Saline Valley area.

Valley report that summertime temperatures exceeding 49°C are common. At elevations above about 1525 m the summer temperatures are pleasant except during occasional hot periods. The winters are mild and nearly frost-free at the lower elevations, but occasional snow has been reported on the valley floor. The winter snowline is usually above about 1525 m, with heavy snow at the high elevations along the crest of the Inyo Mountains.

About two-thirds of recorded precipitation comes from Pacific maritime storms during November through April; the rest from summer thunder showers fed by moist air from the Gulfs of Mexico and California. Distribution of precipitation is erratic in both time and space, with wet years typically receiving three to four times the precipitation of dry years. Years with no precipitation on the valley floor are common. Additional information concerning precipitation in this area may be found in Rantz (1969).

1.5 VEGETATION

Vegetation is sparse throughout most of the study area. The principal vegetation on the floor of Saline Valley is creosote bush which flourishes up to about the 1500 m elevation. A variety of halophilic shrubs are also found around the playa area, especially near the salt lake. Steep slopes are largely bare of vegetation, but moderate slopes and gullies have scattered sagebrush and creosote. Pinon pine and juniper are common above about 1500 m on northern facing slopes and above about 2100 m on south facing slopes. Joshua

trees are locally found above about 1500 m. Large stands of Joshua trees grow in Lee Flat and in portions of the Panamint Range.

1.6 WILDLIFE

Burt and Grossenheider (1976) indicated that approximately forty-four species of mammals live in the region. These include bighorn sheep, deer, two species of rabbits, porcupines, pica, nine species of mice, three species of kangaroo rats, gophers, chipmunks, two species of squirrels, marmots, bobcats, mountain lions, three species of fox, coyote, two species of skunks, badgers, ringtails, black bear and seventeen species of bats.

Stebbins (1966) indicated that approximately twenty-three species of reptiles and amphibians may be found in the region. These include four species of rattlesnakes, ten species of nonvenomous snakes, five species of lizards, chuckwallas, desert iguanas, frogs and toads.

1.7 AVAILABLE PHOTOGRAPHY

The aerial photographs used in this study are from three sources. Black and white photography is available from U.S. Geological Survey Photographic Project GS-CQ (1:37,400) flown in July 1947 and from U.S. Army Map Service Project 109 (1:60,000) flown during October and November 1952. Color photography flown during October 1975 is available from U.S. Bureau of Land Management Photographic Project CM000 (1:20,000). All of the above photographs are standard 23 x 23 cm format. The areas covered by these photographs are shown in Fig. 1.4.

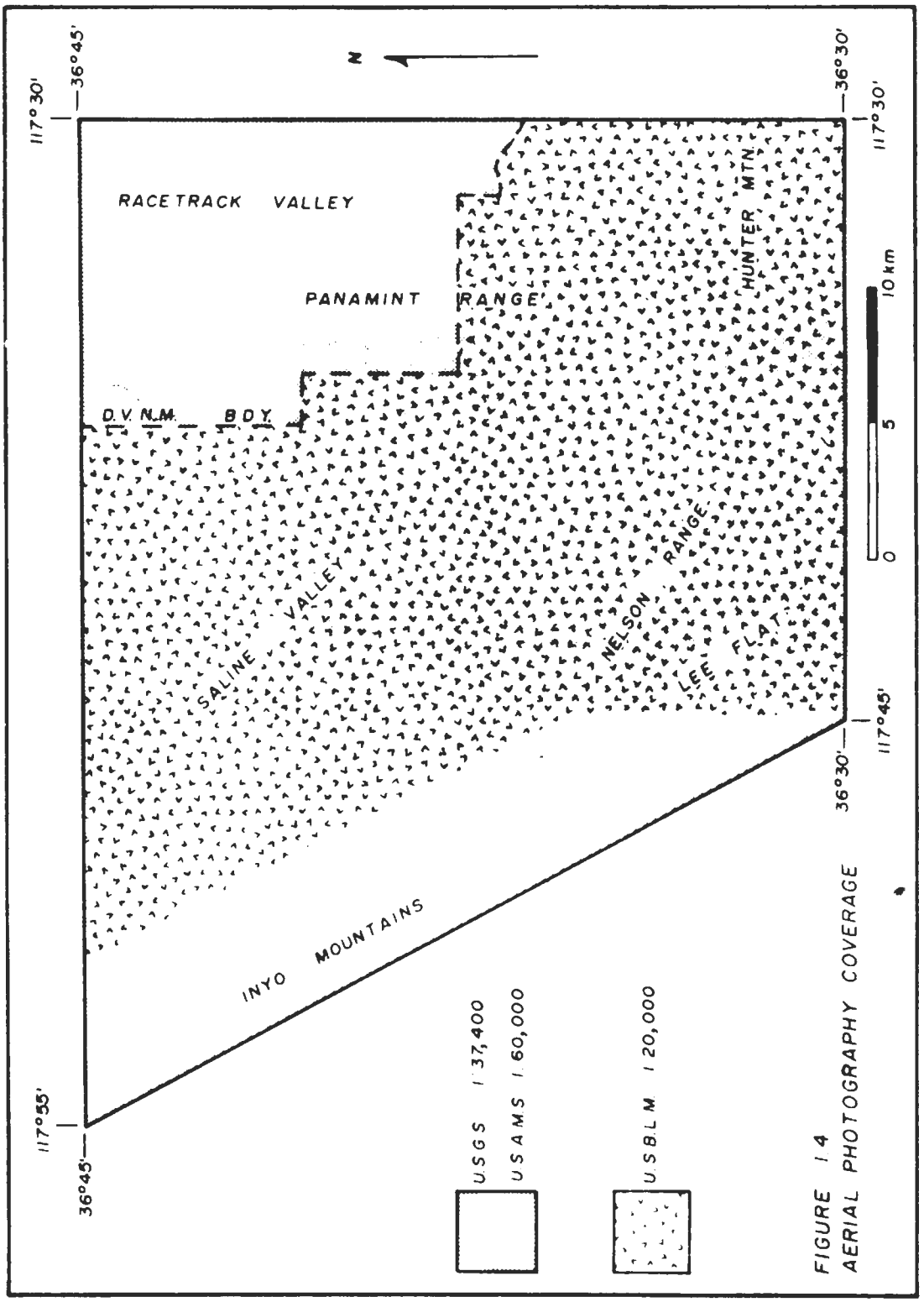

FIGURE 1.4
AERIAL PHOTOGRAPHY COVERAGE

Additional black and white and color photography was obtained in December 1977 and March 1979 during aerial reconnaisance of the area by private aircraft. Numerous color photographs were also taken from ground locations during the period of field work.

1.8 EARLY REGIONAL INVESTIGATIONS

The earliest geologic investigations in the region were generally of a reconnaissance nature, such as those of Whitney (1865), Gilbert (1875), Goodyear (1888), Fairbanks (1896), and Ball (1907). The first detailed study was Walcott's (1897) investigation of the post-Pleistocene elevations of the Inyo Range and the lake beds of the Waucobi Embayment. Spurr (1903) compiled what was then known of the regional geology and published the first geologic map. Waring (1917) produced the first geologic map of Inyo County. Knopf (1918) studied the geology of the Inyo Range and eastern slope of the Sierra Nevada.

As a result of discovery of the Cerro Gordo mining district, in the 1860s, and the salt and borax deposits of Saline and Owens Valleys, there are several early accounts of the economic geology and mining activities of the region. Some of these accounts are: Raymond (1873), DeGroot (1890), Fairbanks (1894), Bailey (1902), Aubury (1908), Knopf (1913), and Waring and Hugueinin (1916).

1.9 INVESTIGATIONS IN THE STUDY AREA

Several studies have focused on portions of the study area. Gale (1912), Lombardi (1963), and Hardie (1968) studied the evaporite deposits of Saline Valley. McAllister (1952, 1955, 1956) reported on

the general and economic geology of the Ubehebe Peak Quadrangle and on the geology of the Quartz Spring area. Merriam (1963) studied the geology of the Cerro Gordo mining district. Lombardi (1964) reported on the deformation of Saline Valley and its relationship to the tectonics of the western United States. Ross (1969) described the petrography of a portion of the Hunter Mountain quartz monzonite. Parker (1976) studied the sedimentology and petrography of the Keeler Canyon Formation near the Ubehebe Mine.

1.10 INVESTIGATIONS IN ADJACENT AREAS

Several investigations have been conducted in areas adjacent to or including portions of the study area. Ross (1965, 1967) mapped the Independence and Waucoba Wash Quadrangles. Burchfiel (1969) reported on the geology of the Dry Mountain Quadrangle and Hall (1971) on the geology of the Panamint Butte Quadrangle. Tucker and Sampson (1938) and Norman and Stewart (1951) reported on the mineral resources of Inyo County. Hall and MacKevett (1958, 1962) studied the economic geology of the Darwin Quadrangle and Hall and Stephens (1963) studied the economic geology of the Panamint Butte Quadrangle.

Smith (1974, 1975a, 1975b, 1978) reported on the late Quaternary pluvial and tectonic history of Panamint Valley. Bachman (1974, 1975, 1978) studied the depositional and deformational history of the Plio-Pleistocene Waucobi Lake beds, the Plio-Pleistocene breakup of the Sierra Nevada-White-Inyo Mountains block, and the formation of Owens Valley. Stevens and Olson (1972) and Kelley and Stevens (1975) studied the nature and significance of thrust faults in the Inyo

Mountains. Carver (1969) studied the Quaternary tectonism and surface faults and Pakiser et al. (1964) studied the structural geology and volcanism in the Owens Valley region.

Miscellaneous investigations in areas adjacent to the study area include Gale's (1914) study of the saline deposits in Owens, Searles, and Panamint Valleys, Schultze's (1937) report on the Plio-Pleistocene Coso fauna, Hopper's (1947) geologic section from the Seirra Nevada to Death Valley, Maxson's (1950) study of the physiographic features of the Panamint Range, and Ross's (1970) study of the volcanic rocks of the Saline Range.

1.11 INVESTIGATIONS IN THE DEATH VALLEY REGION

Numerous geologic studies have been conducted in the Death Valley region. A brief cross section of these includes Campbell's (1902) reconnaissance study of the borax deposits, Beatty's (1961) study of the topographic effects of surface faulting, Denny's (1965) study of alluvial fans, Burchfiel and Stewart's (1966) theory on the origin of the central segment of Death Valley, Hunt and Mabey's (1966) study of the stratigraphy and structure, Hunt's (1966) report on the general geology, Hill and Troxel's (1966) tectonic study of the Death Valley region, and McKee's (1968) study of the age and rate of movement of the northern part of the Death Valley-Furnace Creek fault zone.

Of specialized interest are studies related to the sliding stones on the playa of Racetrack Valley. These stones range in size from pebbles to small boulders weighing up to 25 kg. It has been suggested that the movement of the stones and the resulting furrows in the playa

surface are related to wind or ice movement of the stones. Investigations of this phenomenon were conducted by McAllister and Agnew (1948), Stanley (1955), Sharp and Carey (1975), and Shelton (1953) who tried to move the stones with the propwash from his light aircraft.

1.12 MODERN REGIONAL GEOLOGICAL MAPPING

The study area is shown on geologic maps of the Owens Valley region by Bateman and Merriam (1954), of the Inyo Mountains by Ross (1967), and the Death Valley Sheet by Jennings (1958) and by Streitz and Stinson (1974). Gravity maps of the Death Valley Sheet by Mabey (1963) and Chapman et al. (1971) indicate the main structural and geologic subunits. The study area is also shown on the Fault Map of California (Jennings, 1975).

1.13 REGIONAL GEOLOGIC INVESTIGATIONS

Numerous regional geologic investigations of the western United States and Basin and Range province provide the basis for the understanding of the general geology and tectonic development of the study area. Merriam (1954), Merriam and Hall (1957), Ross (1964), Stewart (1966, 1970), and Miller (1976) studied the pre-Mesozoic stratigraphy. Gilluly (1965), Hamilton and Myers (1966), and Ryall et al. (1966) studied the regional tectonics of the western United States. Nolan (1943), Slemmons (1967), Stewart (1971), Babcock (1974), and Wright (1976) studied the geology and tectonic development of the Basin and Range province. Healy and Press (1964) and Thompson and Burke (1974) conducted geophysical investigations of the Sierra Nevada eastern front and the Basin and Range province.

2.0 REGIONAL TECTONIC SETTING

The study area is located in the southwest portion of the Great Basin in the transition zone between the Basin and Range and Sierra Nevada physiographic provinces. The area has a unique tectonic style by virtue of its location in the transition zone at the boundary of the two distinctly different physiographic and geologic provinces (Figure 2.1). The Basin and Range Province contains north-to-northeasterly trending tilted fault blocks indicative of northwest-southeast to east-west extension totaling between 100 and 300 km (Hamilton and Myers, 1966). Such extension appears to be consistent throughout the province. The regional fault pattern is modified in the transition zone by the Sierra Nevada structure, which is oriented northwest.

The 1000 km long San Andreas fault system with a total right-lateral, strike-slip displacement of scores of kilometers to 200 km (Leet and Judson, 1971) is west of the Sierra Nevada Range. The San Andreas fault forms a portion of Gutenberg and Richter's (1954) Circum-Pacific Belt of great right-lateral, strike-slip fault zones. The associated left—lateral Garlock fault, with a total displacement of 48 to 72 km (Michael, 1966; Dibblee, 1967), extends eastward about 250 km from the San Andreas fault and terminates about 100 km south of the study area.

The Garlock fault is the southern boundary of the transition zone between the Great Basin and Sierra Nevada in California. Ryall et al. (1966) and Troxel et al. (1972) and St. Amand and Roquemore (1979)

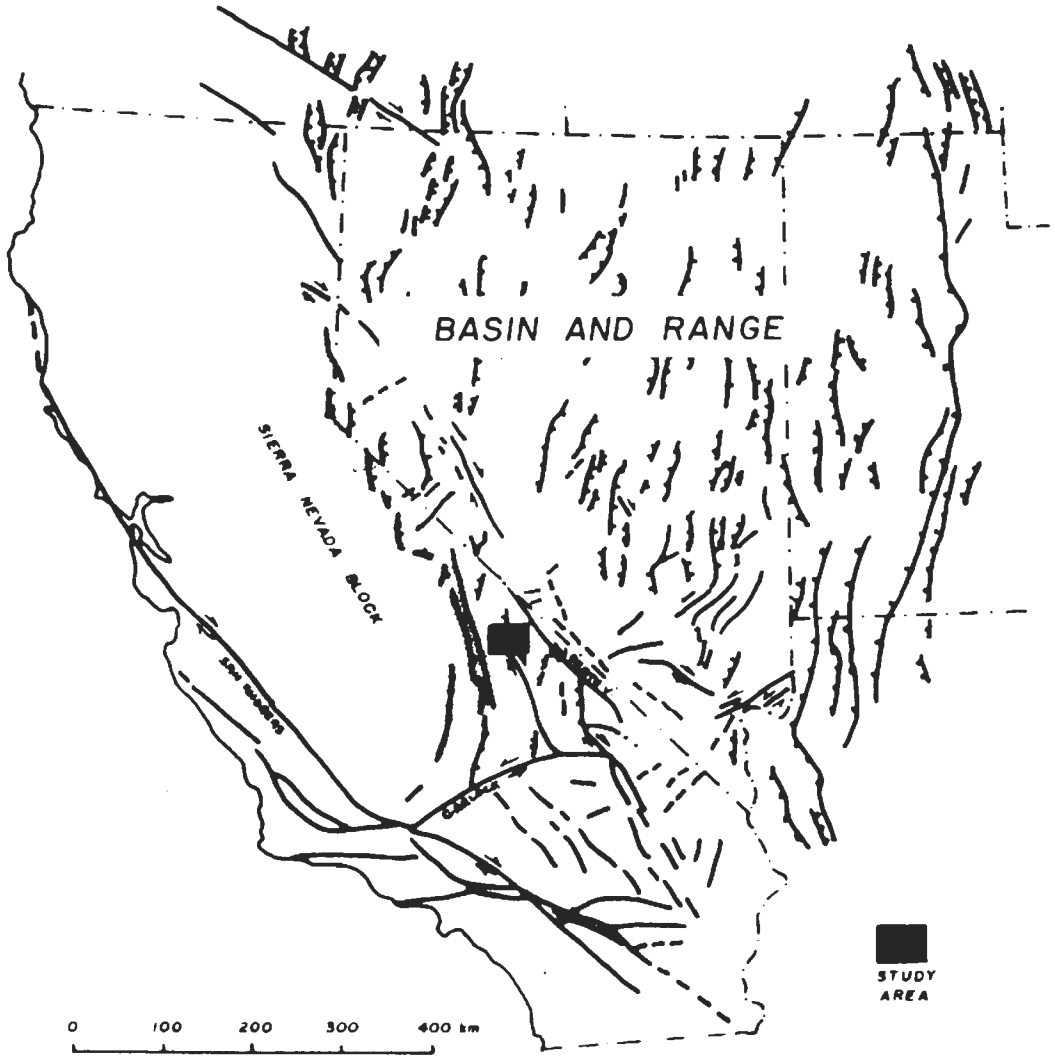

FIGURE 2.1. Major fault patterns in the Sierra Nevada and Basin and Range provinces.

suggest that the Mojave Block, located to the south of the Garlock fault, is tectonically stable while the Great Basin to the north of the fault is seismically active and is undergoing regional extension across normal faults.

The Winnemucca-Ventura Zone of Ryall et al. (1966), a 750 km long belt of historic high seismicity, extends from the Pacific Coast near Ventura, California, through the study area, to near Winnemucca in northern Nevada. This is one of the most seismically active areas in the western United States and has produced numerous surface ruptures during historic times. East of the study area the Walker Lane (Locke et al., 1940), a right-lateral, strike-slip zone of high seismicity, extends approximately parallel to the California-Nevada border for more than 700 km from Pyramid Lake near Reno, Nevada, to near Las Vegas, Nevada. These and other zones of high seismicity are shown in the tectonic flux map of the western United States (Figure 2.2).

Hamilton and Myers (1966) consider that southeastern California, between the Sierra Nevada and the Black Mountains, the Owens Valley-Saline Valley-Death Valley region, is the region of greatest Pliocene and Quaternary faulting in the Basin and Range province.

The following chapters discuss the characteristics of the major zones of active faulting in the Saline Valley area. The patterns, styles and distribution of these faults and related tectonic features were the basis for determining the relationship between the present local tectonic regime and the pattern of regional deformation.

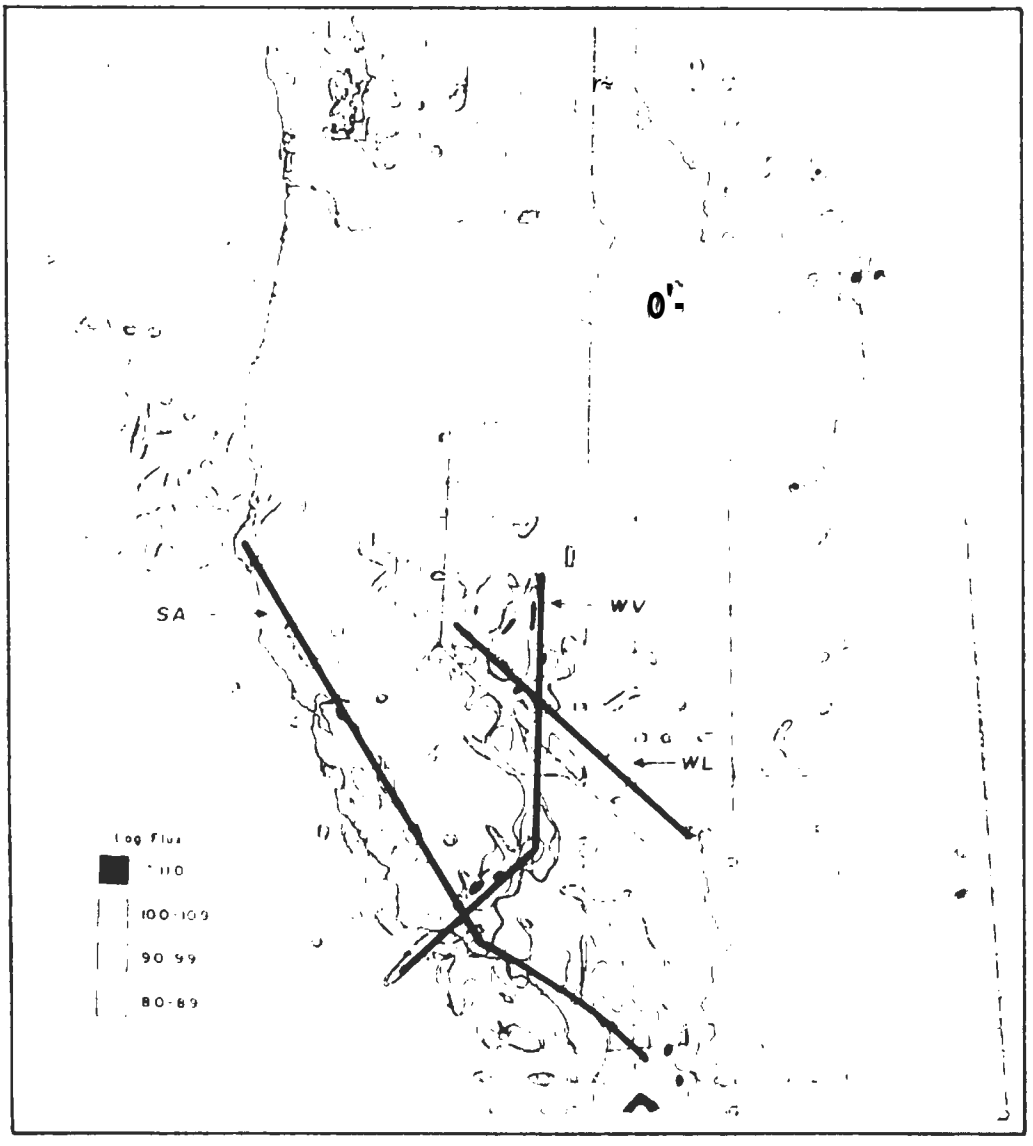

FIGURE 2.2. Tectonic flux map of the Western United States for the period 1769 to 1961 showing areas of seismic energy release (Ryall et al., 1966). SA = San Andreas Zone, WV = Winnemucca-Ventura Zone, WL = Walker Lane Zone.

3.0 DESCRIPTIONS OF ACTIVE FAULT ZONES IN THE STUDY AREA

3.1 INTRODUCTION

This study focuses on the active faults located on the floor and borders of Saline Valley that displace unconsolidated alluvial deposits. The pattern, style and distribution of these active faults form the basis for interpreting the characteristics of the local tectonic regime presently active in the region. These characteristics are used in later sections to infer relationships between the tectonic features in Saline Valley and the structural origin of the Sierra Nevada - Basin and Range transition zone. Although there are numerous bedrock faults in the area, they are generally not considered here unless they affect the young, unconsolidated, alluvial sediments. The older bedrock faults may reflect tectonic regimes that are no longer active, and consequently are of limited interest to this study.

Shown on Plate 3.1 are the active faults in the study area. As used here, "active" refers to any fault that displaces unconsolidated alluvial deposits. Although this definition is based solely on geomorphic data, it is consistent with the criteria given by Slemmons and McKinney (1977).

Plate 3.1a is a simplified geologic map of the study area showing the general distribution of the rock and alluvial units and the major faults, regardless of their activity and the locations of the fault scarp profiles discussed in the text. The faults examined in this study were mapped on the basis of photogeologic interpretation and when possible on direct field evidence.

The active faults in the study area are conveniently grouped into five major zones (Figure 3.1) based on their location and tectonic style. These zones are: 1) the Grapevine Canyon fault zone, 2) the Western Frontal fault zone, 3) the Central Valley fault zone, 4) the East Side fault zone, and 5) the Lee Flat fault zone. Minor zones in Racetrack Valley and Ulida Flat were not studied in detail.

The Grapevine Canyon fault zone is the northern segment of a major regional fault zone that extends from the Garlock fault and through Panamint Valley. In the study area this zone extends from Hunter Mountain to Daisy Canyon with a strike of approximately N60°W. The zone displays normal-slip, right-normal, oblique-slip and right-lateral, strike-slip faulting. The zone trends along the west side of Saline Valley where it offsets bedrock, unconsolidated alluvium and lacustrine deposits.

The Western Frontal fault zone extends from Daisy Canyon to the northern border of the study area along a trend of approximately N40°W. This zone displays normal-slip faulting in bedrock and in unconsolidated alluvial deposits. These are range front faults responsible for uplift of the Inyo Mountains.

Faults in the Central Valley fault zone displace lacustrine and eolian sediments in the playa region of the valley. These faults form northwesterly to westerly trending normal-slip faults and grabens.

The East Side fault zone is located near the northern border of the study area along the western flank of the Panamint Range. The

faults cut unconsolidated alluvial fan, lacustrine and eolian deposits. The zone consists principally of north-south trending horsts and grabens.

The Lee Flat fault zone is located between the Nelson Range and the Inyo Mountains. Faults in this zone generally are normal-slip and displace unconsolidated alluvial sediments and Tertiary basalts. Small grabens occur at several locations.

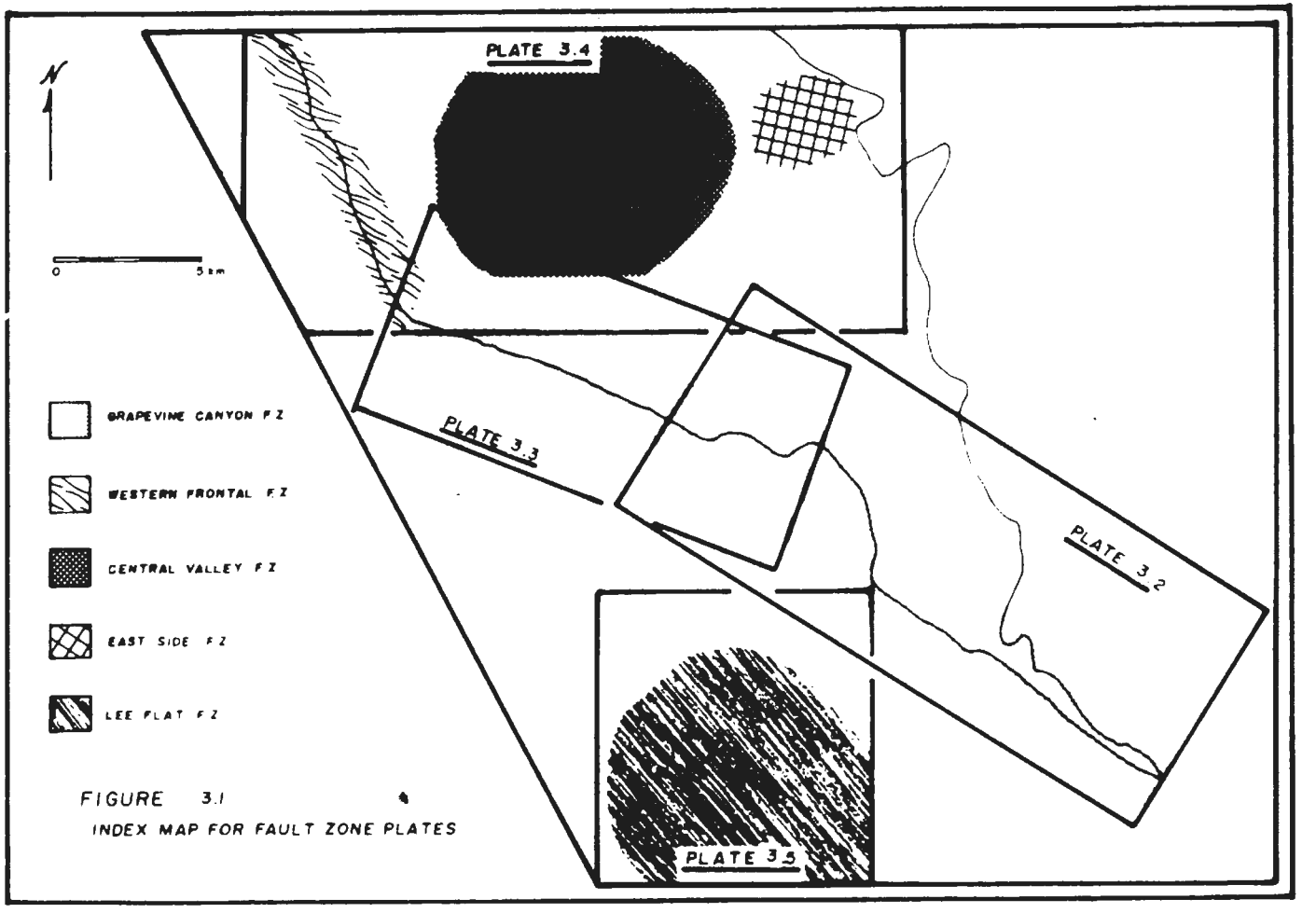

FIGURE 3.1. Index map for fault zones shown on Plates 3.1, 3.2, 3.3, 3.4, and 3.5.

3.2 PANAMINT VALLEY/GRAPEVINE CANYON FAULT ZONE

The Grapevine Canyon fault zone (Plates 3.1, 3.1a, 3.2, 3.3) is the northern extension of the Panamint Valley fault zone. This right-lateral, strike-slip, fault zone extends from the Garlock fault on the south, through Panamint Valley and into Saline Valley, a distance of at least 175 km. The continuance of the fault into Saline Valley was described by McAllister (1956), Lombardi (1963), Babcock (1974), and Smith (1974, 1975a, 1975b) and others. This fault zone is related to other major right-lateral, strike-slip, faults along the western edge of the Basin and Range province. The significance of these faults was briefly discussed by Wright (1976).

Smith (1975b) described the Panamint Valley fault zone as having normal-slip, right-lateral, strike-slip, and thrust fault displacements. Normal-slip displacements total nearly 10,000 m. Strike-slip displacements total between 3000 and 4500 m, with 300 to 600 m of this having occurred during the Quarternary. At the northern end of Panamint Valley the fault thrusts beneath Hunter Mountain with a dip between 17° and 35°. At Grapevine Pass the fault assumes a nearly vertical dip and continues northward as a strike-slip fault into Saline Valley where it becomes a right-normal, oblique-slip fault.

The overall character of the Panamint Valley/Grapevine Canyon fault zone is that of a hinge fault pivoting about Hunter Mountain. Dennis (1967) defines a hinge fault (Figure 3.2) as "a portion of a fault along which displacement increases in one direction with distance from an axis of rotation, or hinge." The Panamint Valley/ Grapevine Canyon fault zone departs from the strict definition in

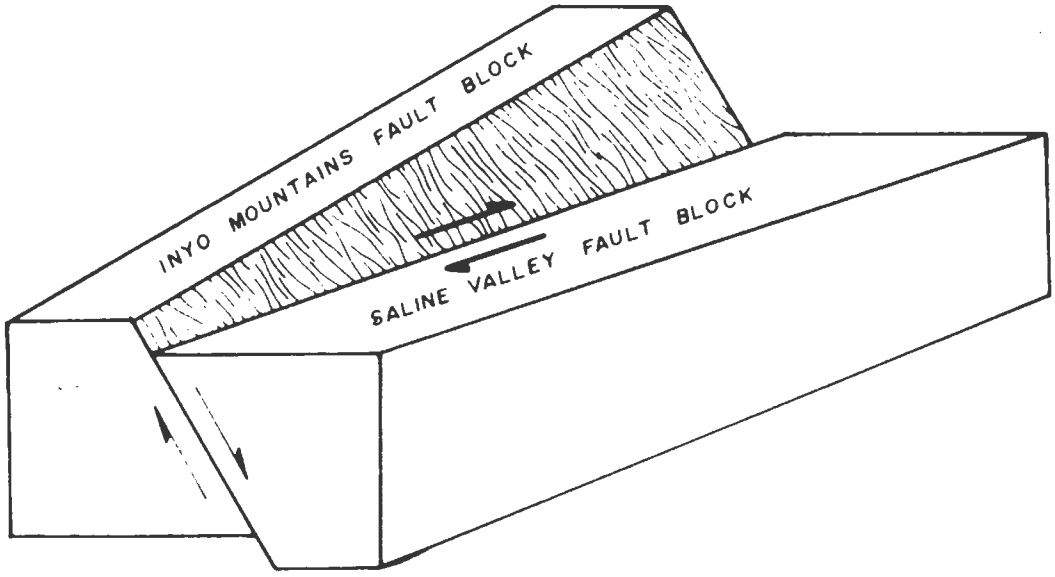

FIGURE 3.2. Displacement of Saline Valley and Inyo Mountains along hinge fault.

that: 1) displacement appears to increase both north and south of the hinge (i.e., forming both Panamint and Saline Valleys), and 2) there is a strong right-lateral, strike-slip component.

The geometry of the faulting suggests that northwest-southeast shearing accompanied the hinging action. Coeval hinge faulting and right-lateral shearing would account for the thrust fault at Hunter Mountain and right-lateral displacements along the zone.

3.3 GRAPEVINE CANYON FAULT ZONE

For convenience the Saline Valley segment of the Panamint Valley/ Grapevine Canyon fault zone is divided into two zones based on their characteristic tectonic styles. These are the Grapevine Canyon and

Western Frontal fault zones. The Grapevine Canyon fault zone is described in this section. The active faults in this zone are shown in Plates 3.1, 3.1a, 3.2 and 3.3.

Displacements along the Grapevine Canyon fault zone change from predominantly right-lateral, strike-slip at Grapevine Pass to predominantly normal-slip at Daisy Canyon. This is explained by the hinge faulting and shearing described earlier. Total normal-slip displacement increases from perhaps tens of meters at Grapevine Pass to at least 6000 m near Daisy Canyon. The maximum displacement is estimated from the present height of the Inyo Mountains above the floor of Saline Valley and the depth of alluvial fill in the valley inferred from gravity data by Mabey (1963). The estimate does not include the amount of material that has been eroded from the crest of the Inyo Mountains. This eroded material could conceivably total thousands of meters. The 6000 m estimate is consistent with Smith's (1975b) estimate of about 10,000 m of vertical displacement in Panamint Valley. In Saline Valley relatively young fault scarps of 20 m or more in height are common in both alluvium and crushed bedrock. Total strike-slip displacements are estimated to be between 700 and 2000 m based on stream offsets. Recurrent recent offsets in unconsolidated lacustrine sediments total at least 20 m at one location.

Photo 3.1 shows several geographic and geologic features near the southern end of the Grapevine Canyon fault zone. These features include Panamint Valley, Grapevine Pass at the summit of Hunter Mountain, Grapevine Canyon, the Nelson Range, Lee Flat, the southern

end of Saline Valley, the Low Granite Hills, the main access road into Saline Valley and the main faullt traces. The view is to the south.

PHOTO 3.1. Aerial view of southern portion of Saline Valley Area showing geographic locations, view to south.

Photo 3.2 shows a 2 m thick tuff bed at the head of Miller Canyon at Grapevine Pass. The tuff was deposited on a relatively level surface. At least locally this surface consisted of mudcracked, fine-grained sand and silt such as is commonly observed on dessicated lake bottoms. The tuff is intercalated within a thick fanglomerate sequence

that dips approximately 20°N. Megascopically, the tuff resembles a distinctive tuff deposit dated at 3 m.y. that crops out about 60 km to the south in the Coso Range. An attempt to determine if these two deposits are correlative is in progress, but not yet complete. An attempt to determine the magnetic polarity of the bed failed because the tuff lacked sufficient magnetic minerals.

PHOTO 3.2. Faulted tuff beds and fanglomerates at Grapevine Pass dipping about 20° to the north. The 2 m thick beds were deposited on a surface locally resembling a dessicated lake. Note "stair-step" offset in foreground.

Since the tuff beds were deposited they have been tilted about 20° to the north and offset by several north-striking normal faults. These offsets commonly exceed 2 m and have an aggregate displacement of tens of meters. Strike-slip offsets were not evident. A "stair-stepping" offset can be seen in the foreground of Photo 3.2. The bed can be seen extending to the east in the background of the photo. Another tuff bed is exposed several meters above this unit. No other tuff beds were observed either above or below the beds shown in the photo.

The tuff outcrop in the foreground of Photo 3.2 is the approximate western extent of the unit. The unit is exposed only near the 1830 m contour on Hunter Mountain on the east side of the Grapevine Canyon fault zone. The unit was probably continuous west of Grapevine Pass but has since been eroded or possibly covered by young basalt flows exposed in the Nelson Range.

If the tuff bed is correlative with the tuff beds in the Coso Formation, it can be used to estimate the minimum age of faulting along the Grapevine Canyon/Panamint Valley fault zone. Dating indicates ages of 40,000 to 3 m.y. for the tuff beds of the Coso formation. Roquemore (Personal Communication, 1979 and 1980) indicated that the tuff beds at Grapevine Canyon are similar to tuff beds of the Coso Formation dated at about 3 m.y. This suggests that faulting along the Grapevine Canyon/Panamint Valley fault zone may have begun less than 3 m.y. ago.

Several branches of the Grapevine Canyon fault zone cut through Grapevine Pass. Total width of the zone is about 800 m. This general

area marks the pivot point of the hinge faulting that was described earlier. South of the hinge, the Panamint Range has been uplifted along the east side of the fault zone relative to Panamint Valley. North of the hinge, the Inyo Mountains and the Nelson Range have been uplifted along the western side of the fault zone relative to Saline Valley.

From Grapevine Pass the fault zone continues north along a nearly linear path through the southwest wall of Grapevine Canyon. The general shape and increased width of the canyon are probably caused by fault splays. Photo 3.3 shows a portion of the fault zone in a road cut about 2.5 km north of Grapevine Pass. On the right side of the photo the Hunter Mountain quartz monzonite is highly jointed but relatively intact. To the left the rock is highly sheared and crushed. The crushed zone is about 10 m wide. The view is to the north.

At the mouth of Grapevine Canyon the fault cuts through alluvial fan deposits that dip northward toward Saline Valley. Numerous fault splays offset these deposits (Photo 3.4). The pattern formed by the splays is similar to the "late stage" structures produced in a Riedel experiment by Tchalenko (1970) using wet clay. In the region between the canyon mouth and the Low Granite Hills is a triangular-shaped wedge (Photo 3.4) about 4 km long and 2 km wide. This wedge appears to have been downfaulted into a tensional zone within the shear system. The pattern formed by the splays and the downfaulted wedge are suggestive of right-lateral, strike-slip faulting.

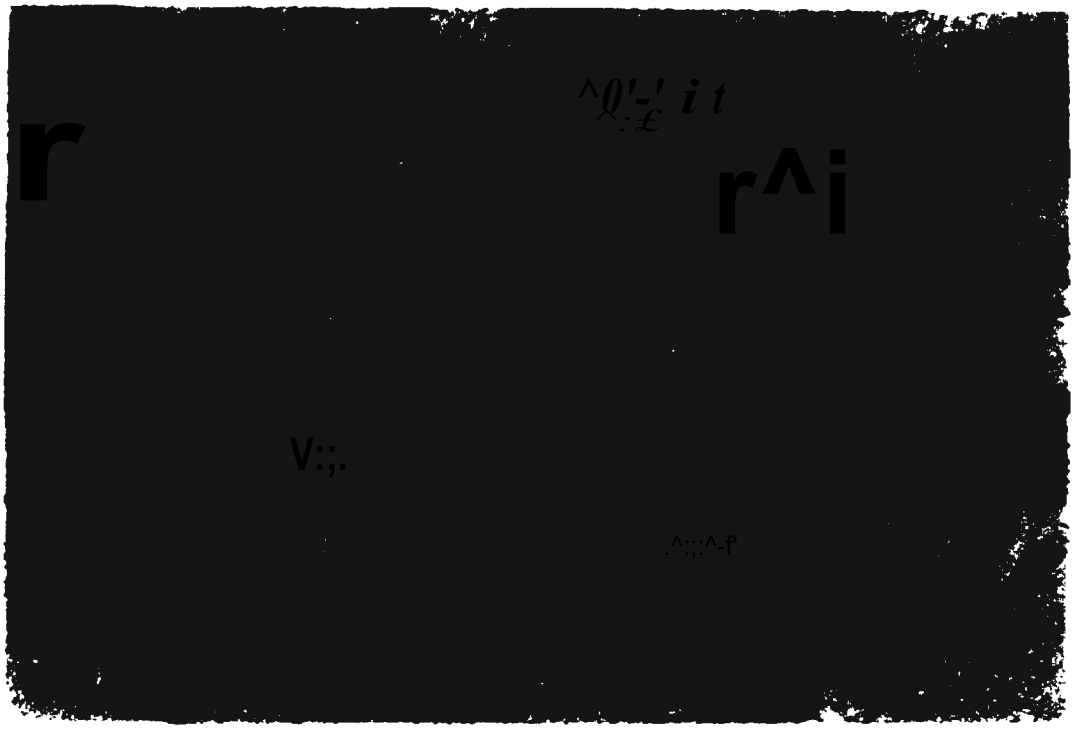

PHOTO 3.3. Grapevine Canyon fault cutting Hunter Mountain quartz monzonite. Note highly crushed rock in center and left portions of photo grading into intact rock at the right side of the photo.

Photos 3.5 and 3.6 are aerial photos showing several details of this portion of the fault zone. Photo 3.5 is a north-looking view along the strike of the main fault zone. The steepness of the scarp is partly due to stream erosion along its base. Because the scarp is probably too high (15 to 23 m) to have been formed by a single earthquake, it is assumed that stream erosion has removed evidence of multiple events. Scarp heights, but not profiles were measured at three locations. Two of these locations and their scarp heights (15 and 23 m) are shown on the photo.

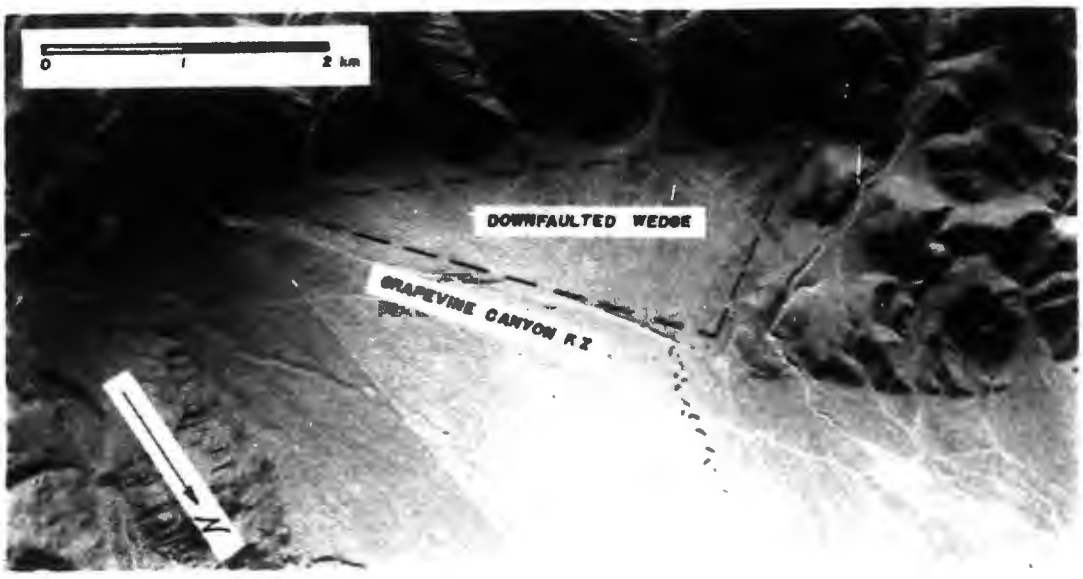

PHOTO 3.4. Vertical aerial photo of southern end of Saline Valley showing downfaulted triangular wedge and main trace of the Grapevine Canyon fault zone.

Photo 3.6 is an east-looking view taken at right angles to the strike of the fault zone. In addition to the several surface ruptures, a light colored, circular area can be seen near the photo center. This circular area contains the lacustrine sediments shown in Photo 3.7. The sediments contain a carbonaceous layer that may be suitable for dating and also tuffaceous material apparently derived from the tuff bed at Grapevine Pass. These sediments may be shoreline deposits representing the high stand of a pluvial lake, but this seems unlikely due to the elevation (945 m) and the lack of other lacustrine features at similar elevations in the valley. These deposits are located more than 600 m above the Saline Valley playa. Consequently, the sediments probably represent localized ponding due to faulting or other causes in the downfaulted triangular zone described earlier and shown in Photo 3.4.

PHOTO 3.5. Aerial view along the strike of the Grapevine Canyon fault zone in the southern portion of Saline Valley. View to north. Note fault scarp heights.

Photo 3.8 is a southwest-looking view of the Low Granite Hills showing several parallel fault traces. In the photo it appears that the hills may be large landslide blocks detached from topographically higher Lee Flat. Sliding, however, is probably only a contributing factor. The fault pattern and morphology of the Low Granite Hills

PHOTO 3.6. Aerial view across the Grapevine Canyon fault zone in southern portion of Saline Valley. View to East. Note fault traces.

suggest that they were detached from the escarpment bordering Lee Flat and the Nelson Range and transported southeastward along parallel right-normal, oblique-slip faults. A schematic cross-section of the Low Granite Hills and Nelson Range is shown in Figure 3.3. Figure 3.4 shows the inferred origin for the Low Granite Hills and other features at the south end of Saline Valley.

Geometrically, the origin of the Low Granite Hills appears to be a combination of northwest-southeast strike-slip faulting and northeast-southwest extension and may be related to the formation of Saline Valley. Such deformation is consistent with first-order Riedel

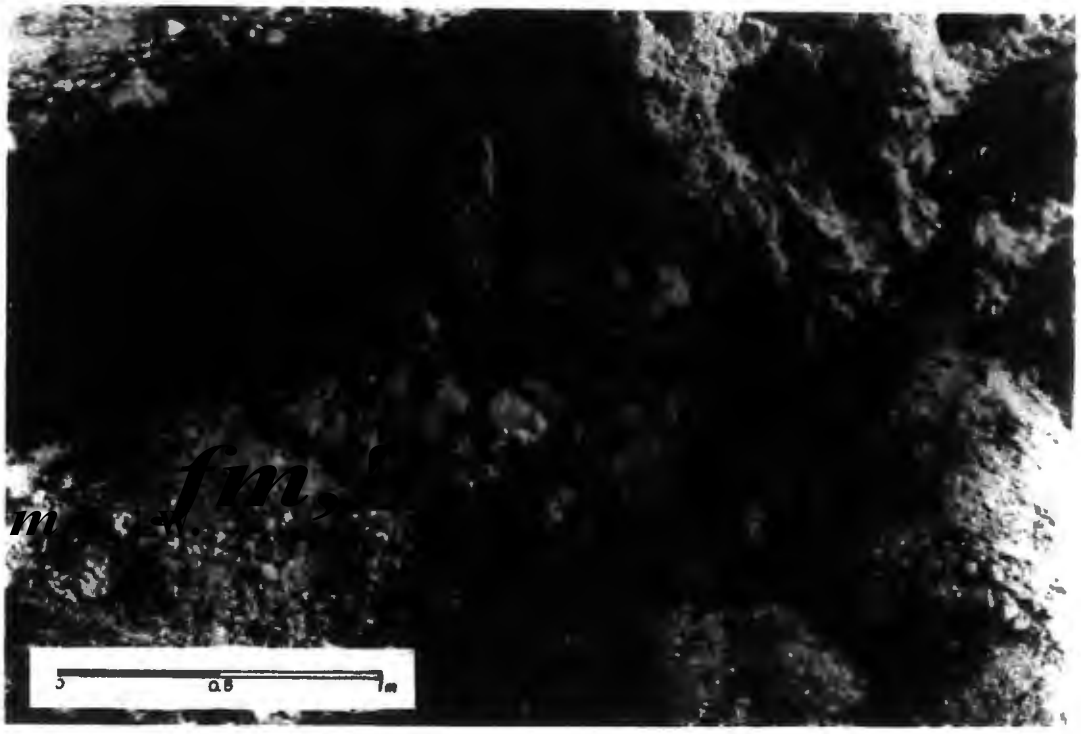

PHOTO 3.7. Lacustrine sediments along trace of the Grapevine Canyon fault zone. The sediments are greenish colored silt and fine sand. The carbonaceous layer can be seen to the left of the hammer head.

shearing associated with the Panamint Valley-Grapevine Canyon fault zone. Riedel shearing can also explain the downfaulted, triangular-shaped segment (Photo 3.4 and Figure 3.5) between the Low Granite Hills and mouth of Grapevine Canyon that was described earlier.

Topographic reconstruction of the Low Granite Hills suggests between 700 and 2000 m of strike-slip displacement and approximately 2500 m of northeast extension. The strike-slip displacement is based on the apparent matching of offset streams. The extensional displacement is based on the position of the Nelson Range relative to the position of the Low Granite Hills.

PHOTO 3.8. Aerial view of the Low Granite Hills with the Nelson Range to south (left) and Lee Flat in background. View to west. Note locations of scarp profiles P1, P2, P3, and P4.

Fault scarp profiles P1, P2, P3 and P4 (Figure B.1 of Appendix) were measured at the southern end of the Low Granite Hills (Plate 3.2, Photo 3.8). These profiles indicate a normal-slip component of approximately 50 m. Bevels on profile P3 indicate that there have been at least three and perhaps five or more periods of uplift. The scarps were formed in the crushed granitic rock that is characteristic of the Low Granite Hills. A caliche-filled fault in young stream channel deposits approximately 1 km southwest of the profile locations

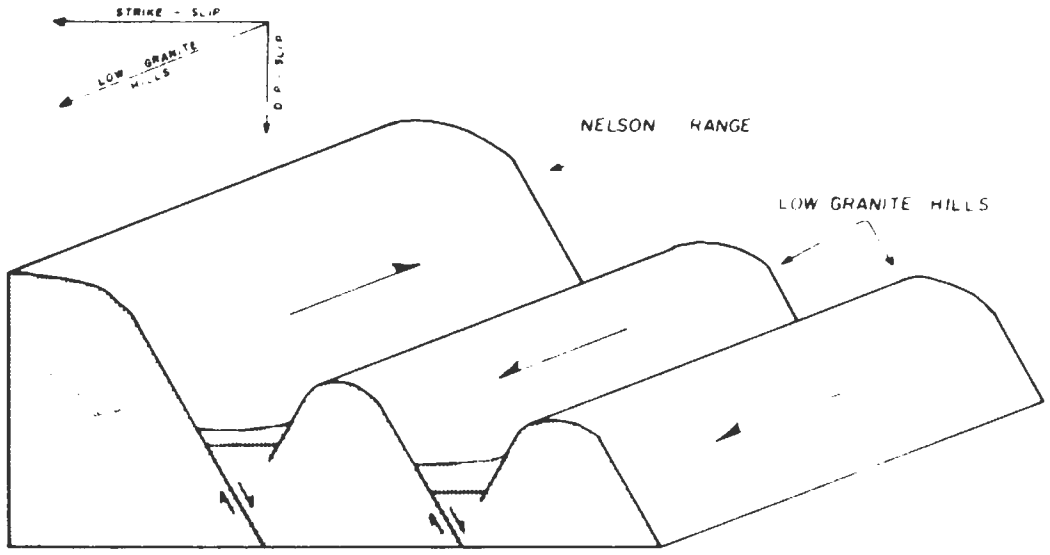

FIGURE 3.3. Schematic cross-section of the Low Granite Hills showing oblique-slip motion along range front faults.

is shown in Photo 3.9. The lower portion of the fault is covered by younger channel deposits. Note the surface offset and slight change of slope of the surface and dip of the beds.

Photo 3.10 is a south-looking view of a fault splay in the Low Granite Hills. In the foreground is the scarp measured for profile P21 (Figure B.1, Plate 3.2). The fault can be seen to continue through the notches in the ridge in the background. Vertical displacement on the scarp is 4.5 m. The angle of the scarp suggests a minimum age of about 350 years based on Wallace's (1977) correlation curve (Figure 4.4). The method of obtaining fault scarp ages from scarp profiles is discussed in the following chapter. The scarp was formed in granitic detritus containing some metamorphic material. The detritus was derived principally from the Nelson Range. Desert varnish

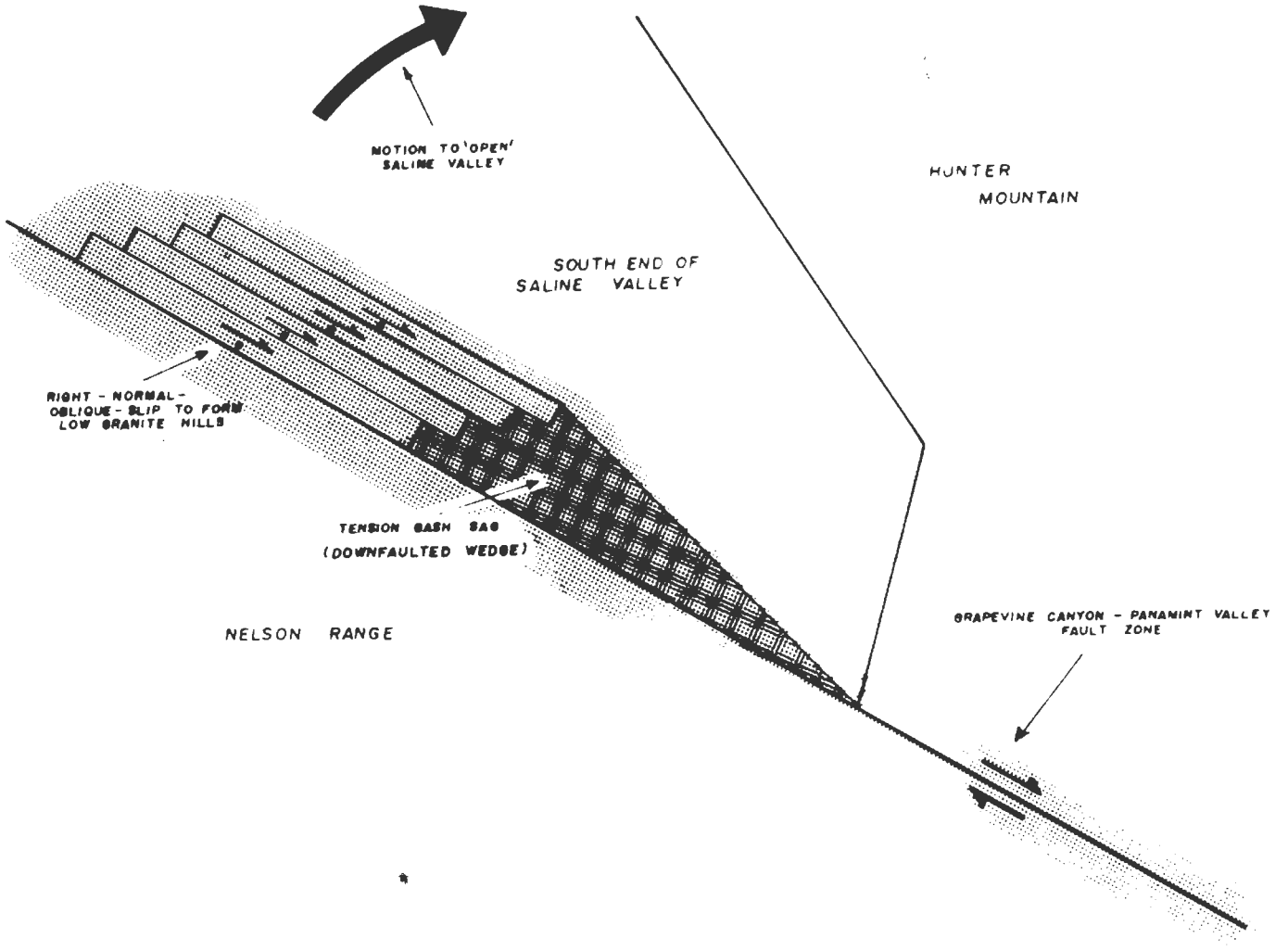

FIGURE 3.4. Inferred origin of structural features at south end of Saline Valley.

PHOTO 3.9. Caliche-filled fault in wall of stream channel. Note surface offset and change of dip of sediments. Younger sediments cover lower portion of fault. Hammer is on left edge of fault plane.

is moderately well developed at the top and base of the scarp, but not on the scarp face. Creosote bushes that are common on the undisturbed alluvial fan surface have not re-established themselves on the scarp face.

Scarp profile P22 (Figure 3.1, Plate 2.2) was measured approximately 0.5 km northwest of P21. This scarp has a vertical displacement of 16 m that occurred during four to six events. The minimum age of the most recent event is about 280 years, based on Wallace's correlation curve (Figure 4.4). The scarp was formed in the same material as profile P21.

PHOTO 3.10. Fault scarp measured for profile P21. View to south along Grapevine Canyon fault zone. Fault continues through notches in skyline.

Profile P20 (Figure B.1, Plates 3.2 and 3.3) was measured about 5 km northwest of P22. The total vertical displacement of 30 m occurred during at least four events. A nearby stream channel indicates that the scarp was formed in thin alluvium and colluvium overlying a shallow bedrock fault in crushed granitic rock. The minimum age determined from the scarp angle may be misleading because the scarp angle may represent crushed granitic rock rather than more easily eroded alluvium and colluvium.

Photos 3.11, 3.12, and 3.13 were taken 1.5 km northwest of San Lucas Canyon (Plate 3.3). These photos and aerial Photo 3.14 show faulted lacustrine silt, sand and gravel at an elevation of 610 m exposed along a shallow range front graben. The unconsolidated, greenish-gray beds are at least 8 m thick. The gravel ranges from sub-rounded to well-rounded. Average diameter of the gravels is about 2.5 cm. The beds strike N20°E and dip 24°W.

PHOTO 3.11. Right-lateral offsets in unconsolidated shoreline deposits along trace of Grapevine Canyon fault zone. View to east.

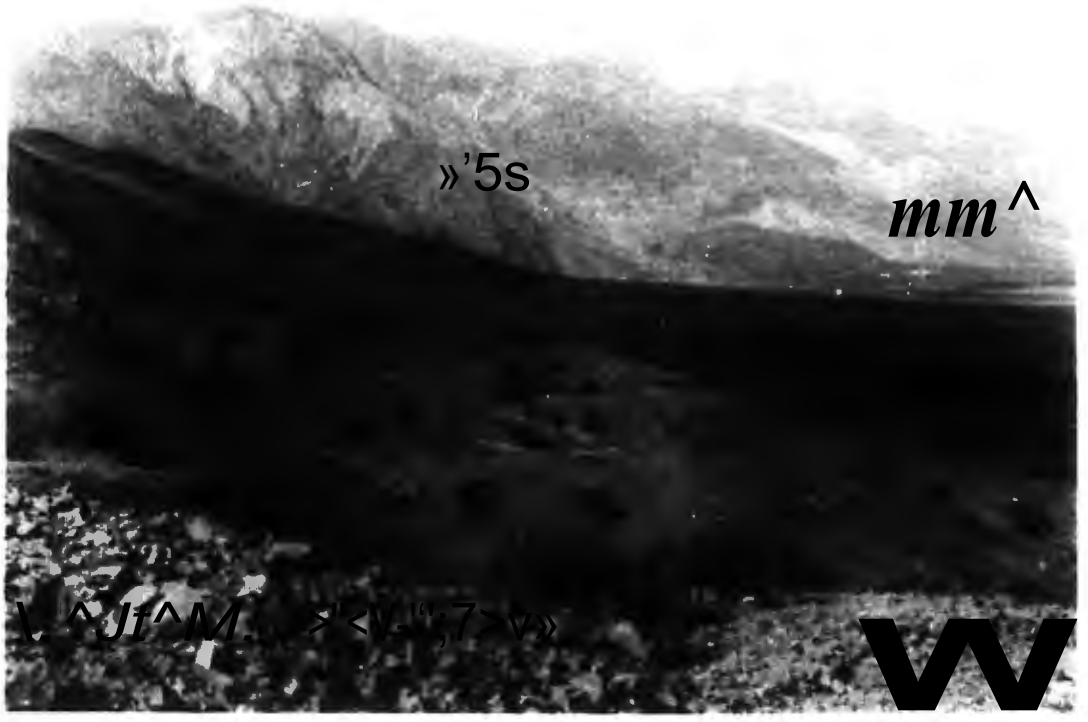

PHOTO 3.12. Down-strike, north-looking view of faulted deposits shown in Photo 3.11.

Some of the beds are highly tuffaceous. The well rounded tuffaceous material was probably derived from the tuff beds at Grapevine Pass. Calcareous material coats and locally cements the lacustrine deposits and also rock fragments derived from the adjacent range front scarp. The scarp and portions of the lacustrine sediments contain calcareous deposits resembling lacustrine tufa. However, since the scarp is in calcareous rock it is not clear if the calcareous material was deposited in a lacustrine environment or was simply leached from the bedrock and redeposited in the sediments.

PHOTO 3.13. Close-up view of unconsolidated sediments in fault zone.

Photo 3.11 is an east, downslope view of the faulted sediments. Right-lateral, strike-slip offsets are clearly visible in the stream alignments. Reconstruction of the stream offsets indicates displacements of 2, 7, 10, 21, 14, 20 and 22 m. The total cumulative displacement is assumed to be 22 m with the smaller displacements representing intermediate offsets. Individual offsets appear to range from 2 to perhaps 7 m.

Photos 3.12 and 3.14 show that the lacustrine deposits are cut by a small range front graben that forms a segment of the Grapevine Canyon fault zone. In addition to the displaced lacustrine deposits, there are numerous vertical and lateral offsets along the fault.

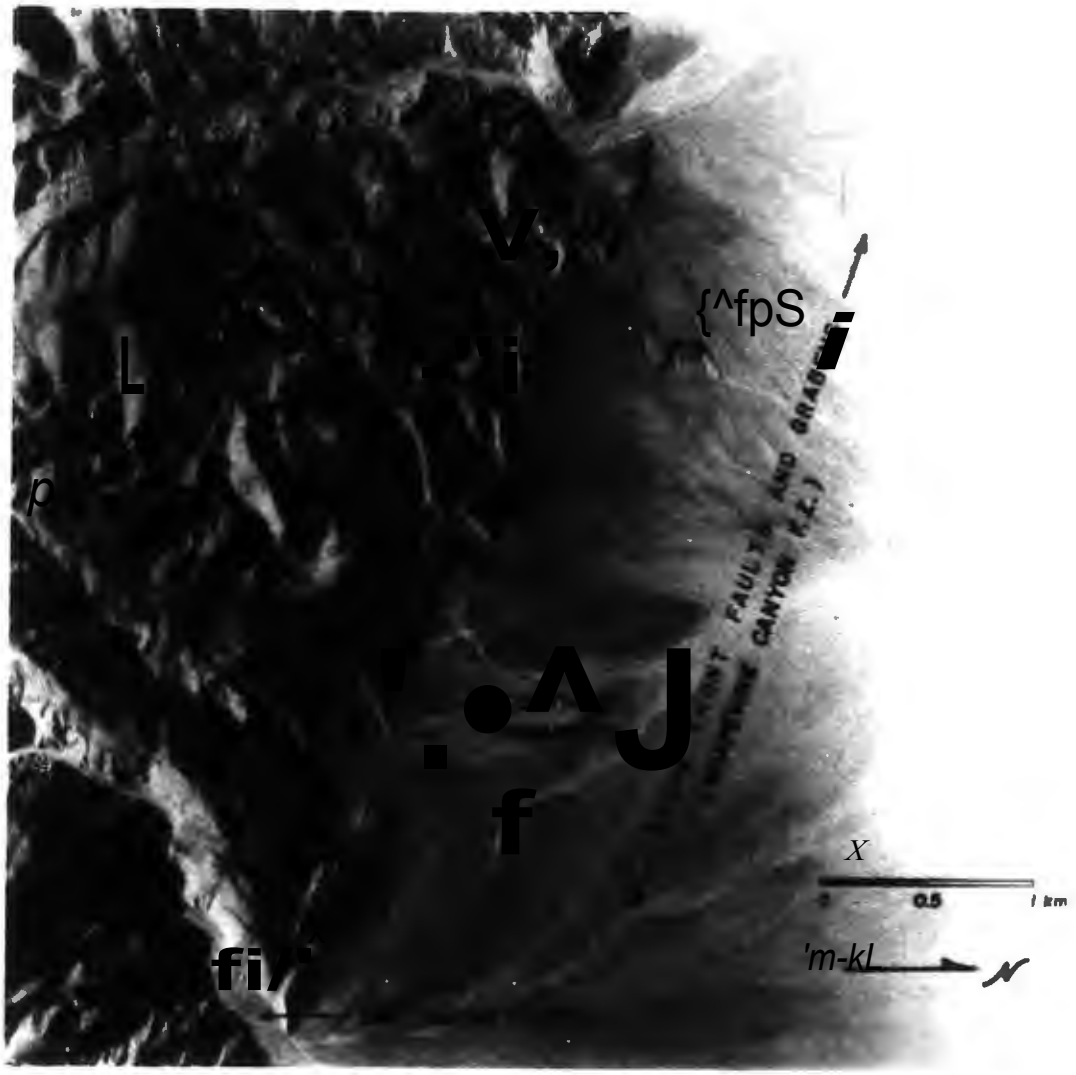

PHOTO 3.14. Vertical aerial photo of the northern segment of the Grapevine Canyon fault zone. Note rangefront graben associated with lacustrine deposits.

These offsets include such features as truncated spurs, faulted alluvial deposits and offset stream channels. The mouth of San Lucas Canyon may be offset nearly 1 km in a right-lateral sense along several parallel faults (Photo 3.14). Similar offsets can be seen in other stream channel alignments along this zone. In general, the

pattern of faulting is similar to that described in the Low Granite Hills region, except that major extensional features are not present. Also, the fault zone is much narrower than in the Low Granite Hills segment and the vertical displacement due to the hinge faulting is much greater.

Photo 3.15 was taken near the location of scarp profile P18 (Figure B.1, Plate 3.3). The photo shows anomalously steep dipping fanglomerates in contact with much shallower dipping modern channel deposits. The modern channel deposits dip slightly steeper than the 4° to 6° generally found on major alluvial fans in Saline Valley (Figure B.4a, B.4b). The dip of the fanglomerates and stream channel deposits shown in Photo 3.15 indicates that they are being tilted to the northeast. Such tilting could be caused by coupling between the uplifting Inyo Mountain block and downdropping Saline Valley block. However, Bachman (1974) reported that tilting of the Waucobi Lake beds and other evidence in Owens Valley indicates westward tilting of the Inyo Mountain block.

This apparent discrepancy can be resolved if step faults are present along the east flank (Saline Valley side) of the Inyo Mountains. Uplift of the moutain "core" would cause drag along the step faults and steepening of the original fanglomerate dips (Figure 3.5). Bachman (1974) reported an uplift rate of 0.5 m per 1000 yr for the White-Inyo Mountains for a total of approximately 1250 m during the last 2-3 m.y. Such uplift can account for the increased fanglomerate and stream channel dips along the west side of Saline Valley.

PHOTO 3.15. Old steep-dipping fanglomerates in contact with shallow-dipping younger channel deposits. View to north.

Profile P19 (Figure B.1, Plates 3.3 and 3.4) was measured approximately 1.5 km northwest of P18 on a 2 km long fault scarp striking nearly perpendicular to the range front. The scarp is about 7.5 m high and was formed by at least three events. The orientation of the scarp relative to the remainder of the Grapevine Canyon fault zone suggests that the scarp is due to tensional failure within the right-lateral Riedel shear system of the Grapevine Canyon fault zone. However, the scarp may also be related to the major tension gash graben extending into Saline Valley from Lee Flat (Photo 3.17) that is discussed in later sections.

Photo 3.16 shows reddish-stained fanglomerate in fault contact with sheared and crushed granitic rock. The view is to the southeast across the mouth of Daisy Canyon near the abandoned tramway. The fanglomerate is a small horst between downfaulted Saline Valley and a graben along the Inyo Mountains rangefront. The small range front graben is located near the intersection of Saline Valley and a major northwest-southeast trending graben. The major graben is shown in Photo 3.17 and 3.18. The graben extends into Saline Valley from Lee Flat and forms the western border of the valley. This results in dramatic changes in the shape of Saline Valley and the orientation of

PHOTO 3.16. View across mouth of Daisy Canyon showing fanglomerates in fault contact with crushed granitic rock. View to southeast.

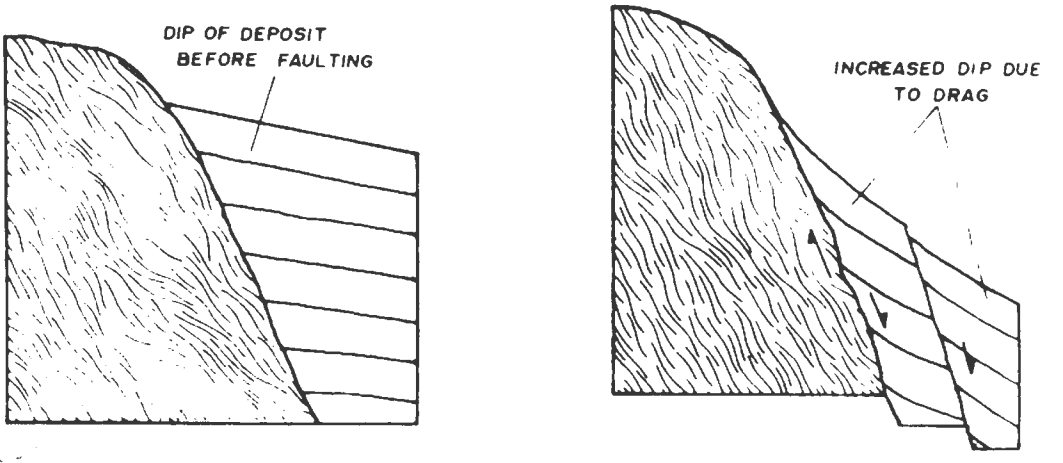

FIGURE 3.5. Steepening of original conglomerate dips by fault drag.

the Grapevine Canyon fault zone. South of the graben the fault zone strikes northwest-southeast, but north of the graben the zone strikes north-northwest--south-southeast; a change of approximately 40°. The graben appears to represent a major tension gash associated with the formation of Saline Valley and the major right-lateral, strike-slip fault zones of the region. This will be explored further in the Regional Tectonic Model section.

Profile P12 (Figure B.1, Plates 3.3 and 3.4, Photo 3.17) was measured adjacent to Daisy Canyon. Total vertical offset is about 30 m. The profile suggests that the alluvium may be underlain by a small bedrock block that is being rotated and detached from the mountain front. The maximum steepness of the scarp indicates a minimum age of about 30 yr. However, there have been no reports of large earthquakes in Saline Valley for at least the last 120 yr. This suggests that there is only a thin veneer of alluvium masking a steep bedrock fault, that the scarp has been artificially steepened by

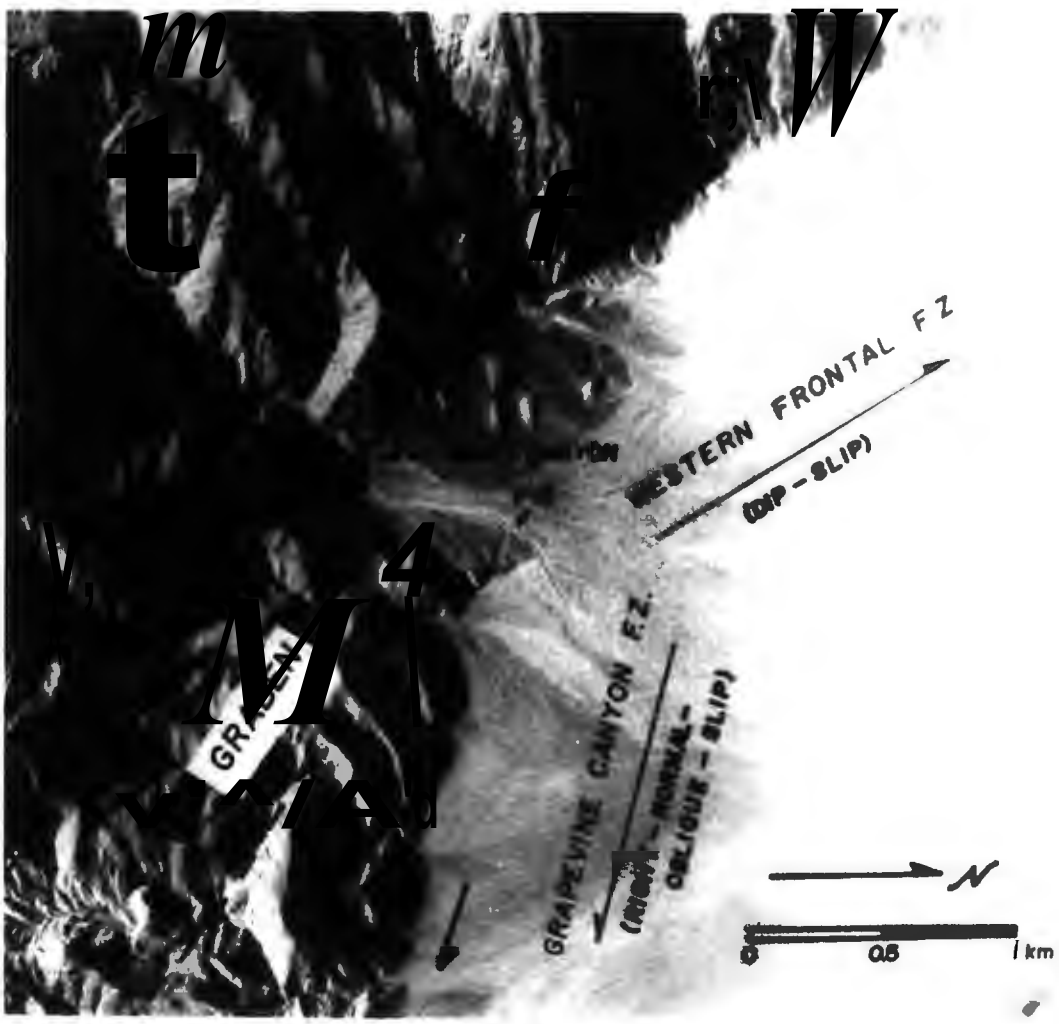

PHOTO 3.17. Vertical aerial photo of Daisy Canyon area showing intersection of Grapevine Canyon and Western Frontal fault zones. Note graben entering Saline Valley from Lee Flat.

erosion, or that Wallace's (1977) age estimation method is inaccurate in this region. The age discrepency is probably a combination of all of these.

PHOTO 3.18. Aerial view of graben extending from Lee Flat into Saline Valley. View to south.

SUMMARY - GRAPEVINE CANYON FAULT ZONE

1) This segment of the Panamint Valley-Grapevine Canyon fault zone is exposed for about 35 km in the study area.

2) At the southern end of the zone displacement is predominantly right-lateral, strike-slip with comparatively minor dip-slip motion. At the northern end of the zone displacement is principally dip-slip. This relationship suggests that the zone is a combination of strike-slip faulting and hinge faulting with a pivot point at Hunter Mountain.

3) The pattern of fault ruptures in the region between the mouth of Grapevine Canyon and the Low Granite Hills results from a combination of right-lateral, strike-slip faulting and

northeast-southwest extension. Strike-slip displacement is estimated at between 700 and 2000 m. The extension may total 2500 m.

4) Unconsolidated lacustrine sediments near San Lucas Canyon may indicate up to 22 m of recent right-lateral, strike-slip offset. The mouth of San Lucas Canyon may be offset by as much as 1 km. This segment of the Grapevine Canyon fault zone is characterized by right-lateral, strike-slip faulting with possible minor extension.

5) For convenience in description, and because strike-slip faulting appears to terminate at this point, the Grapevine Canyon fault zone is considered to terminate at Daisy Canyon. At this location there is dramatic change in the shape of Saline Valley and the style of faulting. The segment of the western border fault of Saline Valley to the north of Daisy Canyon is the Western Frontal fault zone.

3.4 WESTERN FRONTAL FAULT ZONE

The Western Frontal fault zone extends from Daisy Canyon to the northern boundary of the study area, a distance of 13.5 km (Plates 3.1, 3.1a and 3.4). This zone is characterized by dip-slip, range front faulting. No evidence of strike-slip faulting was observed. Total vertical offset is estimated at at least 6000 m. This is based on the height of the Inyo Mountains above the valley floor and the depth of valley fill based on gravity data. No allowance was made for erosion at the crest of Inyo Mountains.

Photo 3.19 shows faulted stream channel deposits and fanglomerates on the north side of Daisy Canyon. The original fan surface has been offset at least 35 m and is about 60 m above the present channel at its highest point. This suggests that the present channel is entrenched approximately 25 m into the downfaulted portion of the original fan. The upfaulted fanglomerate and the present channel dip about 5° while the downfaulted fanglomerate dips about 10°. This relationship suggests steepening of original dips by rotation or drag along fault plane (Figure 3.5).

PHOTO 3.19. Faulted channel deposits in Daisy Canyon. View to north.

Photo 3.20 shows a large landslide located 5 km north of Daisy Canyon, adjacent to the salt lake. The main mass of the slide is 2 km long, 1.5 km wide and 315 m high with a volume of approximately 1.8 x 10^8 m^3. Morphologically the slide appears to be rather young and because it does not display wave cut features, it is probably Holocene in age. A smaller, more recent slide can be seen on the northeast flank of the main slide. It is possible that the main slide occurred in response to seismic activity or to oversteepening of the slope by faulting. Burchfiel (1966) reported a 1.8 x 10^9 m^3 landslide at Tin Mountain, about 60 km northeast of Saline Valley. The Tin Mountain slide occurred on a slope oversteepened by faulting.

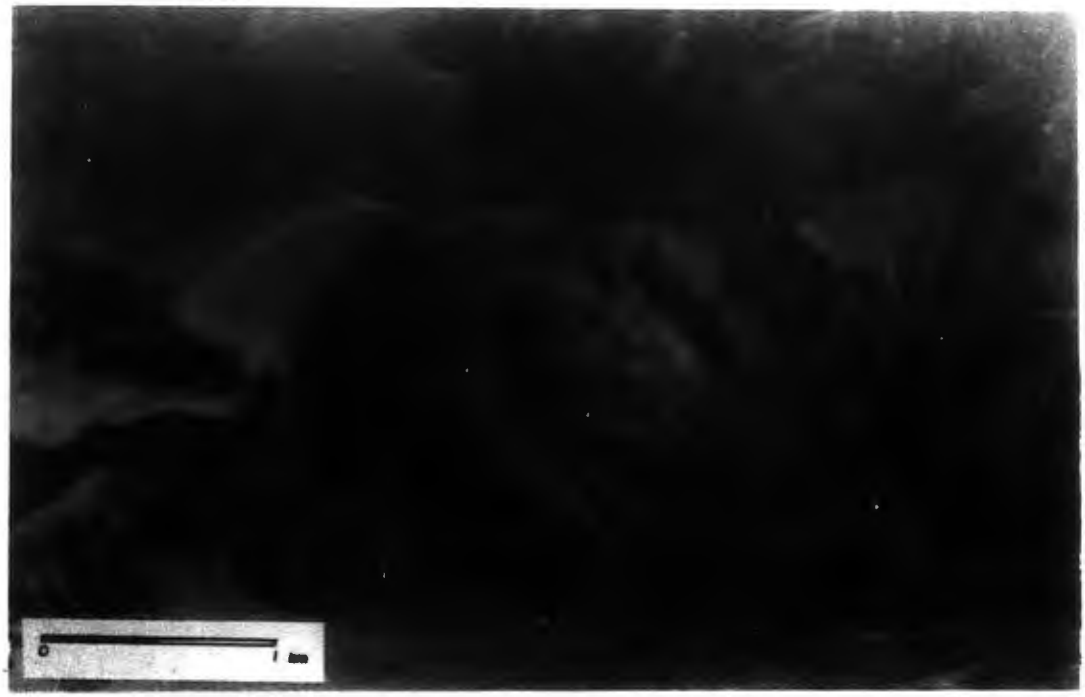

PHOTO 3.20. Aerial view of landslide along west side of Saline Valley. A portion of the salt lake can be seen on the left. View to south.

The Saline Valley landslide has been either rejuvenated or offset by postslide faulting. The complex nature of the fracturing near the surface projection of the range front fault makes an analysis of the relationship between sliding and faulting difficult. It is probable, however, that both faulting and landslide rejuvenation have occurred, perhaps simultaneously.

In general, the rock in and adjacent to the Western Frontal fault zone is highly sheared and crushed. Photo 3.21 shows the fault cutting through granitic rock near Beveridge Canyon. The main trace of the fault is nearly vertical and passes through the low notch on the east (right) side of the photo. A rock hammer is shown in the lower, central portion of the photo for scale.

PHOTO 3.21. Crushed granitic rock along Western Frontal fault zone near Beveridge Canyon. View to north.

Three fault scarp profiles were measured near Beveridge Canyon, P13, P14 and P15 (Figure B1, Plate 3.4). The scarp for profile P14 is shown in Photo 3.22. Profile P15 shows the greatest amount of total displacement, about 15 m. Multiple offsets are indicated on each of the profiles. The minimum age (20 yrs) of the offsets suggested by the scarp angle is probably low by at least an order of magnitude. The reasons for this have been discussed earlier and in other sections.

PHOTO 3.22. Fault scarp measured for profile P14. Near Keynot Canyon.

The original alluvial fan surfaces along the Western Frontal fault zone tend to be steeper than those along the Grapevine Canyon fault zone. This increased steepness may be due to a more rapid

uplift rate and steeper topography north of Daisy Canyon. These two factors would combine to promote more rapid and steeper accumulations of alluvium and colluvium at the base of the scarp. Additional steepening could result from drag along the fault zone (Figure 3.5).

All but the youngest alluvial fans along this zone are faulted. The fans commonly display both simple fault scarps and grabens. The grabens may be due to either step faulting along the range front or simple, tensional failures in the alluvium and colluvium.

Profiles P16 and P18 (Figure B1, Plate 3.4) were measured near Keynot Canyon, approximately at the northern border of the study area. These profiles show maximum vertical offsets of about 8 m and suggest incipient graben development or tensional failure of the fanglomerate. The most recent displacement on profile P16 may be due to landsliding rather than faulting since the profile is similar to that of a small rotational landslide. A portion of the scarp for profile P16 is shown in Photo 3.23. The scarp extends along the slope and on the skyline.

Photo 3.24 shows a section of uplifted fanglomerate in Keynot Canyon. The beds dip about 10° toward Saline Valley and therefore are at or near their original depositional attitude. The surface of the fanglomerate is approximately 120 m above the stream channel at the mouth of Keynot Canyon which is about 500 m to the east. If one assumes that the original depositional attitude of the fanglomerates was 10°, then a simple calculation shows that beds have been uplifted approximately 32 m since their deposition.

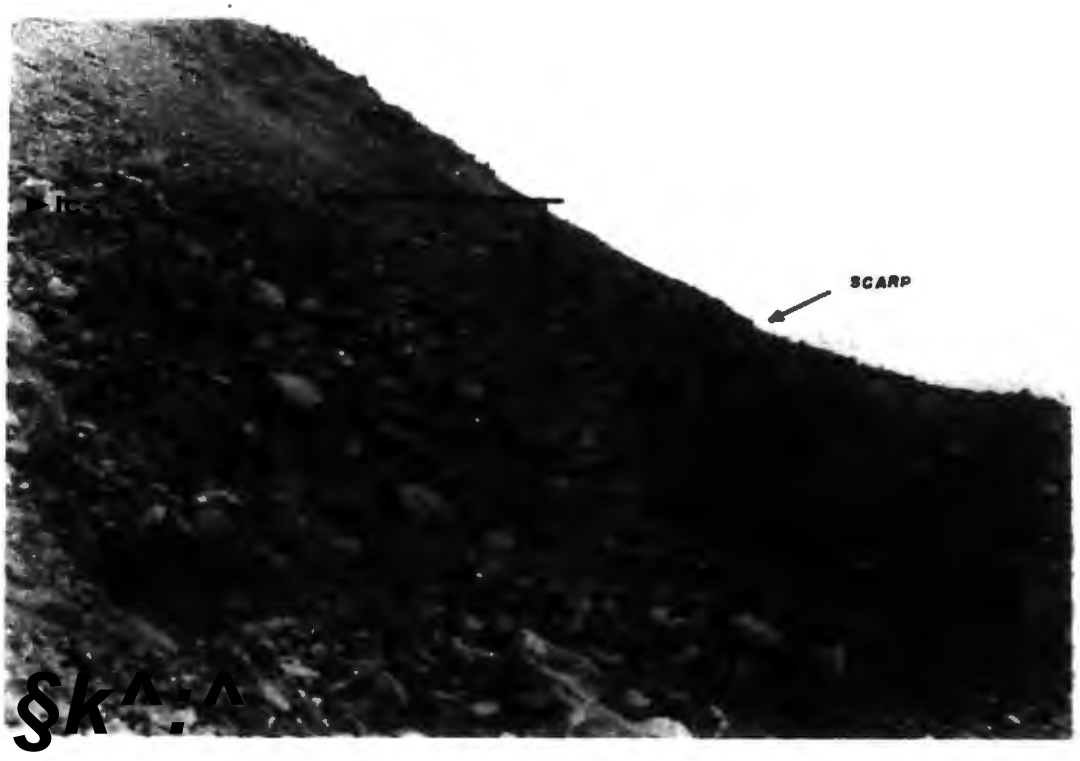

PHOTO 3.23. Fault scarp measured for profile P16. Near Keynot Canyon. Note scarp on skyline.

Photo 3.25 shows offset fanglomerates and colluvium near the mouth of Keynot Canyon. The road is located on a fault plane. The alluvium on the west (right) side of the road has been uplifted approximately 5 m. No profile was measured because of the road construction and related mining activities. The dip of the modern stream channel in the foreground is the same as that of the faulted deposits, suggesting that the faulting did not cause rotation or drag of the deposits. The graben-like features in the background appear to be both fault and landslide induced.

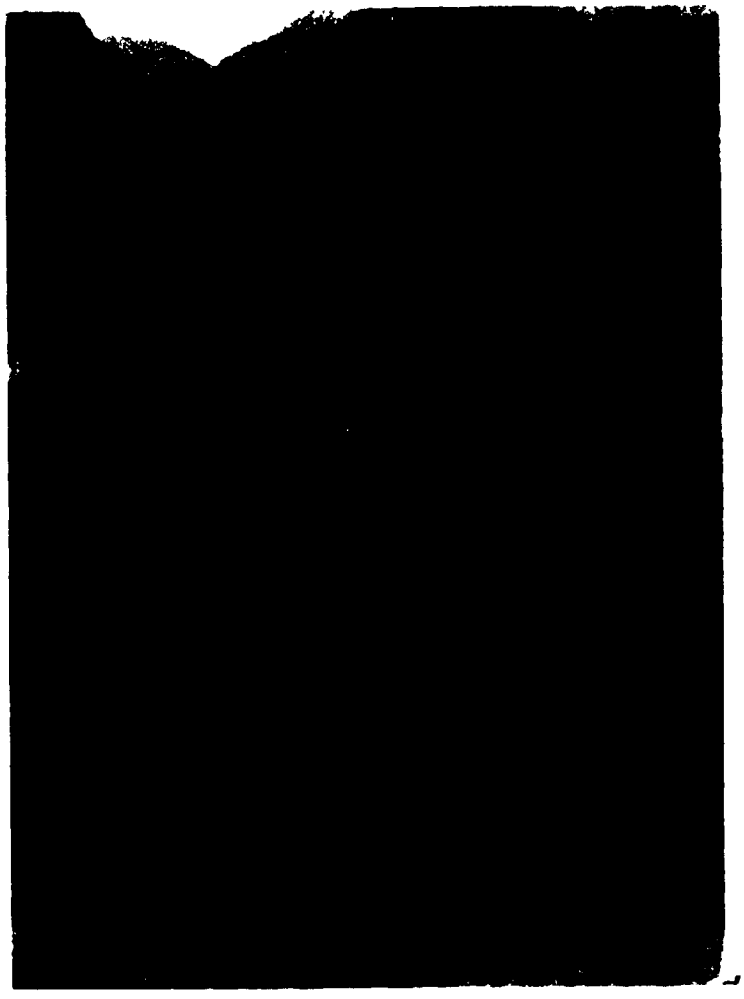

PHOTO 3.24. Uplifted fanglomerate in Keynot Canyon. View to west.

Photo 3.26 shows a fault scarp near Keynot Canyon that displaces a natural levee. Subsequent erosion has removed much of the fault scarp in the channel floor. The levee was offset approximately 1.5 m.

PHOTO 3.25. Faulted alluvial and colluvial deposits near Keynot Canyon. View to south.

Photo 3.27 is a view to the south along the fault zone. The 100 m wide section of lighter colored material in the center of the photo is highly crushed and sheared granitic rock. In the upper right corner of the photo is a 5 m wide vertical zone of fault gouge. Crushing and weathering in the fault zone has converted the rock to a weak, grussy mass. Locally, the features such as quartz veins remain intact.

Photos 3.28 and 3.29 were taken in a small canyon near the northern boundary of the study area. The photos show nickpoints in the stream channel that indicate at least three episodes of faulting in the carbonate rock. The most recent nickpoint forms a dry waterfall

PHOTO 3.26. Offset natural levee along Western Frontal fault zone. Near Keynot Canyon.

10 m high and is located on the fault plane. The height of the waterfall suggests that more than one event was responsible but no evidence for multiple events was observed. However, because of the scarp height and steepness, multiple events over a short period of time probably occurred. The two older nick points are shown more clearly in Photo 3.28. The slopes of the older stream channels are 12°, 20° and 28°. The upper, 12°, channel continues up the canyon with no significant interruptions for perhaps 100 m.

PHOTO 3.27. Crushed granitic rock along trace of Western Frontal fault zone. View to south.

SUMMARY - WESTERN FRONTAL FAULT ZONE

1) The Western Frontal fault zone extends in the study area from Daisy Canyon to the northern border of the study area, a distance of 13.5 km.

2) The zone is characterized by dip-slip faults. No significant, young, strike-slip faults were observed.

3) Offsets in alluvial fan deposits indicate at least 32 m of displacement since their deposition.

PHOTO 3.28. Nickpoints in stream channel showing dry waterfall on fault plane.

4) Locally, there is evidence for at least three episodes of faulting.

5) Faults in the zone range form relatively discrete planes to wide crushed and sheared zones.

PHOTO 3.29. Nickpoints in stream channel.

3.5 EAST SIDE FAULT ZONE

The East Side fault zone (Plate 3.1, 3.1a, 3.4) is located along the northcentral border of the study area. The zone is characterized by a system of grabens trending north-south, primarily through alluvial fan deposits derived from the west flank of the northern Panamint Range. Many of the faults in this zone are shown in Photo 3.30. In the southeast (upper right) corner of the photo Paleozoic sedimentary rocks and Quaternary-Tertiary basalts are truncated by faults along the Panamint Range front. This range front faulting is probably related to faulting in the East Side fault zone.

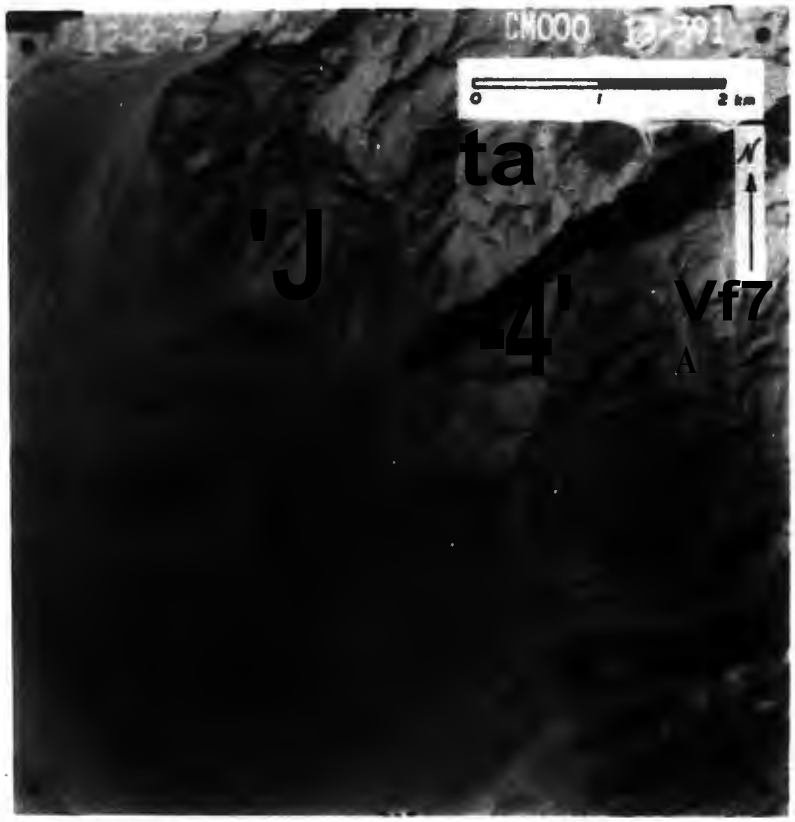

PHOTO 3.30. Vertical aerial photo of the East Side fault zone showing the Panamint Range Front to the east.

Seven fault scarp profiles, P5, P6, P7, P8, P9, P10 and P11, (Figure B1, Plate 3.4, Photo 3.31) were measured in the East Side fault zone. Of these, P6, P7 and P9 suggest at least one episode of faulting, P8 and P11 suggest two episodes of faulting, and P5 and P10 suggest three episodes of faulting. Based on the steepness of the scarps the minimum age of the faulting ranges from 22 to 27,000 yr. The anomolously low ages (22 and 47 yr) can be discounted using the arguments presented in earlier sections. The remaining minimum ages

PHOTO 3.31. Vertical aerial photo of the East Side fault zone showing fault scarp profile locations.

are in the range of 170 to 27,000 yr. These seem reasonable based on geomorphological evidence and the recentness of faulting in adjacent Owens Valley.

The materials in which the scarps are formed range from unconsolidated lacustrine or eolian silt and sand to poorly cemented fanglomerates. Scarp heights range from approximately 2 to 12 m. The

scarps profiled for P6, P7 and P11 are shown in Photos 3.32, 3.33 and 3.34, respectively. In addition to the steepness of the scarps, the recentness of the faulting is also suggested by other factors. In nearly all cases the faulting ruptured a surface with moderately well to well developed desert pavement or desert varnish. Neither pavement nor varnish have formed to an appreciable degree on any of the scarp faces. Also, the creosote bushes are generally smaller and fewer in number than their counterparts in undisturbed areas.

Faults in the East Side fault zone offset all but the most recent deposits and stream channels. Locally the offsets were sufficiently large to cause ponding of flood waters in the grabens. The effect of the ponding is shown in Photo 3.31 where water may have ponded to a depth of about 6 m. The water eventually breached the west wall of the 600 m wide graben and drained toward the playa. The breaching and subsequent erosion of the graben wall may have occurred during a single event but probably occurred in several stages as the graben developed. As can be seen in the photo, some of the water flowed to the north (left) around the uplift block. Also, erosion by the flood waters may have artificially steepened the scarps shown in profiles P7, P8 and P9.

The topographically high area on the north (left) side of the breach channel has been uplifted relative to the original alluvial fan surface. The uplifted surface is approximately 3 m lower than the undisturbed fan surface immediately across the graben, a distance of 380 m. Because the original fan surface dips 5°, the two surfaces should be vertically separated by 33 m. The actual separation

PHOTO 3.32. Fault scarp measured for profile P6.

PHOTO 3.33. Fault scarp measured for profile P7.

PHOTO 3.34. Fault scarp measured for profile P11.

suggests a 30 m uplift along the west side of the graben. Uplift of the block is also suggested by other evidence. Texturally, the uplifted surface is different from the surrounding area in that the surface appears much smoother. This difference is caused by the silt and sand sized material that covers the surface and forms part of the scarp face. Similar material is found only to the west in playa and eolian deposits. This suggests that the block may contain upfaulted playa or eolian sediments. Also the west edge of the block has been dissected.

SUMMARY - EAST SIDE FAULT ZONE

1) The East Side fault zone is largely contained within an area of approximately 13 km^3 in the north central portion of the study area.
2) Faulting in this zone is characterized by normal faults and grabens trending in a north-south direction.
3) The faults are all quite young and generally display multiple offsets.
4) The faults are related to step faulting in the mountains to the east which reflect continuing east-west extension and opening of the Saline Valley.

3.6 THE CENTRAL VALLEY FAULT ZONE

The Central Valley fault zone (Plate 3.1, 3.1a, 3.4) is confined to the playa region of Saline Valley. The zone is characterized principally as a system of northwest-southeast normal faults with small displacements. Locally there is inconclusive evidence for strike-slip faulting. The zone also includes the northeast-southwest and east-west trending faults near the southern edge of the playa. A large portion of the zone is shown in Photo 3.35. The photo is oriented with south to the right to facilitate comparison with Photo 3.36. The East Side fault zone is located immediately to the east of the area shown in Photo 3.35. Lack of access to the area due to the muddy playa surface prevented direct study of the faults.

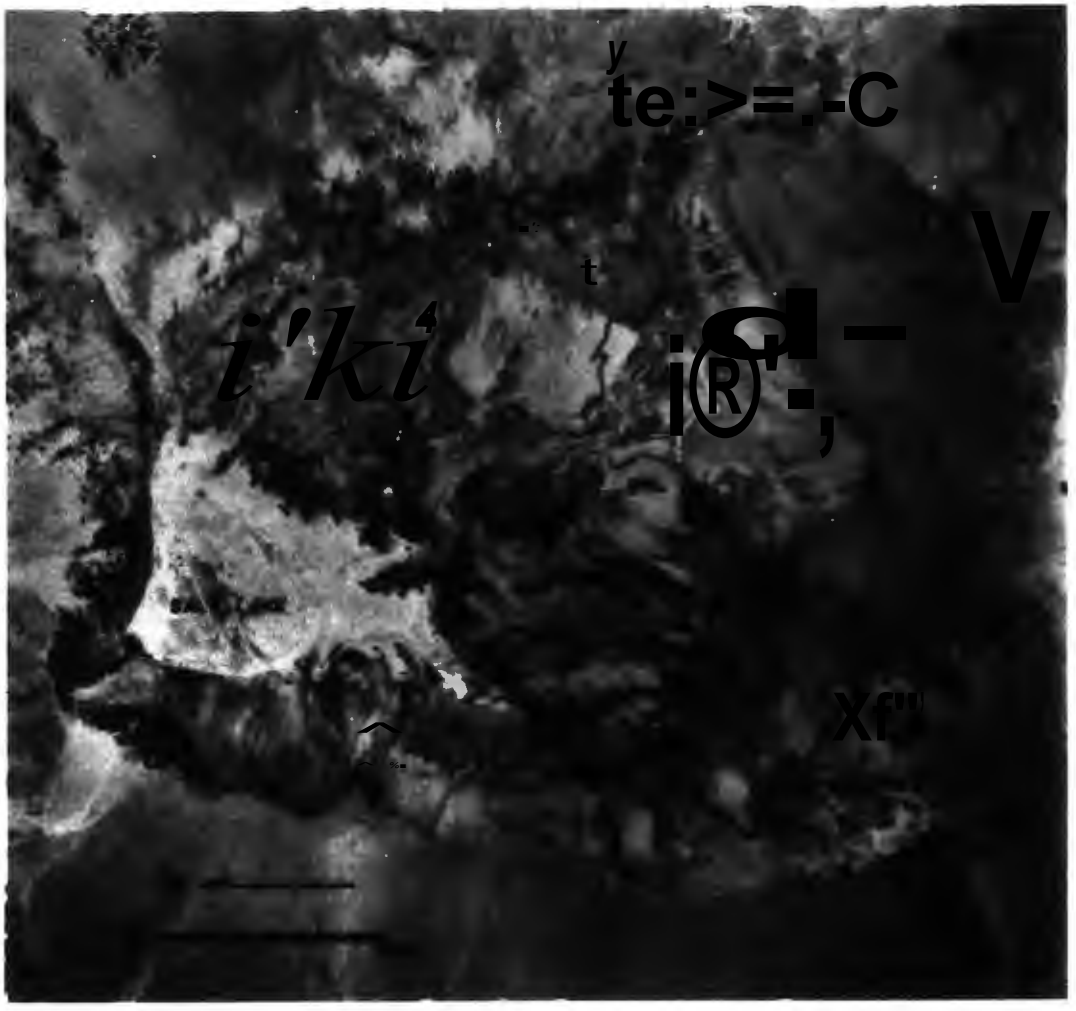

PHOTO 3.35. Vertical aerial photo of Saline Valley playa, showing several young fault traces and location of Photo 3.37. Compare outlined area with area outlined in Photos 3.36 and 3.37.

The playa sediments are composed of lacustrine and eolian sand, silt and clay. In the topographically lower portion of the playa, near the salt lake, the deposits are overlain by a crust of salt, principally NaCl. Exploration drilling by the U.S. Geological Survey (Personal Communication, C. Hedel, 1979) along the northern edge of the salt lake shows that the underlying material is composed

PHOTO 3.36. Oblique aerial view of young fault in playa sediments. Note outlined area and compare with outlined area in Photos 3.35 and 3.36. View to northeast.

principally of greenish-black (greenish gray when dry) mud alternating with layers of salt. The sequence continued to a depth of at least 100 m.

Based on the nature of the playa sediments and preservation of fault traces it is apparent that the faults are relatively recent. Several lines of evidence indicate that deformation of the sediments is still continuing. Lombardi (1963) reported that brine is at the surface at the southwestern end of the playa (the salt lake) but 1 to 1.5 m below the surface elsewhere. He also reported that the playa

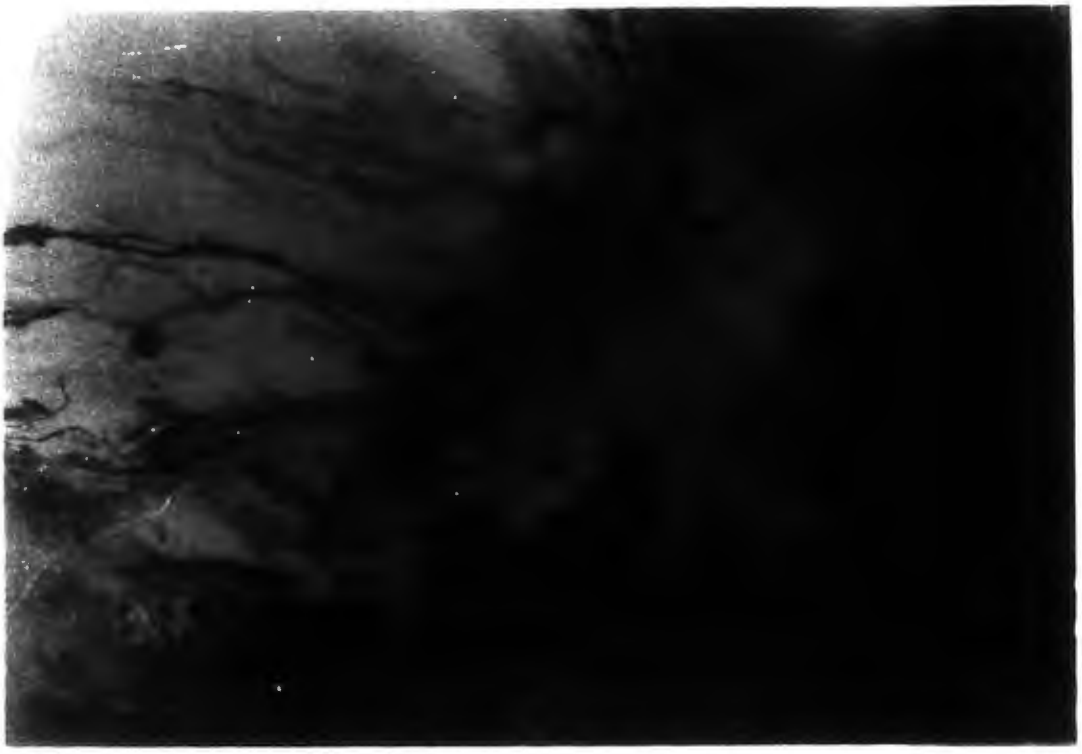

PHOTO 3.37. Vertical aerial photo of Saline Valley playa. Note outlined area and compare with areas outlined on Photos 3.35 and 3.36.

silt deposits are slightly uplifted and tilted to the west near the southern end of the playa. Lombardi's evidence and the general drainage pattern on the playa indicates that the playa is being tilted in a westerly direction along the Inyo Mountain front. This compares favorably with the earlier analyses of the Grapevine Canyon and Western Frontal fault zones.

Additional evidence of modern deformation may be indicated by comparing Photos 3.35, 3.36, and 3.37. In making any comparison the quality and format of the photography as well as the time of year must be taken into account. Photo 3.35 is from a standard 23 cm x 23 cm

black and white vertical aerial photograph taken for topographic mapping purposes at a scale of 1:37,400 in August 1947. Photo 3.36 is from a color slide taken with a handheld 35 mm camera from a private aircraft during March 1979. The original scale is about 1:117,000. Photo 3.37 is from a black and white 10 cm x 12.7 cm format photograph taken by a handheld camera during March 1979. Note the sharp boundary between the light and dark sediments indicated in Photos 3.36 and 3.37. This distinction is not obvious on Photo 3.35. It is possible that groundwater conditions are partly or wholly responsible for the definition of this feature in Photos 3.36 and 3.37 since groundwater elevations should be near their maximum in April and near their minimum in August. However, in view of the evidence for recent and continuing deformation of the playa sediments, it is possible that the feature is due to fault uplift that has increased in displacement during the 32 year period from 1947 to 1979.

Additional support for possible modern deformation is shown in Photo 3.38. This photo shows a low (5-10 cm high) pressure ridge developed in the salt crust near the salt lake. At least three similar ridges were observed. Each continued for several hundred meters approximately parallel to the strike of the Grapevine Canyon fault zone. The ridges appear to have a right-stepping en echelon type of pattern similar to that sometimes associated with strike-slip faults.

An attempt to dig a shallow trench across the pressure ridge was abandoned due to mud and water infilling. Because the pressure ridges are ephemeral features easily eradicated by minor flooding of the

PHOTO 3.38. Pressure ridge linement in playa salt crust. View to southeast. Ridges 5 to 10 cm high.

playa or intense rain, they must be very young. Consequently, the pressure ridges may provide strong evidence for modern deformation of the playa.

SUMMARY - CENTRAL VALLEY FAULT ZONE

1) The Central Valley fault zone is located in the playa region of the Saline Valley.
2) The zone is characterized by small displacement normal faults in lacustrine and eolian sediments.

3) Based on the type of material and its commonly wet condition, and the preservation of the fault traces, the faults must be relatively young.

4) There is strong evidence that the playa is being tilted to the west.

5) Surficial features suggest, but do not confirm faulting of playa sediments during the period 1947 to 1979.

3.7 LEE FLAT FAULT ZONE

The Lee Flat fault zone (Plates 3.1, 3.1a, 3.5) is located in Lee Flat, between the Nelson Range and the Inyo Mountains. The zone is characterized by northwest-southeast trending normal faults. The faults occur in both the alluvium and the Quaternary-Tertiary basalts. Photo 3.39 is a vertical aerial view of the Lee Flat fault zone.

Only one fault scarp profile was measured in Lee Flat. This was profile P23 shown in Figure B.1 and Plate 3.1a and 3.5. The scarp was formed in basalt cropping out along the west flank of the Nelson Range. Total displacement is 28 m. The fault displaces alluvial material both north and south of the profile location.

Photo 3.40 is an aerial view looking south from above Saline Valley into Lee Flat. The view is along the strike of the large graben described in the Grapevine Canyon fault zone section. The photo shows the graben trending into Lee Flat and appearing to widen to encompass the borders of Lee Flat. Consequently, the graben and Lee Flat may be a part of the same structure. The location and geometry of this structure suggest that it is a major tear or tension gash

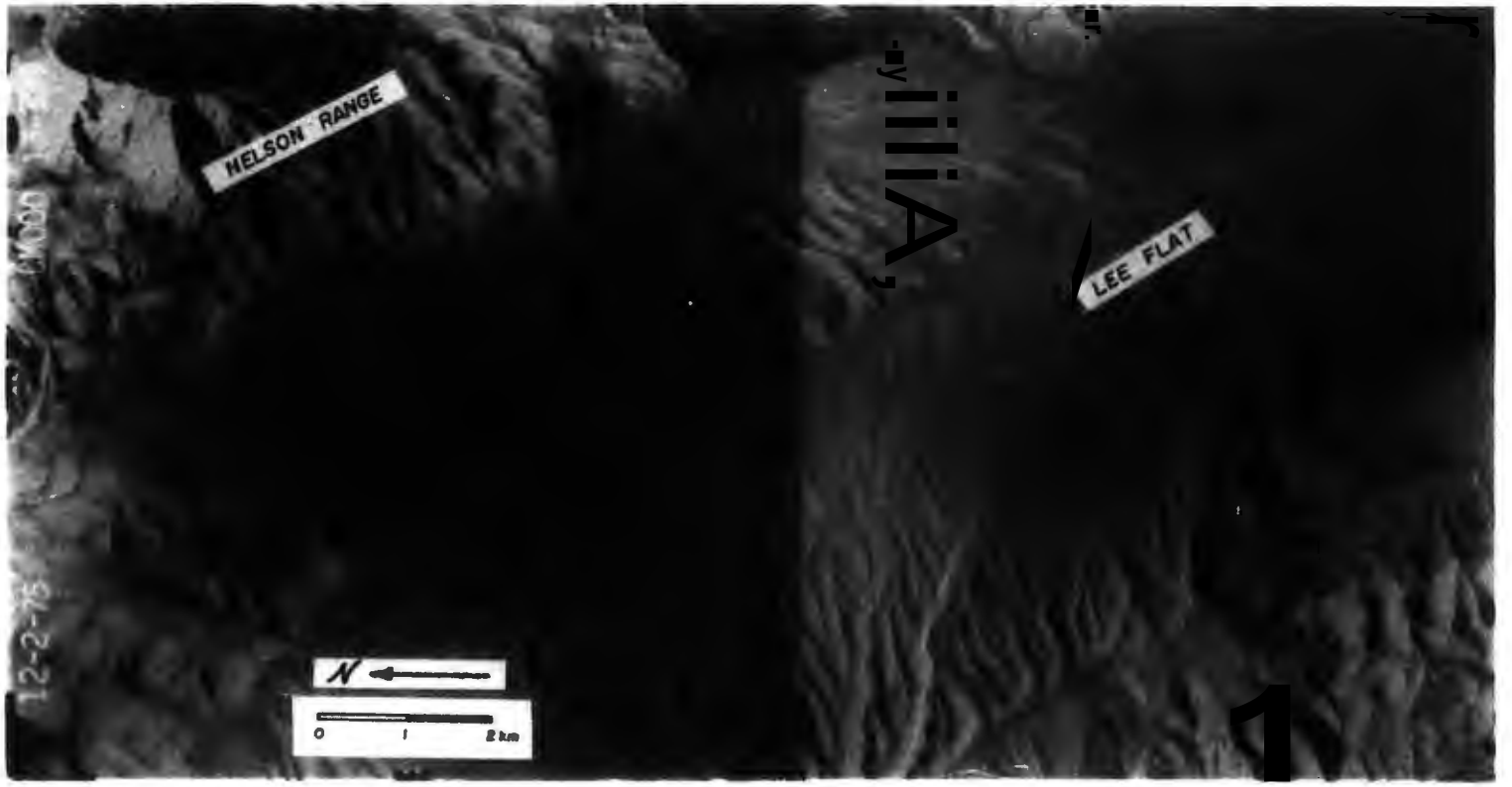

PHOTO 3.39. Vertical aerial photo of the Lee Flat fault zone. Note location of profile P23.

PHOTO 3.40. Aerial view of graben trending into Lee Flat. View to south from Saline Valley.

related to the formation of Saline Valley and the other valleys in the region. This subject will be pursued in more detail in the tectonic model section.

SUMMARY - LEE FLAT FAULT ZONE

1) Lee Flat is characterized by normal faults that trend northwest-southeast through unconsolidated alluvial sediments and basalt flows.
2) Lee Flat appears to represent a portion of a major tear or tension gash related to the formation of Saline Valley.

3) This structure extends from the north border of the study area where it forms the west side of Saline Valley. At Daisy Canyon it becomes a graben cutting across the Inyo Mountains and then widens to include Lee Flat. The structure appears to continue south into Centennial Flat and the Coso Range.

4.0 FAULT SCARP ANALYSIS AND AGE DATING

4.1 INTRODUCTION

No data was found concerning either the absolute age of the young fault scarps in Saline Valley or recurrence rates for fault offsets. To provide estimates of the ages and recurrence rates, the study outlined in this chapter was undertaken. This study of young fault scarps in the Saline Valley region attempts to apply, test, and further develop the method of fault scarp age determination proposed by Wallace (1977). Wallace's method consists of correlating the age of a fault scarp with the angle of the slope resulting from the original formation and gradual erosion of the scarp. A similar study was completed recently by Bucknam and Anderson (1979). The present study uses Wallace's method as a basis, but attempted to correlate such data as seismic velocity and particle size distribution with fault scarp age.

Wallace's (1977) method was developed for an area in northern Nevada, in the central portion of the Basin and Range province. This study applies Wallace's method to an area of extreme aridity in southeastern California, located in the transitional zone between the Basin and Range and Sierra Nevada provinces. The scarps examined in this study are located at elevations ranging from about 500 m to 1000 m and undergo few, if any, freeze-thaw cycles. The scarps studied by Wallace are generally at higher elevations (above 1200 m) and experience up to 160 freeze-thaw cycles per year. Consequently, the present study is concerned with the applicability of Wallace's correlation curve for an area different from that in which it was developed.

This study uses the following information: 1) topographic profiles across each scarp at right angles to the fault strike, 2) the particle size distribution of the alluvial material in which the scarp was formed, and 3) the in-situ seismic velocity of the scarp material. Field data were obtained over a one year period from June 1978 through May 1979.

A total of 22 scarps were profiled during the study. The profiles are shown on Figure B.1 of the Appendix. The locations where the scarps were profiled is shown on Plates 3.1a, 3.2, 3.3, 3.4 and 3.5. Particle size distributions of the alluvium were determined for 17 scarps, and seismic velocities were determined for 12 scarps.

4.2 FAULT SCARP TERMINOLOGY, MORPHOLOGY, AND DEGRADATION

The slope and fault scarp terminology used by Wallace (1977) to describe fault scarp characteristics and evolution is shown in Figure 4.1 and 4.2. This terminology is from Wood (1942), Young (1972), and Cooke and Warren (1973). The upper and lower original alluvial fan surfaces are the segments of the original surface that has been separated by faulting. The toe or base of the scarp and the crest of the scarp are, respectively, the lower and upper extremities of the fault scarp; the free face is the exposed surface resulting from faulting or gravity spalling; the debris slope is the talus slope accumulated below the free face; and the wash slope is any part of the scarp controlled by fluvial erosion or deposition. Wash-control, debris-control, and gravity-control are processes used in discussing slope modification and degradation.

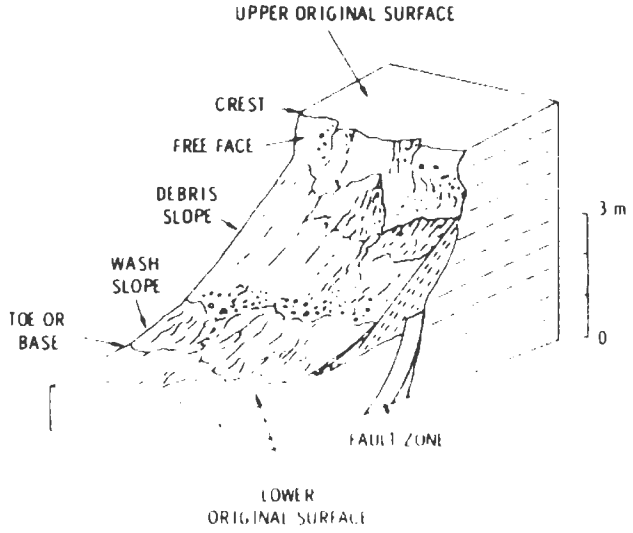

FIGURE 4.1. Fault scarp terminology (after Wallace, 1977).

Wallace (1977) describes the initial fault scarp as a free face in which the original rock, fanglomerate, or colluvium is exposed. The free face immediately begins to spall: pebbles, cobbles, boulders, and finer material break loose and fall from the face and form the debris slope. The crest or crestal break in slope is between the free face and the original upper surface. Initially the crest is a sharp break that persists as long as the free face exists. The crest gradually migrates away from the original scarp and becomes more and more rounded. The debris slope is directly below the free face and is composed of loose material that has fallen from the free face and crest. This material tends to be unstable and generally rests at angles of repose of 34° to 37°. Below the debris slope on young scarps, a wedge of alluvium commonly develops that overlaps the debris slope and the original fan slope. These wash slope deposits

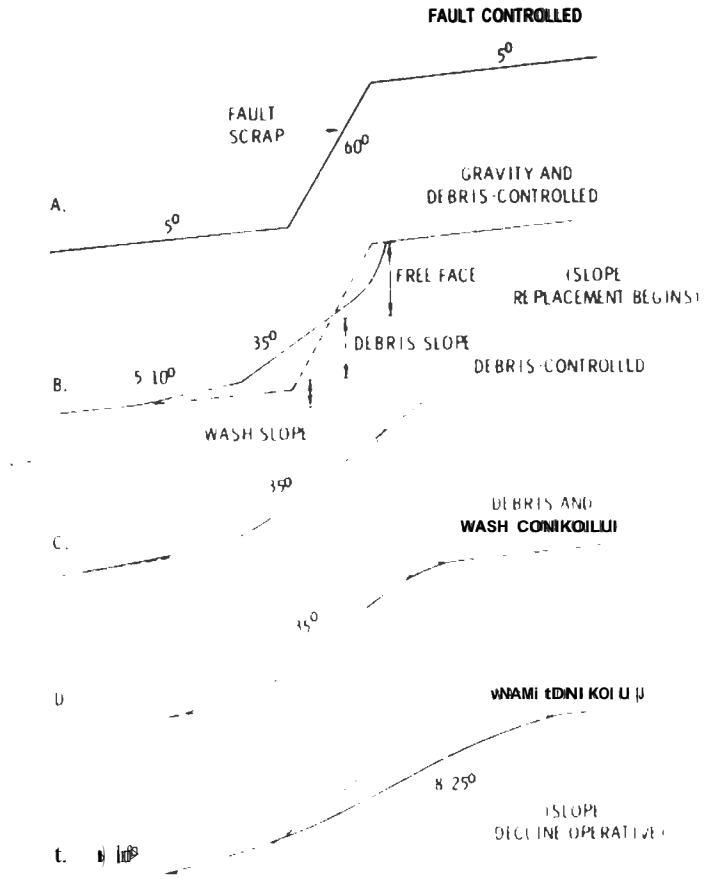

FIGURE 4.2. Slope terminology (after Wallace, 1977).

may be as steep as 10° to 15° while the slope of the original fan before faulting is commonly 3° to 7°.

Wallace (1977) discussed the importance that several factors may have in causing variations in the rate of slope degradation. The most important factors are probably the physical properties of the faulted material. Other variables include the original height of the scarp, the angle between the fault plane and the slope of the displaced surface, the width of the fault zone, the vegetation and the climate.

Wallace's (1977) methodology involves the measurement of fault scarp profiles and estimation of the age of the scarp from its slope angle. This method may also be used to estimate the age of each fault event when multiple bevels exist due to recurring offsets along the same fault (Figure 4.3). Basically the method involves the determination of the slope angle of the fault scarp or bevel (Figure 4.3). Wallace accomplished this by laying a stadia rod directly on the fault scarp and measuring the angle between the rod and the horizontal with an Abney level. The writer believes that this method of angle measurement may introduce operator error, especially if multiple bevels are present, because the operator must visually determine the break in slope between bevels. This task is difficult if the profile is long or if adjacent bevels vary by only a few degrees. The writer prefers to use the continuous profiling method described later in this chapter. In this way, breaks in slope can be determined and the angles measured when the field data is plotted at an exaggerated scale. Once the fault scarp profile is determined, the age of the scarp can be estimated from Wallace's (1977) correlation curve (Figure 4.4). This curve was developed using fault scarps of known age in north-central Nevada. The ages of the fault scarps determined by this method in Saline Valley are given in Table 4.1.

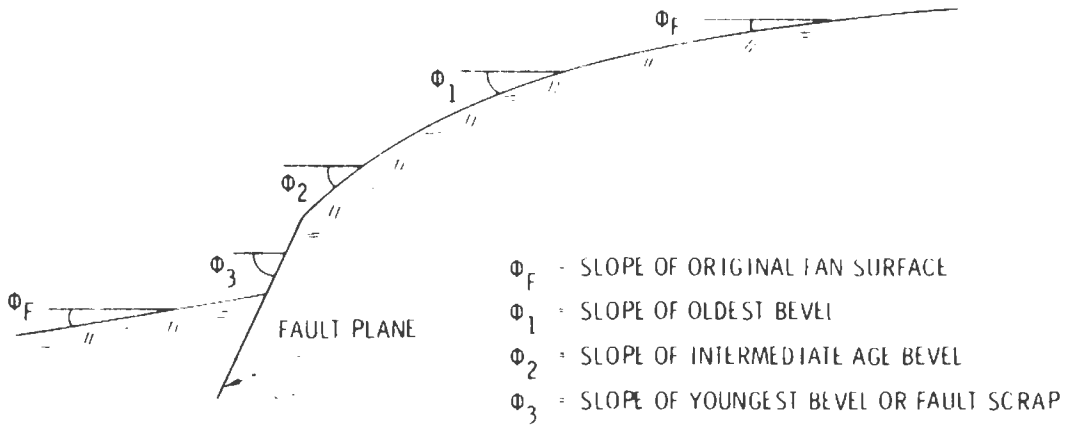

FIGURE 4.3. Fault scarp beveling due to erosion. This figure shows three periods of vertical movement along the fault plane with the most recent indicated by the steepest slope angle, Φ_3, and the oldest by the shallowest slope angle, Φ_1.

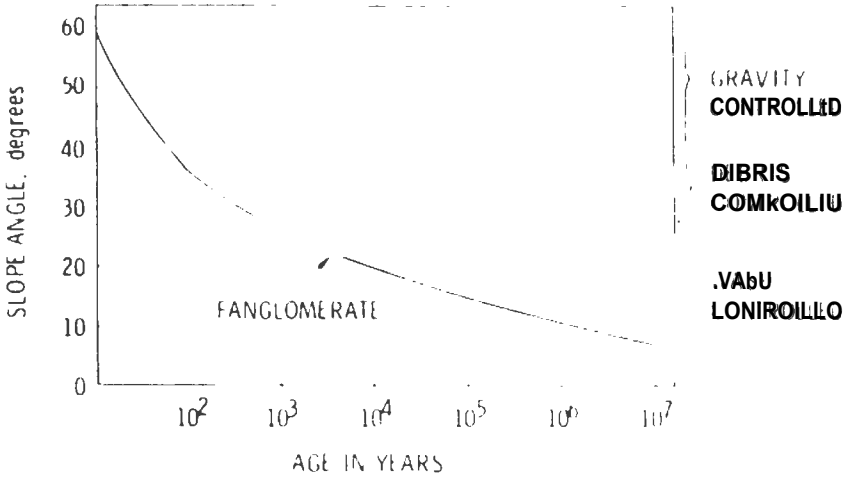

FIGURE 4.4. Relationship between fault scarp slope angle and age for fault scarps in fanglomerates (after Wallace, 1977).

TABLE 4.1. Fault scarp ages.

Scarp	Bevel #	Age
P 2	5.3	10^7 yr
	14.4	80,000
P 3	4.1	10^7
	10.4	10^6
	12.0	240,000
	14.8	75,000
	23.7	2,000
P 4	9.1	10^6
	12.0	110,000
	30.3	280
P 5	4.3	10^7
	5.0	10^7
	9.4	10^6
	13.8	120,000
	22.3	3,000
P 6	2.9	10^7
	49.4	730
P 7	0	10^7
	14.0	100,000
	17.2	21,000
P 8	0	10^7
	2.9	10^7
	4.6	10^7
	7.7	10^7
	21.8	3,700
	31.0	250
P 9	16.7	27,000
	5.7	10^7
	32.7	170
P10	2.1	10^7
	10.2	10^6
	42.0	47
	50.0	22
P11	5.3	10^7
	20.6	5,200
	28.8	420
P12	42.0	46
	8.5	10^6
	11.3	500,000
	31.0	240
	48.2	27
P13	16.0	40,000
	31.6	220
	47.7	27
	30	320
	38.0	12
P14	12.4	250,000
	32.6	170
	53.1	17
P15	18.3	13,000
	59.0	11
P16	16.4	61,000
	13.0	160
	90	0
P18	17.7	17,000
	24.2	6,000
P19	15.1	65,000
	21.8	1,600
	24.7	1,400
P20	19.3	9,000
	24.2	1,600
	31.8	200
	45.2	100
P21	0.6	10^7
	24.4	350
P22	4.0	10^7
	6.3	10^7
	13.8	130,000
	16.7	27,000
	21.4	4,000
	24.0	1,700
	10.8	280
P23	3	10^7
	81.9	100
P24	0	10^7
	21.8	6×10^6
	17.9	2×10^6
	58.6	1,000

4.3 FAULT SCARP PROFILING

In the ideal situation, scarp profiles should be obtained by careful surveying techniques, however, such techniques generally require a two or three man crew. Since the writer worked alone, it was necessary to develop a method by which a single person could expeditiously obtain the required field data. This method is shown diagrammatically in Figure 4.5. For the shorter profiles, e.g., less than about 50 m, a wooden station pole approximately 1.5 m long was placed in an upright position near the crest of the scarp. Attached to this pole was a piece of surveyor's flagging placed at a height equal to the height of a similar, but shorter survey pole. Profiling was accomplished by measuring the slope distance and slope angle from the survey position to the station pole. A Sunto clinometer, type PM-5/360PC, was placed on top of the survey pole and sighted at the flagging on the station pole. In this way the slope angles between the poles at several locations along the profile line were measured. The slope distances between the poles were measured with a 30 m long fiberglass measuring tape. The distance between the measuring points was dependent upon the topography of the scarp and varied from 0.2 to 5 m. Longer profiles were measured in the same manner except that the station pole was relocated as necessary along the profile line.

Horizontal and vertical distances from each of the measuring points to the station pole were calculated using an electronic calculator. The resulting data was plotted on standard graph paper using a vertical exaggeration of 2:1. The fault scarp profile reconstructions are shown in Figure B.1 of the Appendix.

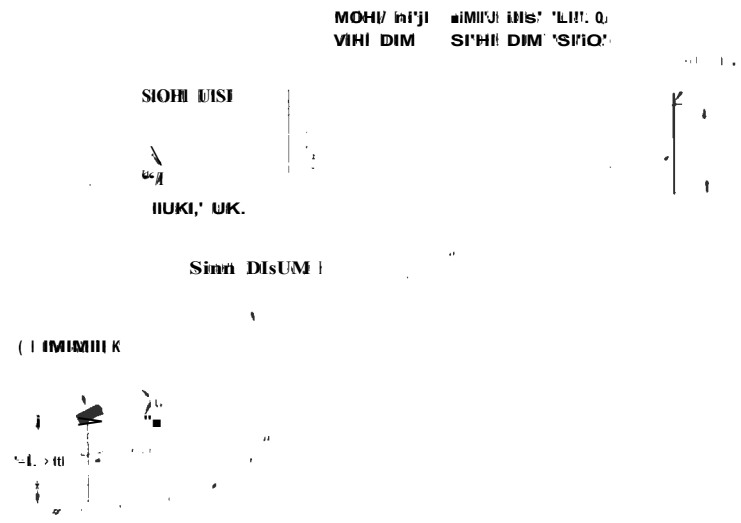

FIGURE 4.5. Fault scarp profiling method used for study.

4.4 PARTICLE SIZE DISTRIBUTION

The generally accepted method of determining the particle size distribution of a sample of unconsolidated material is by sieve analysis of the coarse fraction and hydrometer or pipette analysis of the fine fraction. This is commonly referred to as volumetric or bulk sampling and analysis. Bulk sampling, when applied to alluvial fan deposits, is often difficult, time consuming, and expensive because of the difficulty in obtaining and analyzing statistically significant samples. This difficulty is due to the wide range of particle sizes, often ranging from microns to meters, commonly associated with these deposits. To deal with problems of this sort, Wolman (1954) developed an areal or surface method of sampling coarse river channel material. His method involves the establishment of a grid on the surface to be sampled. The intermediate dimension of the

particle underlying each grid point is measured until a total of 100 particles have been measured. In this way a cumulative curve showing size versus frequency may be plotted. Comparisons of bulk and surface sampling results by Wolman (1954) and later workers have proven the validity of this method. This method has the advantage of using direct measurements rather than relying on the weight of material in a size interval. The method is, however, limited to particle sizes that can be measured in the field.

Denny (1965) applied a slightly modified version of this method in his study of alluvial fan deposits in the Death Valley region. Rather than establishing a grid on the surface, Denny instead laid a 100 ft (30 m) steel tape across the surface to be sampled and measured the intermediate dimension of the particle beneath each 4 ft (1.3 m) mark for a total of 25 measurements.

For the Saline Valley study a 30 m fiberglass tape was laid diagonally across the face of each fault scarp. Uniform sampling distances ranging from 0.2 to 0.5 m were used, depending on the overall coarseness of the material. One hundred measurements were made at each scarp. From this data, the cumulative curves and histograms of the intermediate dimension versus percent frequency were constructed. These are shown in Figures B.2 and B.3 of the Appendix. From the cumulative curves, descriptive measures of particle size distribution were calculated. These measures, based on Inman (1952) include the median, Φ_{50}, the mean, $(\Phi_{16} + \Phi_{84})/2$, and the standard deviation, $(\Phi_{84} - \Phi_{16})/2$. Φ_{16}, Φ_{50}, and Φ_{84} are the

intermediate particle dimensions in phi units corresponding to 16, 50, and 84% finer, respectively on the cumulative curve.

Phi notation, first described by Krumbein (1934), is based on the logarithm to the base two of the particle diameter. The term "phi unit" is synonomous with "Wentworth grade". To emphasize the fact that phi is a dimensionless quantity referring to a nonlinear measurement scale, McManus (1963) gave the following mathematical expression [slightly modified from Krumbein (1934)] for phi:

$$= -\log_2 \frac{\text{particle diameter in mm}}{1.00 \text{ mm}}$$

Several statistical parameters (after Inman, 1952) of the fault scarp material are given in Table 4.2.

4.5 SEISMIC VELOCITY

The in situ seismic velocities of the alluvial fan deposits forming 13 of the fault scarps examined in this study were determined by conventional field methods. A Nimbus Instruments Model ES-1A single channel engineering seismograph was used with a 4.5 kg hammer for an energy source. Because the velocity of only the upper few meters of the scarp-forming material was needed, the profile lines generally did not exceed 15 m in length. Seismic velocities obtained and the profile locations are given in Table 4.3.

TABLE 4.2. Statistical parameters for fault scarp material.

	ϕ_{16}	Median ϕ_{50}	ϕ_{84}	Mean $\frac{\phi_{16}+\phi_{84}}{2}$	Standard Deviation $\frac{\phi_{84}-\phi_{16}}{2}$
P 1,2,3,4	-3.6	-4.75	-6.8	-5.20	1.60
5		N/A			
6	-1.25	-4.25	-6.8	-4.03	2.78
7	-2.3	-4.0	-5.1	-3.70	1.40
8	-0.25	-4.3	-6.3	-4.40	1.90
9	-3.25	-4.5	-6.35	-4.80	1.55
10	-1.75	-3.6	-4.85	-3.30	1.55
11			N/A		
12	0	-3.8	-7.25	-3.63	3.63
13	0	-3.8	-6.55	-3.29	3.29
14	-0.7	-3.25	-5.4	-3.05	2.35
15	-0.8	-4.2	-6.45	-3.63	2.83
16	N/A	-4.2	-7.1		
17			No profile		
18	-2.45	-4.0	-5.2	-3.83	1.38
19	-1.1	-3.6	-5.6	-3.35	2.25
20	-2.0	-4.5	-6.9	-4.45	2.45
21	-2.2	-4.0	-6.2	-4.2	2.00
22	-2.4	-4.2	-6.7	-4.55	2.15
23			N/A		
24			N/A		

TABLE 4.3. Seismic velocity of fault scarp material.

Profile		m/s	Profile	m/s
P 1			P13	488
P 2	General Area	554	P14	436
P 3			P15	N/A
P 4			P16	726
P 5		N/A	P 17 No Profile	
P 6		871	P18	N/A
P 7		484	P19	N/A
P 8		1451	P20	N/A
P 9		762	P21	N/A
P10		736	P22	N/A
P11		N/A	P23	N/A
P12		965	P24	N/A

4.6 ASSUMPTIONS USED IN FAULT SCARP AGE ESTIMATION

In the Saline Valley region, numerous young normal fault scarps in alluvial fans form steps ranging from less than a meter to more than 20 m in height along the bases of the Inyo Mountains and Panamint Range and on the floor of Saline Valley. Several of these scarps appear to have undergone four or more periods of faulting, as indicated by the beveling or segments of increasingly reduced slope uphill from the most recent offset. Although Wallace's (1977) method was developed in a region of different climatic conditions, it appears that it may be used to estimate the minimum age of these scarps.

Several assumptions are implicit in Wallace's (1977) methodology. Of these the most important is that the fault scarps were formed principally by sudden offsets accompanying earthquakes rather than by slow tectonic creep. This is reasonable because tectonic creep on faults within the Great Basin has not been recognized (Slemmons, 1967). Secondly, the initial scarps formed in the alluvial deposits have slopes ranging from about 50° to 90° or even slightly overhanging. Normal fault scarps formed in bedrock generally have slopes averaging about 60°. This is attributed to the mechanics of faulting and physical properties of the material by Billings (1954) and Anderson (1951). Wallace attributes the difference between initial scarp angles in bedrock and in alluvial deposits to tensional fracturing of the sedimentary layer. Thirdly, original alluvial fans commonly have slopes of 3° to 7° but may be as steep as 7° to 10°. Wallace indicates that original slopes greater than about 5.5° are, in many places, the result of tectonic warping or tilting rather than from deposition. The major alluvial fans in Saline Valley (Appendix Fig. B.4, B.5) generally slope between 4° and 6° downstream from the canyon mouth and are steeper in the bedrock upstream from the fault zones. Finally, Wallace assumes that slope degradation rates are greatly affected by climatic conditions and are responsive to climatic changes.

4.7 APPLICATION OF METHOD TO SALINE VALLEY

Wallace's (1977) slope angle-age correlation curve was developed for an area in north central Nevada. This area is considered to be

arid, but the annual precipitation varies widely as a function of local relief. The broad intermountain basins at about 1200 m elevation have between 12 and 20 cm of precipitation annually. The higher ranges, at elevations of 1500 to 3000 m, have 35 to 45 cm of precipitation annually. The number of freeze-thaw cycles per year is between 120 and 130 (Vishner, 1954). Wallace (Personal Communication, 1979) believes that the climate in general, and the number of freeze-thaw cycles in particular, are important factors in the rate of fault scarp degradation.

Because of the importance that the number of freeze-thaw cycles may have on slope degradation, it may not be possible to directly apply Wallace's correlation curve for fault scarps located in the Saline Valley region. The fault scarps studied in this region are generally at elevations of 350 m to 1000 m and have annual precipitation values similar to those reported by Wallace. However, the number of freeze-thaw cycles per year is nearly zero. Lombardi (1963) indicates that a mine camp in Saline Valley at about 500 m elevation is nearly frost-free. Because of the milder winter climate in Saline Valley, ages derived from Wallace's correlation curve are probably too young. There are, however, no precise data concerning the ages of fault scarps in this area. This method can be used, however, to estimate the number of fault events that have occurred along a particular fault segment. Approximate or minimum recurrence rates can be determined from this data.

4.8 RESULTS OF FAULT SCARP ANALYSIS

The purpose of this analysis is to apply, test, and further develop the method of determining the ages for fault scarps proposed by Wallace (1977). Independent dating, properties of the scarp material, seismic velocities, and Wallace's (1977) profile method formed the basis for this study. Independent dating of the scarps is not possible. Age dating of tuff samples by correlating their trace element content with tuffs of known ages is being done, but the data are not yet complete. Absolute dating of the materials was not done due to financial limitations. Lacking these data, there is no way to test Wallace's correlation curve with any degree of certainty.

Based on the degree of dissection, desert varnish development, vegetation growth, and other field criteria, it appears that several surface ruptures have occurred during the Holocene. This conclusion is supported by scarp profile age data which suggest several events during the last 9000 years and many others during the last 100,000 years. The youngest ages determined by this method are anomalously low, i.e., less than 100 years old. In several instances, recurrence rates appear to average about 3.3×10^{-4} yr^{-1} during the Holocene and about 1.7×10^{-4} yr^{-1} during the last 20,000 years. This discrepancy probably reflects the relatively small sample population, the lack of independent dating, correlation curve interpolation errors, and variabilities in fault scarp development, erosion, and material. Scarp material is probably a major factor in determining the apparent age of faulting. Scarps

were profiled in alluvial material ranging in induration from cemented fanglomerates to unconsolidated beach gravel and silt.

Several attempts were made to correlate the seismic velocities and grain size distribution data with the estimated age of the fault scarp. Such correlation efforts were generally unsatisfactory.

5.0 JOINT ANALYSIS

5.1 INTRODUCTION

A study of joint attitudes at Hunter Mountain suggested that many of the high-angle joints probably resulted from post-emplacement tectonic stresses rather than from cooling or intrusion. The orientations of these joints were analyzed to determine the stress pattern responsible for their formation. These data were combined with other information outlined in this paper to develop a model for the tectonic development of the region.

The joint analysis study area occupies an area of about 80 km^2 in the southeast corner of the Ubehebe Peak 15' U.S.G.S. Quadrangle (Figure 5.1). The principal rock unit in this area is the Late Jurassic Hunter Mountain quartz monzonite which forms the bulk of Hunter Mountain. McAllister (1956) indicated that the top of Hunter Mountain is probably very near to the original top of the pluton.

Hunter Mountain, which separates Saline and Panamint Valleys, is cut by a major right-lateral, strike-slip fault system (Grapevine Canyon/Panamint Valley fault zone) trending through these valleys. In Panamint Valley the fault bifurcates into a normal fault system with local right-lateral strike-slip components and forms the east and west boundaries of the valley. At the northern end of the valley the faults join to form a single thrust fault extending beneath the southern edge of Hunter Mountain. The fault continues through Hunter Mountain as a right-lateral, strike-slip fault and becomes principally a normal fault forming the western border of Saline Valley.

5.2 JOINT DATA ACQUISITION

Joint data were obtained at 12 locations on Hunter Mountain from both road cuts and natural outcrops (Figure 5.1). The method of data acquisition used in this study is similar to that recommended by Attewell and Farmer (1976). At each sample location a metric tape measure was stretched across the outcrop to intersect as many joints as possible (Photo 5.1). The attitude of each joint intersected by the tape was measured by placing a Brunton compass directly on the joint surface (Photo 5.2). In situations where the joint surface was not sufficiently exposed, the compass was placed on an aluminum plate approximately 2 mm thick inserted into the joint. If the joint was closed or too narrow for insertion of the plate, the plate was oriented parallel to the joint plane and the plate's attitude determined. The location of each joint relative to the starting point of the survey line was also recorded. A standardized survey line length of 10 m was chosen for the study to permit comparisons among the several traverses. At a few locations natural limitations (e.g., outcrop size) prevented the use of the full 10 m survey line. In these situations as long a line as possible was used and the data later normalized to the full 10 m length (Attewell and Farmer, 1976). Where practical, two intersecting survey lines located as near to 90° to each other as possible were used to provide more complete data acquisition. A total of 550 joint plane attitudes were measured.

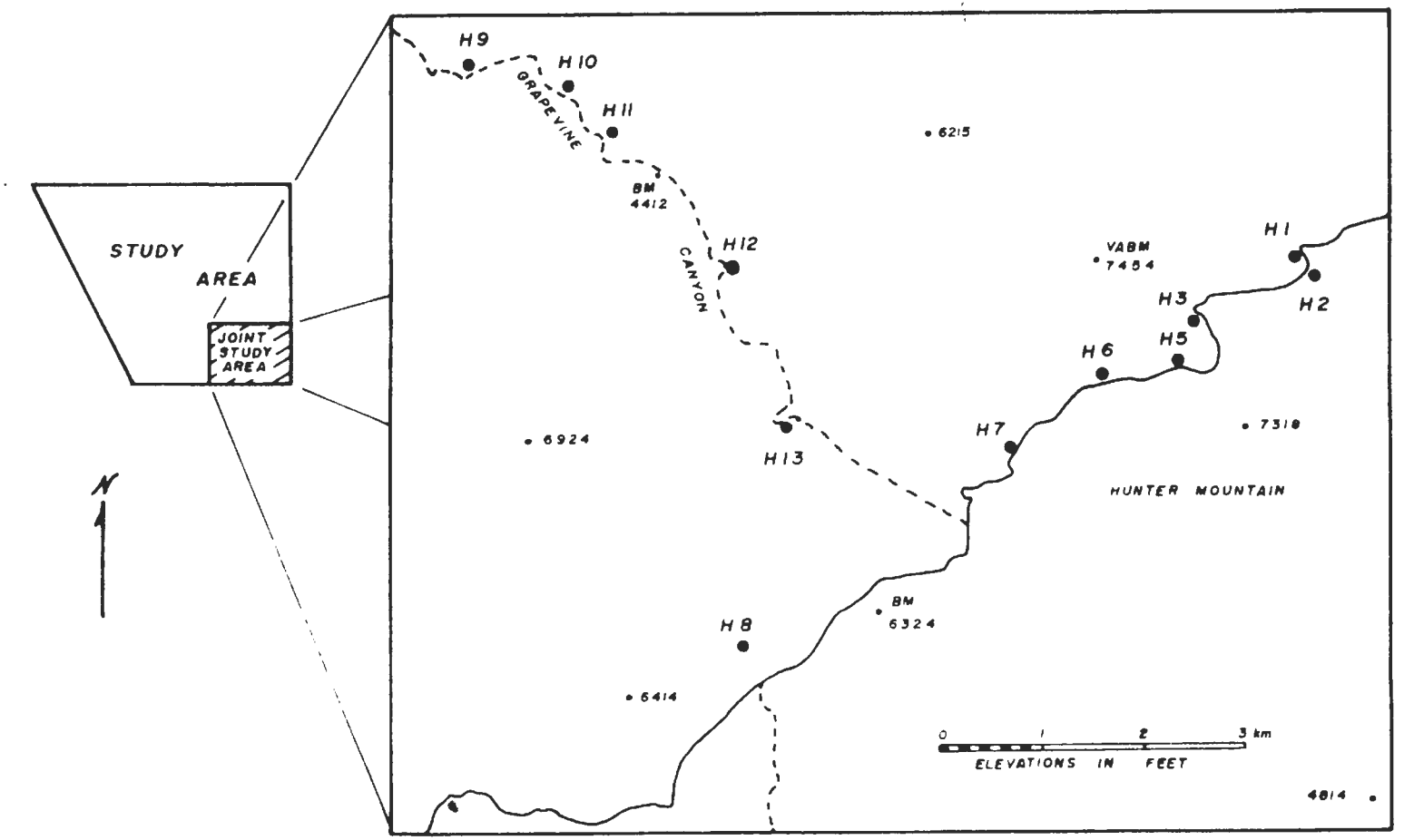

FIGURE 5.1. Location of joint study area. Numbers preceded by letter "H" indicate sample location.

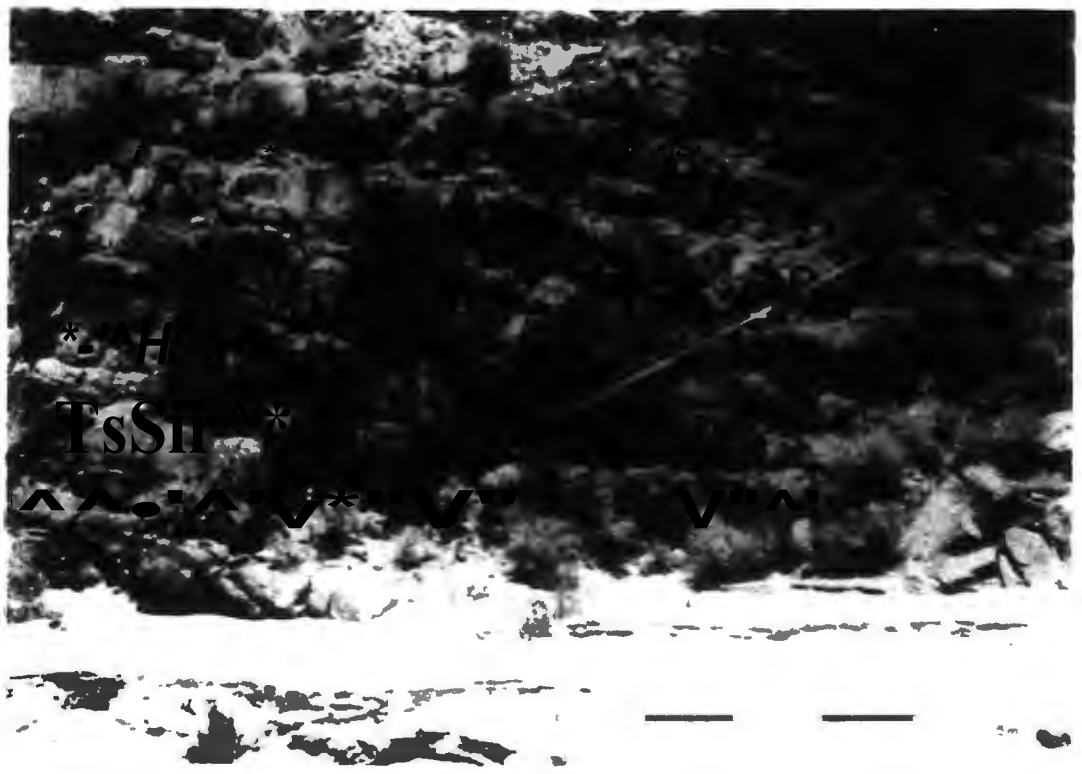

PHOTO 5.1. Jointing in Hunter Mountain quartz monzonite. Note tape measure used in joint attitude survey.

5.3 DATA ANALYSIS METHODS

The joint data used in this study are presented in several formats to facilitate analysis. These formats include stereographic projections, joint strike azimuth rosettes (rose diagrams), joint measurement traverse reconstructions, and tabular and graphical representations.

The stereographic projections of the joint plane poles are shown as upper hemispheric projections. Attewell and Farmer (1976) suggest that although contrary to general structural geology procedure this method has an advantage in that the pole to the joint plane is projected in the same direction as the joint plane dip. A composite

PHOTO 5.2. Brunton compass and aluminum plate used in joint attitude survey.

stereographic projection of all of the data points is shown in Figure 5.2. Stereographic projections for each sample location are shown in Figure B.5 of the Appendix. Joint strike azimuth rosettes for each sample location are shown in Figure B.6 and graphical reconstructions of the traverse lines are shown in Figure B.7.

5.4 JOINT PATTERN ANALYSIS

Approximately 550 individual joint planes at 12 separate locations were analyzed with respect to strike, dip and distribution during this study. Of these 28% were low-angle (dips less than 60°) and 72% were high-angle (dips greater than or equal to 60°). A graph

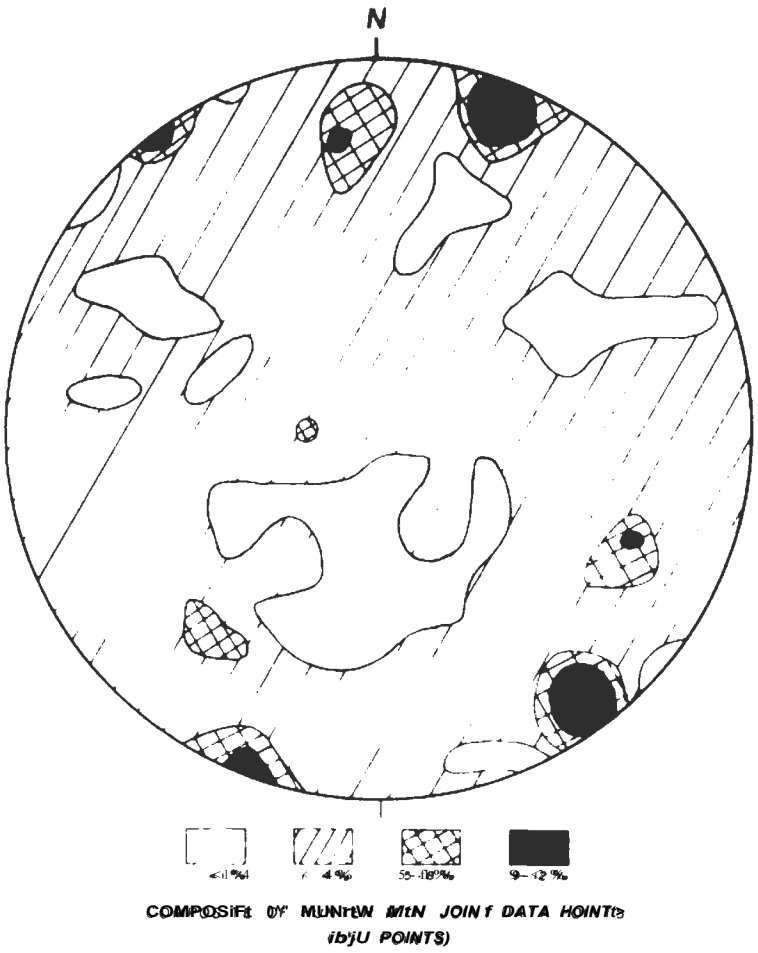

FIGURE 5.2. Composite of all joint data points collected at Hunter Mountain (550 Points).

of joint frequency versus joint dip is shown in Figure 5.3. Firman (1960) noted a similar joint dip distribution in his study of the Eskdale Granite and used it as a partial basis for his analysis. Firman reasoned that the low-angle joints were related to marginal thrusts or flat-lying normal faults. The development of these features along the margins of an intrusion was described by Balk (1937) and shown in Figure 5.4. Balk (1937) also suggested that low-angle joints may develop when the center of an intrusion collapses.

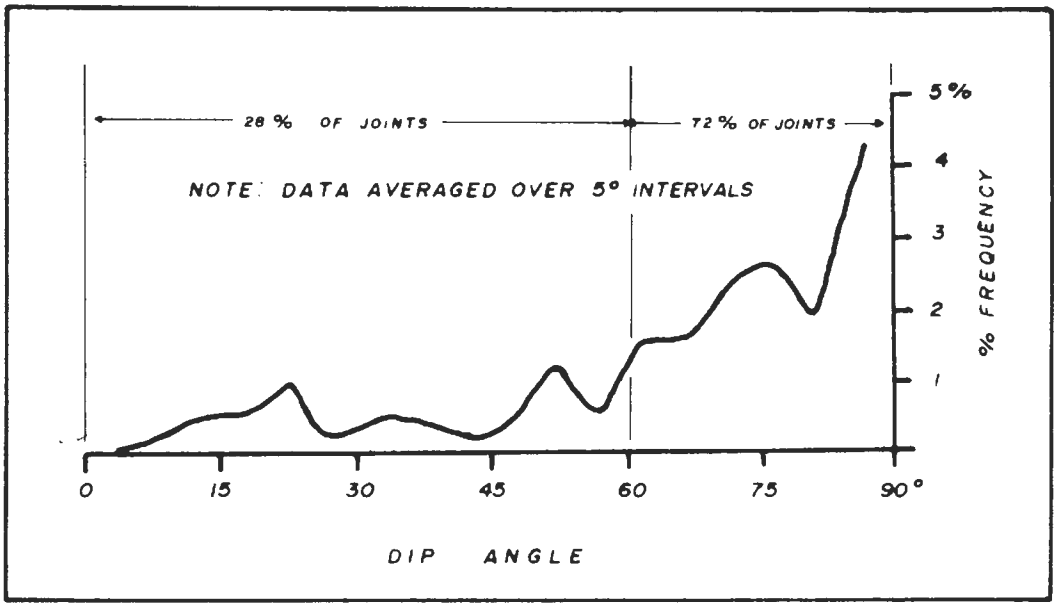

FIGURE 5.3. Plot of dip angle versus frequency for Hunter Mountain joint data.

Firman (1960) suggests that 75% or more of the high-angle joints in the Eskdale Granite were the result of postemplacement stresses. Because of the several similarities between the Eskdale Granite and Hunter Mountain Quartz Monzonite, an analysis method following Firman (1960) is used in this study.

5.5 LOW-ANGLE JOINTS

Low-angle joints are well developed over much of Hunter Mountain. Previous geologic mapping (McAllister, 1956) indicates that this area is located near the original top and margin of the Hunter Mountain batholith. This is confirmed by the apparent attitudes of flow structures in the rock (Figure B.5 of the Appendix). Figure 5.5 shows the orientation of flow structures that may be

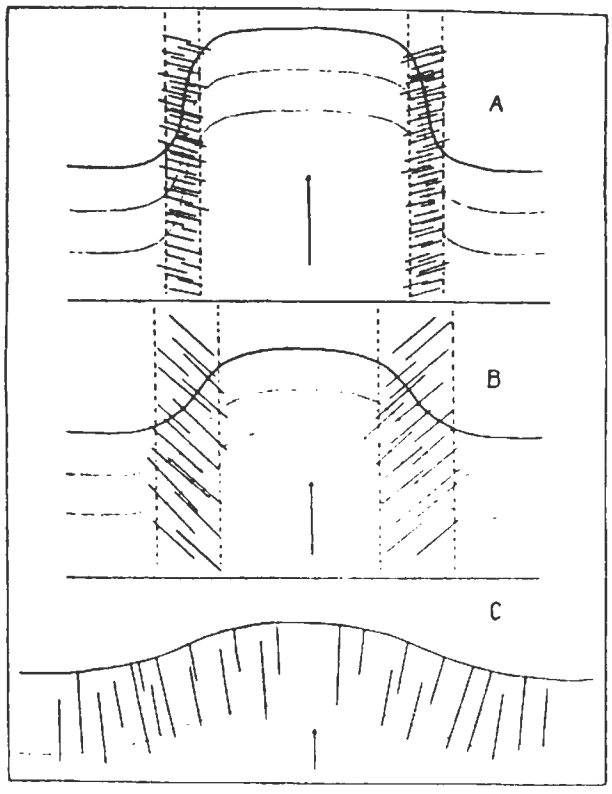

FIGURE 5.4. Bending of weak and strong material and the attendant development of marginal fractures or joint fans. At (A) a weak substance protrudes in the direction of the arrow, between stationary walls to the left and right. The zones of intense legnthening (between the dashed lines) are relatively narrow, as shown by the curvature of the three lines. Under suitable conditions, tension joints open within these zones, approximately normal to the lines of local elongation. In nature, the marginal fissures near intrusive contacts are due to a similar lengthening of the magma. At (B) the material is stronger than in (A). The zone of bending is wider, the elongation per unit area less intense. Fractures within the border zones are more widely spaced, and dip steeper. At (C) a strong substance is bent. Distinct zones of bending disappear, and a continuous symmetric arch results. The fractures are arranged in a broad fan. The fans of tension joints in massifs are believed to form under similar conditions; hence, they are steeper than marginal fissures, and reach from one end of the massif to the other. (After Balk, 1937)

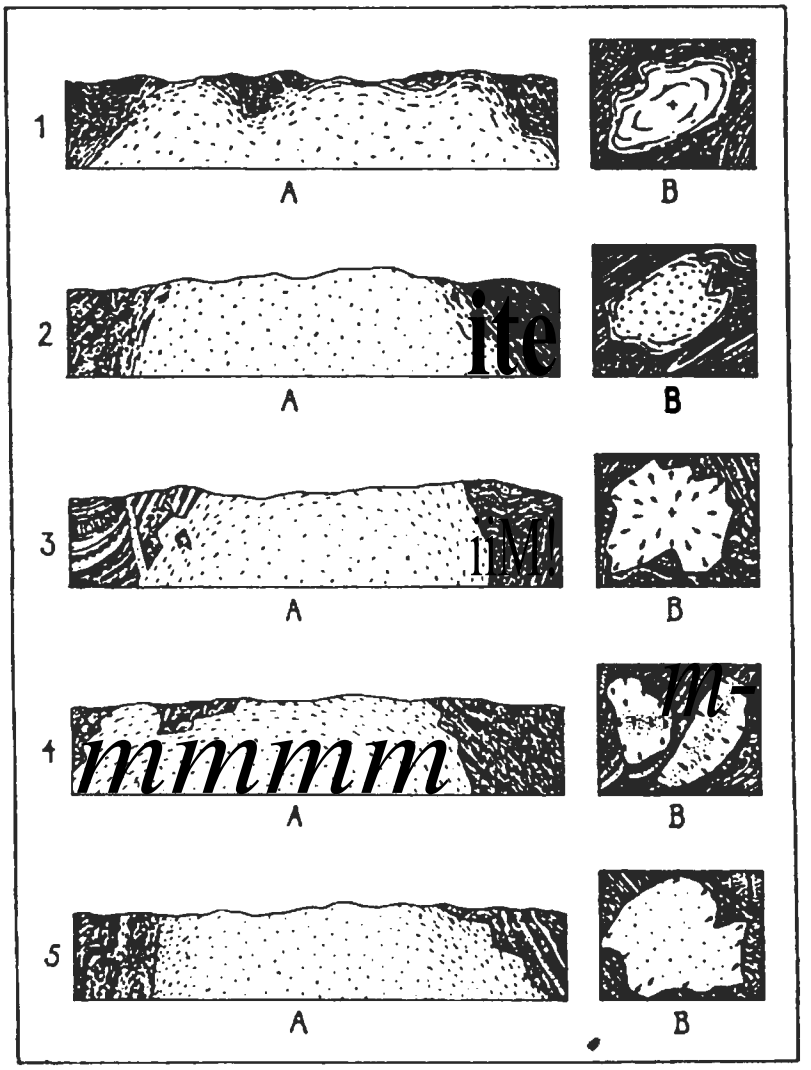

FIGURE 5.5. Ideal structural types of massifs. (A) cross-section, (B) plan. No exact agreement between cross-sections and plans is intended; structures of wall rocks, and details of contacts drawn arbitrarily. (1) Dome of flow layers. (2) Arch of flow layers, massive center. (3) Dome of flow lines (not yet observed iun the field. (4) Arch of flow lines. At 4B, axis of flow lines (shaded area) coincides with axis of massif on the right side, and disregards it on the left. (5) Incomplete arch of flow lines. Arrows show the pitch of flow lines: two-barbed arrow denoted horizontal flow lines. Lines with black triangles refer to strike and dip of flow layers. A cross denotes horizontal flow structures. (After Balk, 1937)

expected in several ideal cases. The low angle joints examined in this study are probably primary emplacement features and not related to later deformational stresses.

5.6 HIGH-ANGLE JOINTS

As shown in Figure 5.3, 72% of the joints examined in this study are steeper than 60°, with many approaching vertical (Figure 5.2). If the majority of these joints are related to post-emplacement stresses their orientations suggest that the intermediate principal stress, σ_2, was nearly vertical at the time of their formation. The directions of the maximum and minimum principal stress, σ_1 and σ_3, were determined on the basis of the orientation of the high angle joints. The orientations of the high angle joints were taken from the stereographic projections and are plotted in Figure 5.6. The orientation of the dominant and secondary joint sets are shown in Table 5.1.

TABLE 5.1. Dominant and secondary joint set orientations for Hunter Mountain joint data.

Location	Dominant Set	Secondary Set
H 1	N85E	N10W
H 2	N80E	N10W
H 3	N65W	--
H 5	N10E	N85W
H 6	N30W	--
H 7	N40E	--
H 8	N55W	--
H 9	N60W	N30W
H 10	N55W	NS
H 11	N10E	N15W
N 12	N65W	N10E
H 13	N55E	N50W

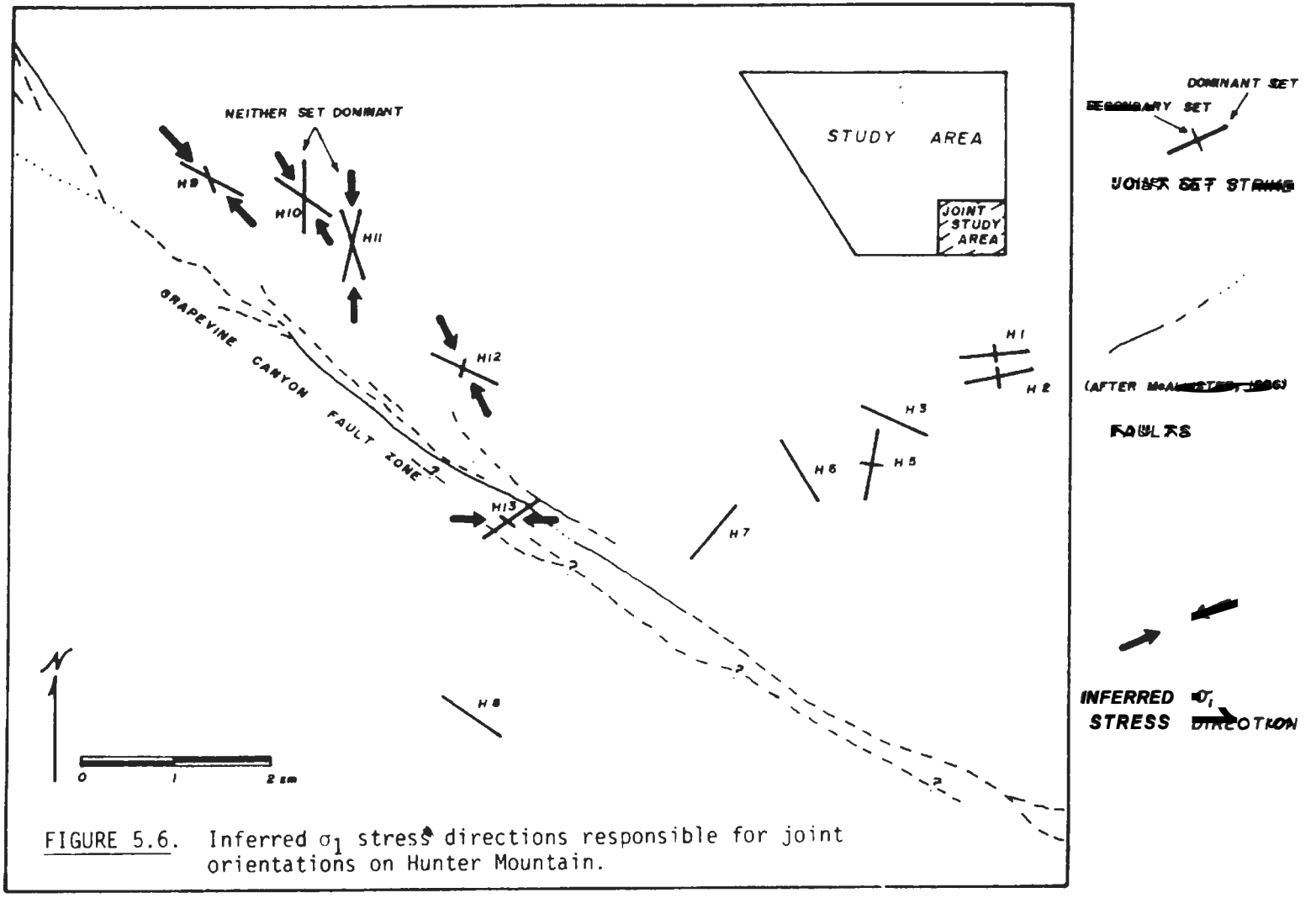

FIGURE 5.6. Inferred σ_1 stress directions responsible for joint orientations on Hunter Mountain.

The joint orientations and inferred principal stress directions suggest a close relationship between the jointing and the Grapevine Canyon fault zone. It appears that both developed in response to the same stress pattern. In general, many of the dominant and secondary joint sets are at orientations parallel to the fault zone or at angles suggestive of their being Riedel shears, complementary Riedel shears, tension joints or marginal fractures (Figure 5.7). The relationship between the faults and joints indicates that both developed in response to a stress pattern in which the maximum principal stress, σ_1, acted in northwesterly - southeasterly direction.

This relationship is shown most clearly by the inferred σ_1 stress directions at locations, H9, H10, H11 and H12 (Figure 5.6). At these locations the joint set orientations suggest a σ_1 stress direction of about N30W - S30E. The Grapevine Canyon fault zone trends about N50W - S50E. The orientations of the joint sets are suggestive of Riedel shearing or tension gashes associated with right-lateral movement of the fault. The orthogonal jointing at locations H1, H2 and H5 probably represents primary stress relief features due to cooling at the top of the Hunter Mountain pluton.

5.7 RELATIONSHIP BETWEEN REGIONAL AND LOCAL STRESS PATTERNS

Many (e.g., Wright, 1976) believe that the late Cenozoic regional stress pattern in the southwestern portion of the Great Basin is oriented with the maximum principal stress, σ_1, in a NNE - SSW to NE - SW direction. If this regional stress pattern is accepted it is probable that the Grapevine Canyon fault zone and

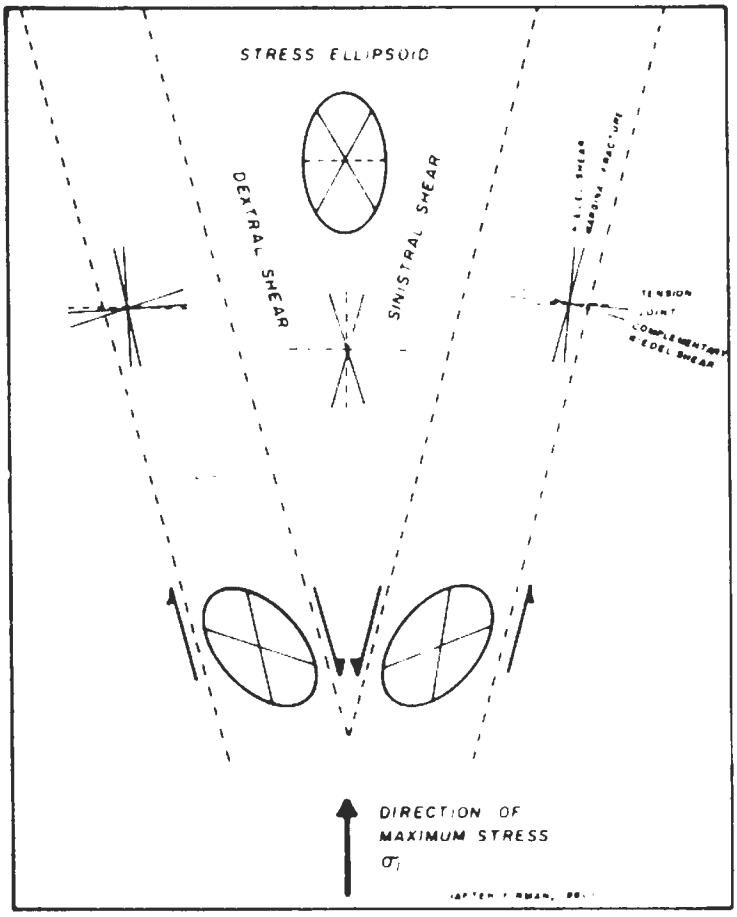

FIGURE 5.7. Stress field and resulting Riedel shears, complementary Riedel shears, tension joints and marginal fractures.

associated jointing represent second- and higher-order Riedel shear systems related to the regional stress pattern. An idealized stress and shear system of this sort is described was Moody and Hill (1956) and is shown in Figure 5.8.

In this figure it is shown that a primary stress orientation can result in the formation of second- and higher-order features. The orientations of the Grapevine Canyon fault zone and high-angle joints

at Hunter Mountain are similar to those that would be predicted on the basis of a NNE - SSW to NE - SW primary stress orientation.

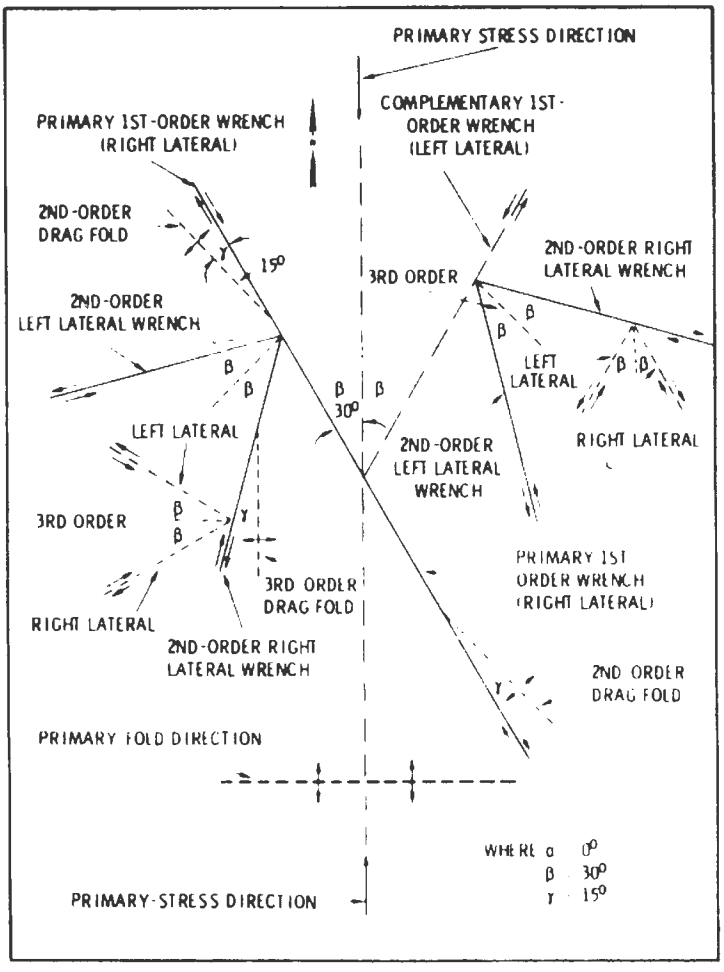

FIGURE 5.8. First-, second- and third-order features related to primary stress direction (after Moody and Hill, 1956).

6.0 SALINE VALLEY RHOMBOCHASM

6.1 INTRODUCTION

This study focuses on the styles and patterns of faults and joints in the southern portion of Saline Valley. The results of this study suggest that Saline Valley is a rhombochasm and indicate that the tectonic stresses responsible for the formation of the valley are still active. Chapters 3 and 5 detail data and present conclusions about the patterns, styles and amounts of deformation in the study area and the regional stress pattern inferred from the deformation. Chapter 4 presents evidence suggesting that the faults offsetting alluvium in Saline Valley have undergone several periods of movement during the Pleistocene and Holocene. This chapter briefly outlines evidence for the rhombochasm origin and continuing deformation of Saline Valley.

6.2 EVIDENCE FOR RHOMBOCHASM ORIGIN AND CONTINUING DEFORMATION OF SALINE VALLEY

Carry (1958) defined a rhombochasm as a parallel-sided gap in the sialic crust occupied by simatic crust. Strictly speaking, this may be incorrect as applied to Saline Valley. However, the mode of origin and the resulting deformation are similar. Burchfiel and Stewart (1966) proposed a similar origin for the central segment of Death Valley (Figure 6.1). Lombardi (1964) appears to be the first to suggest that Saline Valley formed as a rhombochasm as a result of movement along two parallel strike-slip faults. Babcock (1974)

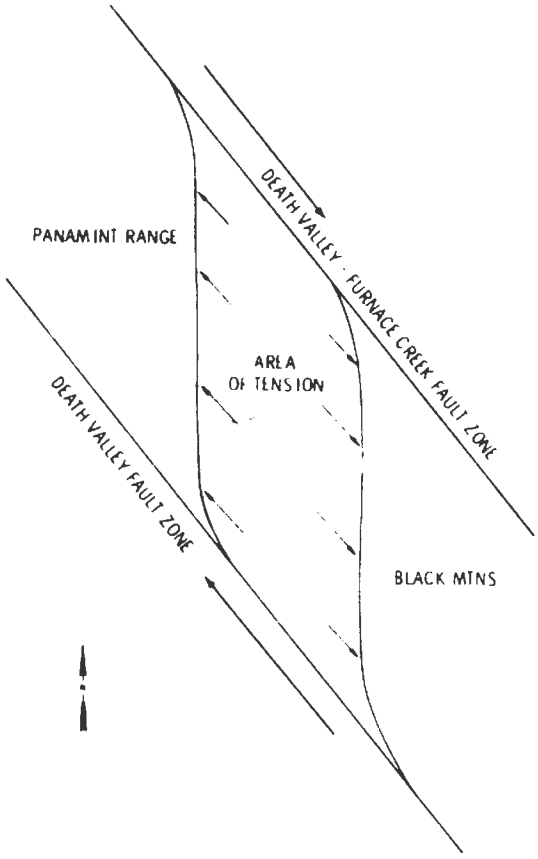

FIGURE 6.1. Origin of the central segment of Death Valley (after Burchfiel and Stewart, 1966).

suggested the same mode of origin. Lombardi's and Babcock's conclusions were based on the geometrical relationships among the topographic and tectonic features observed in the Saline Valley area. These features are shown in Figure 6.2.

If Lombardi's and Babcock's interpretations are correct, one would expect to observe the following features in Saline Valley: 1) the shape of the valley would be rhombohedral, 2) two sides of the valley would be formed by strike-slip or oblique-slip faults, 3) the

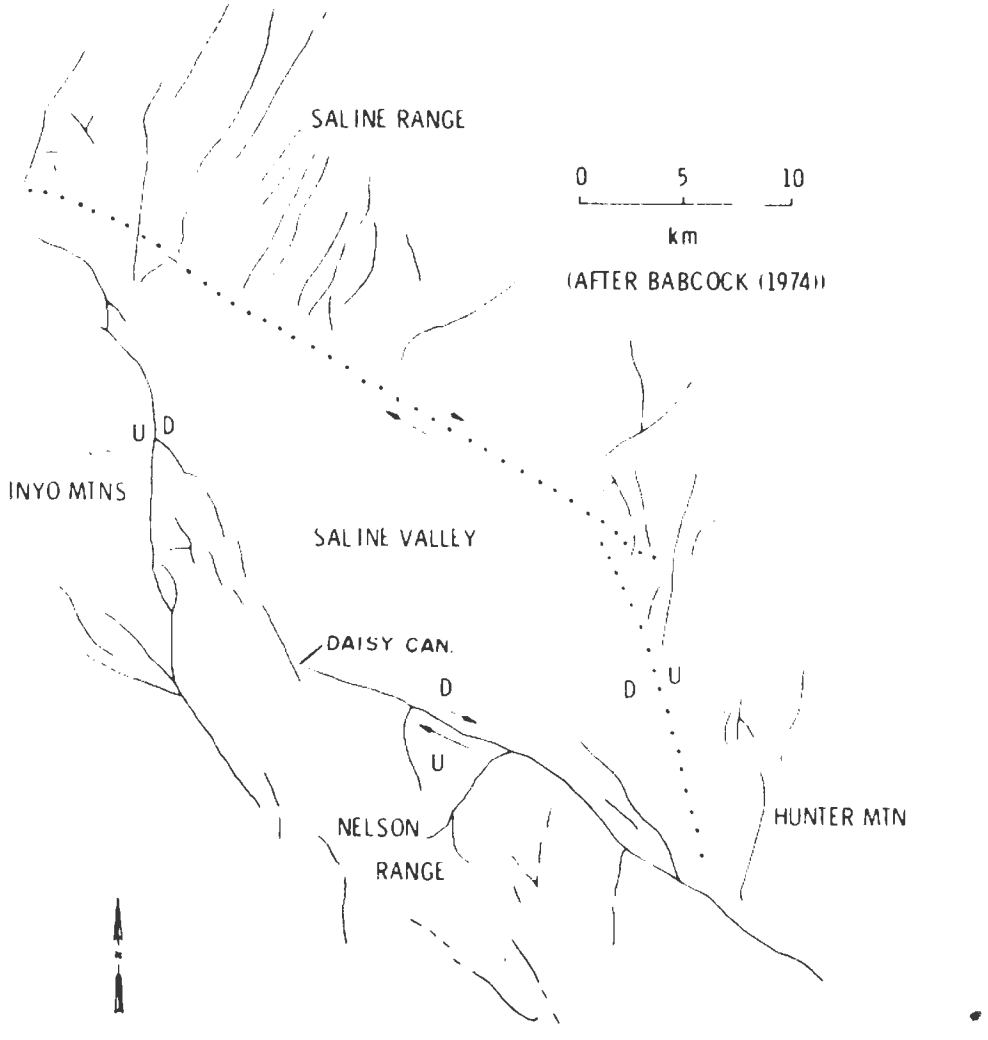

FIGURE 6.2. Major faults and physiographic features of the Saline Valley area (modified from Babcock, 1974).

two remaining sides of the valley would be formed by normal-slip faults, and 4) tensional features would locally form at right angles to the direction of extension.

Although this study focuses principally on the southern portion of Saline Valley, the evidence and conclusions given in Chapters 3, 4 and 5 support Lombardi's and Babcock's proposed mode of origin, and indicate that the valley is continuing to deform. The evidence and

conclusions given in the above chapters are outlined below. The fault zones are shown on Plates 3.1, 3.1a, 3.2, 3.3, 3.4 and 3.5.

1) The Grapevine Canyon fault zone is right-lateral, strike-slip at Hunter Mountain, but becomes increasingly dip-slip as it approaches Daisy Canyon. Strike-slip offset appears to total at least 1 km and dip-slip offset at least 6000 m. Numerous offsets occur in unconsolidated sediments.
2) The Western Frontal fault zone is a normal fault with a throw of at least 6000 m and displays numerous offsets in unconsolidated alluvial sediments.
3) The East Side fault zone consists of parallel, north-south trending horsts and grabens in unconsolidated alluvial deposits. The faults appear to be related to east-west extension of Saline Valley.
4) The ages and orientations of the faults in the Central Valley fault zone suggest that they are also related to east-west extension of Saline Valley and that this extension is still occurring.
5) The Lee Flat fault zone appears to be a part of a graben that extends from Lee Flat into Saline Valley. The orientation of the fault zone and graben suggest that they are related to east-west extension of the Saline Valley area.
6) Topographically, Saline Valley has a rhombohedral shape. Inferences from gravity data suggest that this shape continues at depth.

7) The floor of Saline Valley is tilting in a westerly direction as though it is being downfaulted along the edge of a rhombochasm.

A comparison of the above with the features expected to be associated with a rhombochasm suggest that Saline Valley had this type of origin and that the deformation is still occurring. Saline Valley appears to have developed in a zone of shearing and tension between the Death Valley-Furnace Creek fault zone and the Grapevine Canyon fault zone (see Photo 1.1). The Grapevine Canyon fault zone is the oblique-slip fault bounding the southwest side of the rhombochasm. Along the northeast side of the rhombochasm a series of northerly-trending tension fractures in the Saline Range and northern Panamint Range developed rather than a simple strike-slip fault. The Western Frontal, Lee Flat and East Side fault zones developed in response to east-west extension of the region and related movement along the Grapevine Canyon fault zone. The east side of the rhombochasm is formed by a series of step faults rather than by a narrow fault zone such as the Western Frontal fault zone.

The following chapter is a discussion of the regional implications of the Saline Valley rhombochasm and what can be inferred about the origin of the Sierra Nevada - Basin and Range transition zone.

7.0 REGIONAL TECTONIC MODEL

7.1 INTRODUCTION

In the previous chapter Saline Valley was described as a rhombochasm that developed in response to regional shearing and extension. This chapter is a discussion of what may be inferred about the tectonic development of the Sierra Nevada - Basin and Range transition zone based on topographic and geologic features of Saline Valley and the surrounding region. The discussion uses evidence and conclusions presented in earlier chapters and by other workers as a basis for assessing the relationship between the formation of Saline Valley and the tectonic evolution of the region.

7.2 REGIONAL TECTONIC FEATURES AND DEFORMATION

Wright (1976) proposed the regional stress model shown in Figure 7.1. Such a pattern would lead to regional conjugate strike-slip fault systems oriented northeast-southwest and northwest-southeast. The northeast-trending zones would display left-lateral motion while the northwest-trending zones would display right-lateral motion. East-west extension would develop in response to the north-south compression.

Figure 7.2 shows the regional conjugate strike-slip faults. The Walker Lane, Death Valley-Furnace Creek and Las Vegas zones are right-lateral, strike-slip fault zones along the western border of the Great Basin. The Lime Ridge and Pahranagat zones are two of the left-lateral, strike-slip fault zones along the southeastern border of the

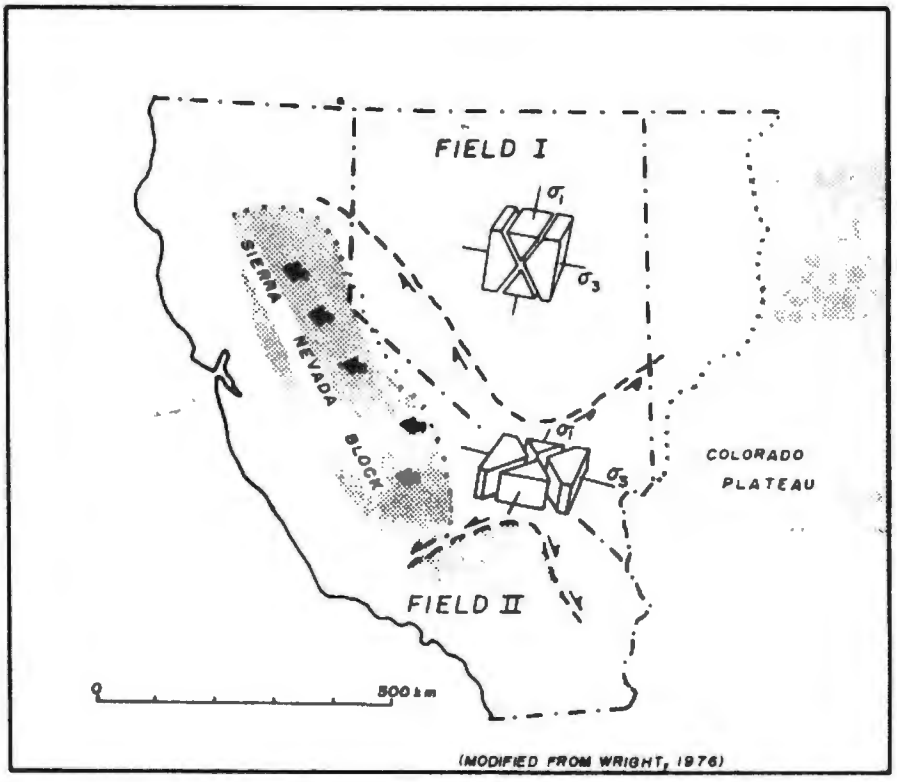

FIGURE 7.1. Deformation fields and principal stress directions for portions of California and Nevada. Field I - generally NNE-SSW trending horst and graben structures. σ_1 vertical. Field II - coeval normal and strike-slip faulting. σ_1 NNE-SSW.

Great Basin. The Garlock fault is a left-lateral, strike-slip fault forming the northwestern border of the Mojave block. Several smaller right-lateral, strike-slip faults form the northeastern border of the block.

In Figure 7.1 the Sierra Nevada is shown as moving to the west. This is due to the east-west extension resulting from regional north-south compression. The normal faults forming the east front of Sierra Nevada and associated normal faults support the existence of a

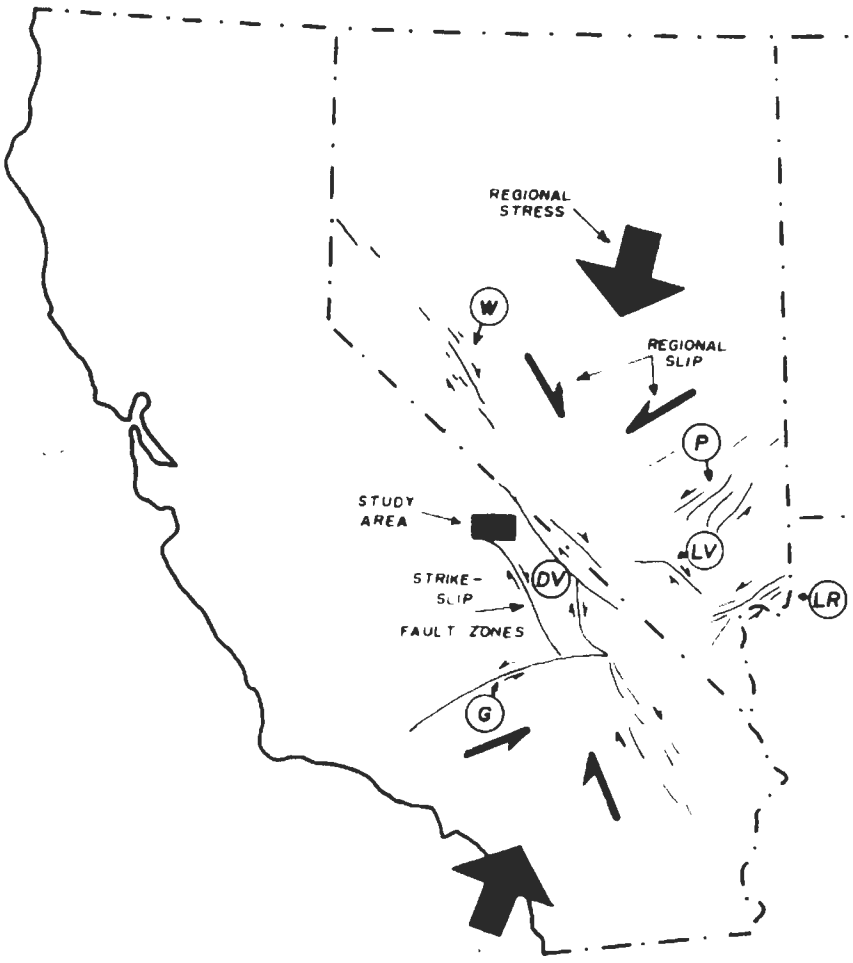

FIGURE 7.2. Regional stress field and related faults in portions of California and Nevada. W = Walker Lane F.Z., DV = Death Valley-Furnace Creek F.Z., LR = Lime Ridge F.Z., P = Pahranagat F.Z., G = Garlock F.Z.

tensional zone in the "wake" of the Sierra Nevada. This tension zone is apparently responsible for many of the major valleys, such as Owens Valley, that border the Sierra Nevada. Right-lateral, strike-slip faults associated with this extension may be responsible for volcanic centers adjacent to the Sierra Nevada (Wright and Troxel, 1968, 1971; Carr, 1974).

The study area is located in the "wake" of the Sierra Nevada and adjacent to right-lateral, strike-slip faults that form the western border of the Great Basin. Thus, the study area is located in a transitional zone between these two provinces. Features in the study area are indicative of both right-lateral strike-slip faulting due to north-south regional compression and east-west tension due to western migration of the Sierra Nevada. McKee (1968) reported total right-lateral offsets of up to 48 km along the Death Valley - Furnace Creek fault zone. Smith (1975b) reported total vertical offsets of up to 10,000 m and right-lateral offsets of up to 4500 m in Panamint Valley. Pakiser et al. (1974), reported vertical offsets totaling up to 6000 m in Owen's Valley. The present study suggests at least 6000 m of vertical offset and perhaps 1000 m of right-lateral offset in Saline Valley. In each case the right-lateral offsets are related to the regional shearing and the vertical offsets are related to down-faulting of the valleys in response to regional extension. Figure 7.3 is a simplified and idealized relief map of the region. Downfaulted valley areas are patternless, mountain blocks are cross hatched and mountain regions suggesting east-west extension, e.g., the Coso Range, are shown by alternating cross hatching and dotted strips.

Saline Valley represents a zone transitional between the east-west extension typified by Owens Valley and Sierra Nevada and the right-lateral, strike-slip faulting typified by the Death Valley - Furnace Creek fault zone. Although right-lateral, strike-slip movements have been reported in Owens Valley, the predominant motion has been dip-slip. Thus, Owens Valley is a deep, narrow graben

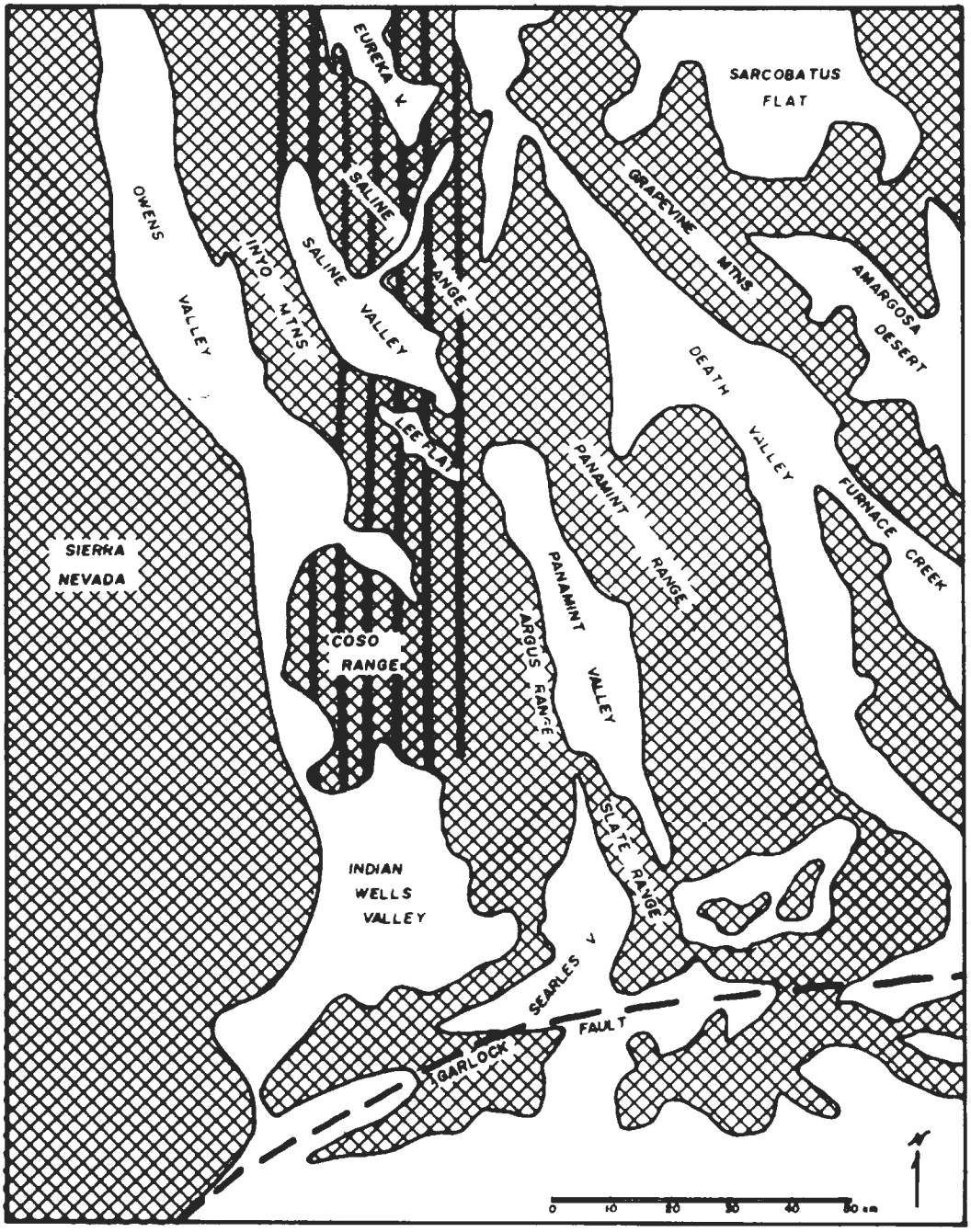

FIGURE 7.3. Simplified and idealized relief map of area. Patternless areas are valleys, cross-hatched areas are mountain blocks, striped areas are mountain blocks undergoing extension.

between the relatively uplifted Sierra Nevada and White-Inyo Mountain blocks. This feature was formed predominantly by extension in an east-west direction. The Death Valley - Furnace Creek zone is a part of the right-lateral, strike-slip zone that forms the eastern edge of the Basin and Range province. Saline Valley has both major strike-slip and dip-slip features.

The Grapevine Canyon fault zone developed in response to strike-slip motion along the Death Valley - Furnace Creek fault zone and tension due to westward migration of the Sierra Nevada block. The Western frontal fault zone developed in response to the east-west tension. The net result of this combined motion is that the western portion of Saline Valley was progressively downfaulted into a rhombochasm along the Inyo Mountains and Nelson Range. This motion caused a hinging action to develop along the Grapevine Canyon - Panamint Valley fault zone at Hunter Mountain. This movement resulted in relative downfaulting of Saline Valley and possible uplift of the Panamint range in Panamint Valley. Geometrically this suggests that the Panamint Range block rotated westward similar to the Sierra Nevada.

Regional shearing related to both the strike-slip faulting and east-west extension caused the formation of the wide fragmented zone extending from the Coso Range, and through the Saline Range north of Saline Valley (Figure 7.3). The zone trends approximately due north-south and forms a 40° angle with the Death Valley - Furnace Creek fault zone. This relationship suggests that the zone is a first order tension gash feature due predominantly to strike-slip

motion of the Death Valley - Furnace Creek fault zone. The formation of Panamint Valley is also related to this motion.

Figure 7.4 is a simplified representation of the major tectonic features in the Saline Valley region similar to that shown in Figure 7.1. The diagram in the left portion of the figure shows the present configuration of the mountains and valleys. By compressing the region in an east-west direction and imposing a left-lateral, northwest-southeast shear (shown by arrows at edge of diagram) the diagram on the right side of the figure can be obtained. This motion is the reverse of that proposed in this study for the development of the Sierra Nevada - Basin and Range transition zone. Therefore, the diagram on the right probably represents an earlier stage of evolution for the transition zone. If the present stress system continues to be active in the future, the valley areas shown in Figure 7.4 will continue to increase in size relative to the mountain areas and the rhombochasm valleys will continue to be downfaulted.

SUMMARY - RELATIONSHIP OF SALINE VALLEY TO REGIONAL TECTONIC DEVELOPMENT

1) Saline Valley is located in the transitional zone between the Sierra Nevada and Basin and Range provinces.
2) The transitional zone is characterized by features suggesting both east-west extension due to western migration of the Sierra Nevada and right-lateral, strike-slip faulting due to north-south compresion and related conjugate shearing.

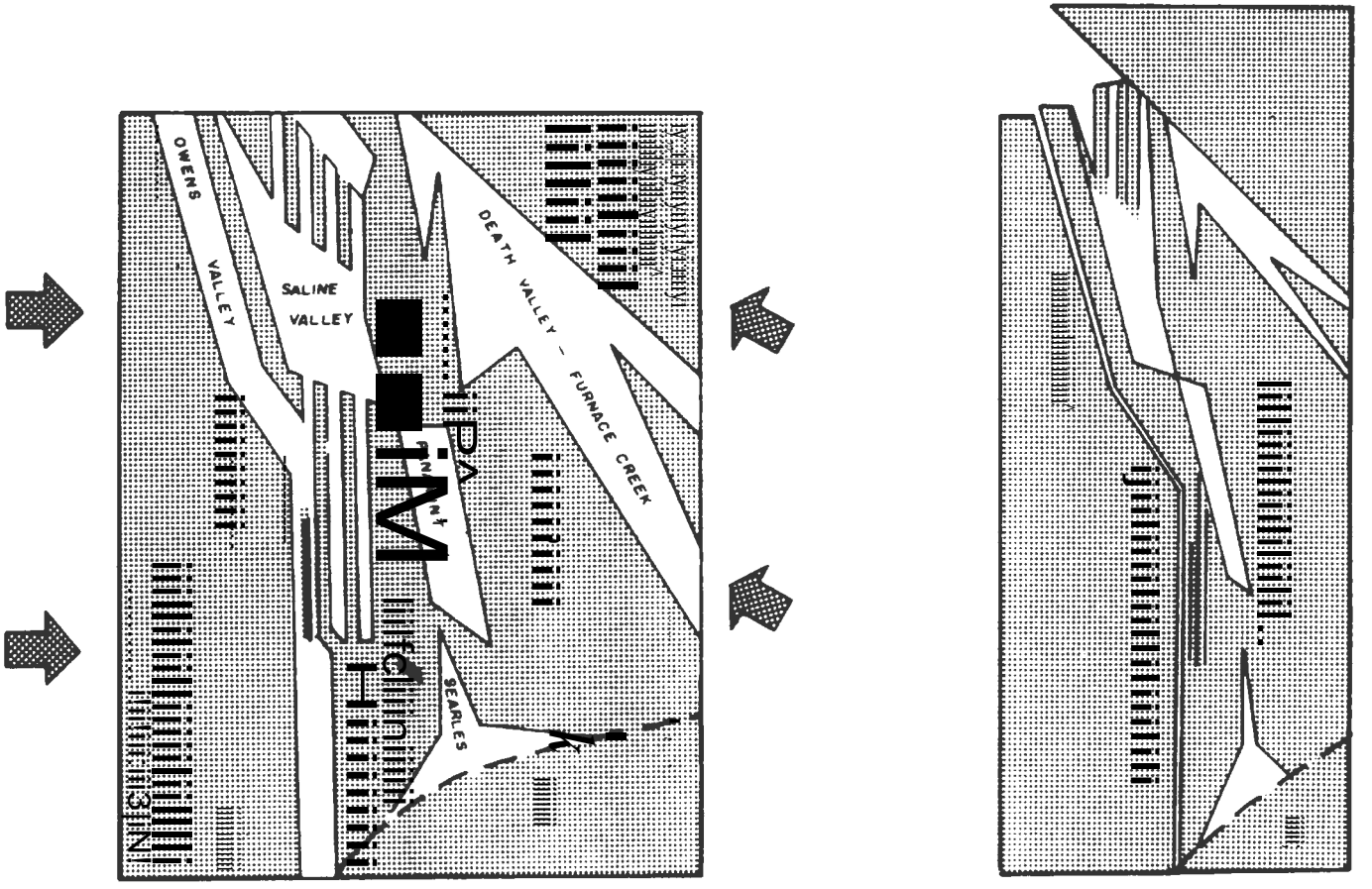

FIGURE 7.4. Idealized representation of study region showing how the major valleys and other extension features can be eliminated by reversing the movement on the faults. Valleys are shown as patternless areas and mountain areas by dotted pattern.

3) Saline Valley is a rhombohedral depression forming part of a regional tension gash zone.
4) Saline Valley formed in response to both east-west extensional forces and northwest-southeast strike-slip faulting.
5) Features observed in Saline Valley are typical of features in the transitional zone.
6) The overall character of the transitional zone is consistent with Wright's (1976) regional tectonic model.

SUGGESTIONS FOR FUTURE WORK

This study proposes that Saline Valley is an actively developing rhombochasm in a zone of extension and shearing transitional between the Sierra Nevada and Basin and Range provinces. To further test the hypothesis the following studies may be useful.

1. Detailed Geophysical Surveys. This should include seismic, gravity and magnetic surveys to better define the subsurface structure and distribution of faults in Saline Valley.
2. Periodic Geodetic Surveys. This should include the establishment and periodic resurveying of a permanent geodetic survey grid to measure both vertical and horizontal changes.
3. Microseismicity. A microseismic array should be established to determine the location and characteristics of deformation in the valley.
4. Dating of Fault Scarps. This study would obtain absolute ages for fault events using ^{14}C or other appropriate dating techniques to better determine the distribution of faulting with time.

5. Fault Scarp Analysis. This would involve detailed surveying of and trench logging of fault scarps to obtain data about the age, number of offsets, amount of offset, recurrence rate, etc.
6. In situ Stress Analysis. This could be obtained through rock mechanics studies in hard rock or inferred from geodetic measurements.
7. Joint Fracture Pattern and Lineament Analysis. This would include a detailed analysis of joint and fracture patterns in the region to help determine the stress pattern responsible for their formation and lineament analysis to help determine regional stress patterns.

8.0 SUMMARY AND CONCLUSIONS

The study area is located in the southwest portion of the Great Basin in the transitional zone between the Basin and Range and Sierra Nevada physiographic provinces. The study focused on the active faults located on the floor and borders of Saline Valley. The pattern, style and distribution of these faults were the basis for interpreting the characteristics of the local and regional tectonic regimes that are currently active. This chapter summarizes the results of the study and presents conclusions based on these results.

8.1 GRAPEVINE CANYON FAULT ZONE

1) This is a segment of the Panamint Valley/Grapevine Canyon fault zone.

2) At the southern end of the fault zone displacement is predominately right-lateral, strike-slip, at the northern end of the zone displacement is principally dip-slip. This relationship suggests that the zone resulted from a combination of strike-slip faulting and hinge faulting with a pivot point near Hunter Fountain.

3) The pattern of fault ruptures in the region between the mouth of Grapevine Canyon and the Low Granite Hills resulted from a combination of right-lateral, strike-slip faulting and northeast - southwest extension. Strike-slip displacement is estimated at between 700 and 2000 m. Extension may total 2500 m.

4) Unconsolidated sediments near San Lucas Canyon indicate up to 22 m of recent right-lateral, strike-slip offset. The mouth of

San Lucas Canyon may be offset by as much as 1 km. This segment of the Grapevine Canyon fault zone is characterized by right-lateral, strike-slip faulting with minor extension.

8.2 WESTERN FRONTAL FAULT ZONE

1) In the study area the western Frontal fault zone extends from Daisy Canyon to the northern border of the study area.
2) The zone is characterized by dip-slip faults.
3) Offsets in unconsolidated alluvial fan deposits indicate at least 32 m of offset since they were deposited.
4) Locally, there is evidence for at least three episodes of faulting.
5) Faults in the zone range from discrete, narrow zones to wide crushed and sheared zones.

8.3 EAST SIDE FAULT ZONE

1) The East Side fault zone is in the northcentral portion of the study area.
2) Faulting in this zone is characterized by horsts and grabens trending in a north-south direction.
3) The faults are quite young and generally display multiple displacements.
4) The faults are related to step faulting in the fountains to the east. These faults reflect continuing east-west extension of Saline Valley.

8.4 CENTRAL VALLEY FAULT ZONE

1) The Central Valley fault zone is located in the playa region

of Saline Valley.

2) The zone is characterized by small displacement normal faults in lacustrine and eolian sediments.

3) Based on the type of material and its commonly wet condition, and the preservation of the fault traces, the faults are quite young.

4) There is strong evidence that the playa is being tilted to the west.

5) Surficial features suggest, but do not confirm faulting of the playa sediments during the period 1947 to 1979.

8.5 LEE FLAT FAULT ZONE

1) Lee Flat is characterized by normal faults that trend northwest - southeast through unconsolidated alluvial sediments and basalt flows.

2) Lee Flat appears to represent a portion of a major tear or tension gash related to the formation of Saline Valley. This structure extends from the north border of the study area where it forms the west side of Saline Valley. At Daisy Canyon it forms a graben cutting across the Inyo Mountains and then widens to include Lee Flat. The structure appears to continue south into Centennial Flat and the Coso Range.

8.6 FAULT SCARP ANALYSIS

1) An analysis of the young fault scarps in the study area indicates that many of the faults have undergone several periods of faulting.

2) Faulting and deformation is still continuing.

3) The ages of faulting determined by Wallace's (1977) method commonly appear to be either too young or erratic.

4) Wallace's method appears to be useful for determining the number of events but not necessarily their ages.

8.7 JOINT ANALYSIS

1) An analysis of joint patterns in the Hunter Mountain batholith suggests that locally the joints are related to movement along the Grapevine Canyon fault zone.

2) The orientation of the joints were used to infer the local and regional stress patterns responsible for their formation.

8.8 SALINE VALLEY RHOMBOCHASM

1) Saline Valley displays characteristics of a rhombochasm formed by regional extension and shearing.

2) The valley is bounded on two sides by normal faults, on one side by oblique-slip faults and on one side by tension gashes.

3) The floor of the valley appears to have been downfaulted into a rhomb-shaped depression.

8.9 REGIONAL TECTONIC MODEL

1) Saline Valley is located in a transitional zone between the Basin and Range and Sierra Nevada provinces.

2) The physiographic features in the transitional zone resulted from a regional north-south compressive stress. This caused westward migration of the Sierra Nevada and northwest - southeast shearing along the west border of the Basin and Range.

9.0 REFERENCES AND SELECTED BIBLIOGRAPHY

A.G.I., 1972, Glossary of Geology, M. Gary, R. McAfee, C. Wolf, ed: American Geologic Institute, Washington, D.C., 857 p.

Allison, I., 1949, Fault pattern of south-central Oregon (abs): Geol. Soc. America Bull. v.60, p.1935.

Anderson, E.M., 1951, The dynamics of faulting and dyke formation with applications to Britian (2nd ed.) revised: Oliver and Boyd, Edinburgh, 206 pp.

Anderson, R., 1973, Large magnitude late tertiary strike-slip faulting north of Lake Mead, Nevada: U.S. Geol. Survey Prof. Paper 794, 18 p.

Attewell, P.B. and Farmer, I.W., 1976, "Principles of engineering geology": Chapman and Hall, London, 1045 p.

Atwater, T., 1970, Implications of plate tectonics for the Cenozoic evolution of North America: Geol. Soc. America Bull. v.81, p.3513-36.

Aubury, L.E., 1908, The copper resource of California: Bull. 50, California Min. Bur. 366 p.

Babcock, J. W. 1974, An Interpretation of late Cenozoic tectonics in the southwestern Great Basin of California: Unpublished manuscript.

Bachman, S.B., 1974, Depositional and structural history of the Waucobi Lake bed deposits, Owens Valley, California: Unpublished M.S., Thesis Univ. Calif., Los Angeles.

Bachman, S.B., 1975, Waucobi Lake bed deposits: evidence of late Tertiary deformation in Owens Valley, California: Geol. Soc. America Abstracts with programs, v.7, no.1, p.292.

Bachman, S.B., 1978, Plio-Pleisto Break-up of the Sierra Nevada - White - Inyo Mountains block and formation of Owens Valley: Geology, v.6, p.461-63.

Bailey, G.E., 1902, The Saline deposits of California: Bull. Calif. Min. Bur., v.24, 216 p.

Ball, S.H., 1907, A geologic reconnaissance in southwestern Nevada and Eastern California: U.S. Geol. Survey Bull. 308, 218 p.

Balk, R., 1937, Structural behavior of igneous rocks: Geol. Soc. America, Memoir 5.

Bateman, P.C., and Merriam, C.W., 1954, Geologic map of the Owens Valley region, California, in Jahns, R.H. ed. Geology of Southern California: Calif. Div. Mines Bull. 170, Map Sheet 11.

Beaty, C.B., 1961, Topographic effects of faulting - Death Valley, California: Assoc. Am. Geographers Annuals, v.51, no.2, p.234-40.

Billings, M.P., 1954, Structural geology, (2nd ed.): Prentice-Hall Inc., 514 pp.

Bishop, D.G., 1968, The geometric relationships of structural features associated with major strike-slip faults in New Zealand: New Zealand Jour. of Geology and Geophysics, v.11, no.2, p.405-17.

Burchfiel, B.C., 1969, Geology of the Dry Mountain quadrangle, Inyo Co., Calif.: California Div. Mines & Geol., Spec. Rept. 99.

Burchfiel, B.C., 1966, Tin Mountain landslide, southeastern California, and the origin of megabreccia: Geol. Soc. America Bull., v.77, p.95-100.

Burchfiel, B.C., and Steward, J.H., 1966, "Pull-apart" origin of the central segment of Death Valley, California: Geol. Soc. America Bull., v.77, p.439-42.

Burt, W.H., and Grossenheider, R.P., 1976, A field guide to mammals (3rd ed.): Houghton Mifflin Company, Boston, 289 p.

Campbell, M.R., 1902, Reconnaissance of the borax deposits of Death Valley and Mojave Desert: U.S. Geol. Survey Bull. 200, 23 p.

Carey, S.W., 1958, The tectonic approach to continental drift, in Carey (ed.), Continental Drift - A Symposium: Hobart Univ., Tasmania, pp.177-355.

Carr, W., 1974, Summary of tectonic and structural evidence for stress orienttion at the Nevada Test Site: U.S. Geol. Survey Open-File Report 74-176, 53 p.

Carver, G.A., 1969, Quaternary tectonism and surface faulting in the Owens Lake basin, California: M.S. Thesis Univ. Nevada - Reno.

Chapman, R.H., Healey, D.L., Troxel, B.W., 1971, Bouguer gravity map of California, Death Valley sheet: Calif. Div. Min. Geol., Map, 1 sheet.

Cloos, E., 1955, Experimental analysis of fracture patterns: Geol. Soc. America Bull., v.66, p.241-258.

Cloos, H., 1936, Einfuhrung in Die Geologie: Berlin, Bebruder Borntraeger.

Cooke, R.U., Warren, A., 1973, Geomorphology in deserts: Univ. Calif. Press., 364 p.

Davis, G.,and Burchfiel, B., 1973, Garlock fault: an intercontinental transform structure, Southern Calif.: Geol. Soc. America Bull., v.84, p.1407-1422.

DeGroot, H., 1890, Inyo County: Calif. Min. Bur. Rept. 10, p.209-218.

Dennis, J.C., (ed), 1967, International Tectonic Dictionary - English Terminology: American Assoc. Petroleum Geologists, Memoir 7.

Denny, C.S., 1965, Alluvial fans in the Death Valley region, California and Nevada: U.S. Geol. Survey Prof. Paper 466.

Diblee, T.W., 1967, Areal geology of the western Mojave Desert, Califiornia: U.S. Geol. Survey Prof. Paper, 522, p.153.

Donath, T.W., 1967, Analysis of basin-range structure, south-central Oregon: Geol. Soc. America Bull. v.73, p.1-16.

Fairbanks, H.W., 1894, Preliminary report on the mineral deposits in Inyo, Mono, and Alpine counties, California: Calif. State Min. Bur. Rept. 12, p.472-78.

Firman, R.J., 1960, The relationship between joints and fault patterns in the Eskdale Granite (Cumberland) and the adjacent Borrowdale Volcanic Series: Geol. Soc. London, Quart. Jour., v.116, Part 3, p. 317-347.

Friedman, M., Handin, J., Logan, J.M., Min, K.D., Sterns, D.W. (1976), Experimental folding of rocks under confining pressure: Part III: faulted drape folds in multilithologic layered specimens: Geol. Soc. America Bull. v.87, p1049-1066.

Gale, H.S., 1912, Salt, borax, and potash in Saline Valley, Inyo County, Calif.: U.S. Geol. Survey Bull. 540, Contributions to Economic Geology, p.416-421.

Gilbert, G., 1874, Preliminary Geological Report, Expedition of 1872: U.S. Geog. and Geol. Survey West of the 100th Merridian, Progress Rept. p.48-52.

Gilbert, G., 1928, Studies of Basin-Range Structure: U.S. Geol. Survey Prof. Paper 153, 92p.

Gilbert, G.K., 1875, Report on the geology of the portions of Nevada, Utah, California, and Arizona: U.S. Geog. Geol. Surveys West of the 100th Merridian, v.3, p.17-187.

Gilluly, J., 1965, Volcanism, tectonism, and plutonism in the western United States: Geol. Soc. America Spec. Paper 80.

Gilluly, J., 1970, Crustal deformation in the western United States: in Johnson, H. and Smith, (eds.), The megatectonics of continents and oceans: New Brunswick, N.J., Rutgers Univ. Press p.47-73.

Goodyear, W.A., 1888, Inyo County: in Report of the State Mineralogist v.8, p.224-309.

Gutenberg, B. and Richter, C., 1954, Seismicity of the earth: Princeton Univ. Press.

Hafner, W., 1951, Stress distributions and faulting: Geol. Soc. America Bull., v.62, p.373-98.

Hall, W.E., 1971, Geology of the Panamint Butte Quadrangle, Inyo, Co., California: U.S. Geol. Survey Bull. 1299.

Hall, W.E. and Stephens, H.G., 1963, Economic geology of the Panamint Butte quadrangle and Modoc District, Inyo Co., California: Calif. Div. Mines and Geol. Spec. Rept. 73.

Hall, W.E. and MacKevett, E.M. Jr., 1958, Economic geology of the Darwin quadrangle Inyo Co., California: Calif. Div. Mines and Geol. Spec. Rept. 51.

Hall, W.E., MacKevett, E.M., Jr. 1962, Geology and Ore Deposits of the Darwin Quadrangle Inyo Co., California: U.S. Geol. Survey Prof. Paper 368.

Hamilton, W. and Myers, W.B., 1966, Cenozoic tectonics of the western United States: Reviews of Geophysics, v.4, no.4, p.509-549.

Handin, J., Freidman, M., Min, K.D., Pattison, L.J., 1976, Experimental folding of rocks under confining pressure: Part II. Buckling of multilayered rock beams: Geol. Soc. America Bull., v.87, p.1035-48.

Hardie, L.A., 1968, The origin of the recent non-marine evaporite deposite of Saline Valley, Inyo, California: Geochim. Cosmochim. Acta. v.32, no.12, p.1279-1301.

Healy, J.H. and Press, F., 1964, Geophysical studies of basin structures along the eastern front of the Sierra Nevada: Geophysics, v.29, no.37, p.337-351.

Hill, M.L. and Troxel, B.W., 1966, Tectonics of Death Valley region, California: Geol. Soc. America Bull., v.77, p.435-38.

Hopper, R.H., 1947, Geologic section from the Sierra Nevada to Death Valley, California: Geol. Soc. America Bull., v.58, p.393-432.

Hunt, C.B., 1966, General geology of Death Valley, California: U.S. Geol. Survey Prof. Paper 494-B.

Hubbert, M.K., 1951, Mechanical basis for certain familiar geologic structures: Geol. Soc. America Bull., v.62, no.4, p.355-72.

Hunt, C.B., and Mabey, D.R., 1966, Statigraphy and structure of Death Valley, California: U.S. Geol. Survey Prof. Paper 494-A.

Inman, D.L., 1952, Measures for describing the size distribution of sediments: Jour. Sed. Petrology, v.22, no.3, p.125-145.

Jaeger, J.C., 1969, "Elasticity, fracture and flow: With Engineering and Geological Applications: Chapman and Hall, London.

Jaeger, J.C. and Cook, N.G.W., 1969, "Fundamentals of rock mechanics": Chapman and Hall, London.

Jennings, C.W., (compiler) 1958, Geologic map of California - Death Valley sheet: Calif. Div. Mines and Geol., map, 1 sheet.

Jennings, C.W., 1975, Geologic data map #1, Fault map of California: Calif. Div. Mines and Geol., Bull. 201.

Keely, J.S., Stevens, C.H., 1975, Nature and regional significance of thrust faulting in the southern Inyo Mountains, eastern California: Geology, v.3, no.9, p.524-26.

King, P., 1959, The evolution of North America: Princeton Univ. Press, 190 p.

Knopf, A., 1913, Mineral resources of the Inyo and White Mountains, California: U.S. Geol. Survey Bull. 540-B.

Knopf, A., 1918, A Geologic reconnaissance of the Inyo Range and the eastern slope of the southern Sierra Nevada, California: U.S. Geol. Survey Prof. Paper 110, 130 p.

Krumbein, W.C., 1934, Size frequency distributions of sediments: Jour. Sed. Petrology, v.4, p.65-77.

LaConte, J., 1889, The origin of normal faults and the structure of the basin region: Am. Jour. Sci., 3rd ser., v.38, p.257-263.

Laubscher, H.P., 1958, Critical examination of the Moody and Hill principles of wrench fault tectonics: Bol. Informativo, Assoc. Venezozana de Geologia, Mineria y Petroleo, v.1, p.14-26.

Leet, L.D., and Judson, S., 1971, Physical geology (4th ed.): Printice-Hall, Inc.

Lensen, G.J., 1958, A method of horst and graben formation: Jour. Geol., v.66, p.579.

Lensen, G.J., 1959, Secondary faulting and transcurrent splay-faulting at transcurrent fault intersections: New Zealand Jour. Geol. and Geophysics, v.2, p.729.

Lensen, G.J., 1976, Earth deformation in relation to town planning in New Zealand: Unpub. Report, New Zealand Geological Survey.

Locke, A., Billingsley, P., and Mayo, E., 1940, Sierra Nevada tectonic pattern: Geol. Soc. America Bull., v.51, p.513-40.

Lombardi, O.W., 1963, Observations on the distribution of chemical elements in the terrestrial saline deposits of Saline Valley, California: N.O.T.S. TP 2916, U.S. Naval Ordance Test Station, China Lake, Calif.

Lombardi, O.W., 1964, Extreme deformation in Saline Valley, California as related to the general deformation of the western states (abs.): Geol. Soc. America Spec.76.

Mabey, D., 1963, Complete bouguer anomaly map, Death Valley Region, California: U.S. Geol. Survey Map GP-305, 1 sheet.

Mackin, J., 1960, Structural significance of Tertiary volcanic rocks in southwestern Utah: Am. Jour. Sci., v.258, no.2, p.81-131.

Maxson, J.H., 1950, Physiographic features of the Panamint Range California: Geol. Soc. America Bull., v.61, p.99-114.

Maxwell, J.C., and Wise, D.V., 1958, Wrench fault tectonics: a discussion: Geol. Soc. America Bull., v.69, no.7, p.927-8.

McAllister, J.F., and Agnew, A.F., 1948, Playa scrapers and furrows on the Racetrack Playa, Inyo Co., California (abs): Geol Soc. America Bull., v.59, no.12, p.1377.

McAllister, J.F., 1952, Rocks and structure of the Quartz Spring area, northern Panamint Range, California: Calif. Div. Mines, Special Rept. 25, 38 p.

McAllister, J.F., 1955, Geology of mineral deposits in the Ubehebe Peak quadrangle, Inyo Co., California: Calif. Div. Mines, and Geol., Spec. Rept. 42.

McAllister, J.F., 1956, Geology of the Ubehebe Peak Quadrangle, California: U.S. Geol. Survey Map GP 95, 1 sheet.

McKee, E.H., 1968, Age and rate of movement of the northern part of Death Valley - Furance Creek fault zone, California: Geol. Soc. America Bull., v.79, p.509-12.

McKinstry, H.E., 1953, Shears of the second order: Am. Jour. Sci., v.251, p.401-14.

McManus, D.A., 1963, A criticism of certain usage of the Phi-notation: Jour. Sed. Petrology, v.33, no.3, p.670-674.

Merriam, C.W., 1954, Rocks of Paleozoic age in Southern California: Calif. Div. Mines, Bull. 170, Ch3, p.9-14.

Merriam, C.W., and Hall, W.E., 1957, Pennsylvanian and Permian rocks of the southern Inyo Mountains: U.S. Geol. Survey Bull, 1061-A, p.1-15.

Merriam, C.W., 1963, Geology of the Cerro Gordo mining district, Inyo Co., California: U.S. Geol. Survey Prof. Paper 408, 83 p.

Michael, E., 1966, Large lateral displacement on Garlock fault, California as measured from offset fault system: Geol. Soc. America Bull. v.77, p.111-114.

Miller, R.H., 1976, Revision of Upper Ordovician, Silurian, and Loser Devonian stratigraphy, southwestern Great Basin: Geol. Soc. America Bull. v.87, p.961-68.

Mohr, O., 1871, 1872, Beitrage Zur Theorie des Erdruchs: Zeitcher Architekten und Ingenieur - Ver Hannover, v.17, p.334; v.18, p.67,245.

Mohr, O., 1882, Uber die Darstellung des Spannungzustandes Eines Korpelementes: Zivil Ingenieur, p.113.

Mohr, O., 1900, Welche Umstande Bedingen die Elastizitat und den Bruch eines Materials: Zeitschr. Vereins Deutsches Ing. p.1524.

Moody, J.D., and Hill, M.H., 1956, Wrench fault tectonics: Geol. Soc. America Bull. v. 67, p.1207-46.

Moody, J.D., and Hill, M.G., 1964, Moody and Hill system of wrench fault tectonics: reply: Bull. American Assoc. Pet. Geol. v.48, no.1, p.112-122.

Nadai, A., 1952, "Theory of fracture and flow of solids" (2nd ed.) v.1: McGraw-Hill, N.Y.

Nolan, T.B., 1943, The Basin and Range province of Utah, Nevada, and California: U.S. Geol. Survey Prof. Paper 197-D, p.141-196.

Norman, L.A., and Stewart, R.M., 1951, Mines and mineral resources of Inyo Co., California: Jour. of Mines and Geol., v.47, p.17-223.

Pakiser, L.C., Kane, M.H., 1964, Structural geology and volcanism of Owens Valley region, California - a Geological Study: U.S. Geol. Survey Prof. Paper 438.

Parker, T.S., 1976, The sedimentology and petrography of the Keeler Canyon Fm. at Ubehebe Mine Canyon, California: MS Thesis, Stanford Univ. Calif.

Price, N.J., 1966, Fault and Joint Development in brittle and semibrittle rock: Pergamon Press, 176pp..

Prucha,. J.J., 1964, Moody and Hill system of wrench fault tectonics: discussion: Bull. American Assoc. Pet. Geol., v.48, no.1, pp.106-11.

Ramsay, J.G., 1962, The geometry of conjugate fold systems: Geological Magazine, v.99, no.6.

Rantz, S. E., 1969, Mean annual precipitation in the California region, U.S. Geol. Survey Water Resources Division, Basic Data Compilation, Map, 2 sheets.

Rankine, W.J.M., 1957, On the stability of loose earth: Royal Society of London, Philos, Tr., v.147.

Raymond, R.W., 1873, Statistics of mines and mining in the states and territories west of the Rocky Mountains for 1872: 5th Ann. Rept., U.S. Commissioner Mining Statistics, U.S. Treasury Dept. p.1-550.

Ross, R.J., 1964, Middle and Lower Ordovician formations in southernmost Nevada and Adjacent California. U.S. Geol. Survey Bull. 1180-C, 101pp.

Ross, D.C., 1967a, Generalized geologic map of the Inyo Mountains region, California: U.S. Geol. Survey Miscellaneous Geologic Investigations, Map I-506.

Ross, D.C., 1967b, Geologic map of the Waucoba Wash quadrangle, Inyo Co., California: U.S. Geol. Survey Map GQ-612.

Ross, D.C., 1969, Descriptive petrography of three large granitic bodies in the Inyo Mountains, California: U.S. Geol. Survey Prof. Paper 601, 47 pp.

Ross, D.C., 1970, Pegmatitic trachyandesite plugs and associated volcanic rocks in the Saline Range - Inyo Mtns. region, California: U.S. Geol. Survey Prof. Paper 614-D, 29pp.

Ryall, A., Slemmons, D.B., and Gedney, L., 1966, Seismicity, tectonism and surface faulting in the western United States during historic times: Bull. Seismol. Soc. America, v.56, p.1105-35.

St. Armand, P. and Roquemore, G. R., 1979, Tertiary and Holocene development of the southern Sierra Nevada and Coso Range, California: Tectonophysics, 52(1979) 409-410.

Sanford, A.R., 1959, Analytical and experimental study of simple geologic structures: Geol. Soc. America Bull., v.70, pp.19-52.

Schultz, J.R., 1937, A late Cenozoic fauna from the Coso Mountains, Inyo Co., California: Carnegie Inst. Washington, Pub. 487, p.75-109.

Scholz, C., Barazangi, M., and Spar, M., 1971, Late Cenozoic evaluation of the Great Basin, western United States, as an ensialic interarc basin: Geol. Soc. America Bull., v.82, p.2979-2990.

Sharp, R.P. and Carey, D.L., 1975, Sliding stones, Racetrack Playa, California Geol. Soc. America Abst. with programs, v.7, no.7, p.1267.

Shawe, D.R., 1965, Strike-slip control of basin-range structure indicated by historical faults in western Nevada: Geol. Soc. America Bull., v.76, p.1361-78.

Shelton, J.S., 1953, Can wind move rocks on Racetrack Playa?: Science, v.117, no.3042, p.438-9.

Slemmons, D.B., 1967, Pliocene and Quarternary crustal movements of the Basin and Range Province, U.S.A.: Jour. Geoscience, Osaka City Univ., v.10, Art. 1-11, p.91-103.

Slemmons, D.B., and McKinney, R., 1977, Definition of "active fault": Misc. Paper S-77-8, U.S. Army Engineer Waterways Experiment Station, Soils and Pavements Laboratory, Vicksburg, Miss.

Smith, R.S.U., 1974, Quarternary thrust movement on a boundary fault at the north end of Panamint Valley, western Basin-and-Range, Calif.: Geol. Soc. America Abstracts with Programs, Cordilleran Section.

Smith, R.S.U., 1975a, Late-Quarternary pluvial and tectonic history of Panamint Valley, Inyo and San Bernadino Counties, California: Ph.D. Thesis, Calif. Inst. Tech.

Smith, R.S.U., 1975b, Guidebook to the Quarternary tectonics of Panamint Valley, California: Geol. Soc. America Field Trip, Cordilleran Section.

Smith, R.S.U., 1978, Pluvial history of Panamint Valley, California: Guidebook for the Friends of the Pleistocene, Pacific Cell.

Spurr, J.E., 1903, Descriptive geology of Nedvada south of the 40th parallel and adjacent parts of California: U.S. Geol. Survey Bull. 208, 229p.

Stanley, G.M., 1955, Origin of playa stone tracks, Racetrack Playa, Inyo Co., California: Geol. Soc. America Bull., v.66, no.11, p.1329-1350.

Stebbins, R.C., 1966, A field guide to western reptiles and amphibians: Houghton Mifflin Company, Boston, 277p.

Stevens, C.H., and Olson, R.C., 1972, Nature and significance of the Inyo thrust fault, eastern California: Geol. Soc. America Bull., v.83, no.12, p.3761-3768.

Stewart, J.H., 1966, Correlation of Lower Cambrian and some Precambrian strata in the southern Great Basin, California and Nevada: Geol. Sur. Res. 1966, Prof. Paper 550-C, p.C66-C 72.

Stewart, J.H., 1970, Upper Precambrian and Lower Cambrian strata ain the southern Great Basin, California and Nevada: U.S. Geol. Survey Prof. Paper 620, 206pp.

Stewart, J.H., 1971, Basin and Range structure: a system of horsts and grabens produced by deep-seated extension: Geol. Soc. America Bull., v.82, p.1019-1040.

Streitz, R., and Stinson, M., 1974, Geologic map of California, Death Valley Sheet: Calif. Div. of Mines and Geology, map, 1 sheet.

Tchalenko, J.S., 1970, Similarities between shear zones of different magnitudes: Geol. Soc. America Bull., v.81, p.1625-40.

Thompson, G., 1966, The rift sytem of the western United States: in. The World Rift System - International Upper Mantle Commission Symposium, Ottawa: Can. Geol. Surv. Paper. 66-14, p.280-290.

Thompson, G.A., and Burkee, D.B., 1974, Regional geophysics of the Basin and Range province: Annual Review of Earth and Planetary Sciences, v.2, p.213-237.

Tschanz, C. and Pampeyan, E., 1970, Geology and mineral deposits of Lincoln Co., Nevada: Nev. Bur. Mines Bull. 73, p.83-84.

Tucker, W.B., and Sampson, R.J., 1938, Mineral resources of Inyo Co. California: Jour. of Mines and Geology, v.34, no.4, p.368-500.

Visher, S.S., 1954, Climatic atlas of the United States: Harvard Univ. Press, Cambridge, Mass., Harvard Univ. Press, 403p.

Walcott, C.G., 1897, The post-Pleistocene elevations of the Inyo Range, and the lake beds of Waucobi Embayment, Inyo, Co., California: Jour. of Geol., v.5, p.340-348.

Wallace, R.E., 1977, Profiles and ages of young fault scarps, northcentral Nevada: Geol. Soc. America Bull., v.88, no.9, p.1267-81.

Waring, C.A., and Huguenin, E., 1916, Inyo Co.: California Min. Bur. Rept. 15, p.25-130.

Waring, C.A., 1917, Geological map of Inyo Co., California: Calif. State Min. Bureau, Map 14.

Whitney, J.D., 1865, Geological survey of California Vol.1: Geology, 498pp.

Wolman, M.G., 1954, A method of sampling coarse river-bed material: Transaction, American Geophysical Union, v.35, no.6.

Wood, A., 1942, The development of hillside slopes: Geologists Assoc. Proc., v.53, p.128-140.

Wright, L.A., and Troxel, B.W., 1968, Evidence of northwestward crustal spreading and transform faulting in the southwestern part of the Great Basin, California and Nevada (abs): Geol. Soc. America Spec. Paper 121, p.580-81.

Wright, L.W., and Troxel, B.W., 1971, Thin-skinned megaslump model of Basin-Range structure as applicable to southwestern Great Basin: Geol. Soc. America Abs. with Programs, v.3, p.758.

Wright, L., 1976, Late Cenozoic fault patterns and stress fields in the Great Basin and westward displacement of the Sierra Nevada block: Geology, v.4, p.489-94.

Young, A., 1972, Slopes: Oliver and Boyd, Edinburgh, 288p.

APPENDIX A

STRATIGRAPHY

A.1 PALEOZOIC SEDIMENTARY ROCKS

Detailed differentiation and descriptions of the Paleozoic sedimentary rocks cropping out in the study area are given by McAllister (1952, 1955, 1956), Nolan (1943), Hunt and Mabey (1966) and Ross (1967). Because this study is concerned principally with the tectonic development of the region, these units are of significant importance only when affected by late Cenozoic faulting or deformation. Consequently, only brief descriptions of the units, based of the above references are given.

CAMBRIAN

Bonanza King Formation

The Bonanza King Formation (Racetrack Dolomite of McAllister, 1956) consists of beds of dolomite ranging from nearly black to grayish yellow. The unit contains varied quantities of nodular chert and locally in a lower section shaley dolomite. Where exposed, the top of the unit is marked by the distinctive shale and chert beds at the base of the overlying Nopah Formation.

Nopah Formation

The Nopah Formation consists principally of gray and grayish-yellow dolomite beds. Locally, the dolomite contains irregularly distributed chert nodules. The basal portion consists of brownish-

weathering shale, cherty limestone, and dolomite. The formation is approximately 490 m thick in the study area. Upper Cambrian fossils are common.

ORDOVICIAN

Pogonip Group

The lowest portion of the Pogonip Group (Pogonip Limestone of McAllister, 1956) consists of medium-gray dolomite similar to the underlying Nopah Formation. It weathers to yellow-tinged gray and contains some limestone and thin lenses of light-gray chert. The middle section contains light-brown shale, shaley limestone and siliceous limestone that has a characteristic crepe structure and weathers conspicuously brown. The upper section of the formation consists of gray dolomite that weathers yellowish-gray and locally contains irregularly distributed sandy or quartizitic sections. Both the middle and upper portions are fossiliferous. Total thickness in the area is about 440 m.

Eureka Quartzite

The lower portion of the Eureka Quartzite consists of slabby iron-bearing quartzite weathering to brown with some interstratified shale. The upper portion is massive vitreous quartzite that is nearly white and weathers to pale tints. Both sections contain some cross stratification. No fossils have been identified in this unit. Total thickness in the area is about 122 m.

Ely Springs Dolomite

The Ely Springs Dolomite has a lower section of dark-gray dolomite containing chert nodules. The unit grades upward from the dark-gray dolomite at the base to medium gray dolomite. The unit has a maximum thickness of about 185 m in the area. The dark-gray lower section is fossiliferous.

SILURIAN - DEVONIAN

Hidden Valley Dolomite

The Hidden Valley Dolomite consists of cherty, medium-gray dolomite in the lower section, very light-gray (nearly white) coarse grained dolomite in the middle section, and medium-gray dolomite, which tends to weather light olive gray, in the upper section. The thickness of each of these sections is highly variable. the formation boundaries poorly defined. The cherty, moderately dark lowest section resembles the dark, cherty section of the underlying Ely Springs Dolomite but is distinguished by its olive gray weathering and abundant fossils. Total thickness at the type locality is 416 m.

DEVONIAN

Lost Burro Formation

The Lost Burro Formation consists predominantly of light- and dark-gray interbedded limestone and dolomite. Brownish-weathering siliceous beds mark the upper and lower boundaries. The basal dolomite is locally cherty and shaley but is principally sandy or quartaitic. The upper boundary of the formation is marked by a much

thinner sandy and quartzitic zone, which weathers brown in contrast to the bulk of the formation. Total thickness at the type locality is 465 m.

MISSISSIPPIAN

Tin Mountain Limestone

The Tin Mountain Limestone consists of uniformly dark limestone in contrast to the underlying, striped Lost Burro Formation. The lower part consists of thin, dark limestone beds interstratified with some light brownish-gray to pale-red calcareous shale. The upper section consists of cliff-forming, dark limestone, with some pale-red shaley partings along the beds. The unit also contains thin chert lenses that are larger and more noticeable in the upper section. Total thickness at the type locality is 145 m.

Perdido Formation

The Perdido Formation is lithologically transitional between the underlying Tin Mountain Limestone and overlying Rest Springs Shale. The Perdido Formation consists of limestone interbedded with shale, chert, calcareous siltstone, fine-grained sandstone, sandy limestone, and minor conglomerate. Vertical and lateral diversity is characteristic of the formation. The lower portion of the unit is predominantly dark limestone with interstratified shale and chert beds. The upper part, which weathers to yellowish- or reddish-brown, consists of siltstone, sandstone, and quartzite. The top of the unit is marked by a thin limestone bed lying on reddish or light-gray, very soft shale. The unit is 183 m thick at the type locality.

PENNSYLVANIAN

Rest Springs Shale

The Rest Springs Shale consists of dark-gray or olive-gray, fine-grained clastic constituents and minor limestone. The lower shale section grades upward into sandstone, which in the type locality contains some quartzite and a few thin beds of pebbly conglomerate. Because the unit is highly incompetent, measured thicknesses range from 61 to 305 m. Only a few poorly preserved fossils have been found.

PENNSYLVANIAN - PERMIAN

Keeler Canyon Formation

The Keeler Canyon Formation [part of McAllister's (1956) Bird Springs Formation] consists of thinly-bedded, bluish-gray, silty and sandy, limestone, clean limestone, limestone breccia, shale, and locally, minor siltstone. The unit has a banded appearance formed by alternating bluish-gray limestone and thin white or light-gray bands of marble. The lower portion contains chert nodules 1 to 5 cm in diameter. The thickness varies from 556 to 1220 m.

PERMIAN

Owens Valley Formation

The Owens Valley Formation [part of McAllister's (1956) Bird Springs Formation] consists of three informal units. The lowest and most widely distributed unit consists principally of thin-bedded, fine-grained calcarenite. Shaley limestone, lenses of pure limestone

and limestone breccia, shale, and siltstone are common. Lenses of massive bluish-gray limestone and limestone breccia are characteristic of the lower portion of the unit. The middle portion consists predominantly of shale, but also contains lesser amounts of siltstone and limestone. The upper unit has a basal 20 m thick limestone conglomerate, a middle 10 m thick section of light-gray, fine-grained orthoquartzite, and an upper 30 m thick section of light-yellow and yellowish-brown-weathering siltstone and light-gray calcarenite with minor yellowish-weathering pebble conglomerate. Total thickness of the formation is 970 m.

A.2 MESOZOIC INTRUSIVE ROCKS

JURASSIC

Hunter Mountain quartz monzonite

The Hunter Mountain Quartz Monzonite (McAllister, 1956) consists predominantly of light-gray, medium- to coarse-grained hornblende quartz monzonite. Associated with the quartz monzonite are a wide range of border facies, commonly syenodiorite, monzonite, and syenite with lesser amounts of pegmatite, aplite, and lamprophyre. Coarse textures commonly display a local subparallel arrangement of elongate feldspars. Inclusions are locally abundant in the finer-grained portions of the quartz monzonite. A typical specimen of the quartz monzonite consists of the following: 40% orthoclase, 40% plagioclase, 14% quartz, 4% horn-blende, nearly 1% each of magnetite and sphene, and traces of biotite, apatite, epidote, and sericite. Based on

radiometric dating of similar granitic bodies in the area, the Hunter Mountain Quartz Monzonite is considered to be approximately 180 million years old, or early Jurassic.

A.3 LATE CENOZOIC VOLCANICS

McAllister (1956) described the 8 to 16 m thick olivine basalt flows as remnants of thick volcanic sequences that are extensively exposed in the region. These flows are thought to be between 2 and 3 my (per com., P. St. Amand, 1979) The flows are commonly medium dark-gray, but range from dark-gray through medium-gray to light brownish gray, and readily acquire a brownish-black desert varnish. Some of the flows are amygdaloidal and vesicular. The textures are aphanitic or porphyritic-aphanitic with phenocrysts of olivine and clear plagioclase. Reddish-brown scoria and fragmental olivine basalt underlie the dark flows. Scoria and volcanic bombs locally mark possible vent locations. The flows continue virtually without interruption southwestward of the study area to the type locality of the Cosco Formation which is late Pliocene or early Pleistocene in age.

A white, 2 m thick tuff bed is exposed on the divide between Grapevine and Mill Canyons near the summit of Hunter Mountain. Tuffaceous detritus has been identified by Lombardi (1963) in alluvium underlying the olivine basalt flows. Tuffaceous detritus is also found in unconsolidated lacustrine sediments exposed about 4 km northwest of the mouth of Grapevine Canyon and in unconsolidated beach gravels and sands at the juncture of the Inyo Mountains front and alluvial apron about 5 km southeast of the tramway.

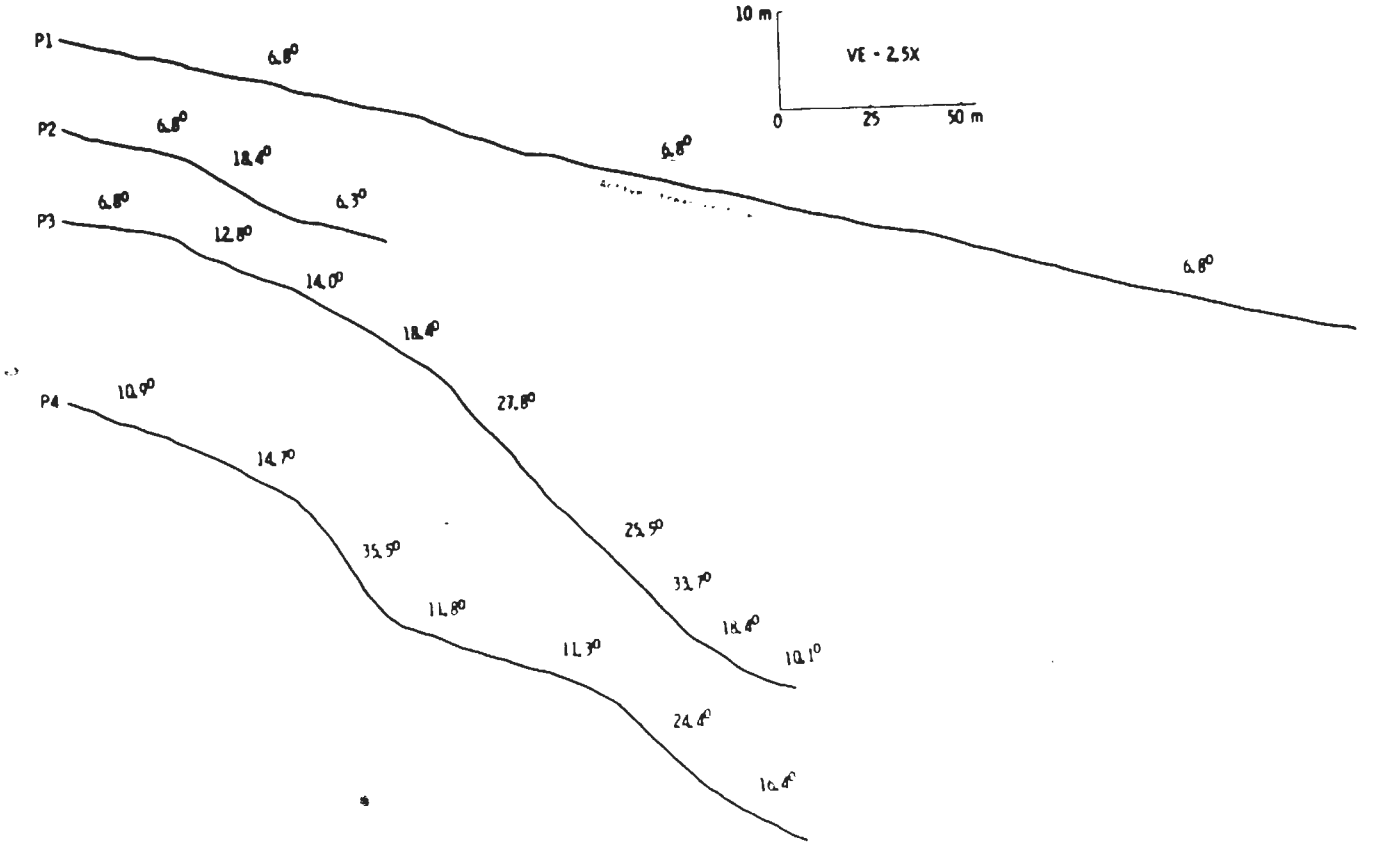

FIGURE B.1. FAULT SCARP PROFILES

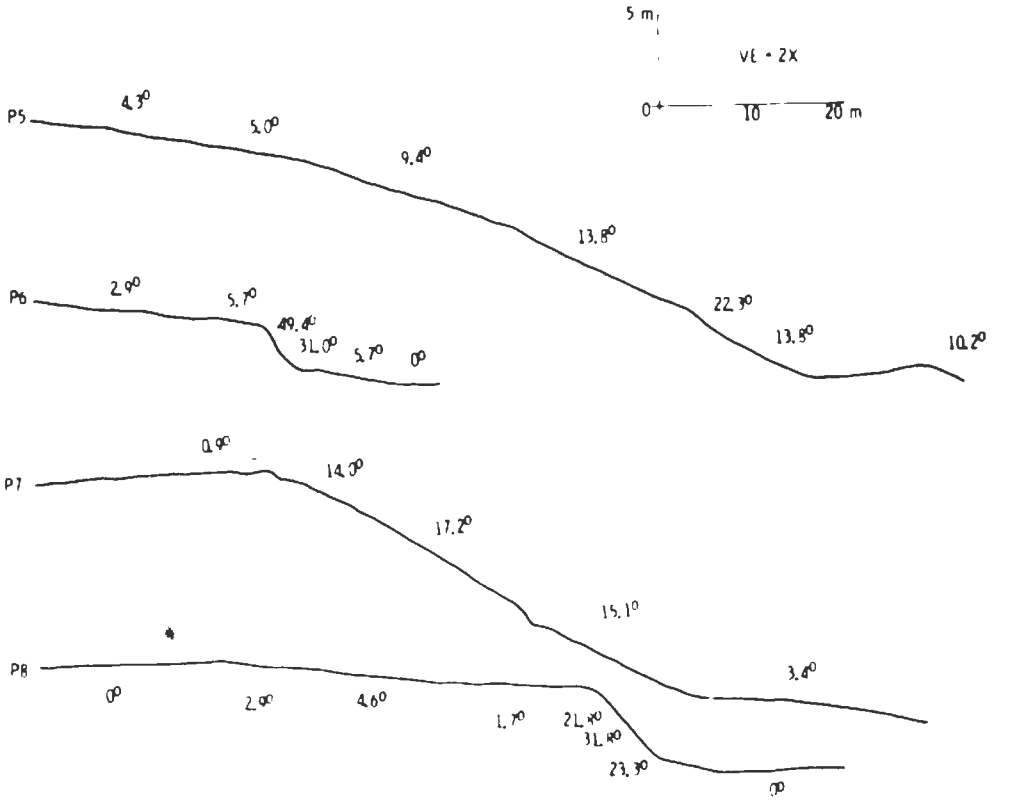

FIGURE B.1. (CONT)

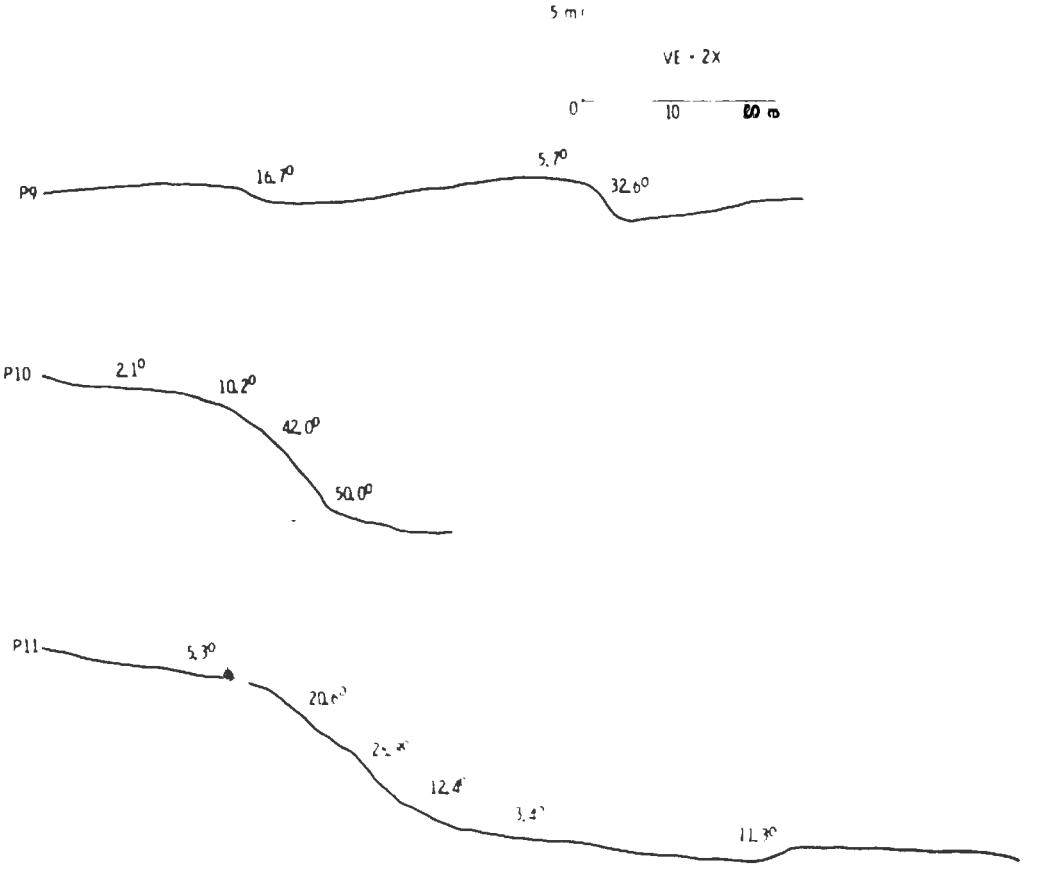

FIGURE B.1. (CONT.)

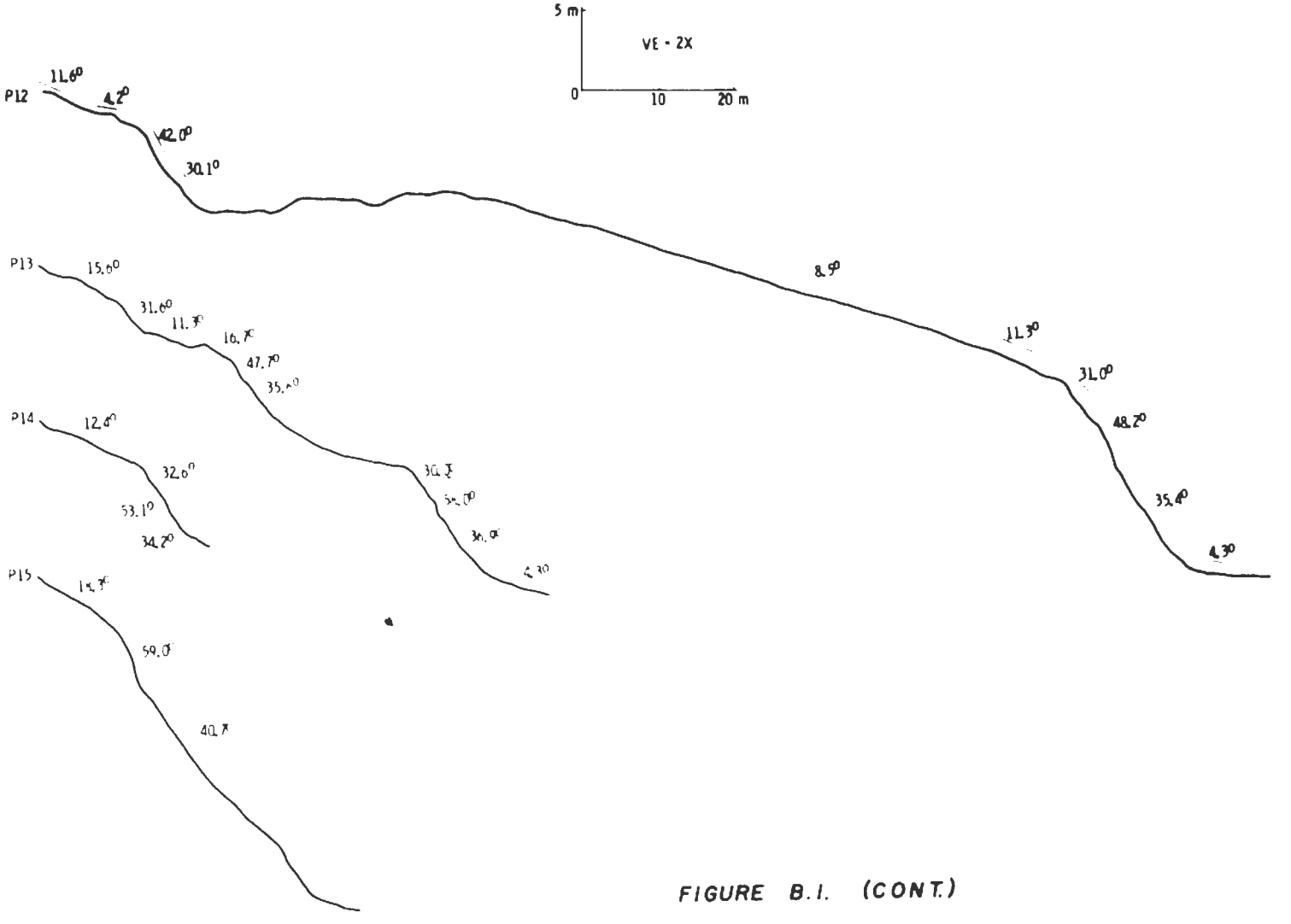

FIGURE B.I. (CONT.)

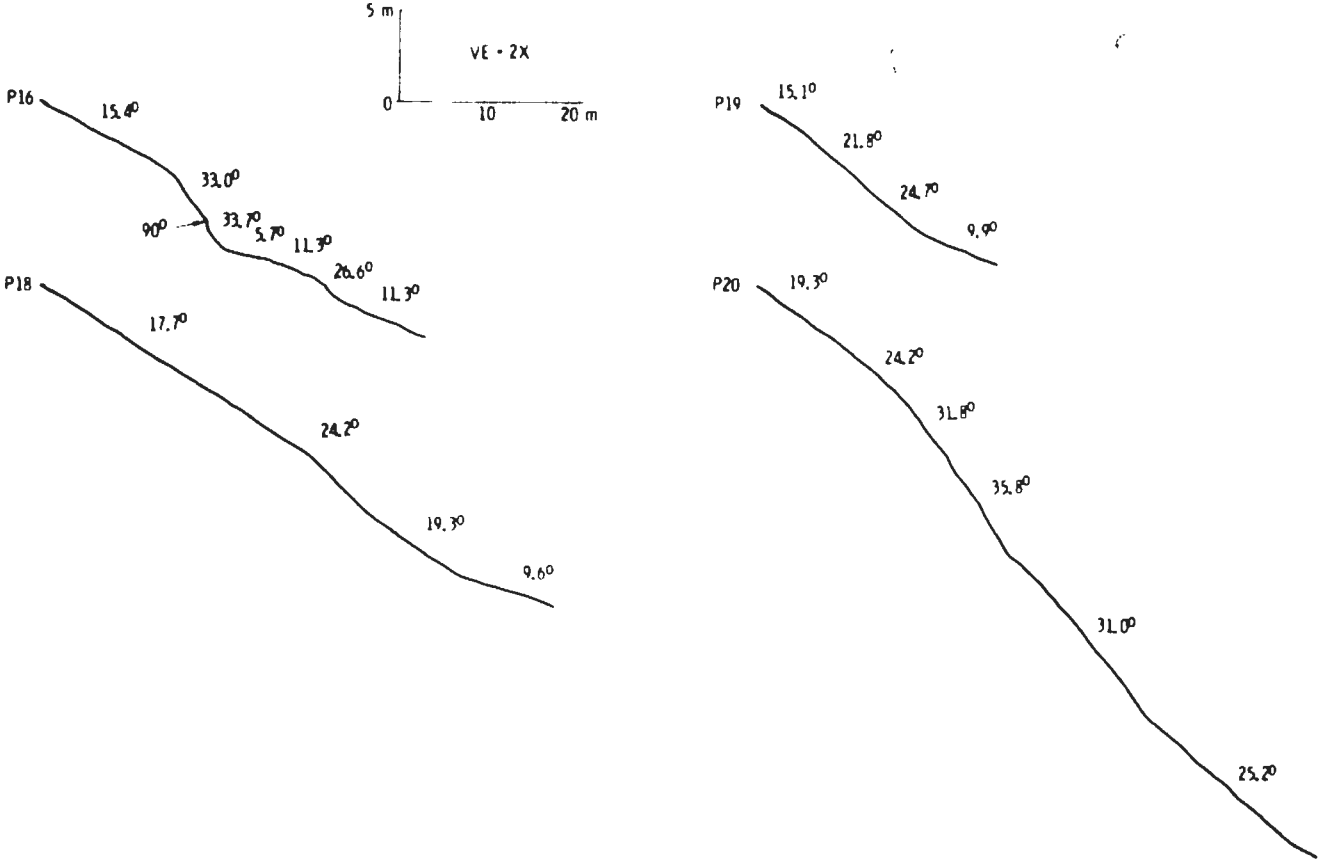

FIGURE B.1. (CONT'D)

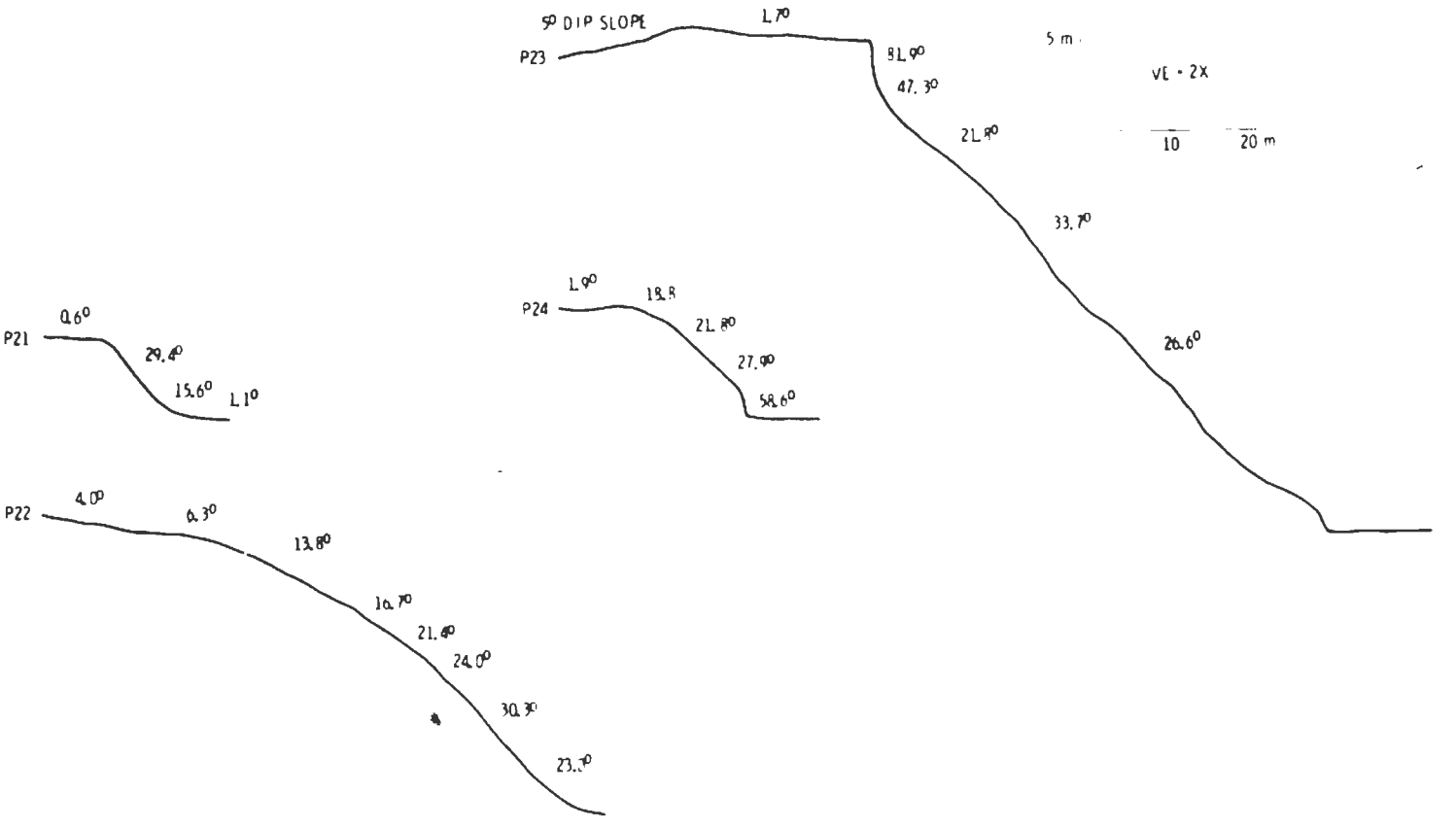

FIGURE B.1. (CONT)

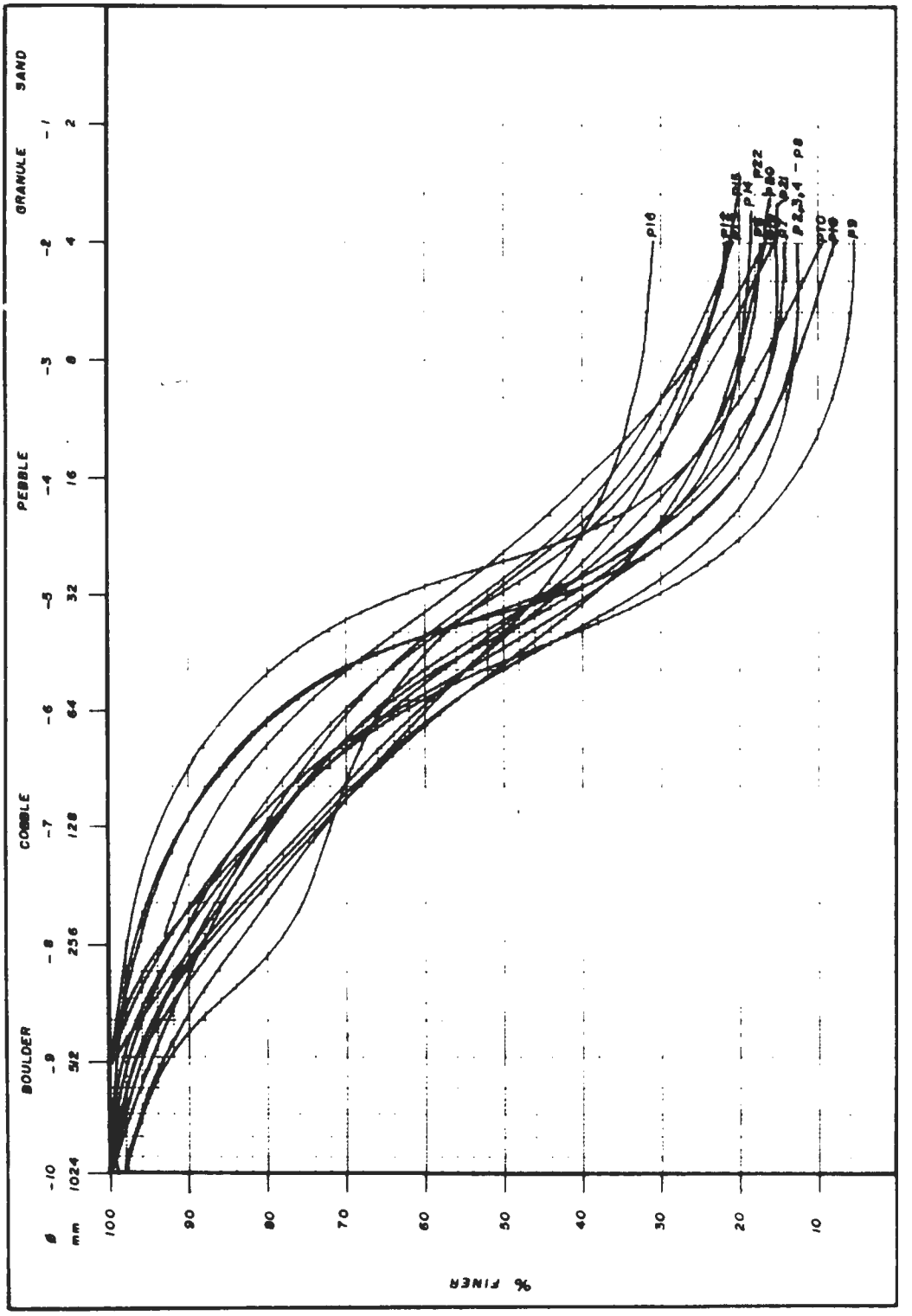

FIGURE 8.2. [illegible] SOARP MATERIAL SIZE DISTRIBUTION

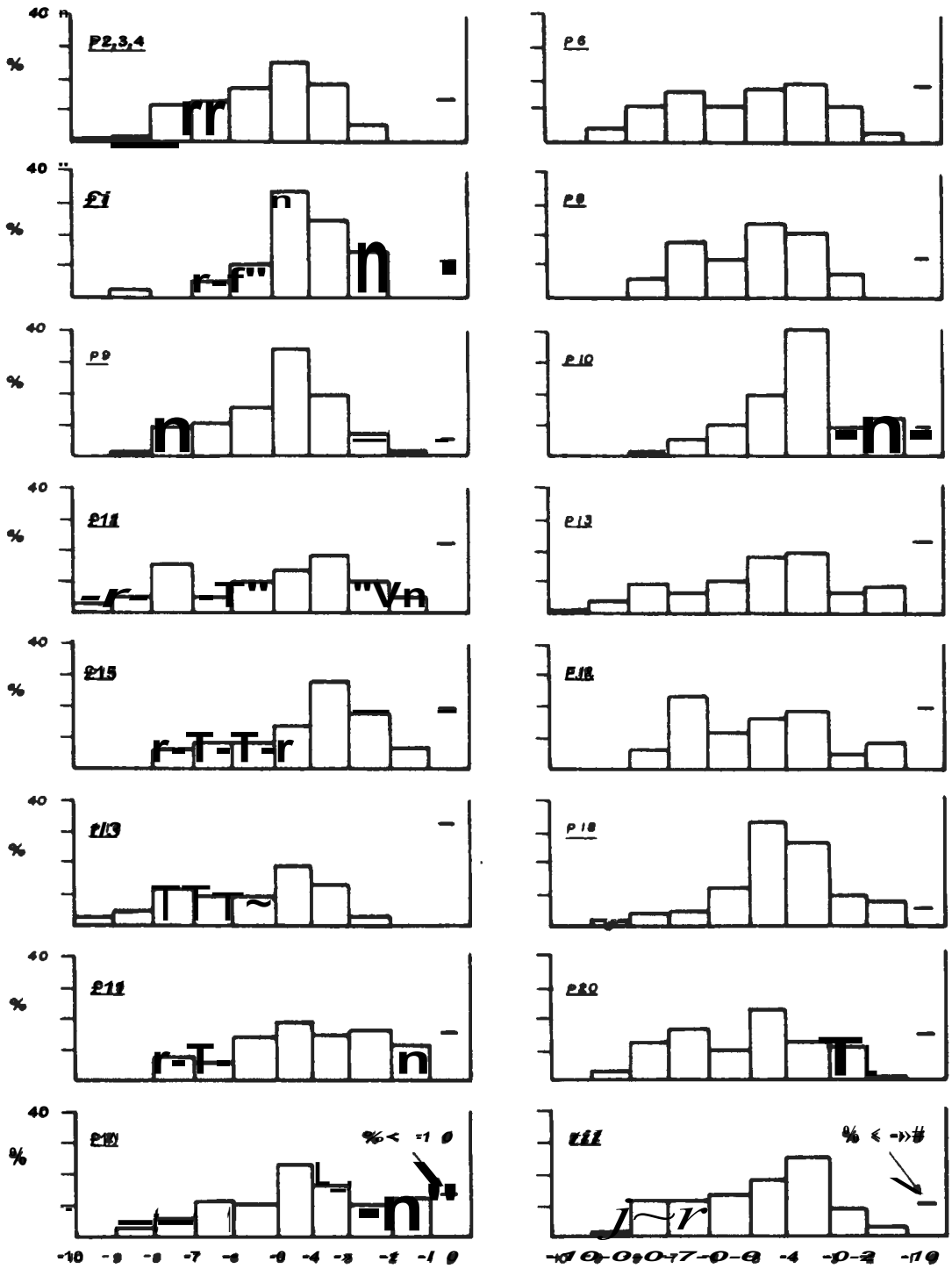

FIGURE B.3. FAULT SCARP MATERIAL SIZE DISTRIBUTION HISTOGRAMS

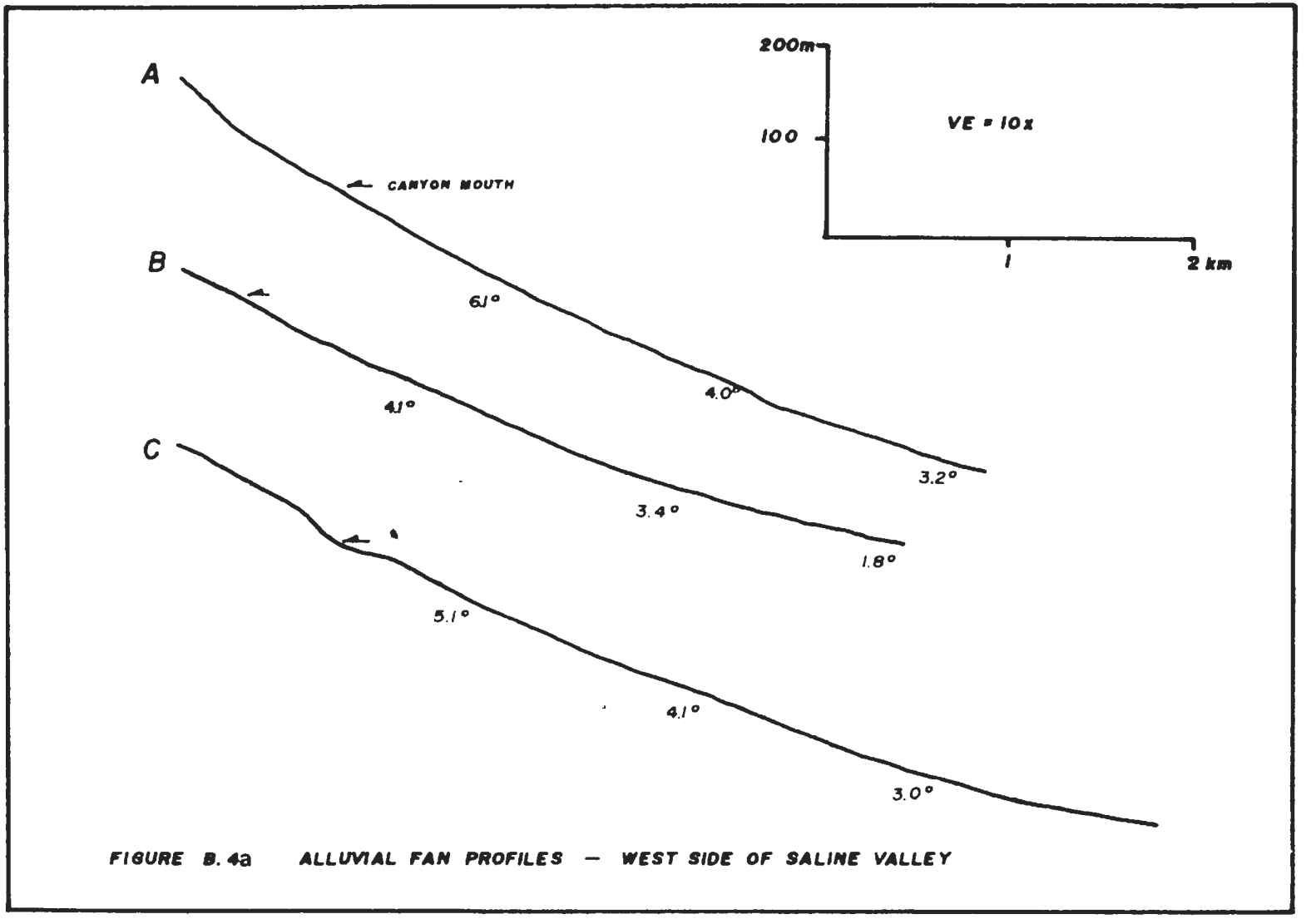

FIGURE B.4a ALLUVIAL FAN PROFILES — WEST SIDE OF SALINE VALLEY

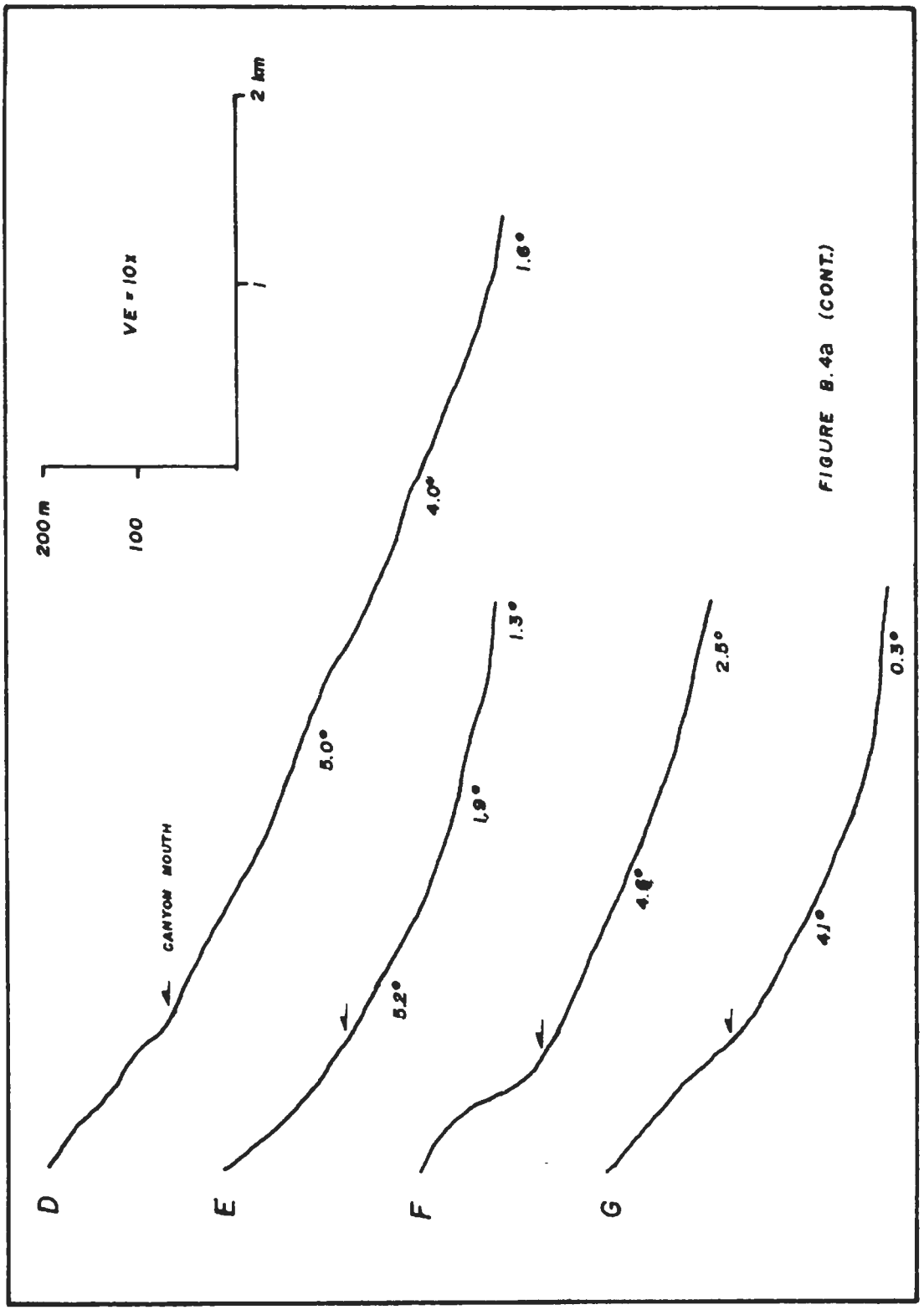

FIGURE 8.4a (CONT.)

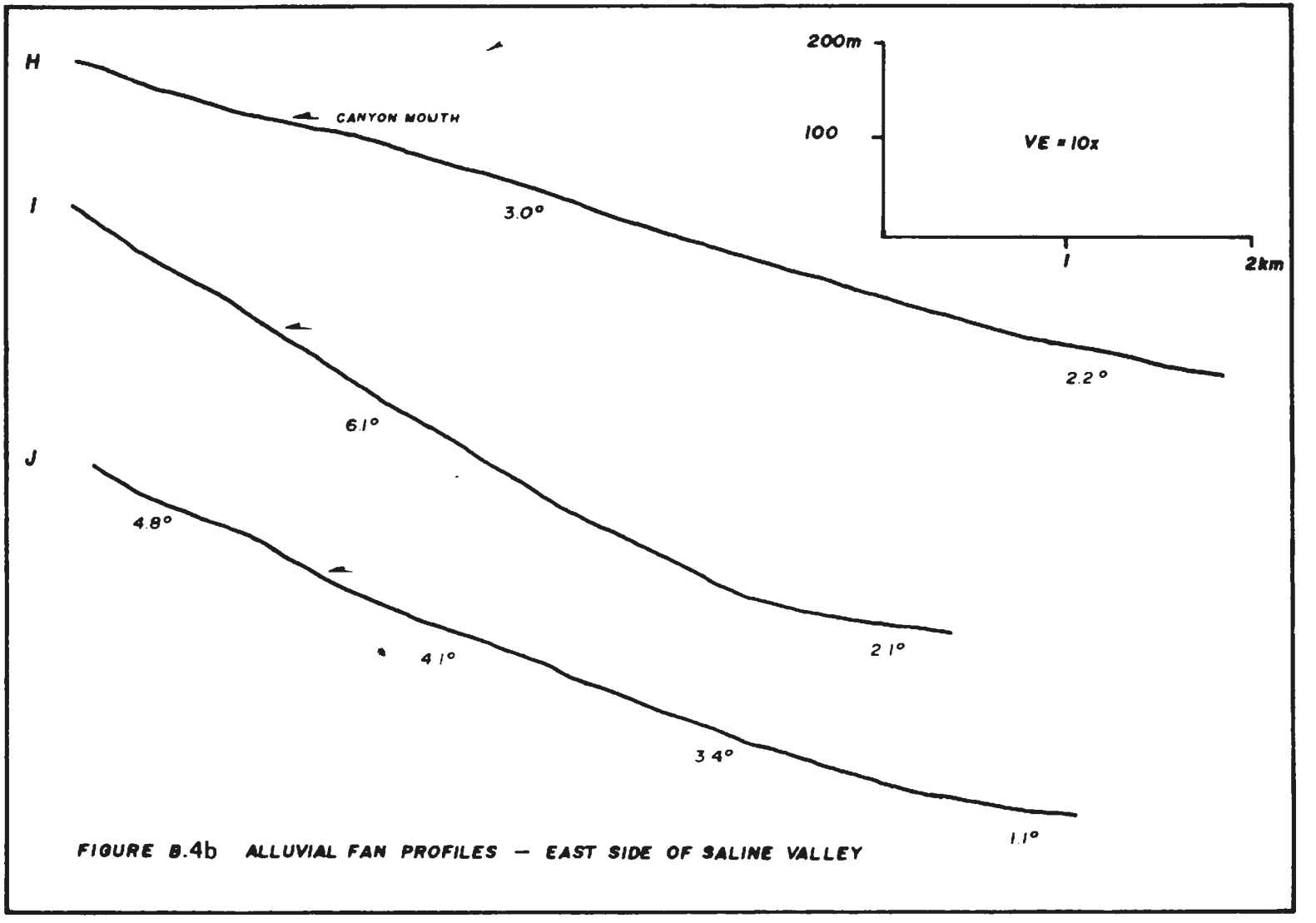

FIGURE B.4b ALLUVIAL FAN PROFILES — EAST SIDE OF SALINE VALLEY

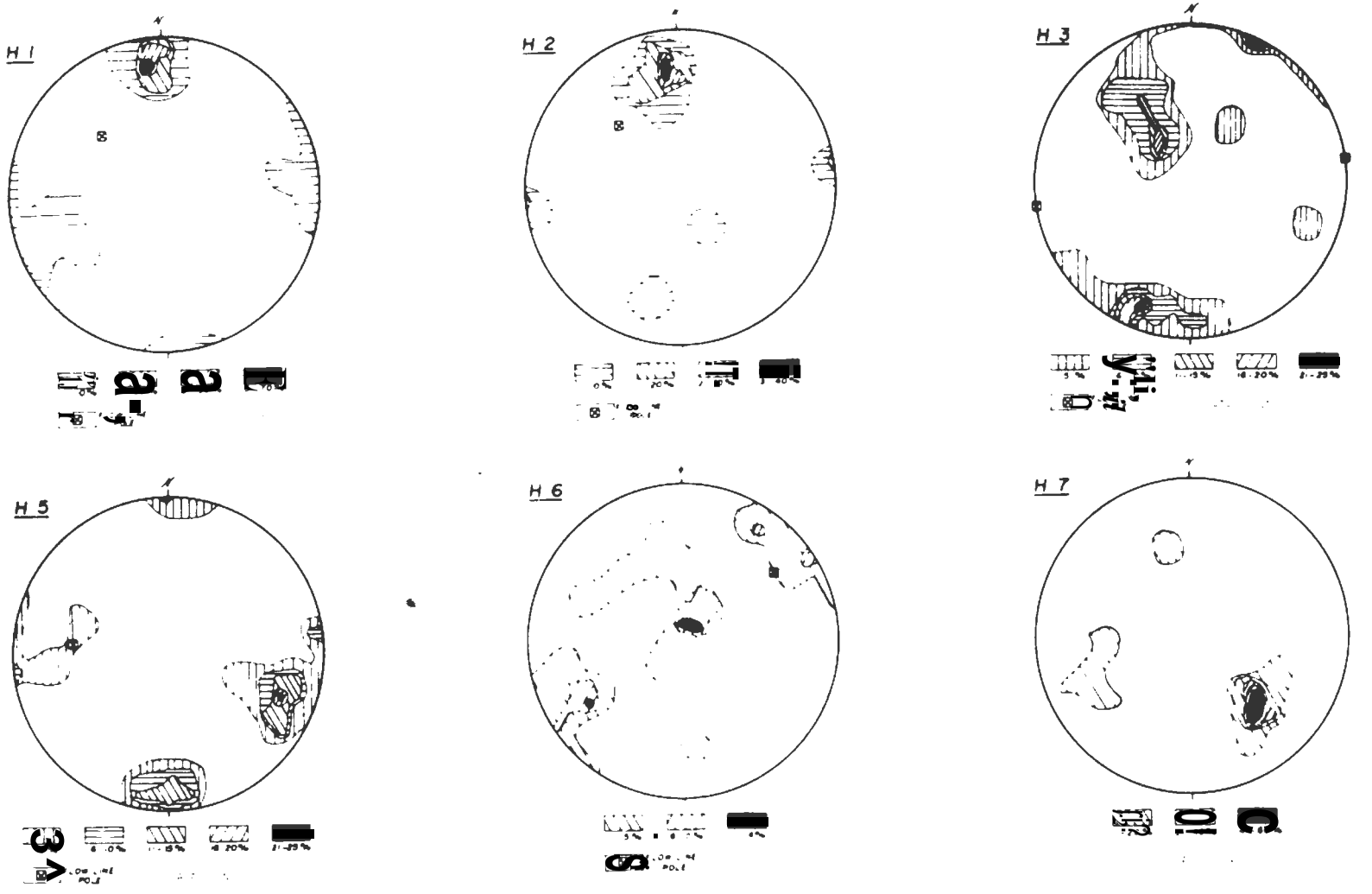

FIGURE B.5. UPPER HEMISPHERE STEREOGRAPHIC PROJECTIONS OF JOINT DATA.

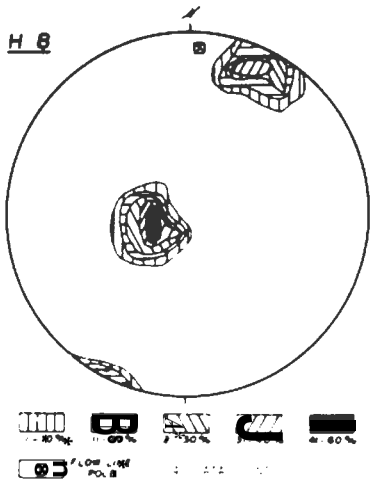

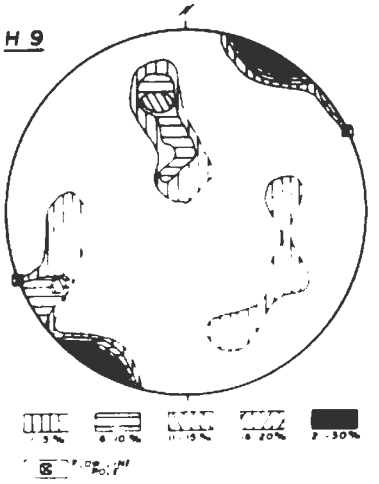

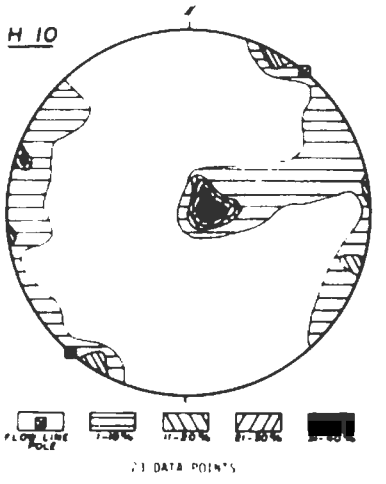

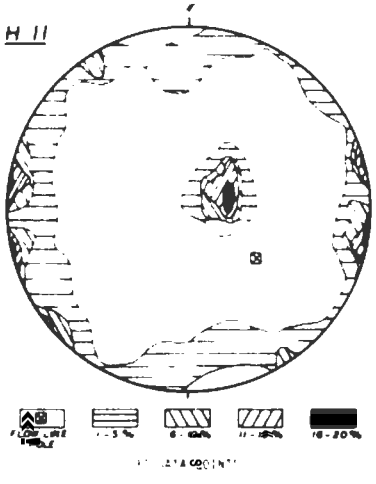

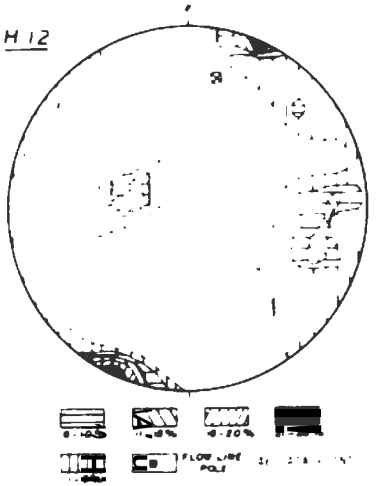

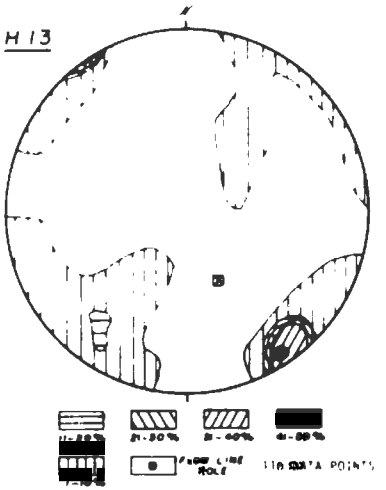

FIGURE B.8. (CONT)

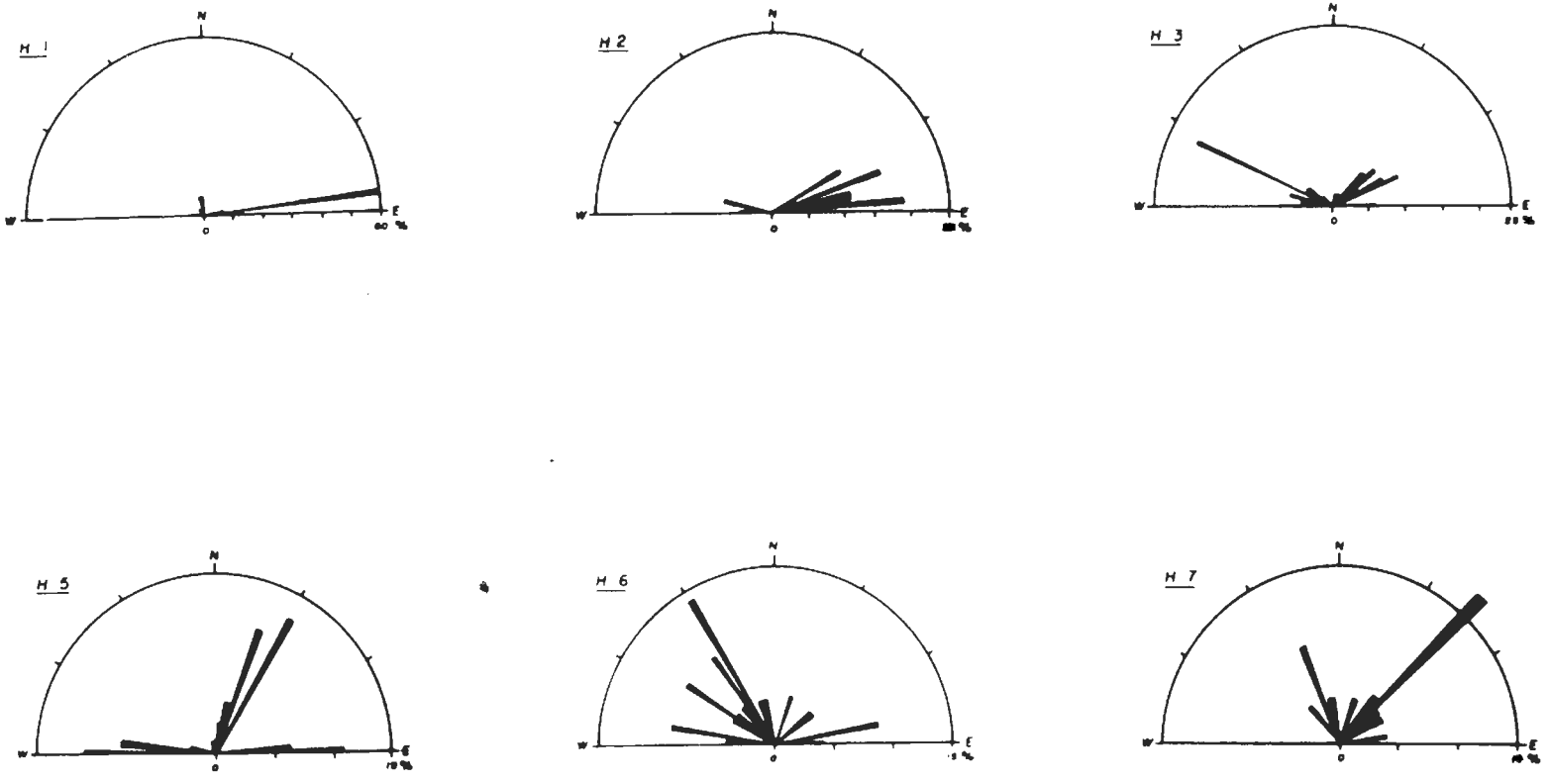

FIGURE 2.6. JOINT STRIKE AZIMUTH ROSETTES.

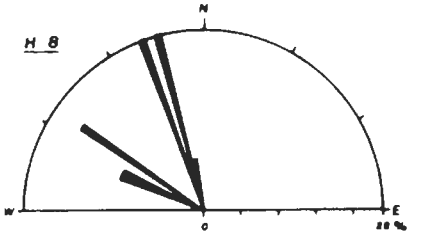

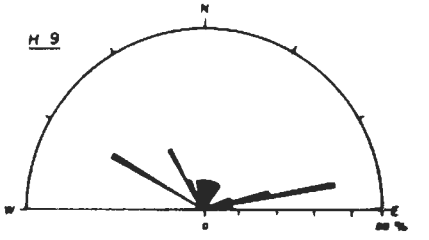

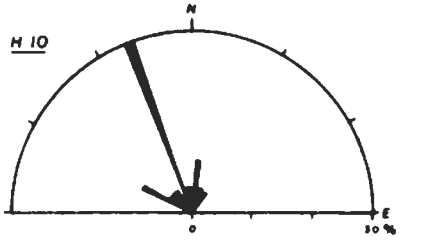

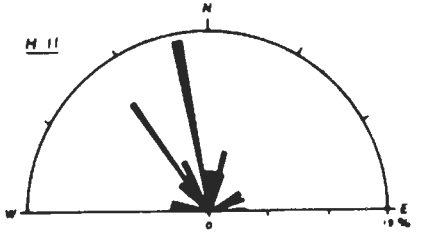

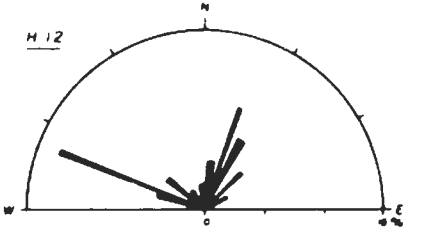

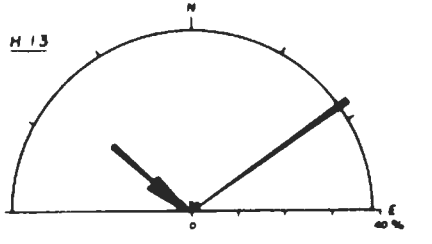

FIGURE B.6. (CONT.)

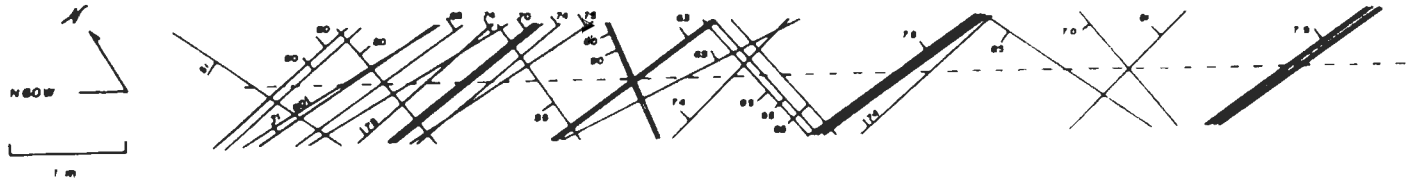

H 1

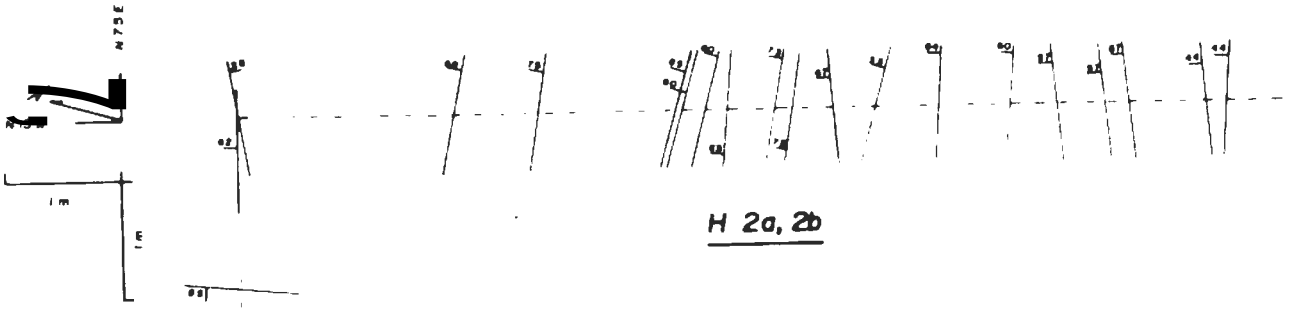

H 2a, 2b

FIGURE 8.7 JOINT TRAVERSES

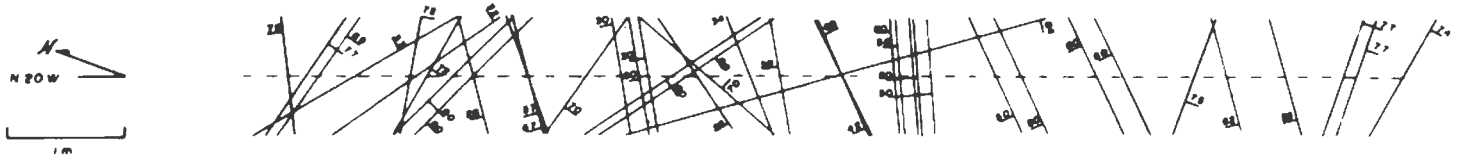

M 3

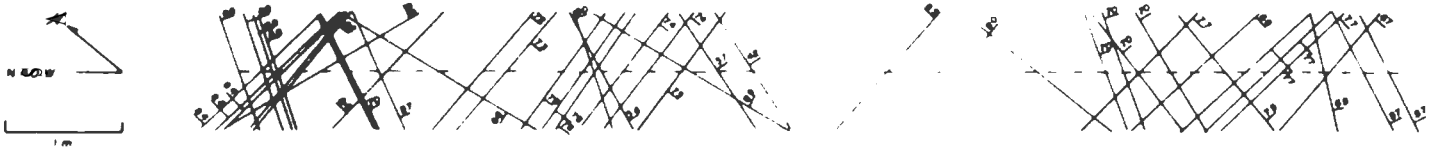

M 5

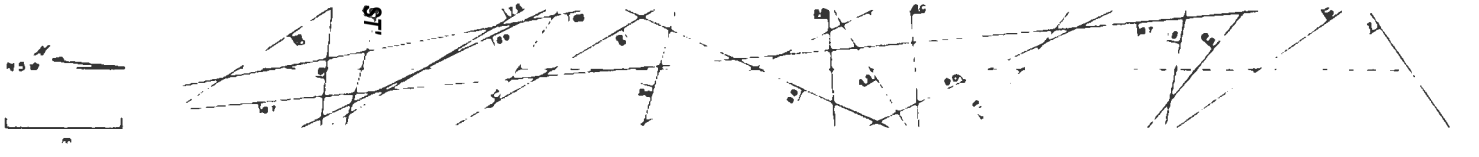

M 6

FIGURE B7 (CONT.)

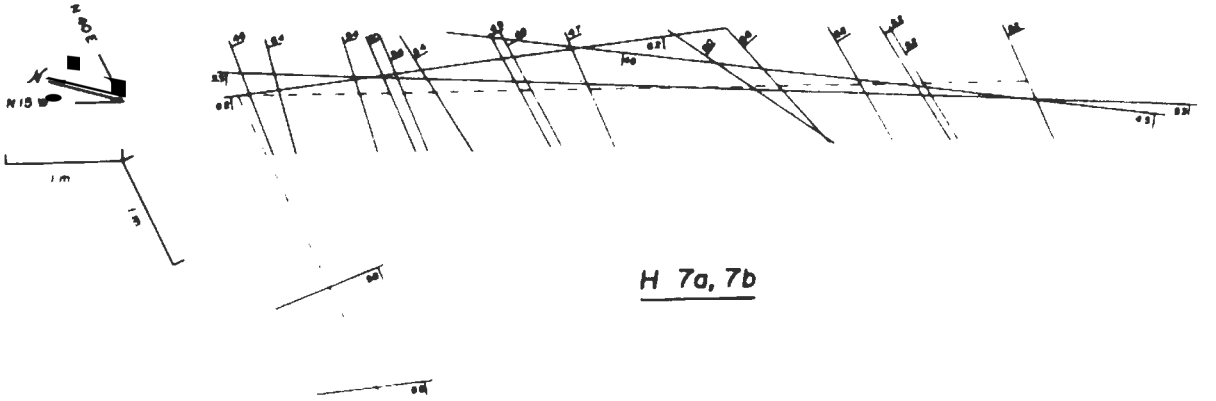

H 7a, 7b

FIGURE B.7 (CONT.)

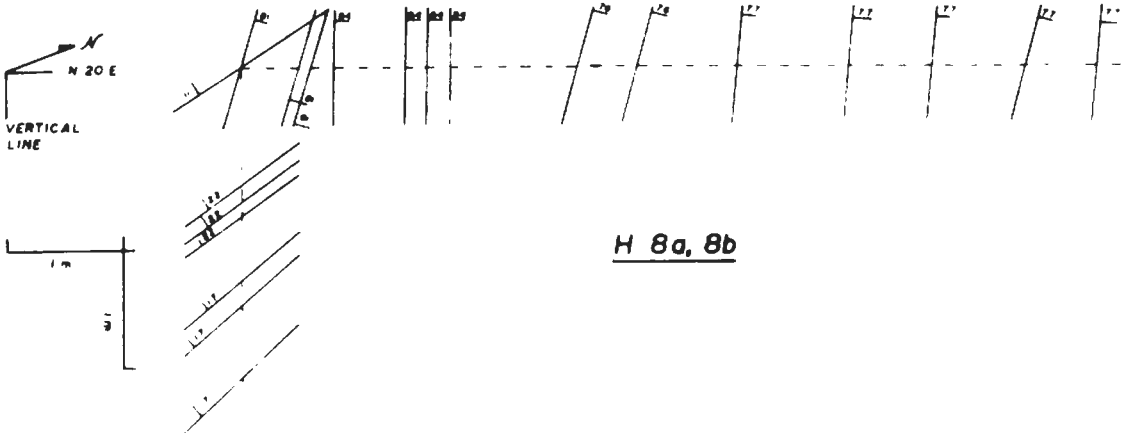

FIGURE B.7. (CONT.)

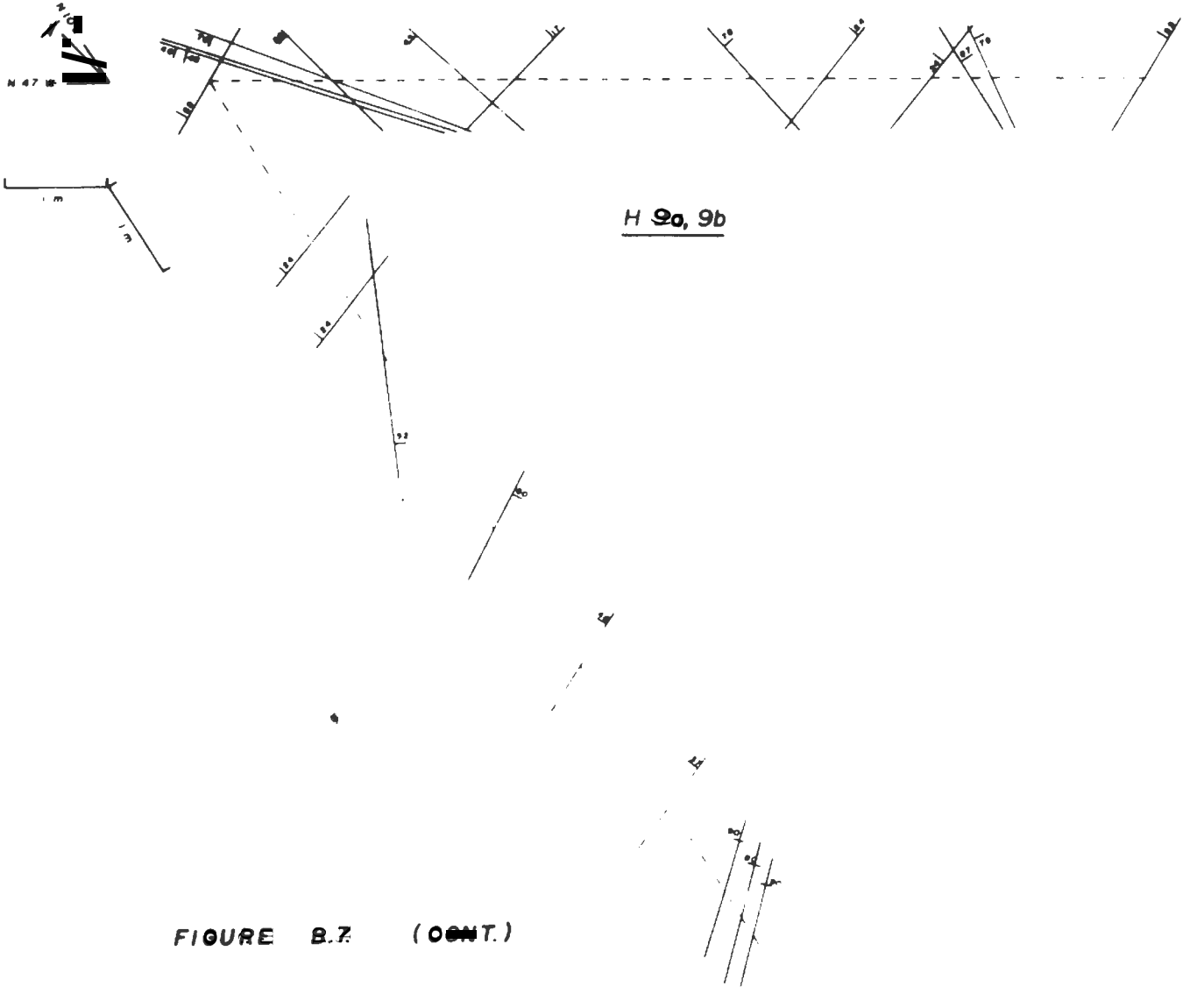

FIGURE B.7 (CONT.)

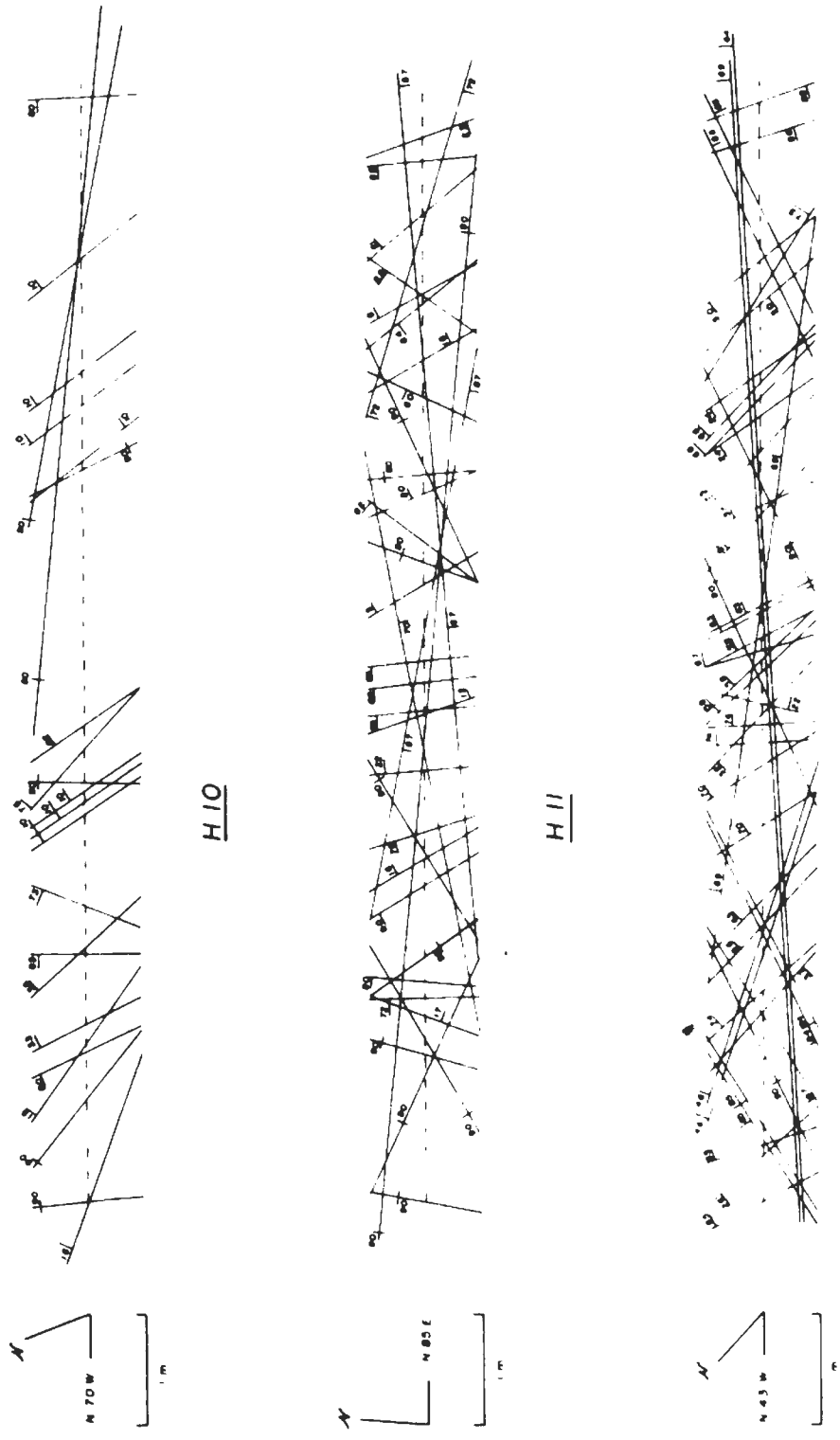

FIGURE B.7. (CONT.)

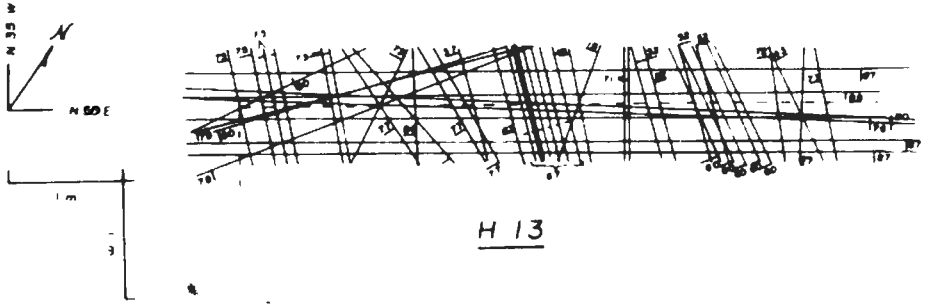

H 13

FIGURE B.7 (CONT.)

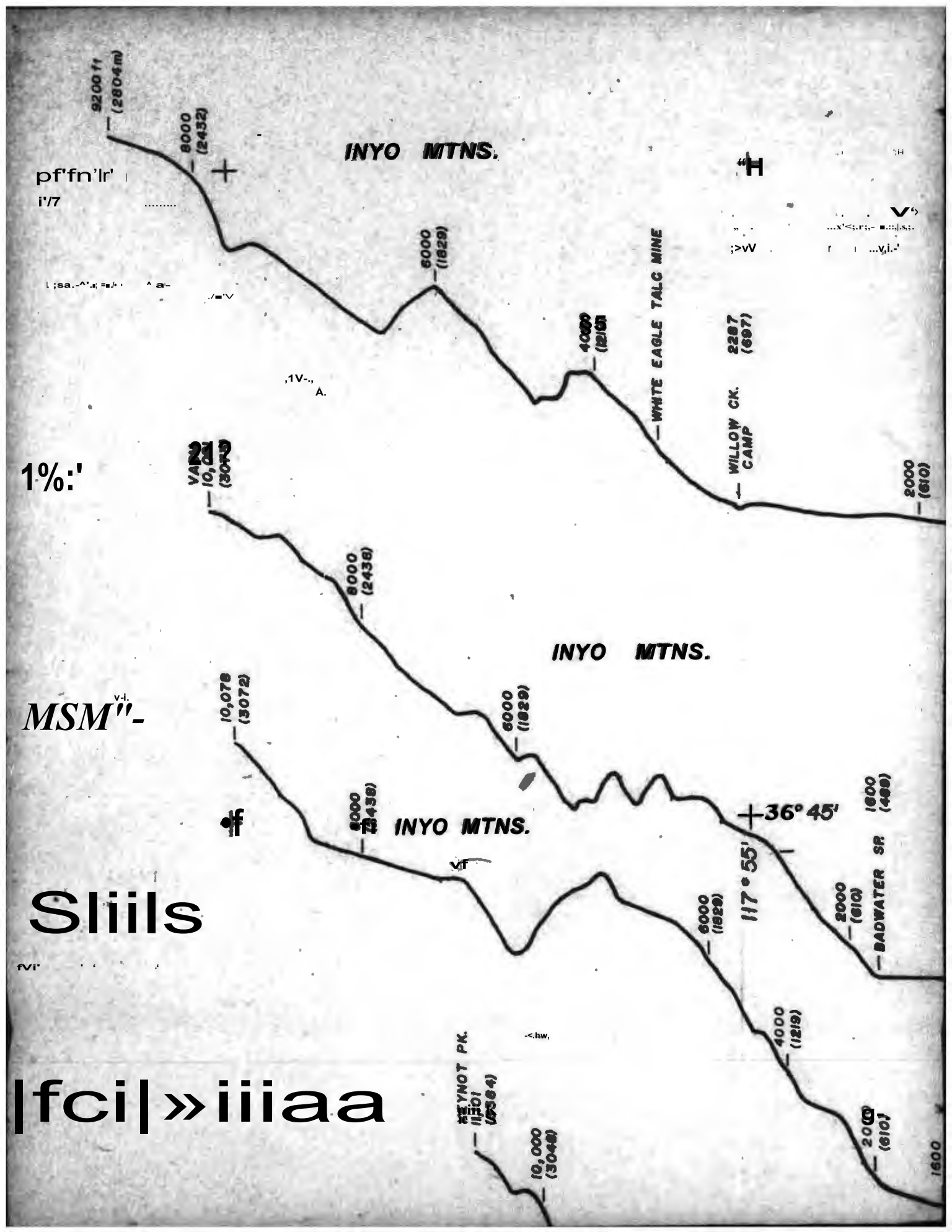
INYO MTNS.
INYO MTNS.
INYO MTNS.
WHITE EAGLE TALC MINE
WILLOW CK. CAMP
2287 (697)
BADWATER SR
36° 45'
117° 55'
9200 ft (2804m)
8000 (2432)
6000 (1829)
4000 (1219)
2000 (610)
10,078 (3072)
8000 (2438)
6000 (1829)
4000 (1219)
2000 (610)
1600 (488)
10,000 (3048)

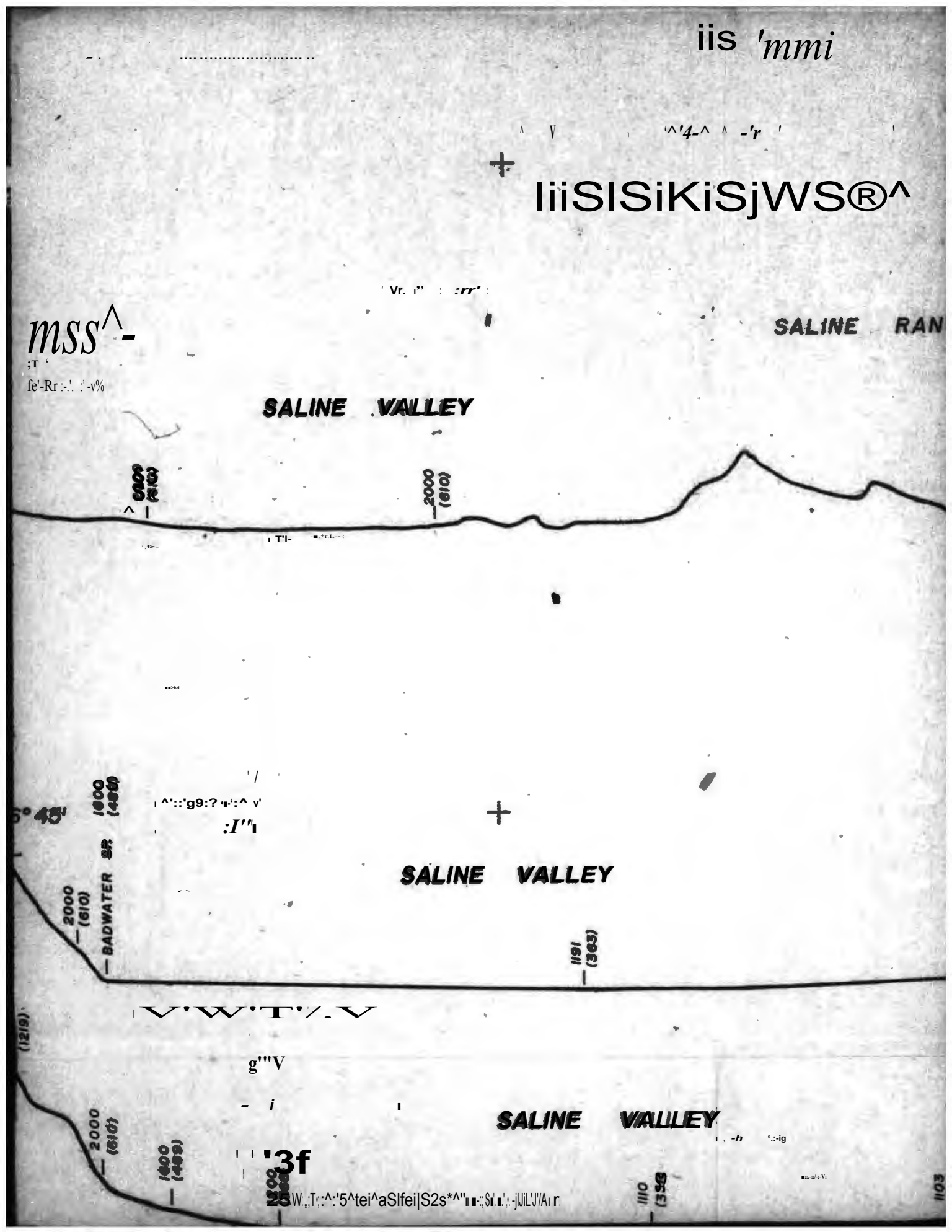
SALINE RAN
SALINE VALLEY
2000 (610)
SALINE VALLEY
BADWATER
2000 (610)
1191 (363)
SALINE VALLEY
2000 (610)
1110 (338)

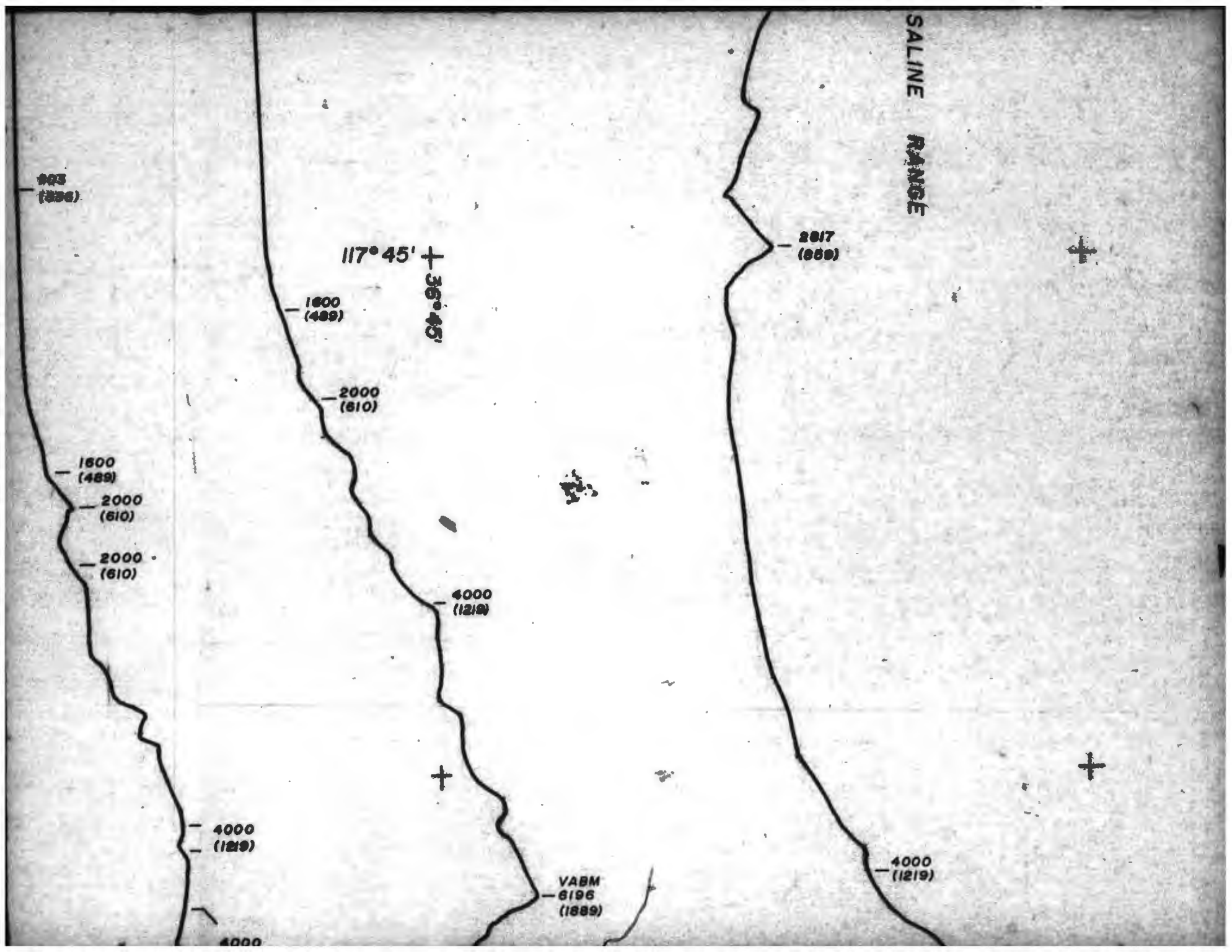
SALINE RANGE
903
(275)
1600
(489)
2000
(610)
2000
(610)
4000
(1219)
117° 45'
36° 45'
1600
(489)
2000
(610)
4000
(1219)
2917
(889)
4000
(1219)
VABM
6196
(1889)

PANAMINT RANGE

DVNM BDY.

6000 (1829)

4000 (1219)

PANAMINT RANGE

VABM 6196 (1889)

4000 (1219)

DVNM BDY.

4000 (1219)

PANAMINT RANGE

TEAKETTLE JCT.

4000 (1219)

4000 (1219)

DVNM BDY.

4000 (1219)

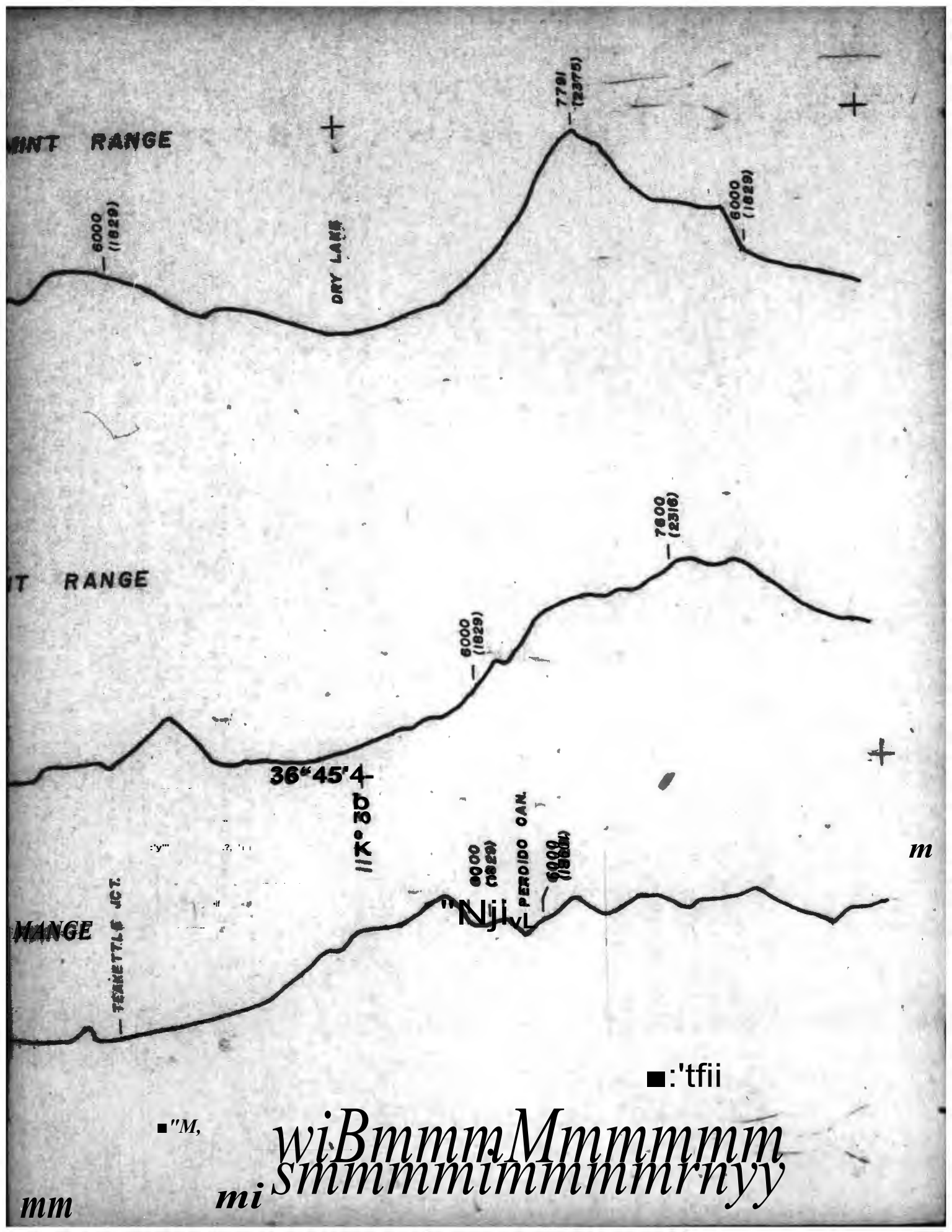
7791 (2375)
6000 (1829)
6000 (1829)
DRY LAKE
7600 (2316)
6000 (1829)
36"45'4-
6000 (1829)
PERDIDO CAN.
TEEKETTLE JCT.

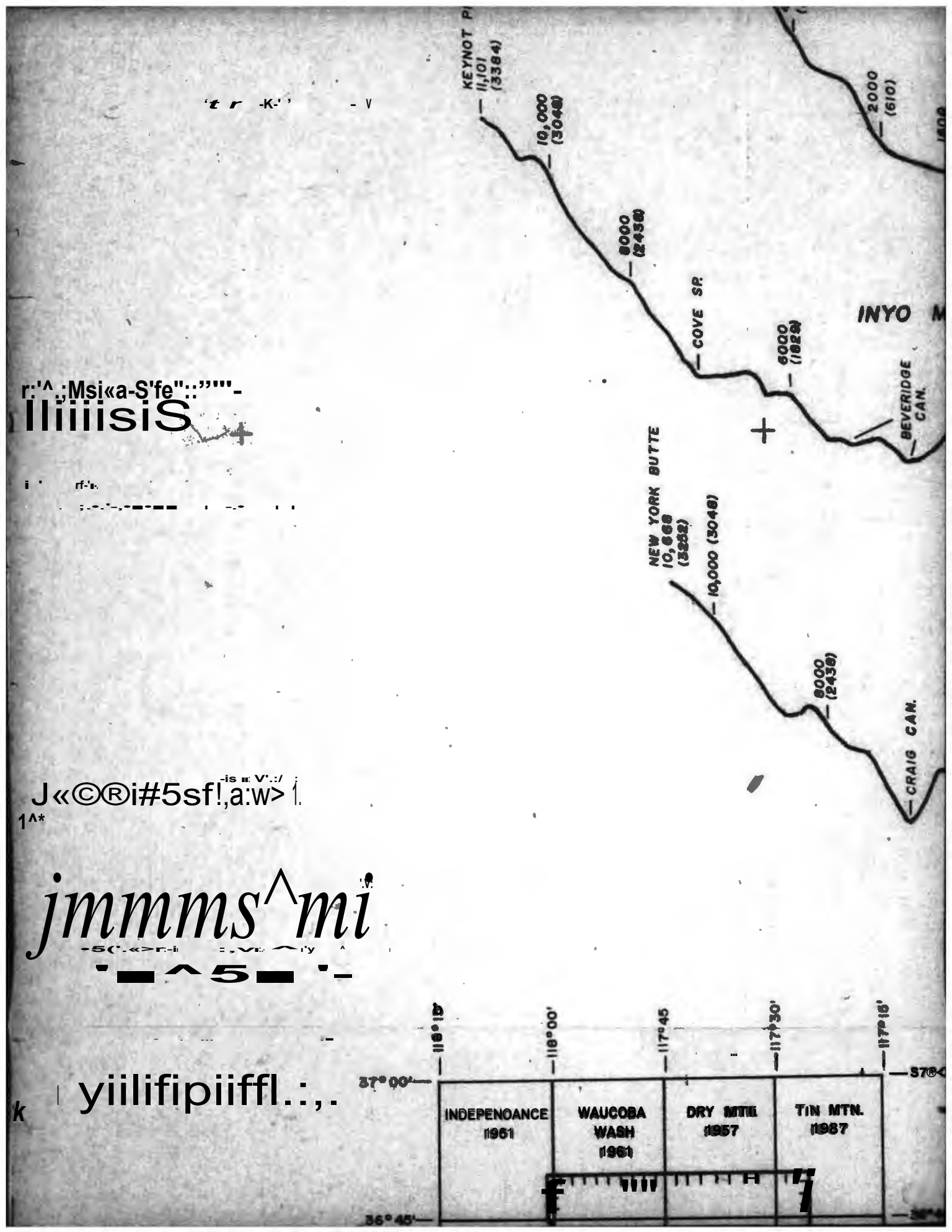
KEYNOT P
11,101
(3384)
10,000
(3048)
8000
(2438)
COVE SP.
6000
(1829)
2000
(610)
INYO M
BEVERIDGE
CAN.
NEW YORK BUTTE
10,668
(3252)
10,000 (3048)
8000
(2438)
CRAIG CAN.
INDEPENDANCE
1961
WAUCOBA
WASH
1961
DRY MTN.
1957
TIN MTN.
1987
37°00'
36°45'
118°15'
118°00'
117°45'
117°30'
117°15'

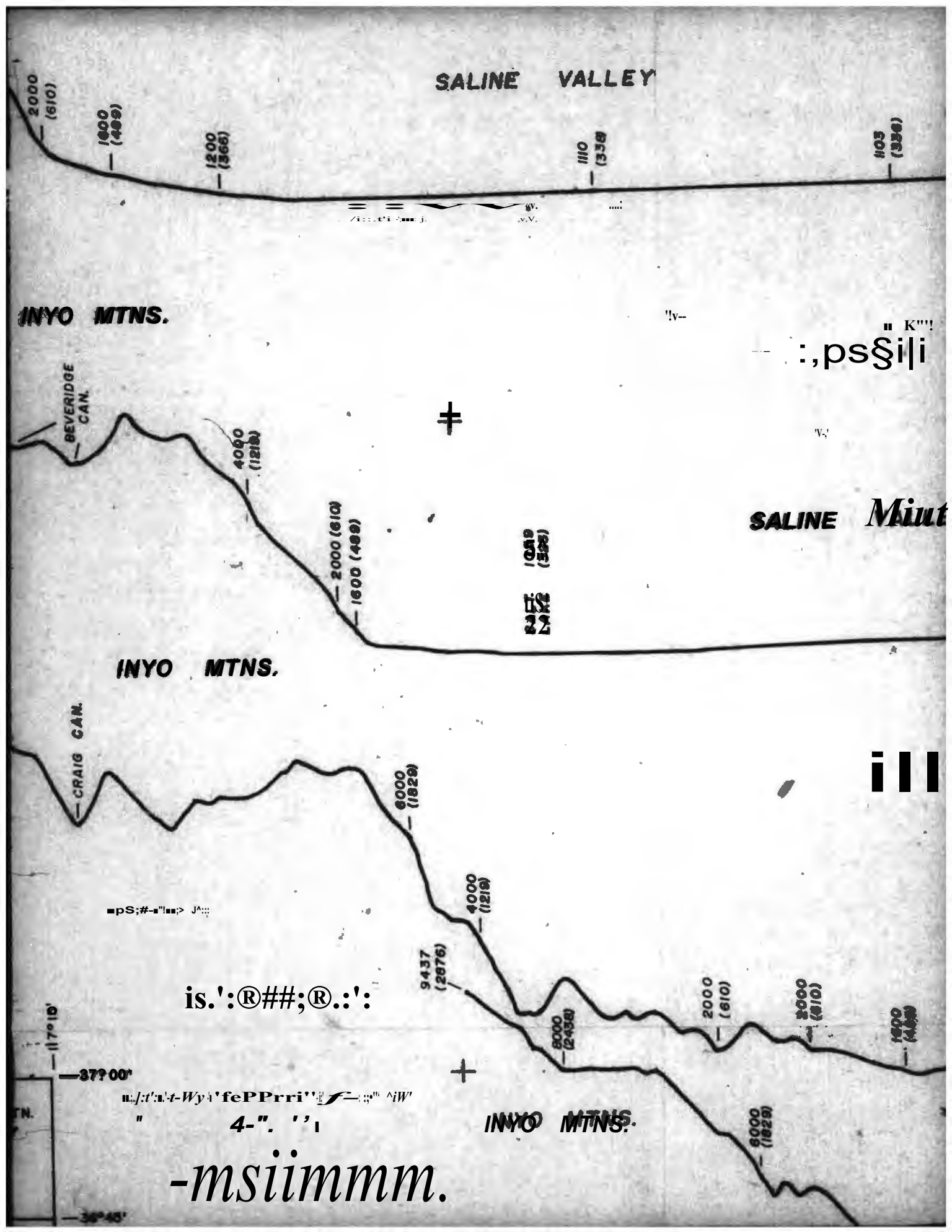
SALINE VALLEY
2000 (610)
1800 (488)
1200 (366)
1110 (338)
1103 (336)
INYO MTNS.
BEVERIDGE CAN.
4000 (1219)
2000 (610)
1800 (488)
SALINE
INYO MTNS.
CRAIG CAN.
8000 (1829)
4000 (1219)
9437 (2876)
8000 (2438)
2000 (610)
117°10'
37?00'
INYO MTNS.
8000 (1829)
36°45'

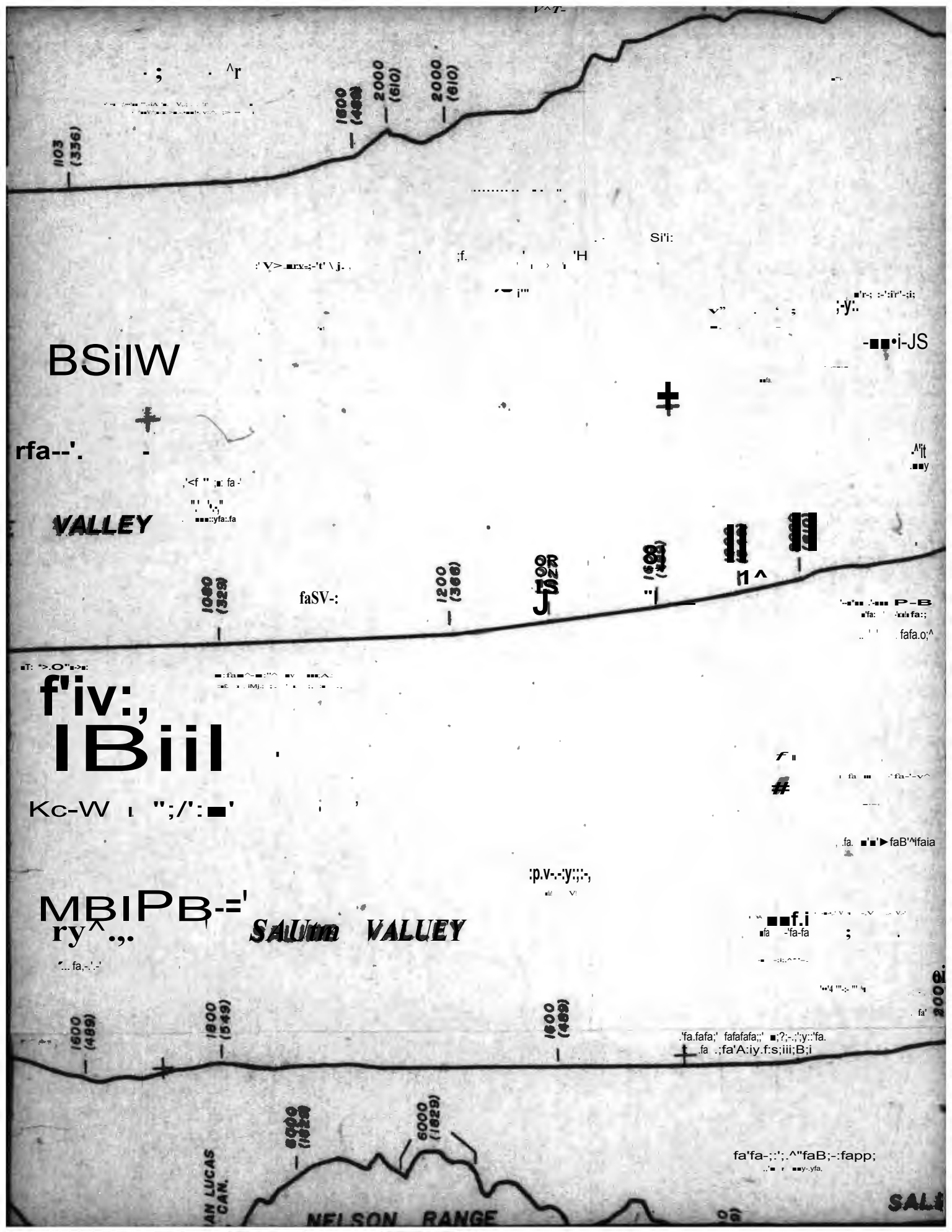
BSilW
rfa--'.
VALLEY
faSV-:
f'iv:,
IBiil
Kc-W
MBIPB-='
ry^.,.
SALUm VALUEY
NELSON RANGE
SAL

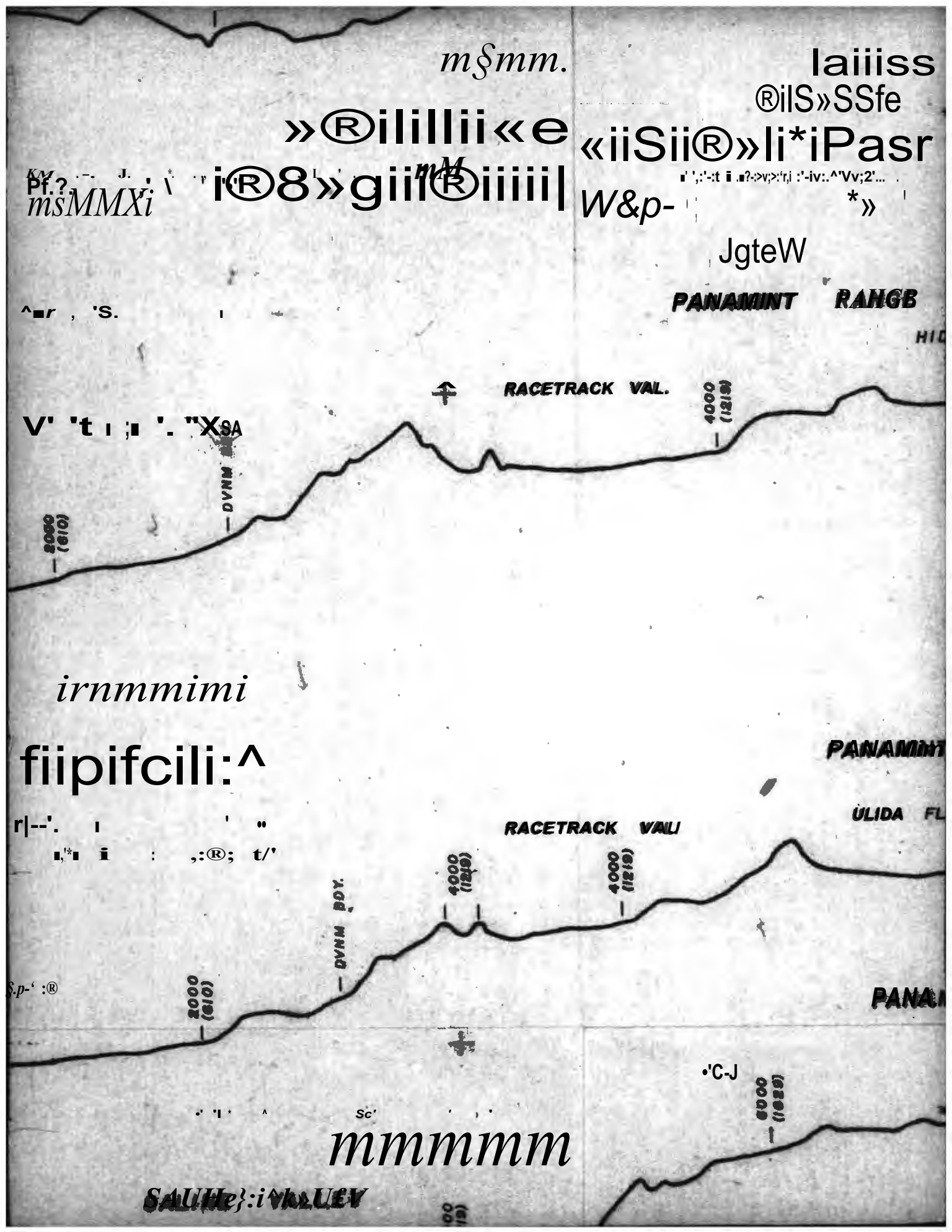
RACETRACK VAL.
4000 (1219)
2000 (610)
RACETRACK VALI
4000 (1219)
4000 (1219)
2000 (610)
PANAMINT RANGE
ULIDA FL
PANAMINT

WtMW-H

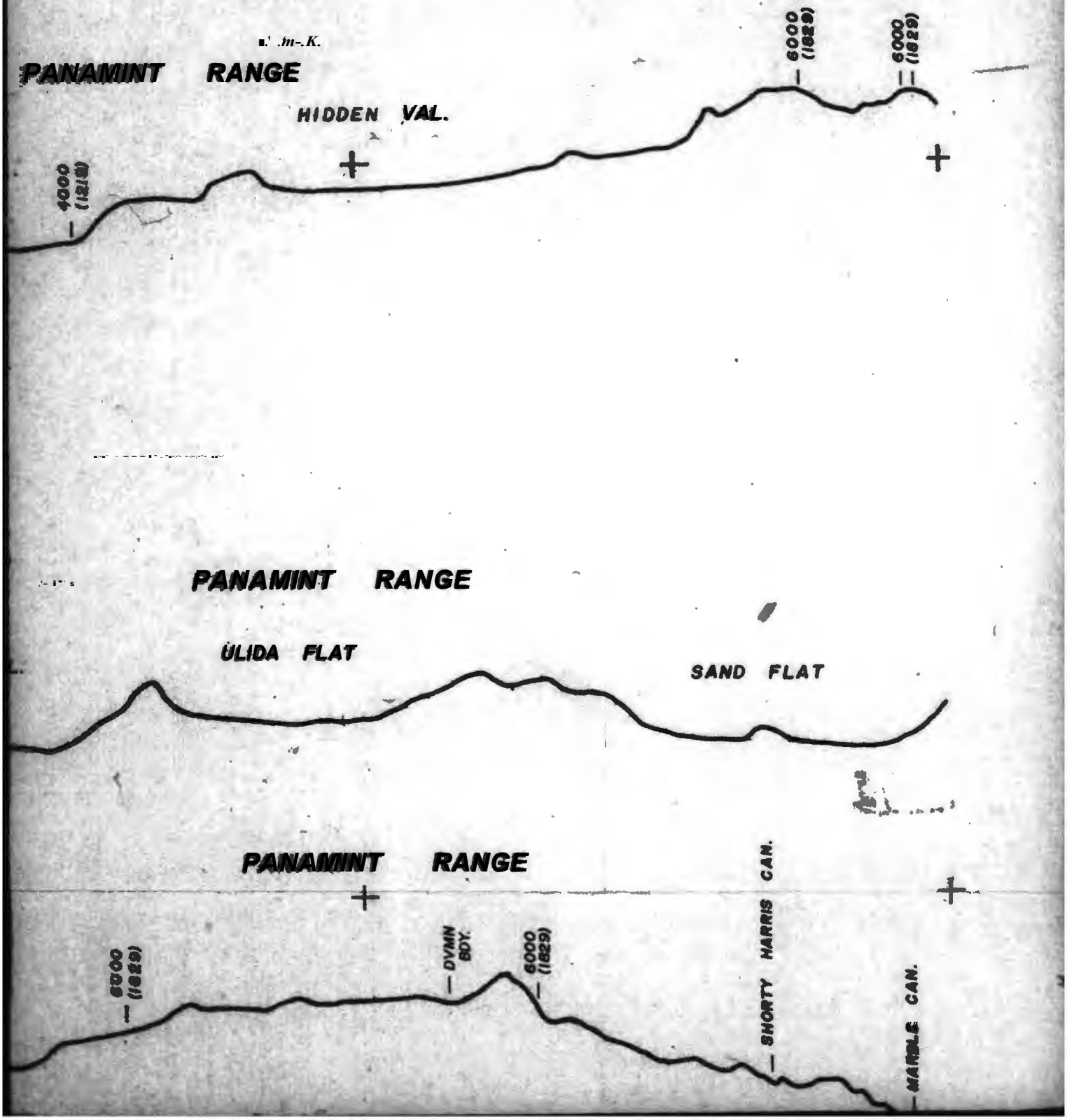
PANAMINT RANGE
HIDDEN VAL.
4000 (1219)
6000 (1829)
6000 (1829)
PANAMINT RANGE
ÚLIDA FLAT
SAND FLAT
PANAMINT RANGE
6000 (1829)
DVMN BDY.
6000 (1829)
SHORTY HARRIS CAN.
MARBLE CAN.

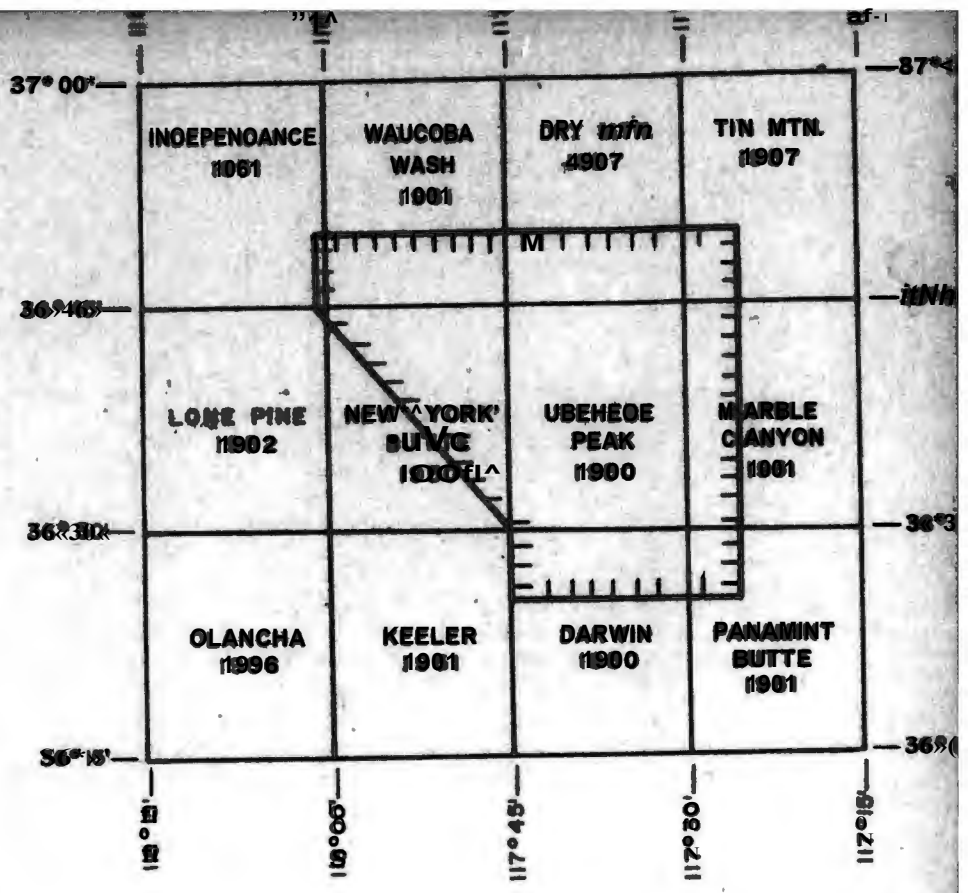

TOPOGRAPHIC PROFILES GEOGRAPHICALLY CORRE

METERS FEET

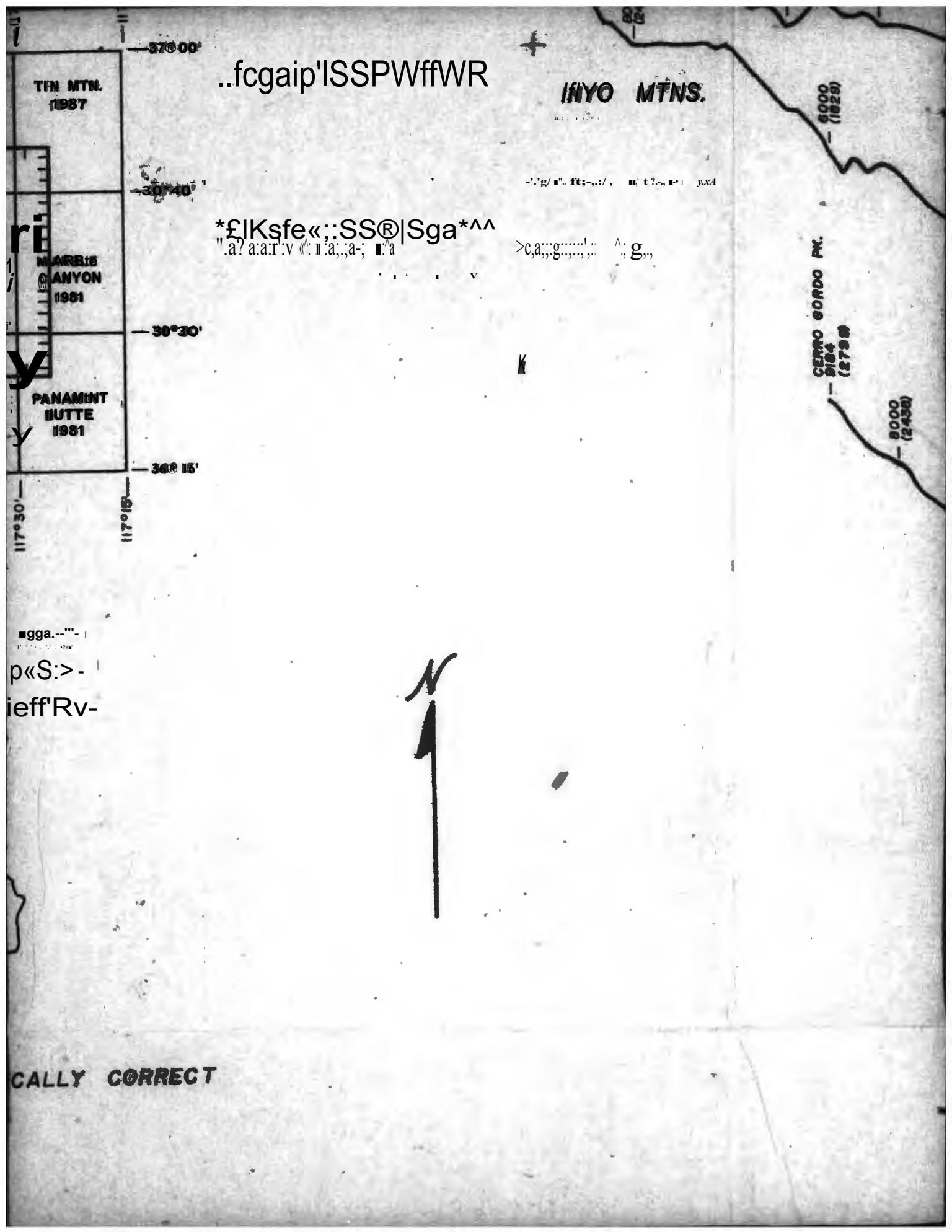
37°00'
TIN MTN.
1987
30°40'
MARBLE
CANYON
1981
36°30'
PANAMINT
BUTTE
1981
36° 15'
117°30'
117°15'
INYO MTNS.
8000
(1829)
CERRO GORDO PK.
9184
(2798
8000
(2438)
CALLY CORRECT

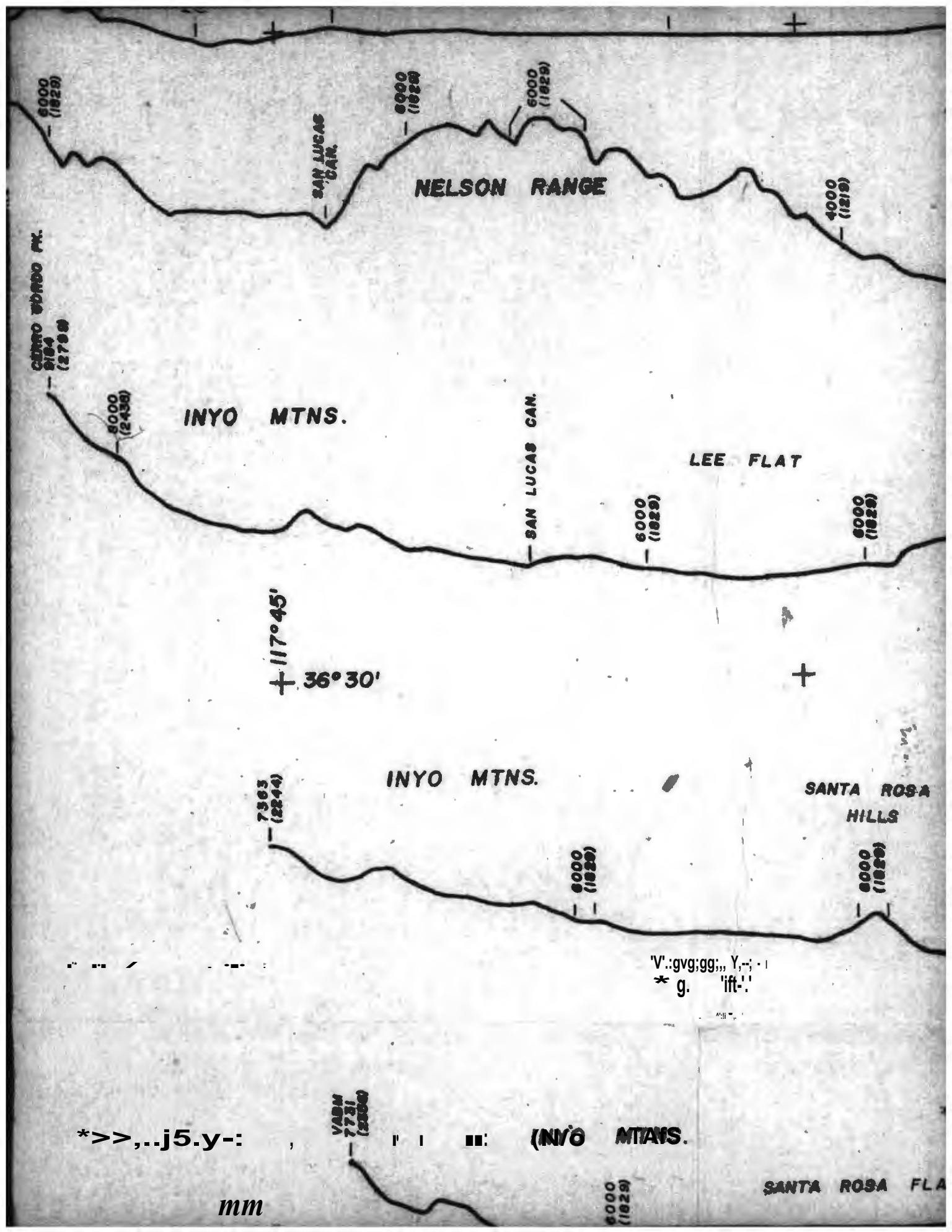
6000 (1829)
SAN LUCAS CAN.
6000 (1829)
6000 (1829)
NELSON RANGE
4000 (1219)
CERRO BONDO PK.
9184 (2799)
6000 (2438)
INYO MTNS.
SAN LUCAS CAN.
LEE FLAT
6000 (1829)
6000 (1829)
117°45'
36°30'
INYO MTNS.
7365 (2244)
SANTA ROSA HILLS
6000 (1829)
6000 (1829)
(INYO MTNS.
SANTA ROSA FLA
6000 (1829)

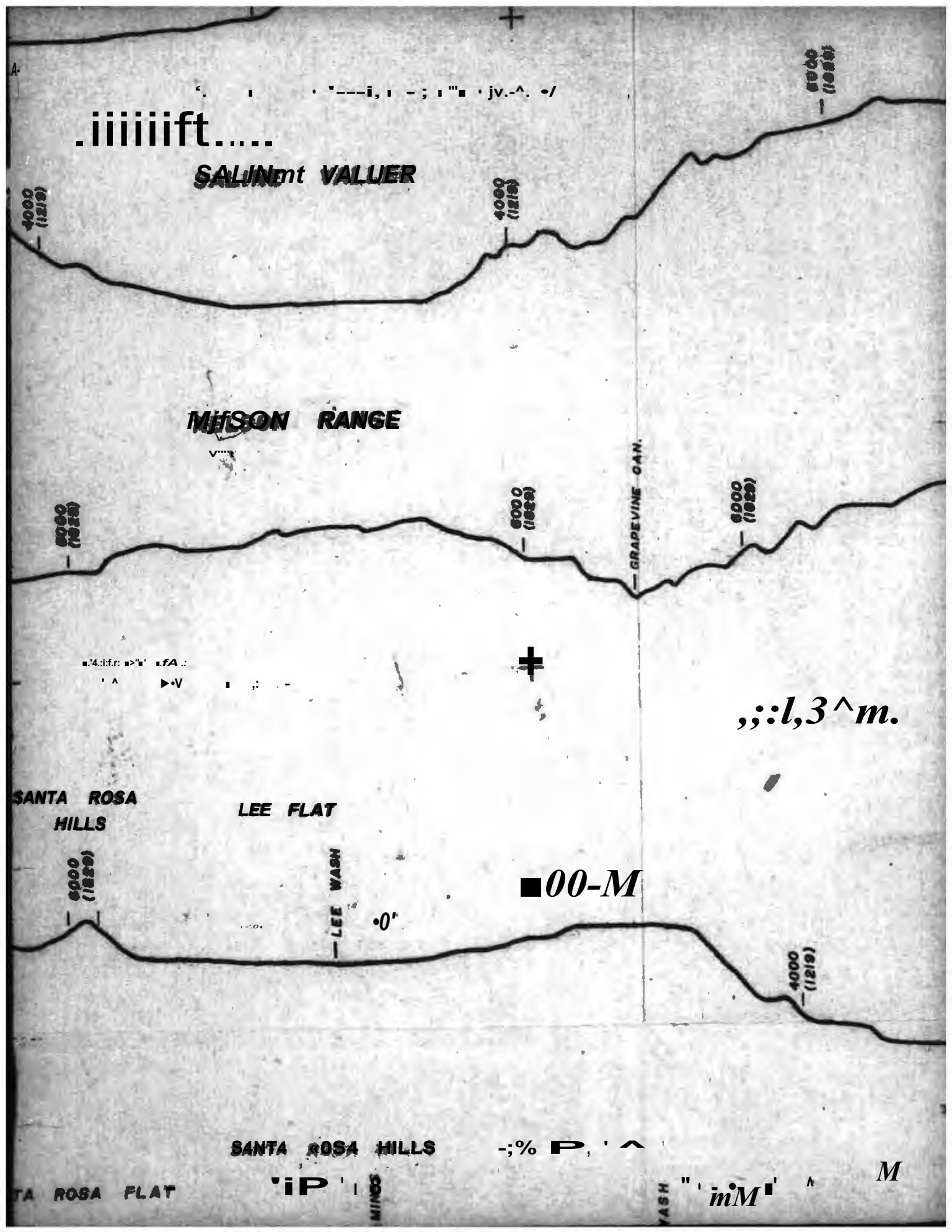
SALINE VALLEY
MjfSON RANGE
GRAPEVINE CAN.
SANTA ROSA HILLS
LEE FLAT
LEE WASH
SANTA ROSA HILLS
TA ROSA FLAT
4000 (1219)

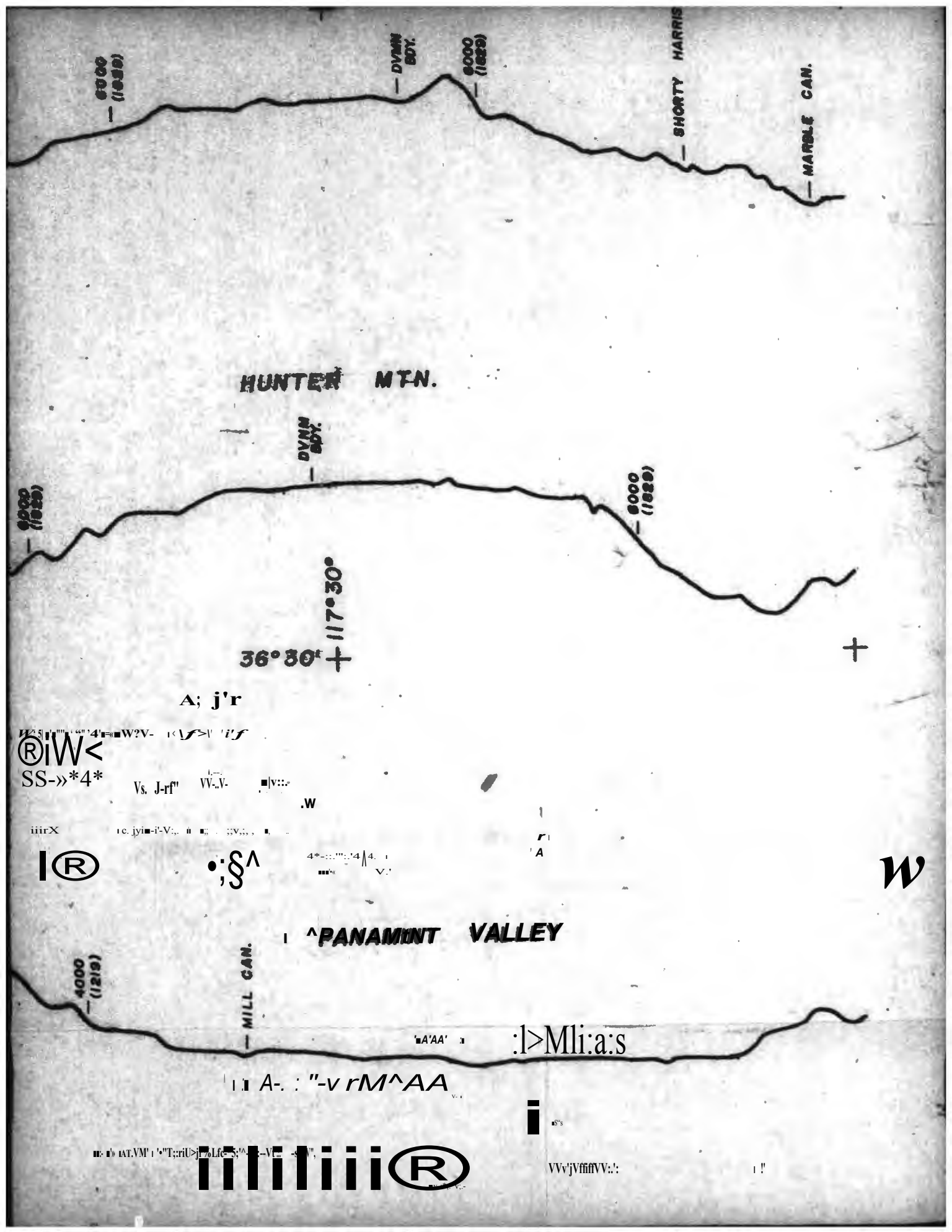
8000 (1829)
DYNN BDY.
8000 (1829)
SHORTY HARRIS
MARBLE CAN.
HUNTER MTN.
DYNN BDY.
8000 (1829)
8000 (1829)
117°30'
36°30'
PANAMINT VALLEY
4000 (1219)
MILL CAN.

TOPOGRAPHIC PROFILES GEOGRAPHICALLY CORREC

MWK&tmMy-

P«« *15?"

pftisr"-..

K%afeDa;«5s^

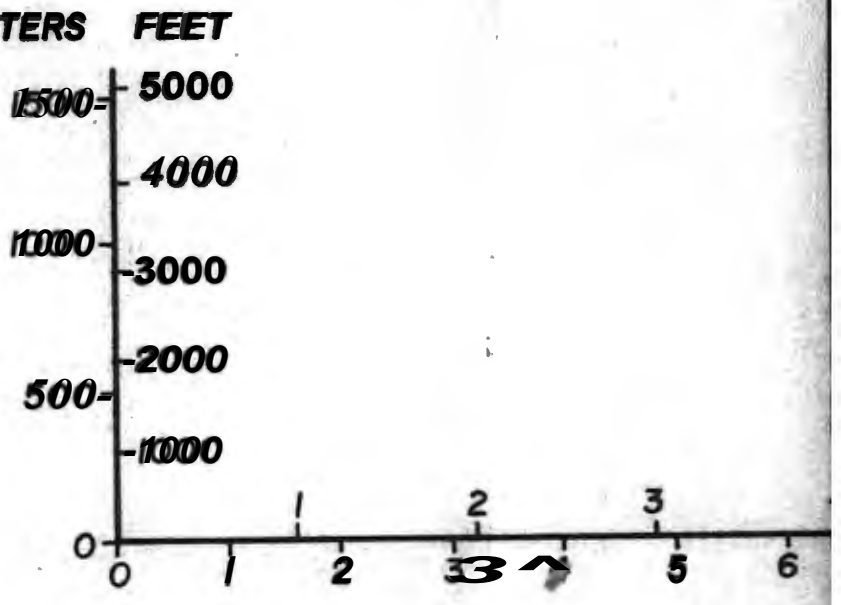

VERTICAL EXAGGERATION

J.T. ZELLMER (1980)

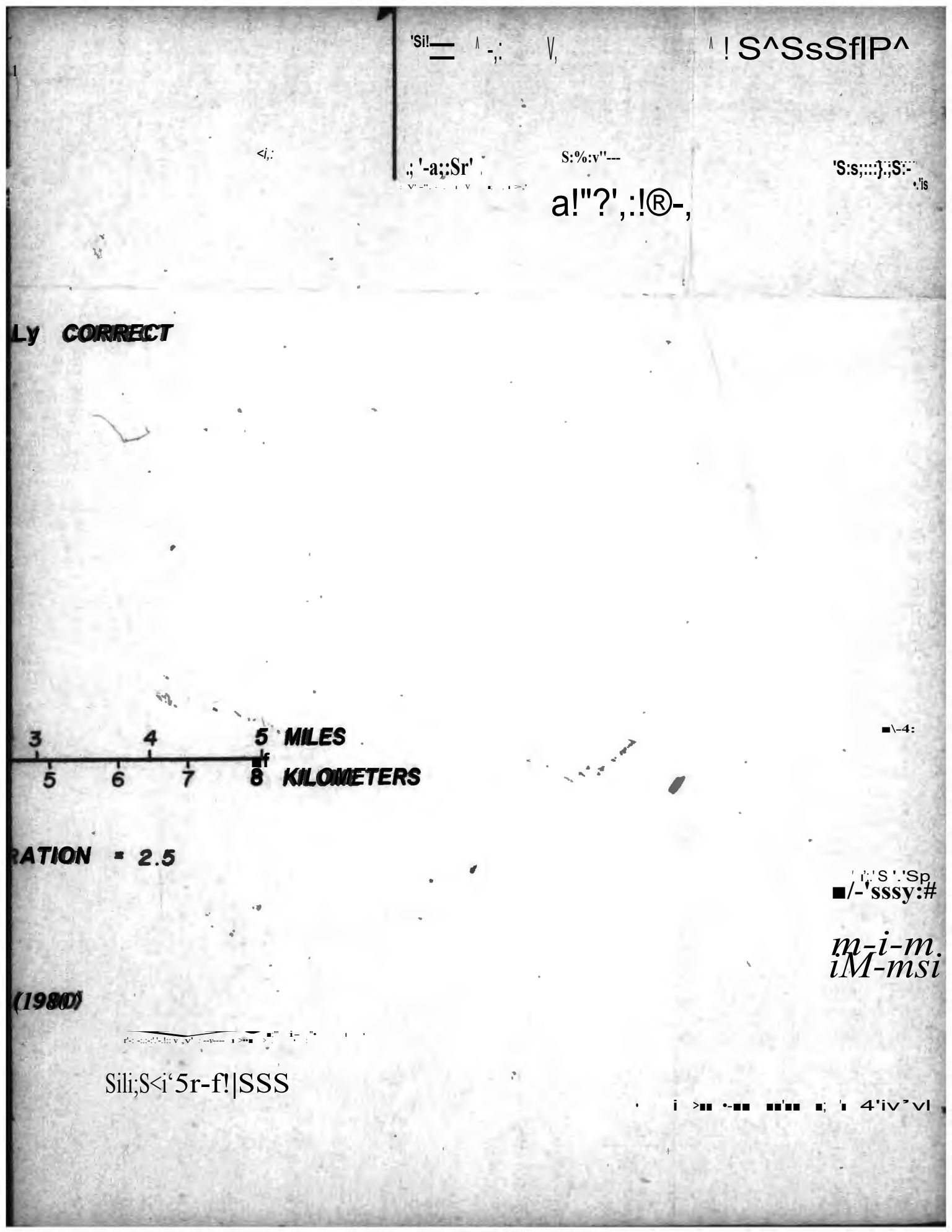
Ly CORRECT
3 4 5 MILES
5 6 7 8 KILOMETERS
RATION = 2.5
(1980)

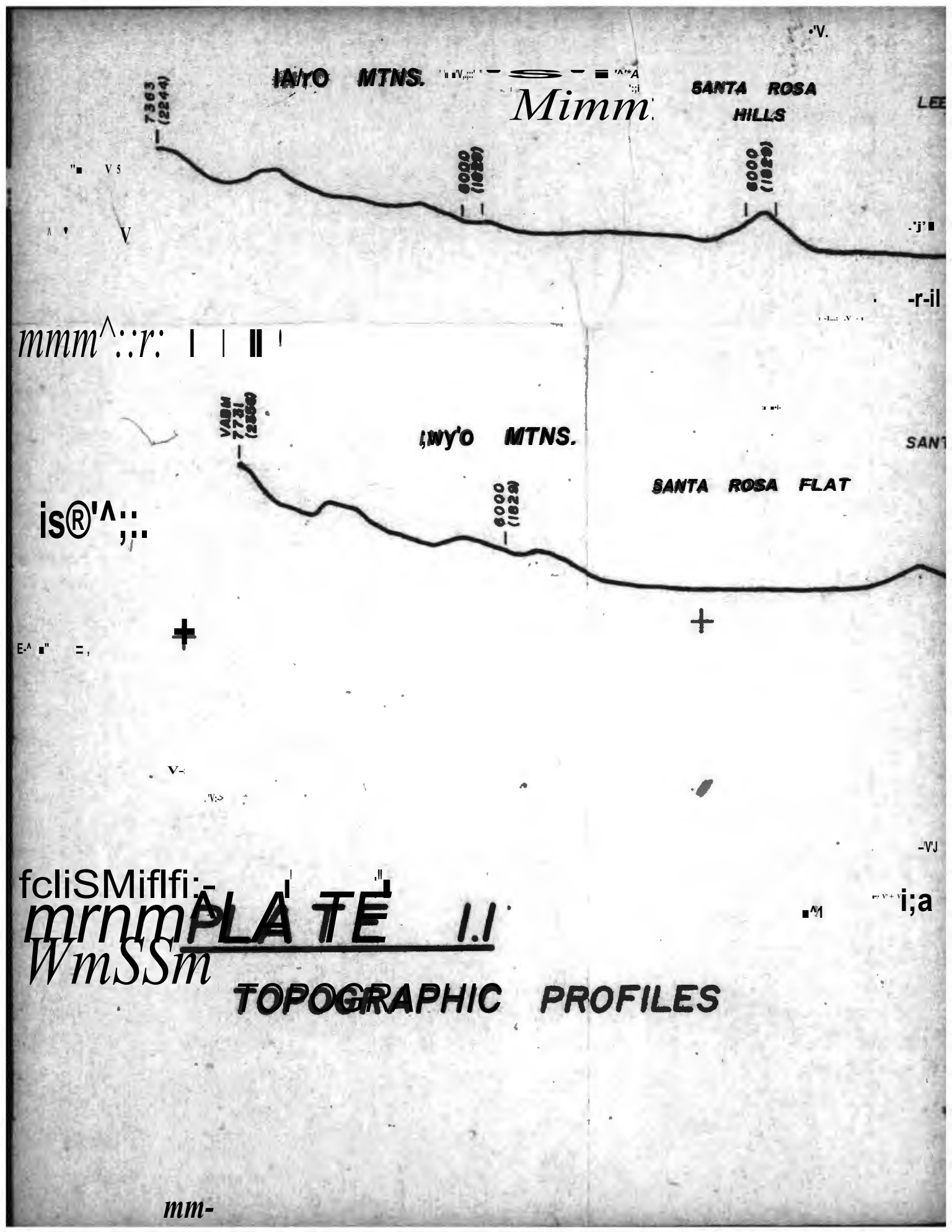

PLATE I.I

TOPOGRAPHIC PROFILES

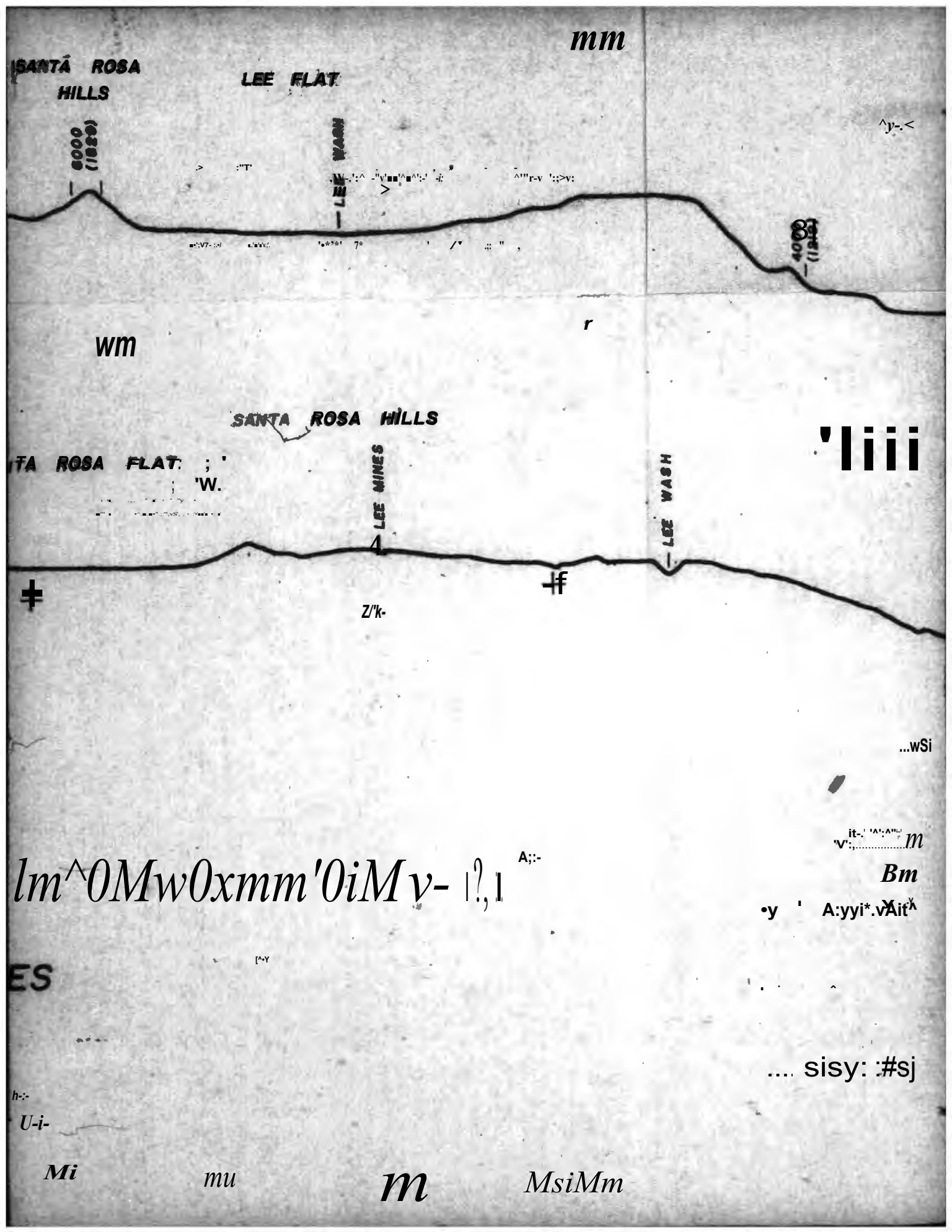
SANTA ROSA HILLS
LEE FLAT
LEE WASH
SANTA ROSA HILLS
LEE MINES
LEE WASH

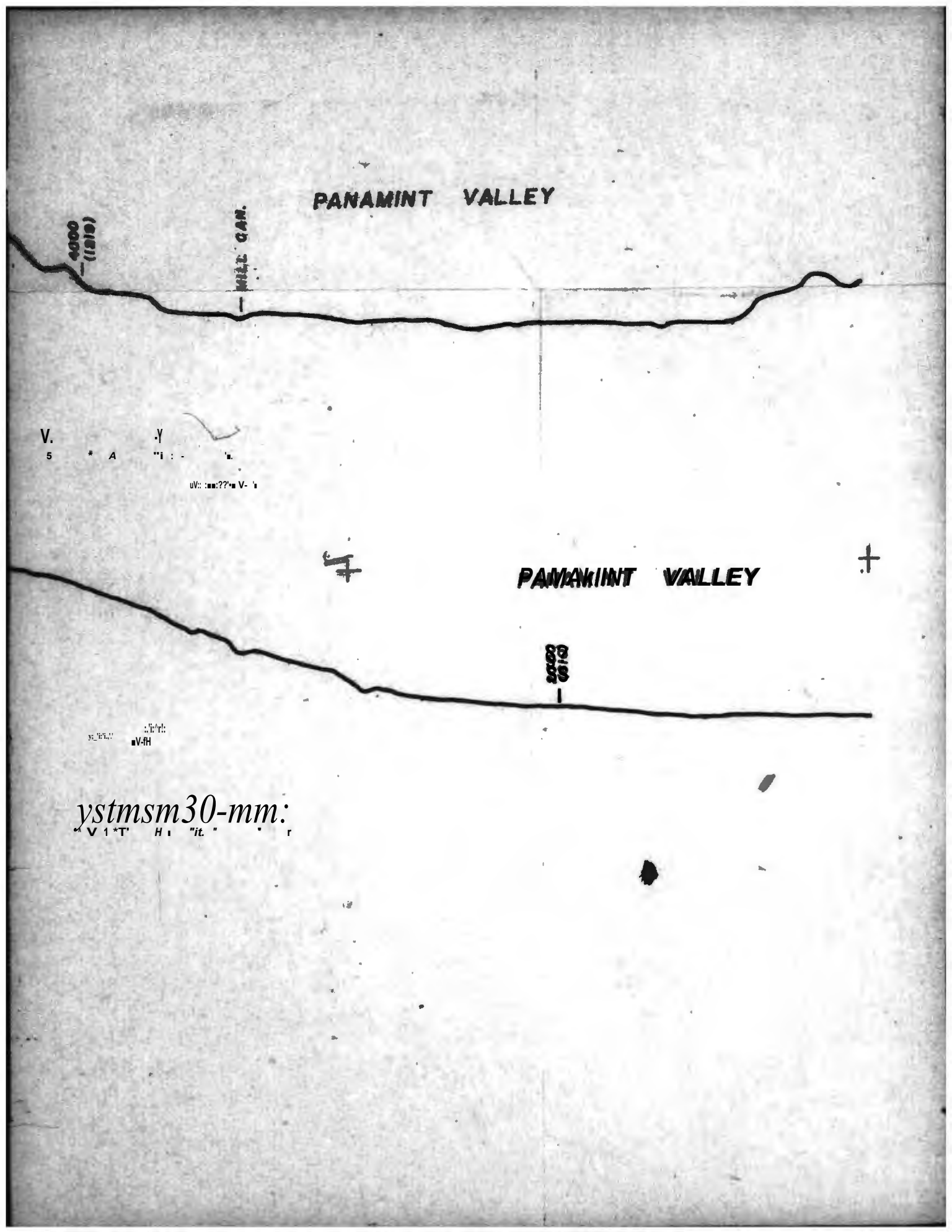
PANAMINT VALLEY
MILL CAN.
PANAMINT VALLEY

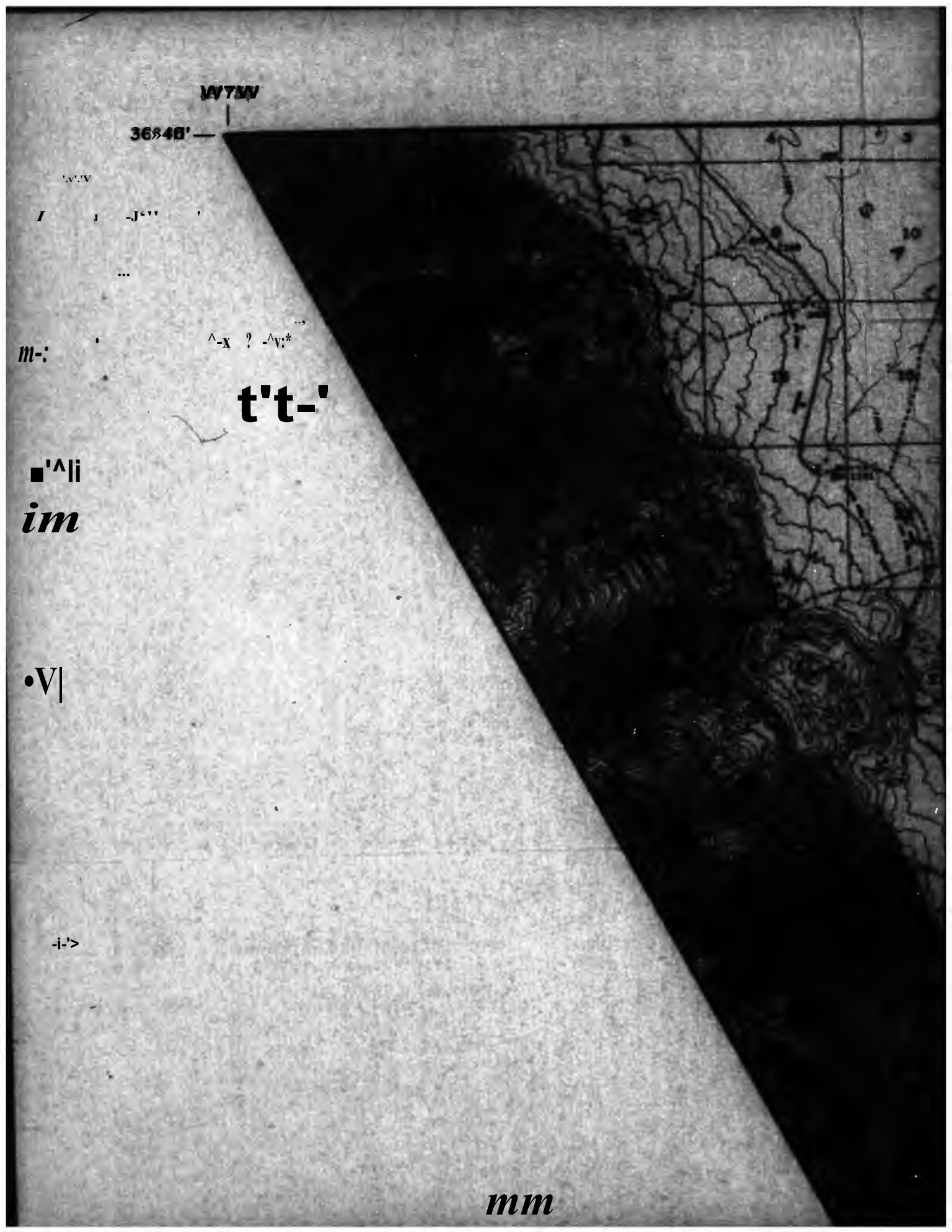

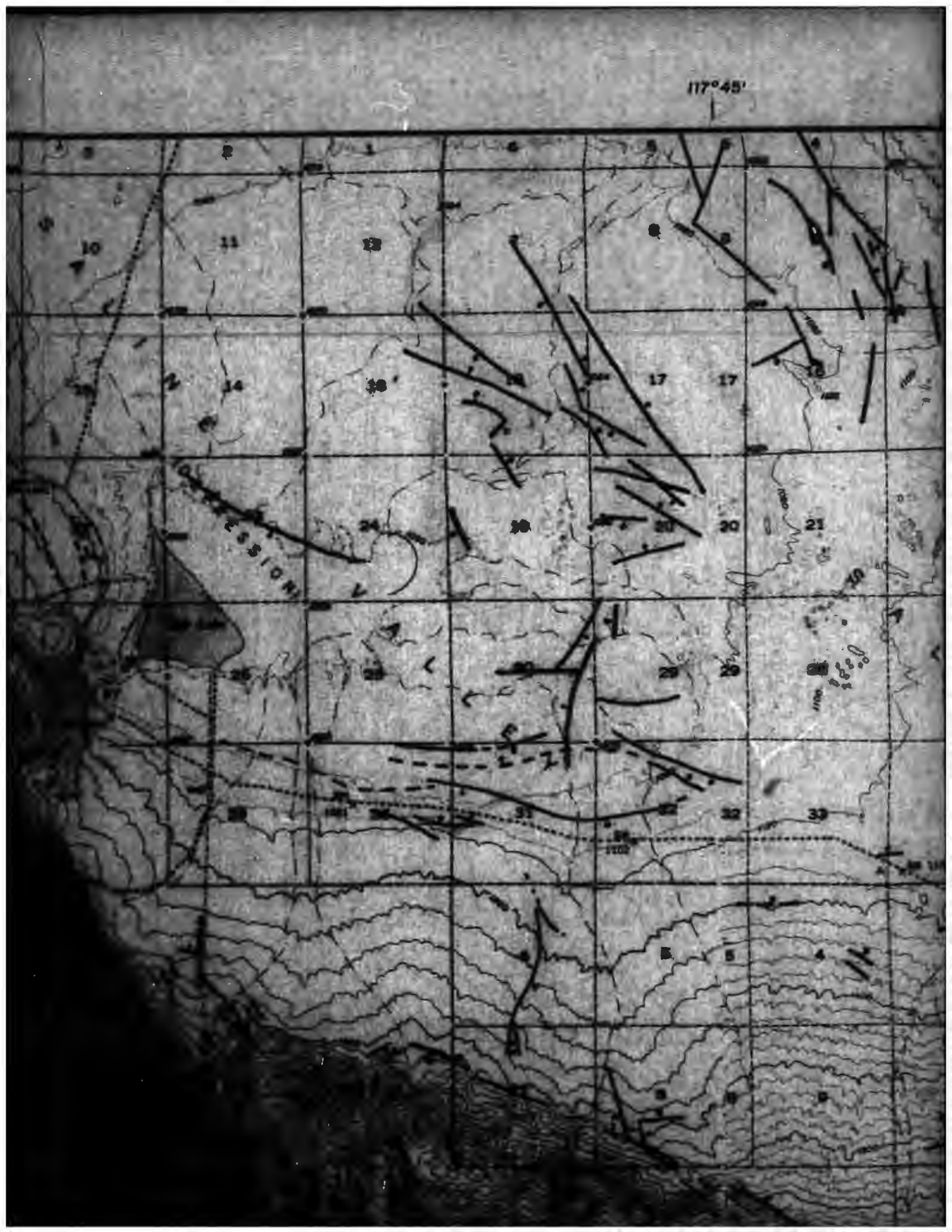
117°45'

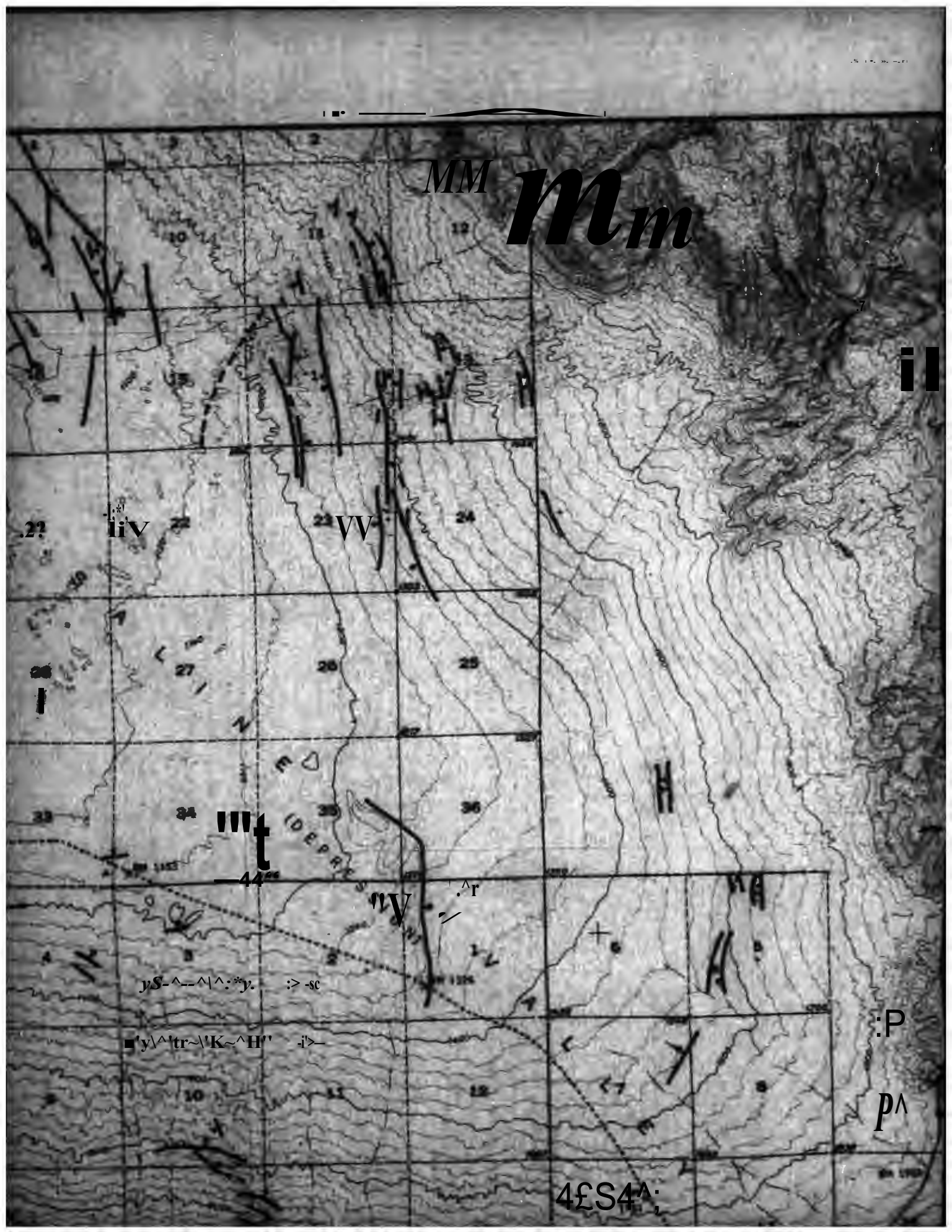

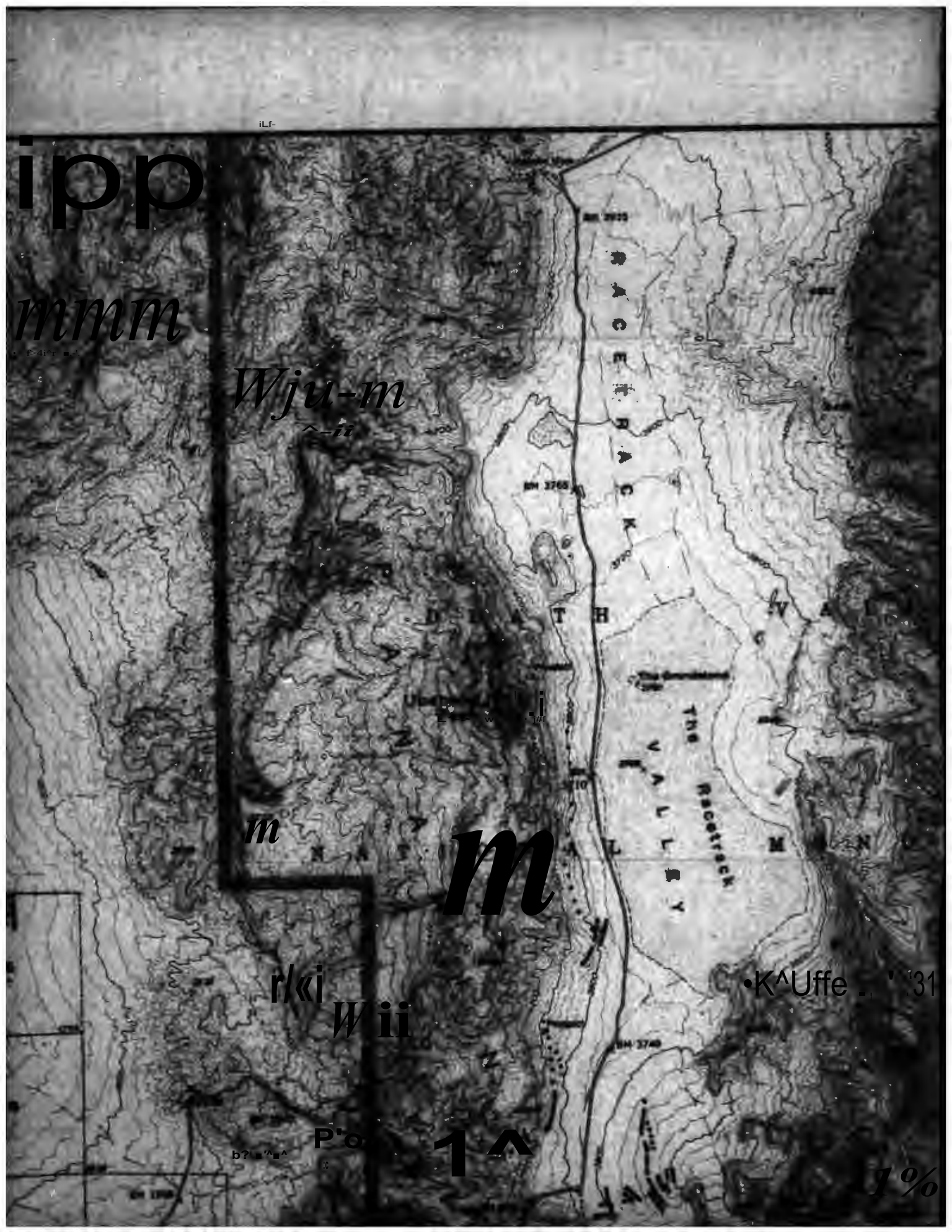
ipp
mmm
Wju-m
^-ii
m
m
r/«i
W ii
•K^Uffe
1^
1%

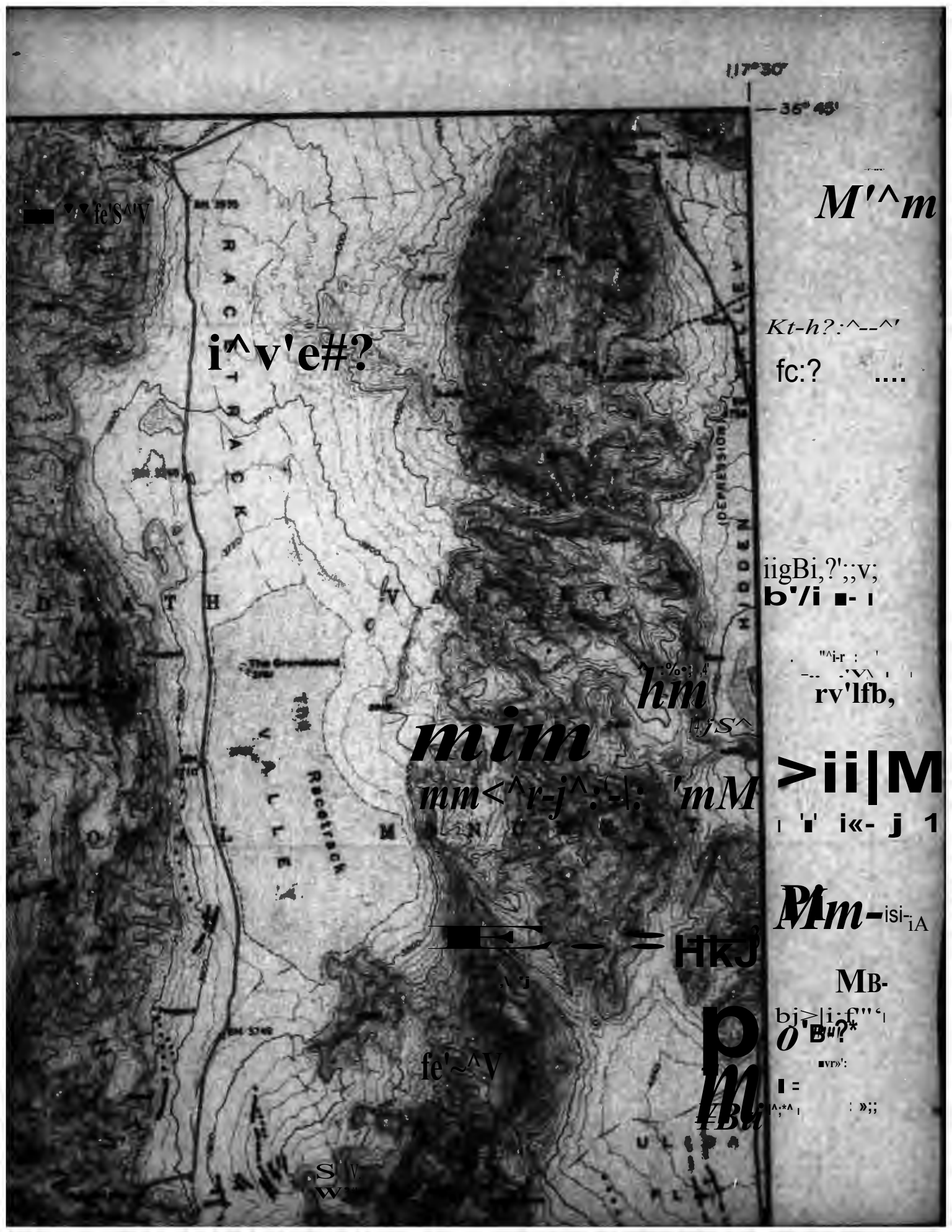
117°30'
36° 45'
RACETRACK
DEATH
VALLEY
Racetrack
HIDDEN
(DEPRESSION)

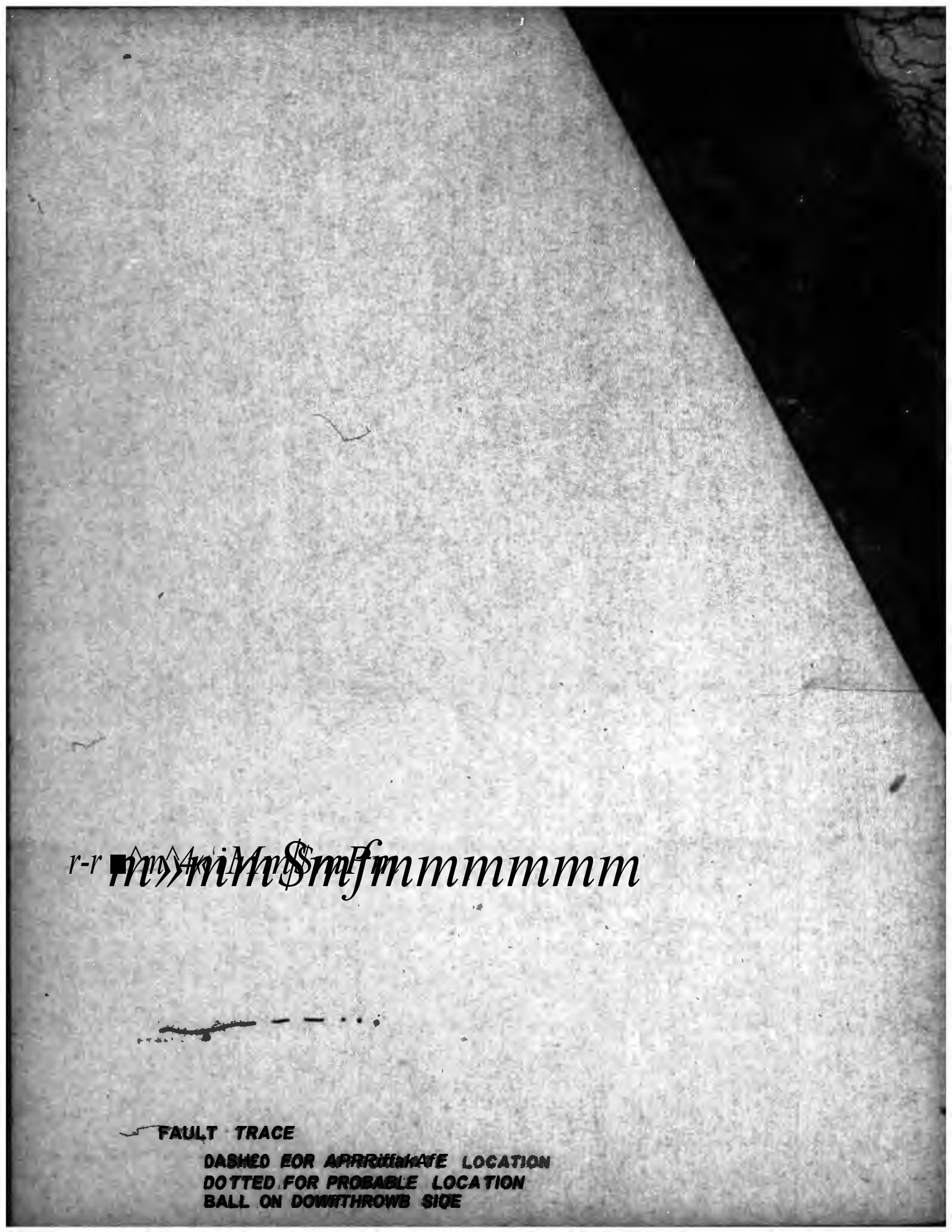
FAULT TRACE
DASHED FOR APPROXIMATE LOCATION
DOTTED FOR PROBABLE LOCATION
BALL ON DOWNTHROWN SIDE

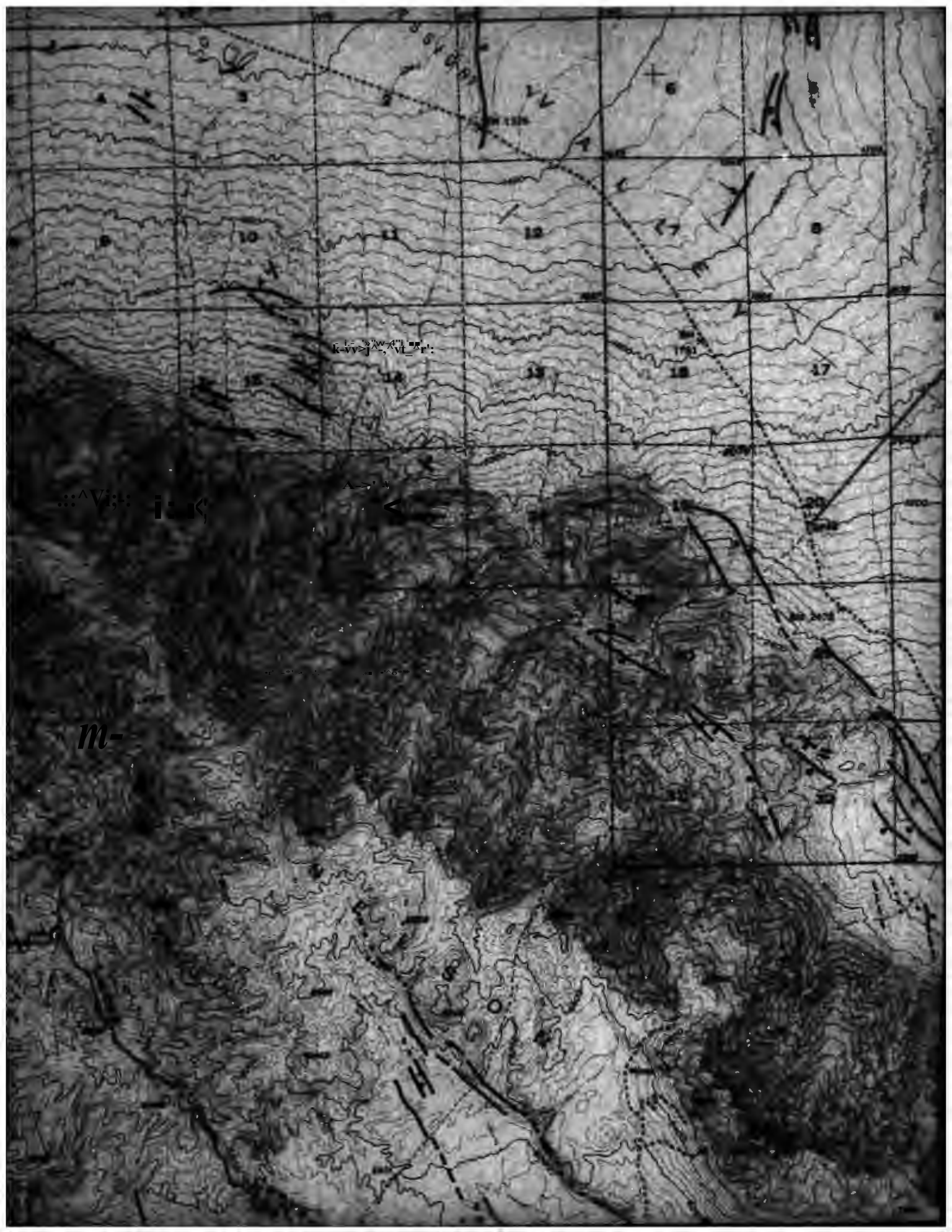


sm< Si&ts
a-. ^liS^fi^
M.
ii'!ii£i
ra/
P
i;#j3f?
li?Wra
SS
PPK


mm
raw
3m",
Pmiva
111
IliH
If-"#
iif%
M:Mtk
mm
m
iOT
fJiSSM
CS

FAULT TRACE

DASHED FOR APPROXIMATE LOCATION

DOTTED WHERE CONCEALED

BALE ON DOWNTHROWN SIDE

PLATE 3.1

FAULTS DISPLACING UNCONSOLI

at ZEELMER (1980)


36°30'
117°45'

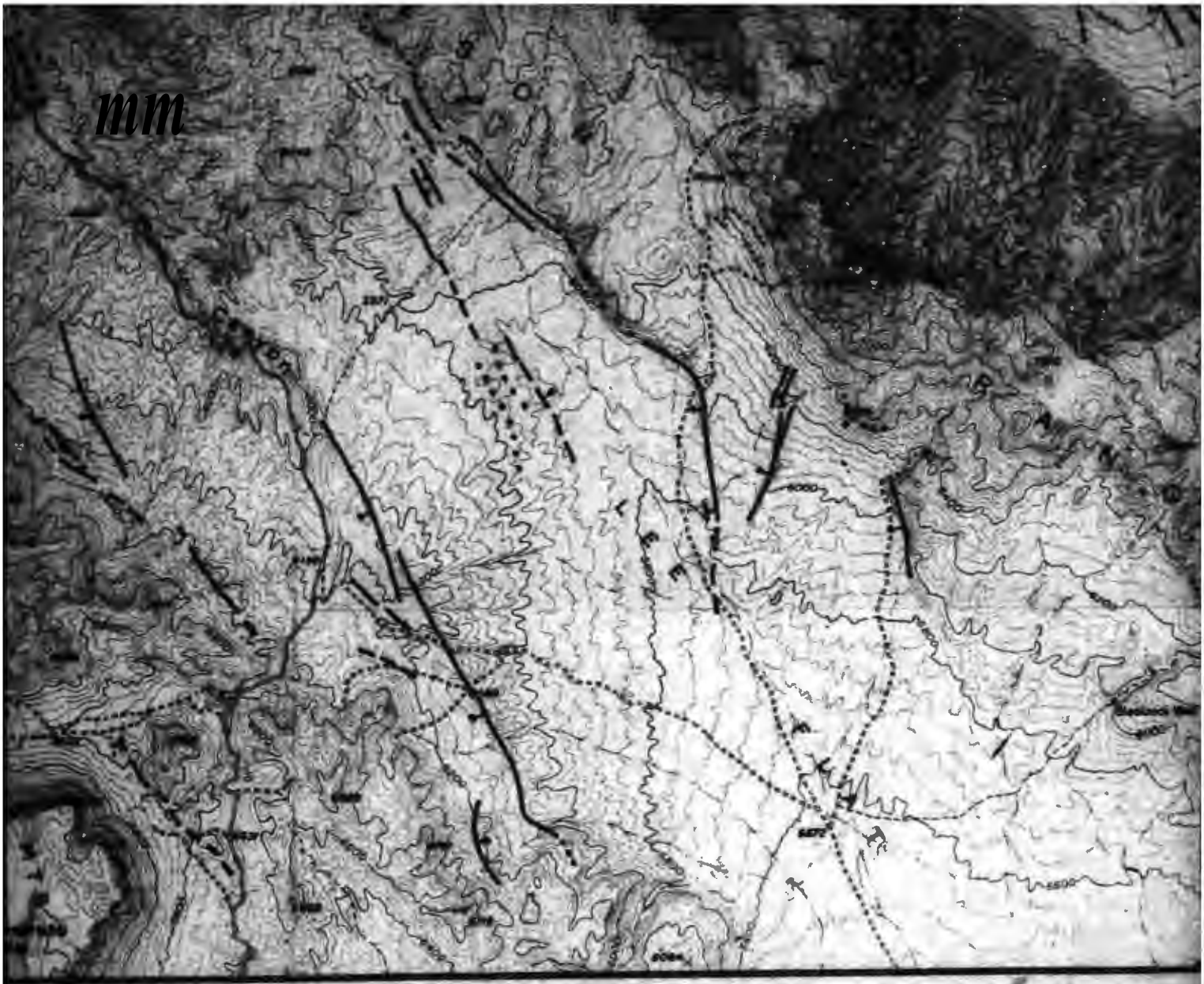

SCALE 1:

0 0.5 1 2

0 0.5 1 2 3

CONTOUR INTERVAL VARIA

SCALE 1:50,000

2 3 4 5 MILES

2 3 4 5 6 KILOMETERS

CONTOUR INTERVAL VARIABLE: 20 TO 80 Ft.

N

5 M/LES

6 KILOMETERS

N

1950 MAGNETIC DECLINATION

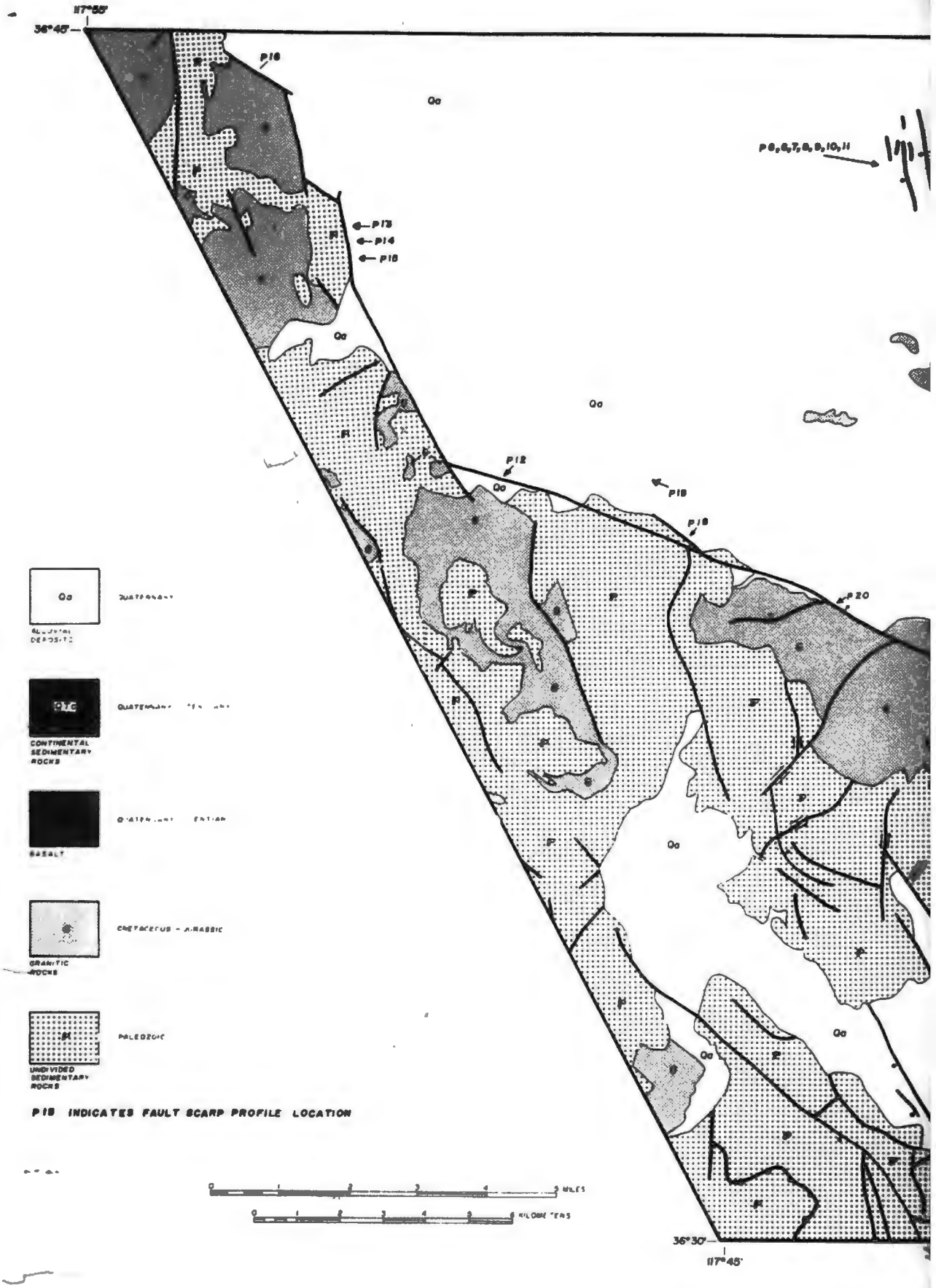
117°50'
36°45'
P16
Qa
P1, 2, 3, 4, 5, 6, 7, 8, 9, 10, 11
P13
P14
P15
P12
P17
P19
P20
Qa
Pl,C
CONTINENTAL SEDIMENTARY ROCKS
BASALT
GRANITIC ROCKS
PALEOZOIC
UNDIVIDED SEDIMENTARY ROCKS
P18 INDICATES FAULT SCARP PROFILE LOCATION
MILES
KILOMETERS
36°30'
117°45'

PLATE 3.1a.

TE 3.1a. SIMPLIFIED GEOLOGIC MAP

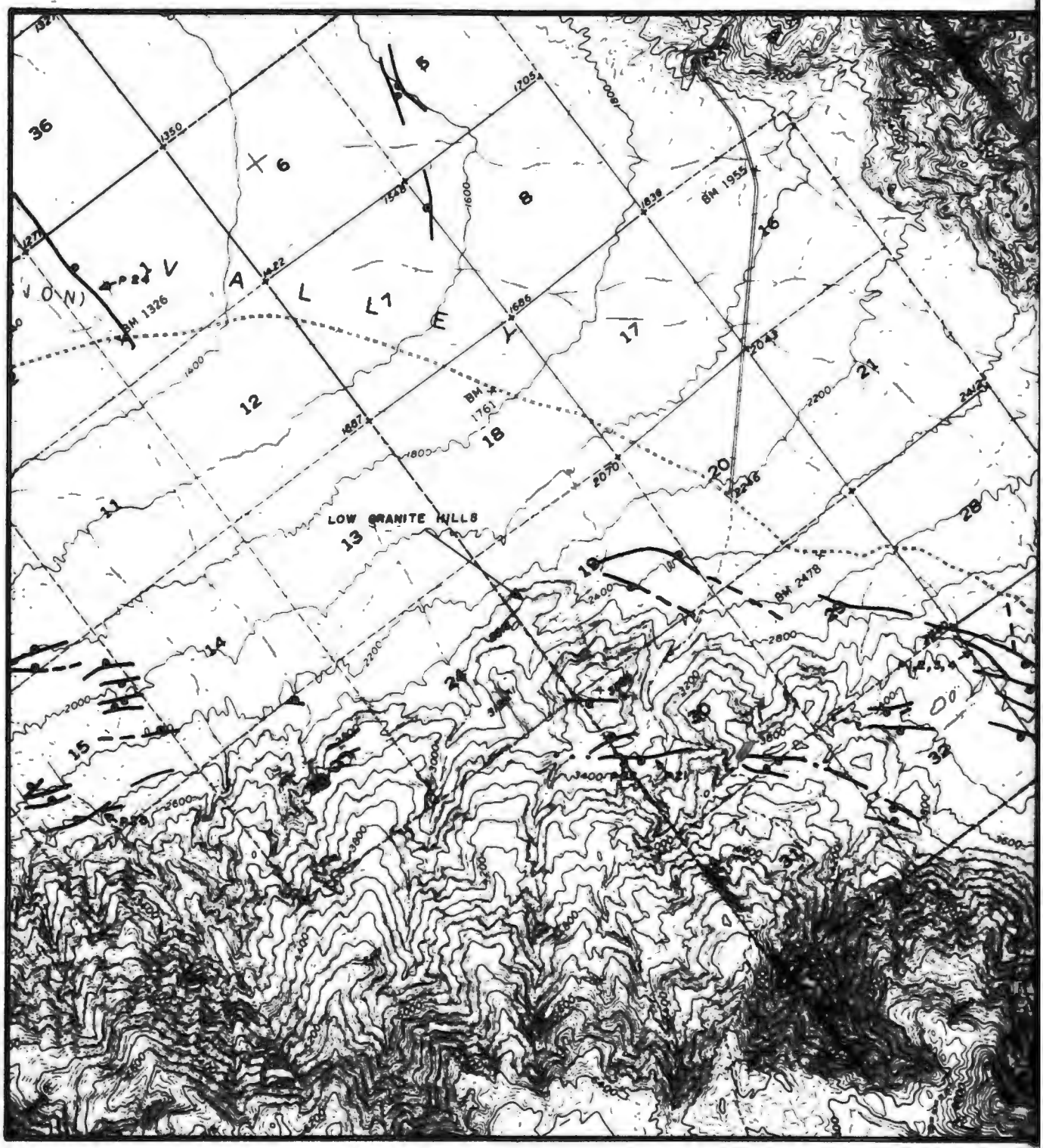

PLATE 3.2. FAULT ZONE LOCATI

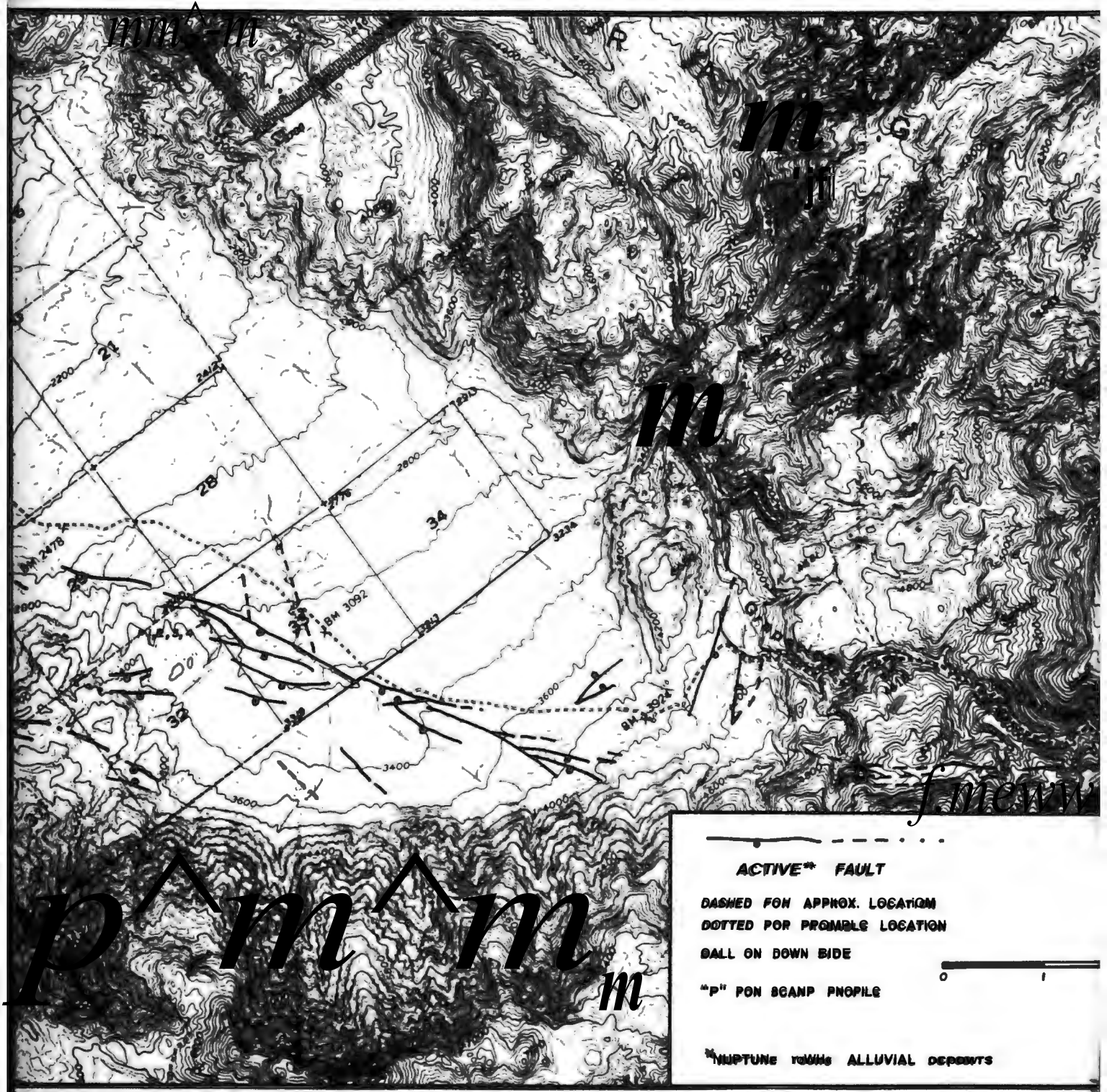

ZONE LOCATION – SOUTH END GRAPEVINE CANYON F.Z.

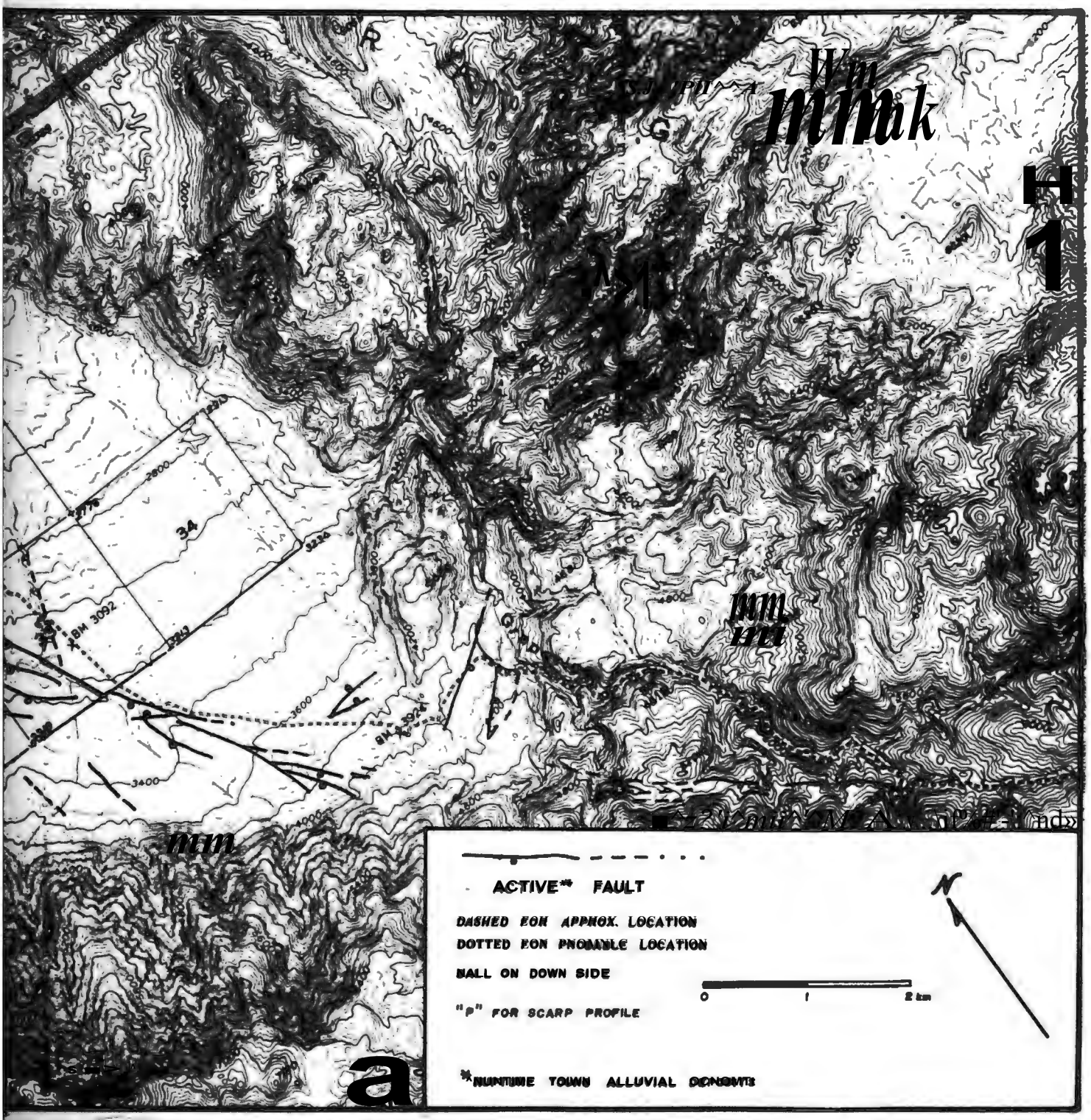

ION — SOUTH END GRAPEVINE CANYON F.Z.

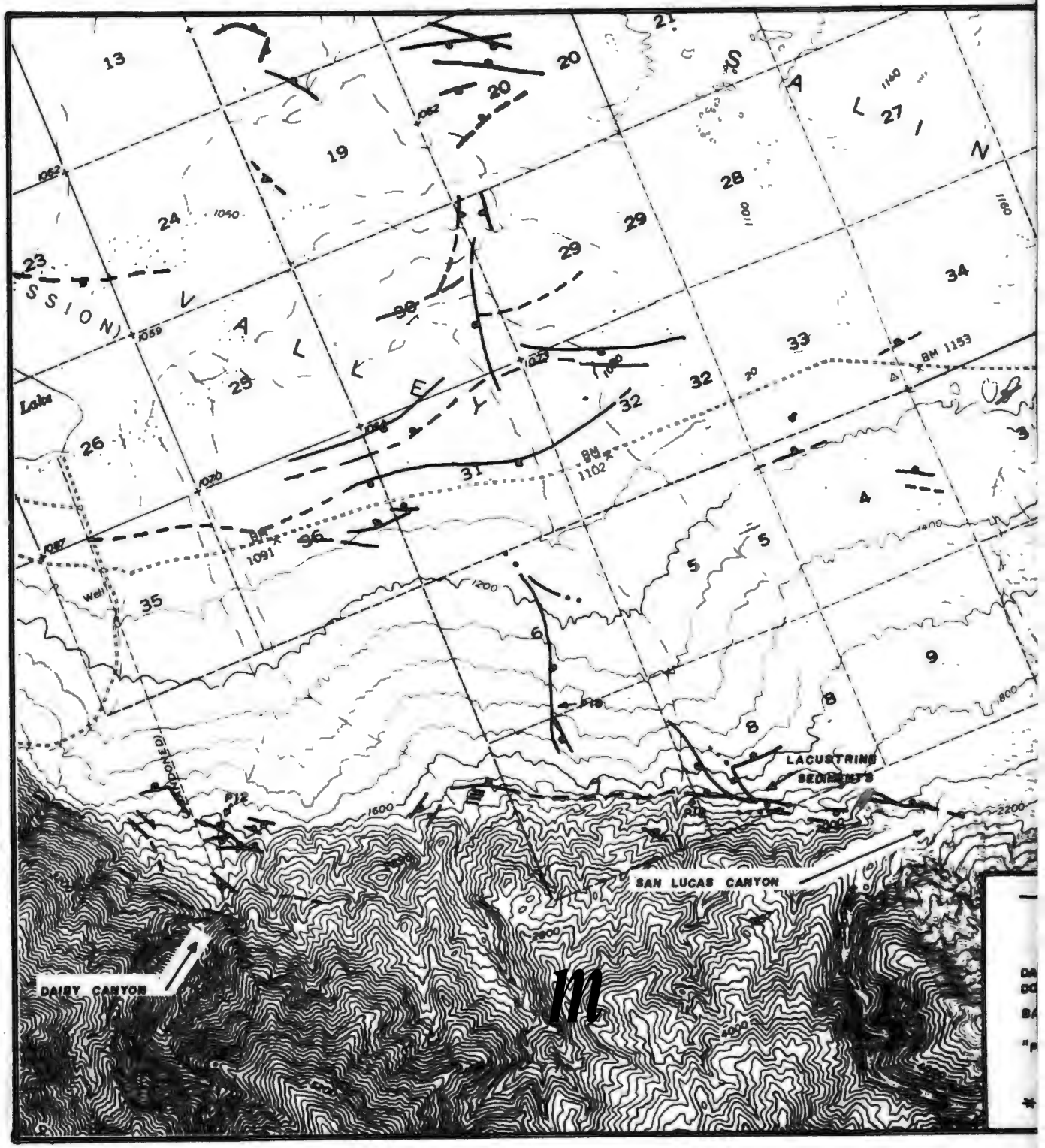

PLATE 3.3. FAULT ZONE LOCATIONS – N

CANYON, PORTION OF

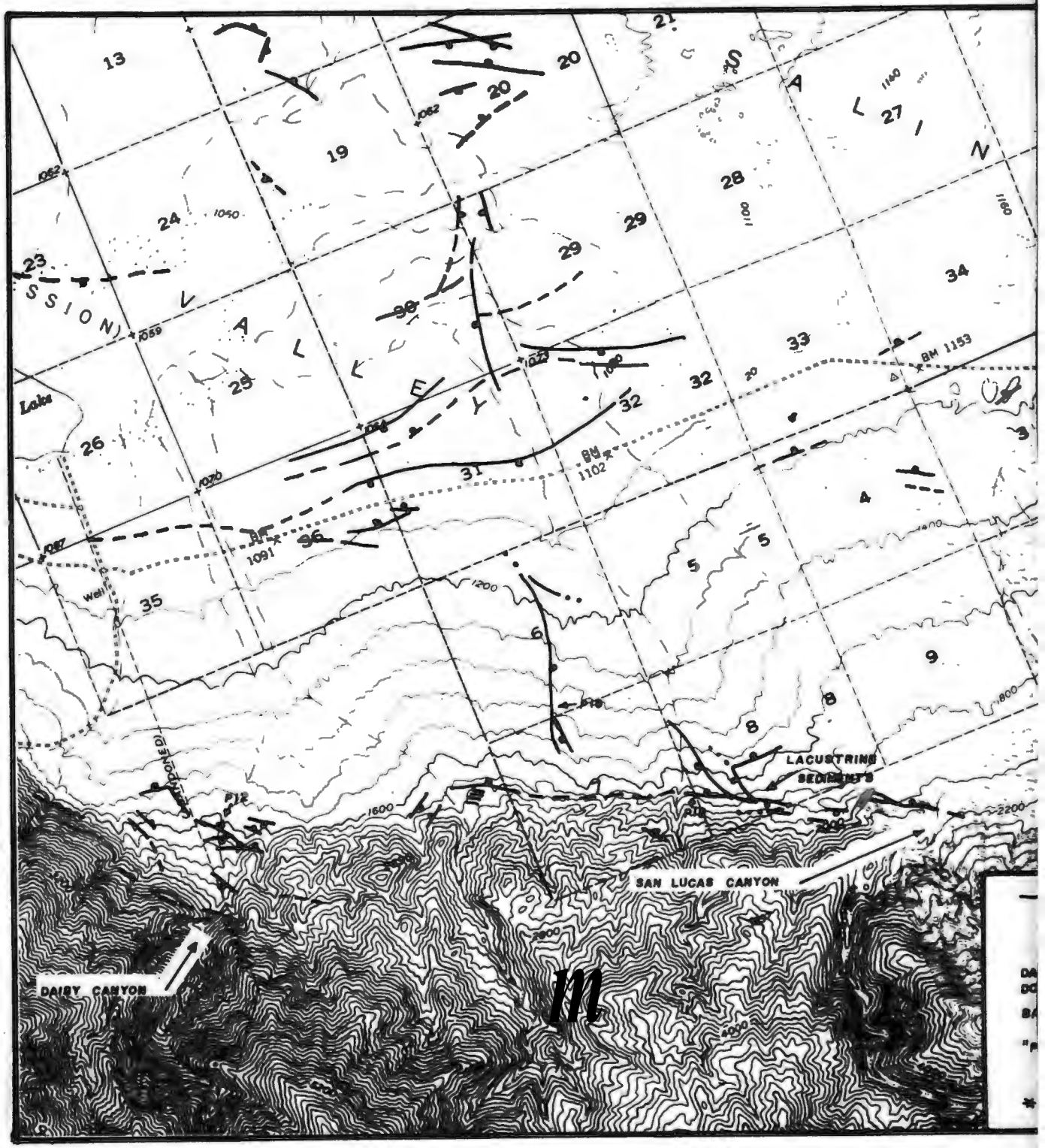

PLATE 3.3. FAULT ZONE LOCATIONS – N

CANYON, PORTION OF

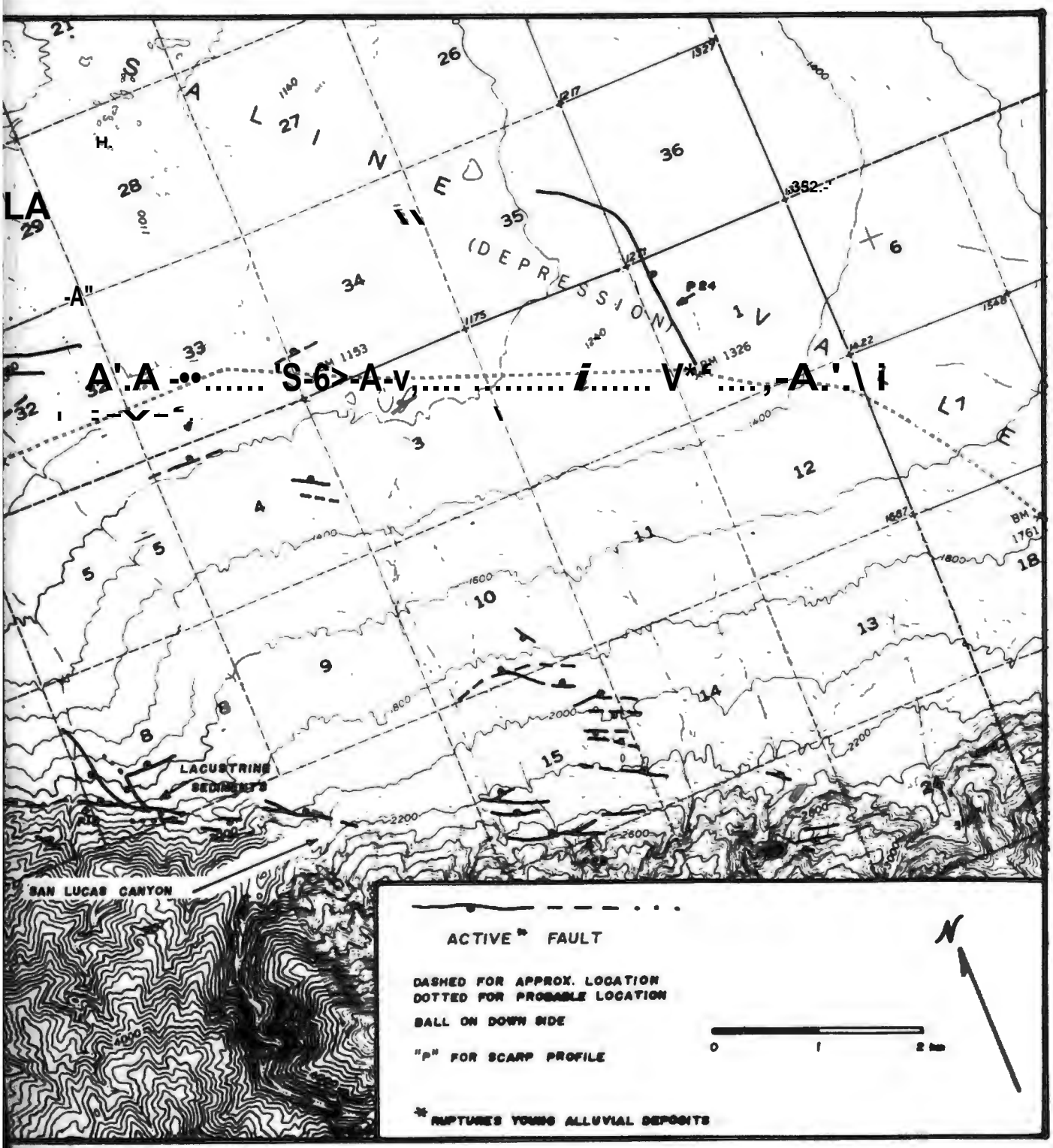

ZONE LOCATIONS – NORTH END GRAPEVINE CANYON, PORTION OF CENTRAL VALLEY F.Z.

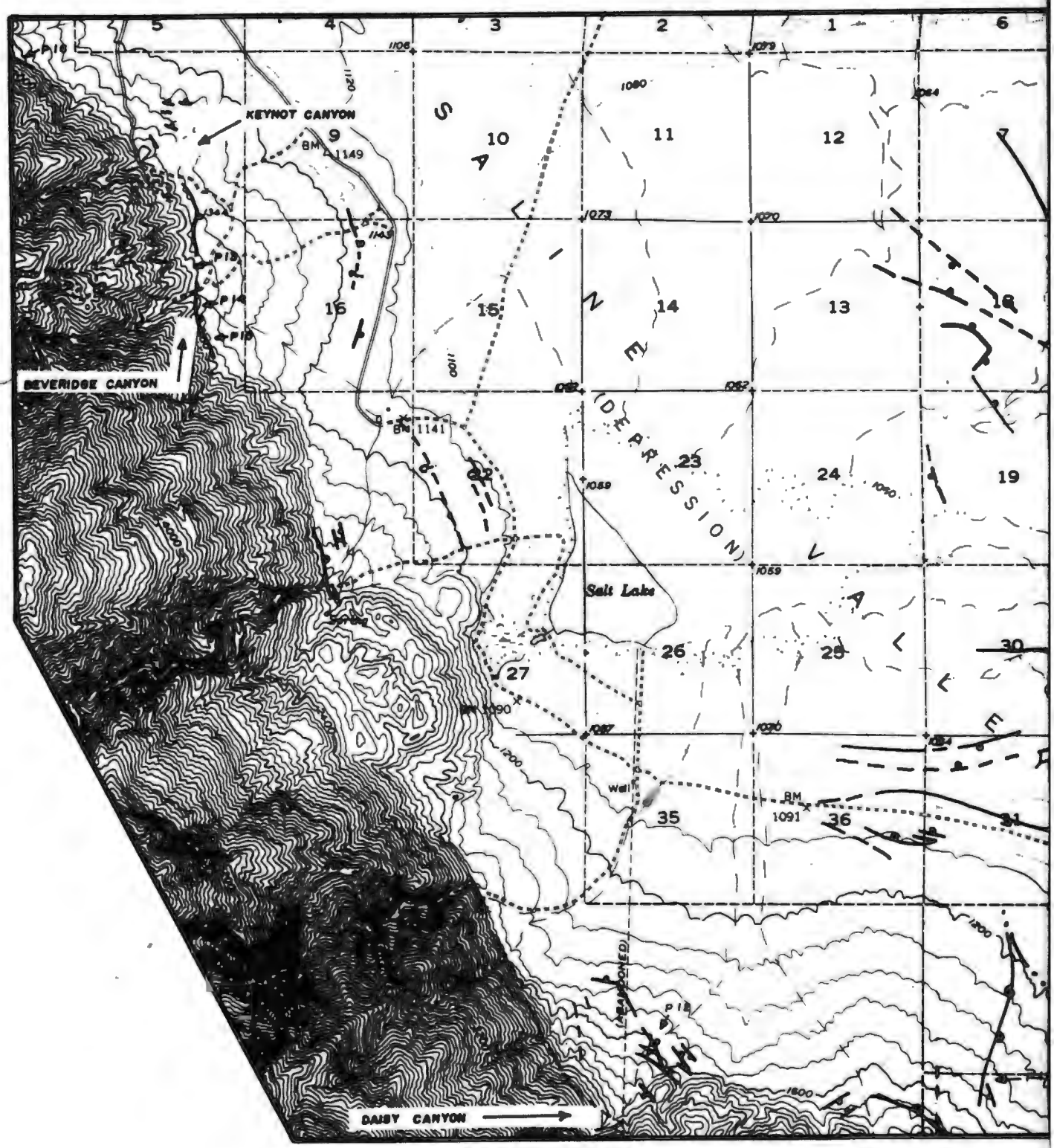

PLATE 3.4. FAULT ZONE LOCAT

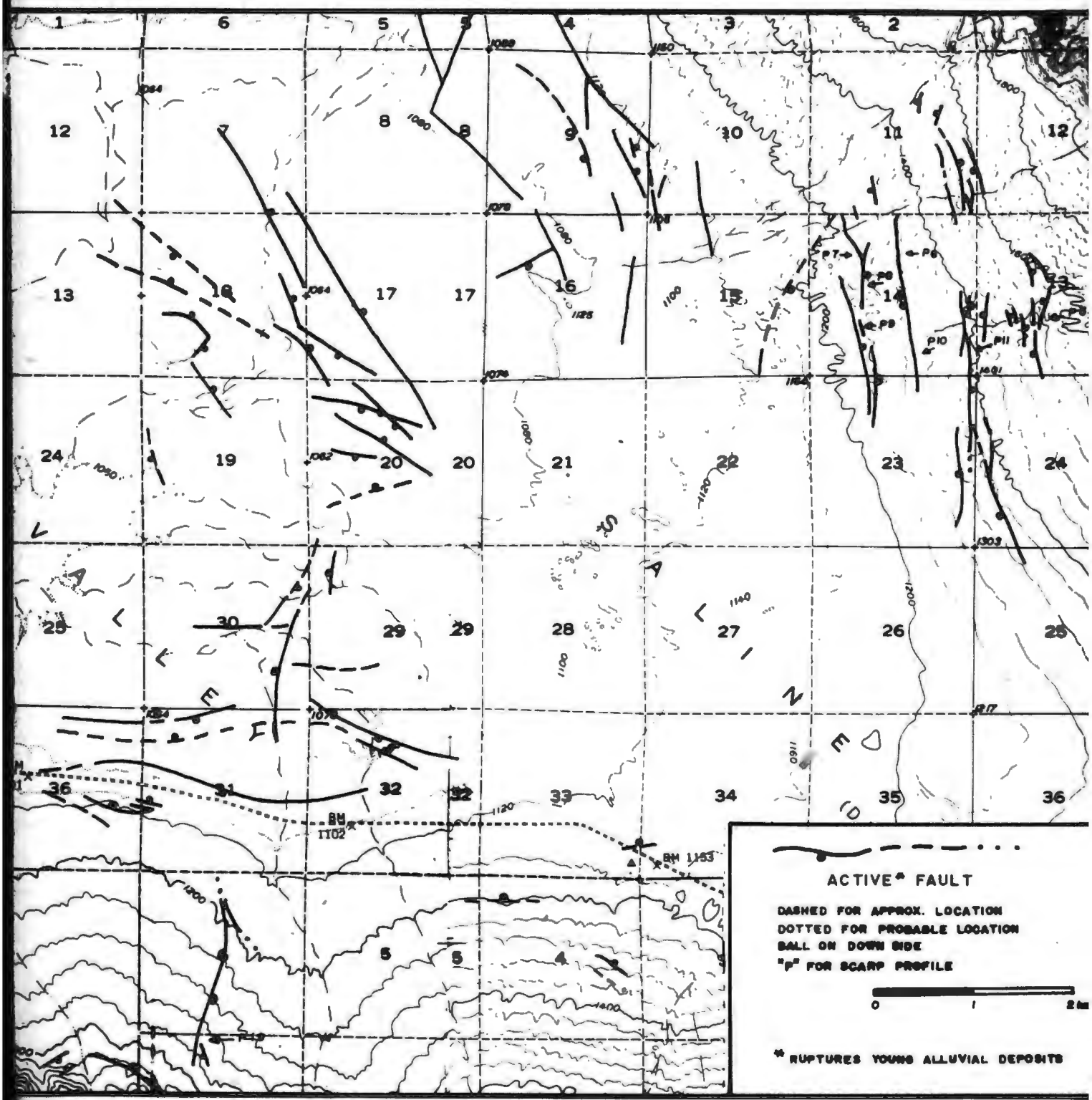

ZONE LOCATIONS - WESTERN FRONTAL, CENTRAL VALLE
EAST SIDE. F.Z.

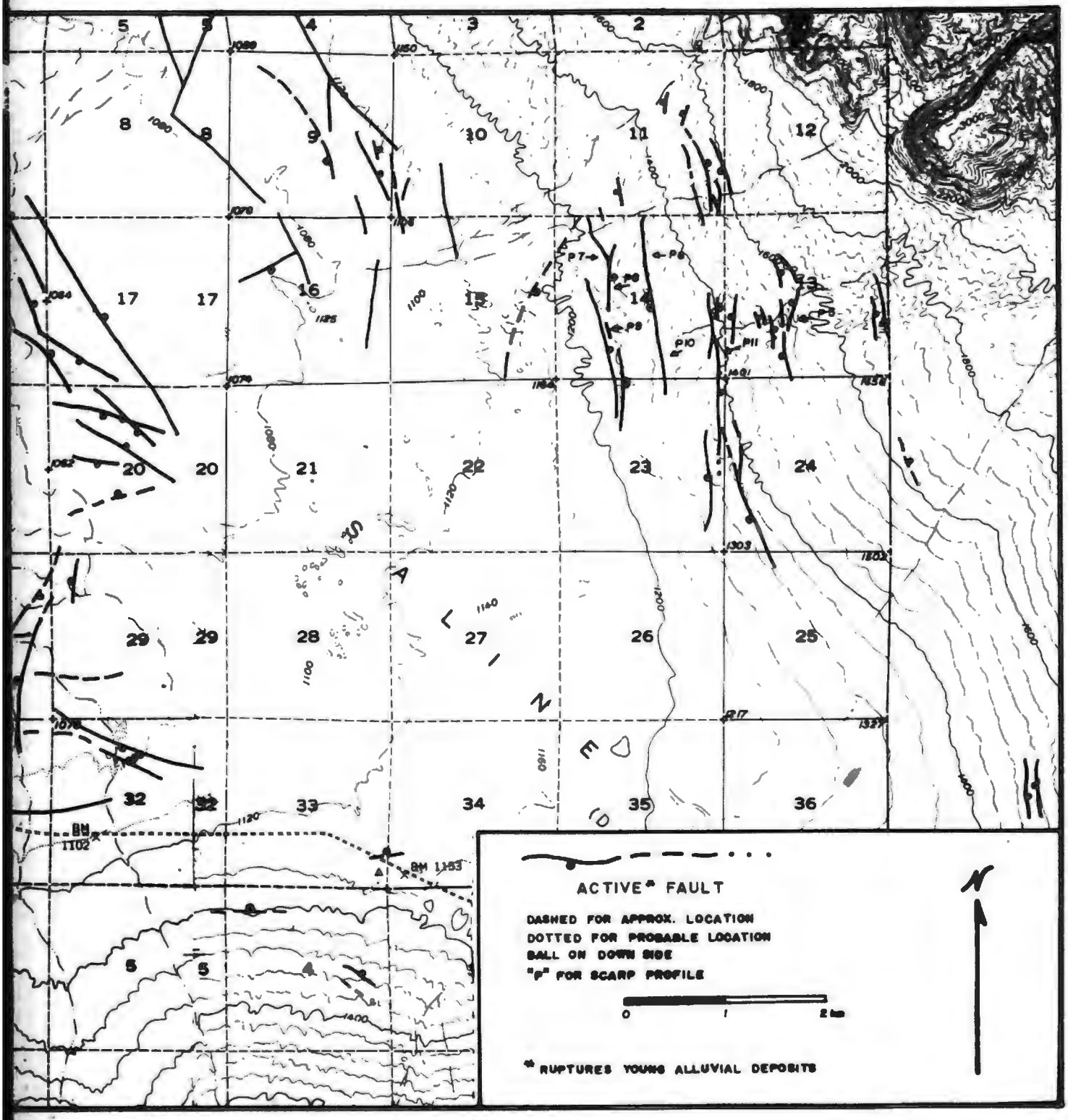

ONS - *WESTERN FRONTAL, CENTRAL VALLEY, EAST SIDE. F.Z.*

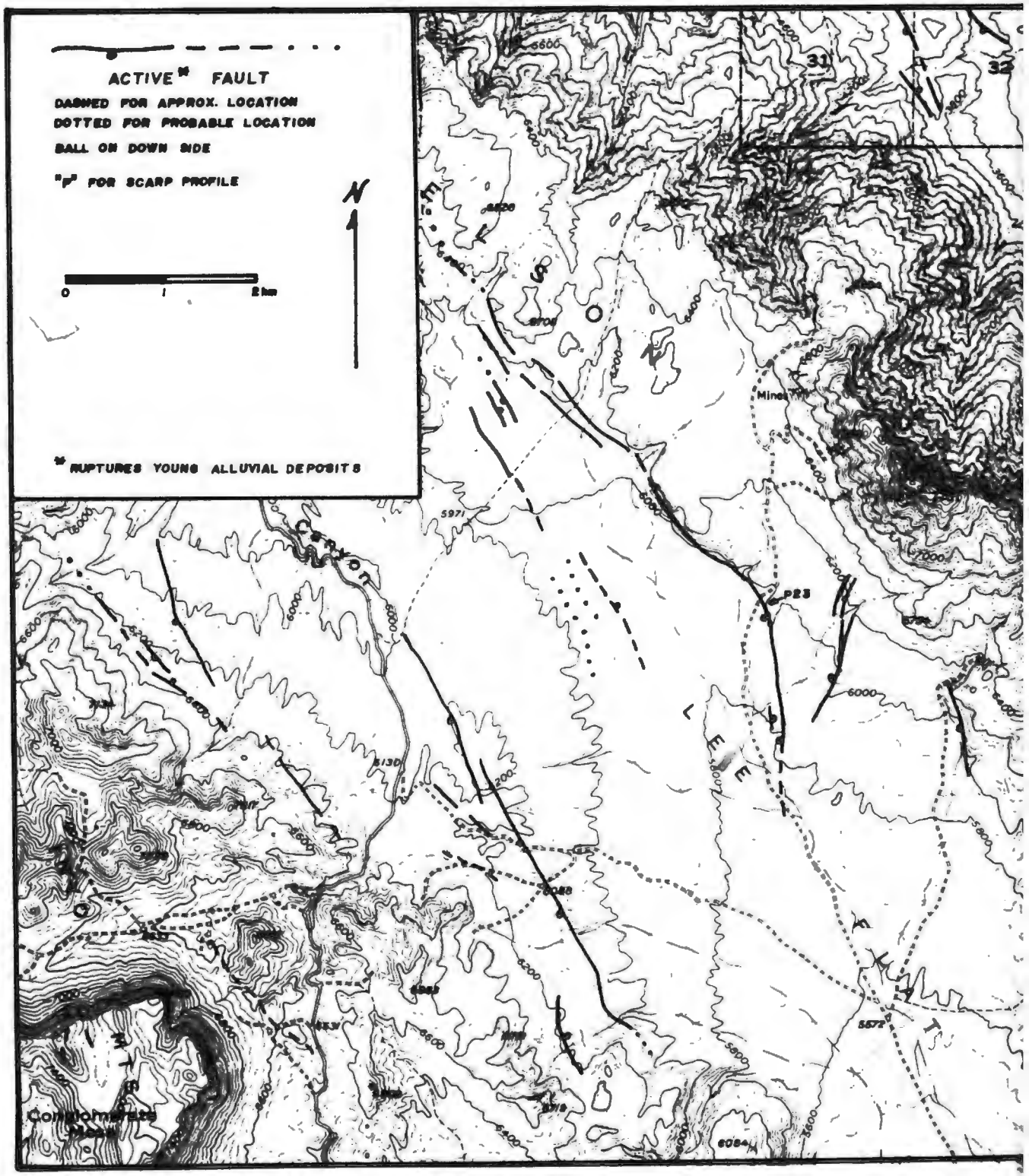

PLATE 3.5. FAULT ZONE LOCATION - LEE FLAT

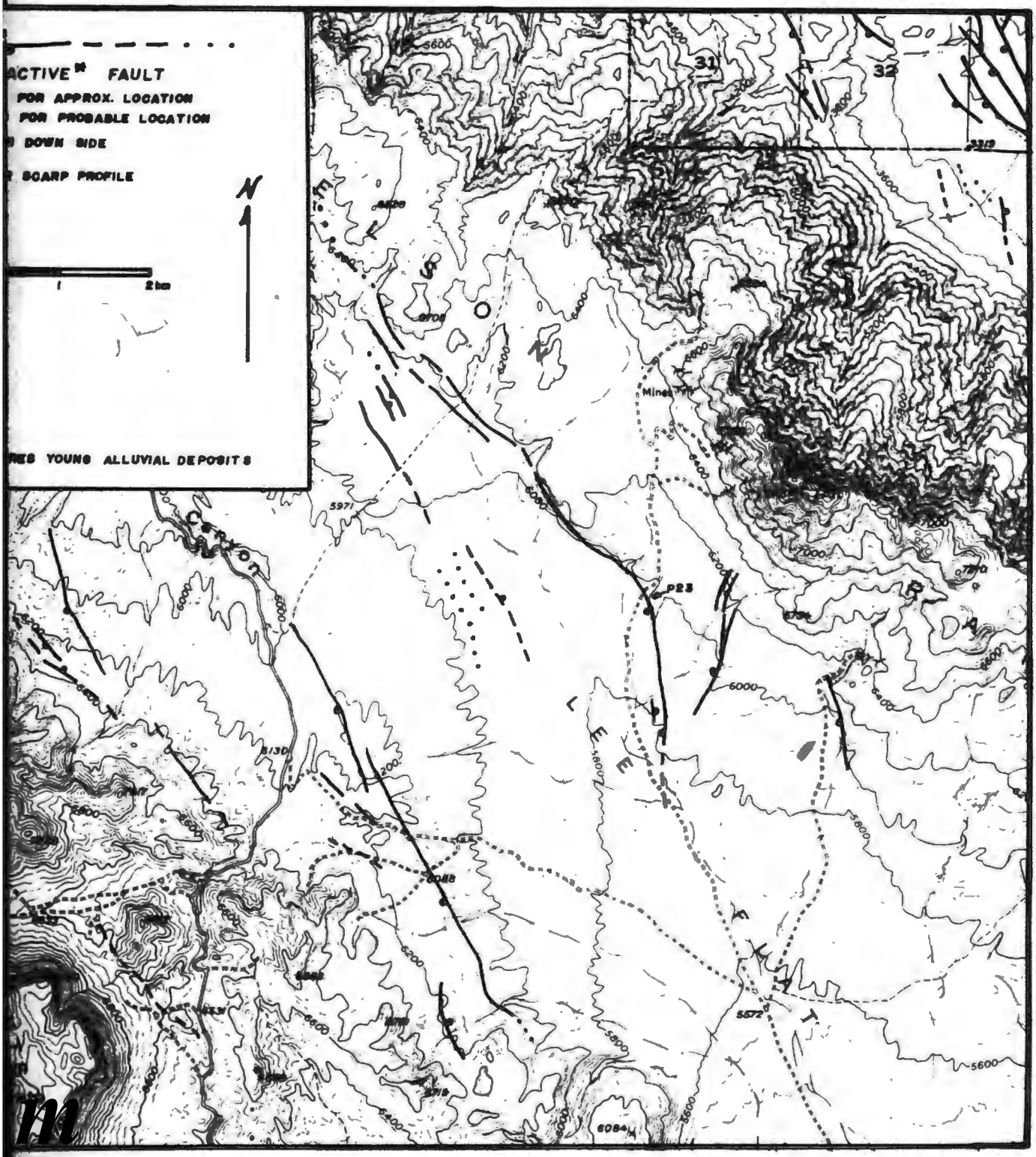

E 3.5. FAULT ZONE LOCATION – LEE FLAT F.Z.